André Miguel da Costa Lopes

Mestre em Biotecnologia

Valorisation of lignocellulosic biomass with ionic liquids in the frame of green chemistry and biorefinery concepts

Dissertação para obtenção do Grau de Doutor em Química Sustentável

Orientador:	Dr. Rafal Marcin Lukasik, Investigador Principal, Laboratório Nacional de Energia e Geologia, I.P.
Co-orientador:	Prof. Dr. Manuel Nunes da Ponte, Professor Catedrático, Faculdade de Ciências e Tecnologia, Universidade Nova de Lisboa

Júri:

Presidente:	Prof. Doutora Ana Isabel Nobre Martins Aguiar de Oliveira Ricardo
Arguentes:	Prof. Doutor Jyry-Pekka Mikkola Prof. Doutora Susana Filipe Barreiros
Vogais:	Doutor Francisco Manuel Ferreira Gírio Doutor Alexandre Babo de Almeida Paiva Doutor Rafal Marcin Lukasik

FACULDADE DE CIÊNCIAS E TECNOLOGIA
UNIVERSIDADE NOVA DE LISBOA

October 2017

André Miguel da Costa Lopes

Mestre em Biotecnologia

Valorisation of lignocellulosic biomass with ionic liquids in the frame of green chemistry and biorefinery concepts

Dissertação para obtenção do grau de
Doutor em Química Sustentável

FACULDADE DE
CIÊNCIAS E TECNOLOGIA
UNIVERSIDADE NOVA DE LISBOA

October 2017

Valorisation of lignocellulosic biomass with ionic liquids in the frame of green chemistry and biorefinery concepts

Para a minha família, namorada e amigos

Agradecimentos

Assim termina um longo período de crescimento profissional e pessoal que me marcou e que levo de recordação para o resto da minha vida.

Agradeço primeiramente ao meu orientador Doutor Rafal Lukasik que foi fundamental para chegar a este patamar. Um muito obrigado pela disponibilidade, colaboração e atitude crítica no acompanhamento do meu trabalho ao longo destes anos de orientação (e foram mais do que 4 anos!!), e sobretudo por toda a ajuda que me foi dada, tanto dentro como fora do LNEG, em momentos que mais precisei. Partilhámos momentos bons e menos bons, alguns divertidos e únicos cheios de peripécias para contar, e no final o balanço é bastante positivo. Um grande abraço!!

Agradeço também ao meu co-orientador Professor Doutor Manuel Nunes da Ponte pela disponibilidade e sabedoria que foram necessários ao longo destes 4 anos.

Obrigado Rita Morais por todo o teu companheirismo no LNEG e acompanhamento desta fase que ambos sabemos que não é fácil, mas que fomos os dois ultrapassando todos obstáculos que foram surgindo. Agradeço a todas as pessoas que passaram pelo LNEG que contribuíram para o desenvolvimento do meu trabalho: obrigado Sara Magalhães ("Oh Márcio!!!"), Vanessa Carvalho, Susana Peleteiro ("que dices?? no entiendo nada" espanholita querida!!!), Miriam Brenner, Roberto Lins (grande Robert!!!).

Obrigado Doutora Luísa e Doutor Roseiro, duas pessoas muito queridas para mim, que eu estimo e respeito muito, serão sempre um exemplo pessoal e profissional que levo de Lisboa. Obrigado Doutor Luís, Doutora Florbela e Doutora Patrícia Moniz pela disponibilidade e amizade. Obrigado Céu Penedo e Belina Ribeiro por toda a ajuda prestada e pela boa disposição que tinham todos os dias. Não me podia esquecer da minha querida Sofia Graça, que sempre tinha tempo para barafustar e embirrar comigo (é que não havia um dia!!! ☺). Agradeço também aos colegas e amigos que passaram pelo LNEG que tive muito gosto em conhecer. Obrigado Joana, Sérgio, Cadinho e Cordeiro, e claro, um grande obrigado à minha grande amiga Cláudia, por ouvires os meus desabafos, foste fundamental a ajudar-me a ultrapassar os maus momentos, sei que posso contar contigo para a vida e sabes que também podes contar com o teu "PêhDê".

Agradeço também aos meus amigos de Lisboa. Obrigado Luís ("gajo cheio do guito") foste o meu grande amigo ao longo destes 6 anos que estive em Lisboa, e continuarás a ser um dos meus melhores amigos. Ajudaste-me a viver este período desafiante sempre com a disposição em alta. Aquelas corridas pela Quinta das Conchas, aquelas "tainadas" a ver o grande FCP a jogar que serão sempre épicas com uma Maredsous a acompanhar e aquela competição Masterchef lá de casa, vão estar sempre na minha recordação. Obrigado Hélder Edral, Joana Frutuoso, Sónia, Filipe e Juliana vou sentir saudades vossas.

Agora mais a Norte, nas minhas origens, muito obrigado "amigos de Aveiro", Pinho, Queirós e Chica, são os mais antigos e sempre com uma amizade pura e fiel, porque quando regressava a Aveiro era sempre uma festa. Muito obrigado aos "amigos de Oliveira", e em especial ao meu grande amigo Zinho

e à minha querida amiga Maria João, com vocês já partilhei momentos únicos que contribuíram para a minha felicidade e continuarão a haver muitos mais.
Por fim deixo um eterno obrigado às pessoas mais importantes da minha vida. Aos meus pais devo tudo o que sou hoje, e é difícil retribuir a força, amor e carinho que mais ninguém dá como vocês. Obrigado mãe, por seres a minha conselheira, és sem dúvida um dos meus maiores suportes na vida e tu és uma das razões por todo o sucesso que até hoje tenho conquistado. Obrigado pai pela força que me foste dando até hoje para ultrapassar as adversidades. Obrigado minha irmã, sei que estás longe, mas sempre estiveste para mim quando mais precisei. Um muito obrigado minha querida Rita, és o meu braço direito e ajudaste-me em todas as etapas deste percurso difícil, partilhámos momentos únicos e espero continuar a vivê-los contigo. A tua amizade e amor são insubstituíveis, não há ninguém como tu. Obrigado Sr. Amílcar e Dona Lídia pela coragem e força que sempre me foram dando neste período. Por fim, todos os meus restantes familiares e queridos amigos um muito obrigado pois sempre estiveram quando mais precisava.

Resumo

Atualmente existe a necessidade de apostar nos conceitos de bioeconomia e economia circular. A utilização de biomassa lenhocelulósica, como fonte renovável de carbono, para a produção de combustíveis, compostos químicos e materiais é uma potencial solução que tem sido vastamente explorada nos últimos anos. Neste âmbito, a presente tese demonstra o desenvolvimento de novas tecnologias com líquidos iónicos (LIs) para a valorização de biomassa lenhocelulósica, seguindo os conceitos de química verde e biorrefinaria.

O trabalho foi realizado através de duas abordagens, dependendo das características químicas dos LIs estudados (acidez e basicidade), que permitiram o fracionamento da biomassa nos seus componentes principais, nomeadamente, celulose, hemicelulose e lenhina, quer nas suas formas poliméricas ou hidrolisadas. A primeira estratégia abordou a utilização do LI básico acetato de 1-etil-3-metilimidazólio no desenvolvimento de um processo de fracionamento de palha de trigo em três passos, que permitiu a separação seletiva de frações de celulose, hemicelulose e lenhina com elevada pureza. No final do processo verificou-se a presença de compostos fenólicos dissolvidos no LI recuperado, que foram extraídos e purificados através da utilização de resinas poliméricas e CO_2 supercrítico. Na segunda estratégia, os processos de pré-tratamento, hidrólise, e conversão de biomassa foram integrados num único passo, através da utilização de LIs ácidos contendo anião do tipo imidazólio e o catião hidrogenossulfato. Estes LIs revelaram a capacidade de hidrolisar e converter seletivamente a fração hemicelulósica da palha de trigo produzindo pentoses e/ou furfural. A presença de água no sistema demonstrou favorecer a produção de pentoses. Para além disso, o processo produziu um sólido constituído por celulose e lenhina, os quais foram fracionados em glucose, lenhina de elevada pureza e compostos fenólicos. Em ambas as abordagens, os LIs foram recuperados e reusados com sucesso, e desta forma, os processos desenvolvidos demonstraram ser eficientes e sustentáveis para implementação em biorrefinarias.

Palavras-chave

Biomassa, biorefinaria, líquidos iónicos, fracionamento, hidrólise, química verde

Abstract

The current need to move from a fossil-derived economy to sustainable bio-based and circular economy is highly demanding. The utilisation of lignocellulosic biomass, as a renewable carbon source, for the production of fuels, chemicals and materials is a promising solution that has been widely explored in recent years. In this framework, the present thesis discloses the development of novel technologies using ionic liquids (ILs) for biomass valorisation following the green chemistry and biorefinery concepts.

Two different approaches, on the basis of the chemical character of examined ILs, *i.e.* acidity and basicity, paved the way for a fractionation of wheat straw into main components, namely cellulose, hemicellulose and lignin, either in their polymeric or hydrolysed forms. A first strategy relied on the development of a three-step fractionation process using alkaline 1-ethyl-3-methyimidazolim acetate ([emim][OAc]) allowing selective separation of cellulose, hemicellulose and lignin as high purity fractions. The recovered IL demonstrated the presence of soluble phenolic compounds, which were extracted and purified by means of polymeric resin and supercritical CO_2 extraction methods. The second strategy integrated a pre-treatment, hydrolysis and conversion of biomass in a single step process through the employment of acidic imidazolium ILs containing HSO_4 anion. These ILs revealed the ability to selectively hydrolyse and convert the hemicellulosic fraction of wheat straw into pentoses and/or furfural, in which the formation of pentoses are favoured in presence of water. The resulting solid composed mainly of cellulose and lignin was fractionated and processed towards the production of glucose, highly pure lignin and also phenolic compounds. Both types of ILs were recovered and reused without losing their performances in biomass valorisation, showcasing efficient and sustainable processes for implementation in biorefineries.

Keywords

Biomass, biorefinery, ionic liquids, fractionation, hydrolysis, green chemistry

Table of Contents

List of Figures

Chapter I

Chapter II

Chapter III

Chapter IV

Chapter V

Chapter VI

Chapter VII

List of Tables

CHAPTER I

CHAPTER III

CHAPTER IV

CHAPTER V

CHAPTER VI

CHAPTER VII

APPENDIX A

APPENDIX B

APPENDIX C

List of Publications

The current thesis is based on the following scientific papers:

S. P. Magalhães da Silva, A. M. da Costa Lopes, L. B. Roseiro and R. Bogel-Lukasik, Novel pre-treatment and fractionation method for lignocellulosic biomass using ionic liquids., *RSC Adv.*, 2013, **3**, 16040-16050..... CHAPTER III

A. M. da Costa Lopes, M. Brenner, P. Fale, L. B. Roseiro and R. Bogel-Lukasik, Extraction and purification of phenolic compounds from lignocellulosic biomass assisted by ionic liquid, polymeric resins and supercritical CO_2., *ACS Sustain. Chem. Eng.*, 2016, **4**, 3357-3367. ..... CHAPTER IV

A. V. Carvalho, A. M. da Costa Lopes and R. Bogel-Lukasik, Relevance of the acidic 1-butyl-3-methylimidazolium hydrogen sulphate ionic liquid in the selective catalysis of biomass hemicellulose fraction., *RSC Adv.*, 2015, **5**, 47153-47164. ..... CHAPTER V

A. M. da Costa Lopes, R. M. G. Lins, R. A. Rebelo and R. M. Lukasik, Biorefinery approach for lignocellulosic biomass valorisation with acidic ionic liquid. *Energ. Environ. Sci.*, 2017. (submitted). ..... CHAPTER VI

A. M. da Costa Lopes and R. M. Lukasik, A comprehensive study for the separation and recovery of hemicellulose-derived sugar produced from biomass hydrolysis by acidic ionic liquid. *ACS Sus. Chem. Eng.*, 2018. (submitted) .....CHAPTER VII

During my studies I have also contributed to the following scientific productions which are not included in this thesis:

A. M. da Costa Lopes and R. Bogel-Łukasik, Acidic ionic liquids as sustainable approach of cellulose and lignocellulosic biomass conversion without additional catalysts, *ChemSusChem*, **2015**, 8, 947-965.

A. M. da Costa Lopes, L. B. Roseiro and R. Bogel-Łukasik, Relevance of Ionic Liquids and Biomass Feedstocks for Biomolecule Extraction, in Ionic Liquids in the Biorefinery Concept: Challenges and Perspectives, ed. R. Bogel-Łukasik, *RSC*, Cambridge, **2015**, chapter 5, pp. 121-167

S. Peleteiro, A. M. da Costa Lopes, G. Garrote, J. C. Parajó, R. Bogel-Łukasik, Simple and Efficient Furfural Production from Xylose in Media Containing 1-Butyl-3-Methylimidazolium Hydrogen Sulfate, *Ind. Eng. Chem. Res.*, **2015**, 54 (33), 8368-8373.

S. Peleteiro, A. M. da Costa Lopes, G. Garrote, R. Bogel-Łukasik, J. C. Parajó, Manufacture of furfural in biphasic media made up of an ionic liquid and a co-solvent, *Ind. Crop. Prod.*, **2015**, 77, 163-166.

M. H. L. Silveira, A. R. C. Morais, A. M. da Costa Lopes, D. N. Olekszyszen, R. Bogel-Łukasik, J. Andreaus and L. Pereira Ramos, Current Pretreatment Technologies for the Development of Cellulosic Ethanol and Biorefineries, *ChemSusChem*, **2015**, 8, 3366-3390.

M. Arshadi, et al., Pre-treatment and extraction techniques for recovery of added value compounds from wastes throughout the agri-food chain, Green Chem., **2016**, 18, 6160-6204.

A. M. da Costa Lopes, A. R. C. Morais and R. M. Lukasik, Sustainable catalytic strategies for C_5-sugars and biomass hemicellulose conversion towards furfural production., in *Production of Platform Chemicals from Renewable Resources*, eds. Z. Fang, R. L. J. Smith and X. Qi, Springer, **2017**, ch. 2, pp. 45-80.

CHAPTER I

Introduction

1.1. Circular economy and bioeconomy

European Union (EU) has been struggling to boost a response to key economic and environmental challenges that society is facing today. The current fossil-based economy has been pointed out as non-renewable, non-sustainable, environment hazardous and lacks to manage waste and to preserve natural resources for world society.[1] On the other hand, environmental concerns have been growing with problems related to climate change and efforts to achieve a sustainable low carbon future as aimed and agreed at the 21st Conference of the Parties (*Paris Climate Agreement*)[2] are expected. Therefore, EU has been propelling alternatives to fulfil these gaps without compromising economic growth, social development and the environment protection. In the front line of such response, two distinct but well paired concepts have been tentatively proposed, namely circular economy and bioeconomy.[3-5] Circular economy represents an ideology of preserving the value of products, materials and resources in the economy for as long as possible, minimising the generation of waste.[4] On the other hand, the utilisation of biomass resources as feedstocks, for the production of food, materials and energy is the basis of a bioeconomy.[3, 5] From the communion of both concepts (Figure 1) is expected the utilisation, production, consumption, storage, recycling and reuse of biological and renewable resources towards:

i) sustainable global population growth;
ii) rational management of available resources;
iii) sustainable value chain creation in industry;
iv) zero or low impact in the current and future environmental issues.[3-5]

To turn this concept into practise, European Commission have been launching several R&D programmes at different levels of implementation.[6] Particularly, a development of advanced technologies for the efficient processing and transformation of null or low price biomass feedstocks into desired products, substituting those derived from petroleum refinery, are key challenges to overcome. In this context, a successful valorisation of biomass raw materials has been pursued at scientific level and it is expected to be upgraded into an industrial activity of industrial infrastructures called biorefineries. A forecasted implementation of biorefineries would create new jobs and generate economic profit from the high level of commodities produced from biomass refining. Furthermore, taking into the account the current environmental issues, the implementation of biorefineries are expected to reduce gas emissions, to use less hazardous chemicals and to avoid residues disposal, bringing environmental benefits in detriment of current petroleum refineries.[1, 6, 7]

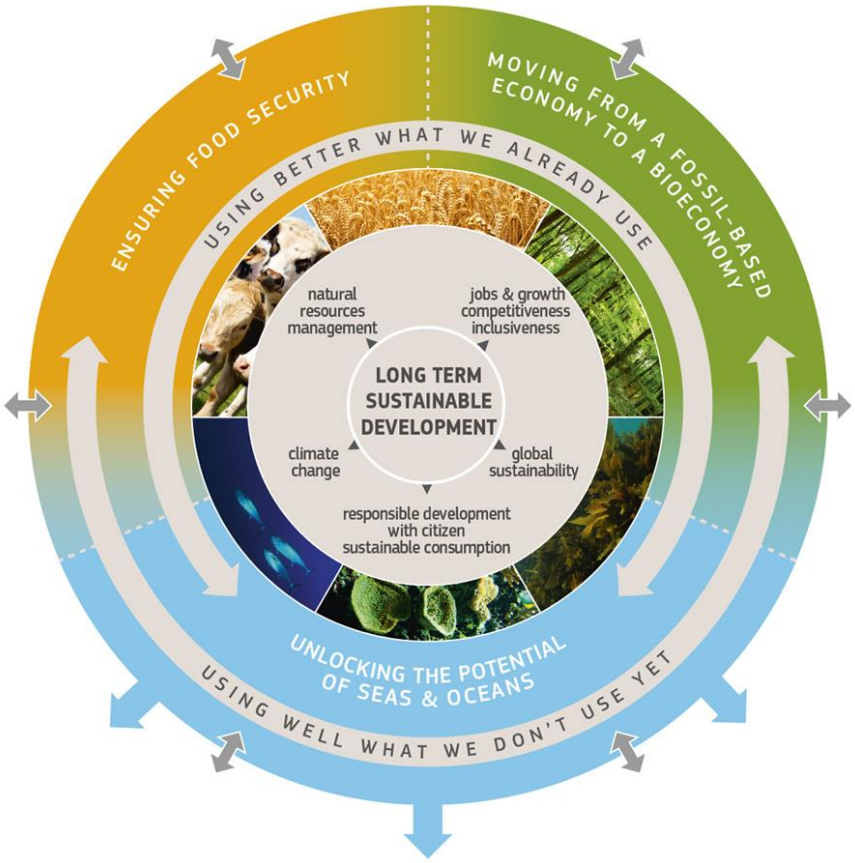

Figure 1.1. Illustrative example of both circular economy and bioeconomy concepts.[8]

1.2. Biorefinery and green chemistry concepts

The biorefinery concept relies on the valorisation of all biomass fractions in the production of energy, materials and value-added products.[9, 10] This activity embraces, in general, three different platforms. The biochemical platform is based on the use of biological technologies to convert biomass-derived sugars into biofuels and value-added products (*e.g.* organic acids, polyols and bioplastics). On the other hand, the thermochemical platform transforms biomass into energy, gaseous fuels (*e.g.* hydrogen and methane) and value-added chemicals (*e.g.* aromatic compounds).[11] The conversion of biomass into respective products can be also independently performed through chemical or thermochemical platforms, although combination of them is possible and might offer advantages for biomass valorisation, meeting the goals of the biorefinery concept.[11]

The operations established in a biorefinery highly depends on the type of biomass feedstock to be processed and the products generated from it, as depicted in Figure 2. There are numerous examples of biomass materials, such as forestry, agriculture, aquaculture, industrial residues, municipal organic wastes and aquatic biomass (algae and seaweeds).[1] From each of these feedstocks, different paired technologies might be developed and applied to efficiently convert them into desired products.

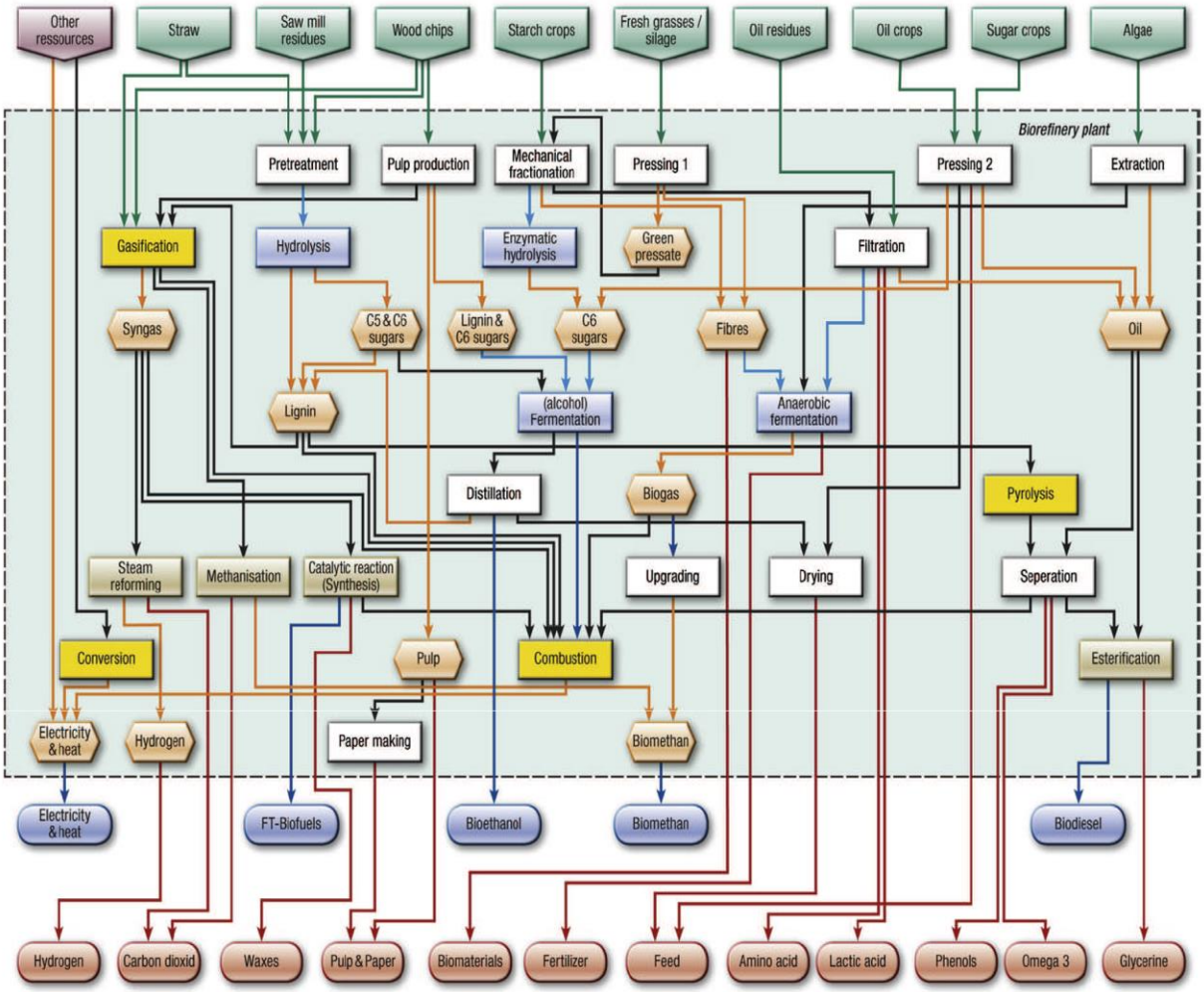

Figure 1.2. Scheme representing multi-step processing of several biomass raw materials in a forecasted biorefinery. Reprinted from [1] with permission of Elsevier.

As outlined before, a biorefinery is expected to process biomass feedstocks into desired products within sustainable paths. Therefore, the application of green chemistry in biorefinery processes can be an ideal solution. Green chemistry is a concept that arose from the more sustainable use of resources and minimisation of the harmful consequence of the chemical process. In this context, twelve principles were postulated and became a widely accepted set of criteria for the evaluation of chemical products and processes regarding the environmental and health safety issues. The twelve principles of green chemistry proposed by Anastas and Warner[12] are as following:

(i) Prevention of waste to avoid treating or cleaning up waste after it has been created;

(ii) Atom economy through new synthetic methods designed to maximise the incorporation of all materials used in the process into the final product;

(iii) Less hazardous chemical syntheses designed to use and generate substances that possess little or no toxicity to human health and the environment;

(iv) Designing safer chemicals able to carry out the desired function while minimising their toxicity;

(v) Avoiding wherever possible or minimising the use of auxiliary substances (*e.g.* solvents, separation agents, and others), and introducing safer solvents and auxiliaries that are innocuous when they have to be used;

(vi) Design for energy efficiency of chemical processes to minimise their environmental and economic impacts and if possible, to introduce synthetic methods to be conducted at ambient temperature and pressure;

(vii) Use of renewable feedstocks instead of depleting ones whenever technically and economically practicable;

(viii) Reduce derivatives through minimising or avoiding the use of blocking groups, protection/deprotection, and temporary modification of physical/chemical processes that require additional reagents and can generate waste;

(ix) Catalytic reagents as selective as possible;

(x) Design for degradation of chemical products at the end of their function into innocuous degradation products not persisting in the environment;

(xi) The development of analytical methodologies needs to allow real-time analysis for pollution prevention, in-process monitoring and control prior to the formation of hazardous substances;

(xii) Inherently safer chemistry for accident prevention by choosing substances and the form of a substance used in a chemical process that minimise the potential for chemical accidents, including releases, explosions, and fires.

Therefore, in parallel to the goal of reaching economic feasibility of biorefinery processes, it should also aim good practices in biomass processing to not compromise the environment and health safety. The application of green chemistry in biomass valorisation is thus a challenge that must be tackled according to aforementioned principles.

1.3. Lignocellulosic biomass as renewable resource for fuels, energy and chemicals

Lignocellulosic biomass is abundant and renewable carbon source with a great potential for valorisation. Among lignocellulosic biomass, the most represented are forest residues (*e.g.* branches, sawdust, thinning rests), grasses (*e.g.* switchgrass, miscanthus), agriculture (*e.g.* wheat straw, corn stover, rice hulls, sugarcane bagasse) and industrial residues and others.[13, 14] The annual production of these materials is *ca.* billion tonnes,[6] and still limited valorisation technologies make biomass a low price feedstock, which is very interesting raw-material for biorefinery.

Plant cell walls structuring lignocellulosic biomass are constituted by three major macromolecular components: cellulose (40-50 wt.%), hemicellulose (20-30 wt.%) and lignin (20-30 wt.%).[15] Cellulose is a homopolysaccharide that presents a semi-crystalline fibrous structure, whereas hemicellulose is a heteropolysaccharide characterised by an amorphous structural organisation.[16] In contrast, lignin is constituted by phenylpropanoid units forming an amorphous aromatic polymer.[17] These three main fractions constitute strongly integrated and complex matrix as presented in Figure 3.

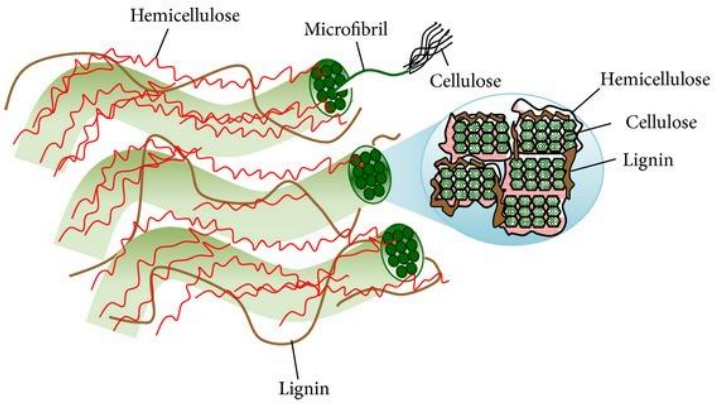

Figure 3. Representation of a plant wall structure showing the organisation of cellulose micro and macro-fibrils embedded in a matrix of hemicellulose and lignin. Reprinted from [15] with permission of Creative Commons Attribution License 3.0 (Copyright © 2014 H. V. Lee *et al.*).

Cellulose is structured into micro- and macrofibrils, while hemicellulose polymers are positioned between cellulose fibrils forming an open network. Lignin fills up the spaces left by cellulose and hemicellulose and provides a protective barrier for plant cell permeability and resistance against microbial attacks. Lignin can be found in both interfibrous area as well as on the cell wall surface.[15]

Lignocellulosic biomass also presents in its constitution minor fractions, such as starch, pectins, proteins, extractives (*e.g.* phenolic compounds, free saccharides), ash (*e.g.* inorganic minerals) and others. These compounds have lower impact in giving rigidity to lignocellulosic matrix, but they influence the efficiency of biomass processing technologies related to fractionation of macromolecular components, formation of inhibitor compounds, process issues, etc.[18]

1.3.1. Cellulose

Cellulose is a linear homopolysaccharide solely composed by cellobiose units linked each other by β-(1→4) glycosidic bond. Cellobiose is formed by two glucose molecules, where the hemiacetal form of a glucose unit is bonded to a C-4 carbon of another glucose unit[19] as shown in Figure 4.

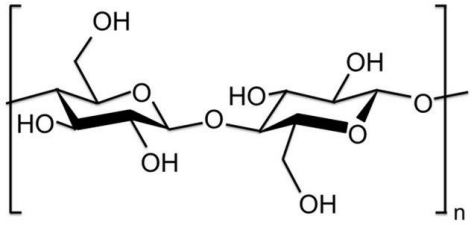

Figure 1.4. Molecular structure of a cellulose polymer chain. Reprinted from [20] with permission of Creative Commons Attribution License 4.0. (Copyright © 2013 Serge Rebouillat and Fernand Pla.).

The number of units in a single cellulose chain dictates the degree of polymerisation (DP), which highly depends on the source of cellulose material. For instance, agriculture residues, such as wheat straw and sugarcane bagasse, are composed of cellulose chains with lower DP (≈ 1000) than that constituting softwoods and hardwoods (≈ 5000).[21] In general, higher DP makes the cellulosic material more rigid. Furthermore, the fact that each glucose unit contains three hydroxyl groups evenly distributed on both sides allows the formation of intra- and intermolecular hydrogen bonds.[22] Through this arrangement, several cellulose polymer chains interact in parallel providing a network of strong hydrogen bonds. This interaction leads to the formation of micro and macro-fibrils with highly ordered structure and spatial conformation contributing to cellulose crystallinity. However, less ordered regions (amorphous cellulose) are present at some extent in lignocellulosic materials.[23] In this context, the strength of a cellulose material relies on the DP value and on the ratio between crystalline and amorphous regions present in cellulose matrix.

The dissolution and processing of cellulose in classical molecular solvents is challenging due to its fibril structure and aforementioned hydrogen bond network. For instance, cellulose is a relatively hygroscopic material, but its solubility in water is null. Actually, the hydroxyl groups of glucose units by interacting each other make a hydrophobic environment impeding solvation by water molecules (even at high temperatures).[15] The disruption of such hydrogen bond network is thus the key for an efficient dissolution of cellulose. To achieve an extended dissolution of cellulose, a combination of high temperature and solvents capable to swell and dissolve cellulose fibres is needed. The swelling process allows disruption of crystalline structure and afterwards cellulose fibres are susceptible for solvation by solvent molecules.[24, 25] Bi-component solvent systems such as diacetylamide/LiCl and NaOH/urea have been used in the processing of cellulose.[26, 27] Lately, ionic liquids demonstrated ability to dissolve high amount of cellulose by efficiently disrupting its crystalline organisation and transforming it into an amorphous structure.[28]

In a biorefinery context, cellulose is expected to have an important role as starting material for the production of biofuels, chemicals and materials. Depolymerisation of cellulose through enzymatic hydrolysis is a key process of biorefineries to produce glucose as pivot compound. Afterwards, glucose can be either chemically or biologically transformed. For instance, dehydration and hydrogenation

reactions of glucose leads to the production of 5-hydroxymethylfurfural and sorbitol, respectively.[29, 30] On the other hand, the use of glucose as substrate for fermentative processes allows the production of biofuels (*e.g.* bioethanol and biobutanol)[31, 32] or value-added products (*e.g.* organic acids and polyhydroxyalkanoates).[33, 34] Furthermore, cellulose could be chemically modified into derivative materials through a series of reaction of the free hydroxyl groups.[35] In that way, cellulose can be used as a starting material for a variety of products, including cellulose acetate, carboxymethylcellulose and others.[36-38]

1.3.2. Hemicellulose

Hemicellulose is an amorphous heteropolysaccharide, which composition varies depending on the lignocellulosic biomass specie. This macromolecular component can be represented by a complex family of polysaccharides such as xyloglucans, xylans, arabinoxylans, arabinogalactans, mannans, glucomannans, and galactoglucomannans, among others.[39] Contrary to cellulose, hemicellulose polysaccharides are characterised by lower DP (mostly 80-200) and are formed by a wide variety of carbohydrates including pentoses units (*e.g.* xylose and arabinose), hexoses units (*e.g.* glucose, mannose and galactose) and associated uronic acids (*e.g.* 4-*O*-methyl-glucuronic and galacturonic acids).[40] A high complexity of hemicellulose is mostly devoted to the type of carbohydrate units constituting the polysaccharide chain and the ratio between them. Furthermore, hemicellulose structure can be branched with a variable degree, unbranched or helical.[41] For instance, the most typical hemicellulose is rod-shaped and branched with side chains folded back to the main chain linked by hydrogen bonds. This rod-like structure facilitates their interaction with cellulose fibrils, resulting in a tight association that gives great stability to the lignocellulosic complex.[41]

Xylans are one of the main hemicellulose polymers existing in agriculture residues, such as wheat straw, rice straw and sugarcane bagasse. This type of polysaccharide is formed by a backbone chain of xylose units linked each other by β-(1→4) glycosidic bonds, similarly to those established by glucose units in cellulose.[42] The branching in xylans is very common and is produced by chemical linkages between xylose constituting xylan backbone with acetyl groups or other carbohydrates, such as arabinose and glucuronic acids. This type of structure was demonstrated in a recent structural analysis of hemicellulose from sugarcane bagasse and sugarcane straw.[42] Figure 5 depicts empirical structures of xylans extracted from those agriculture residues.

The highly branched character gives to hemicellulose an amorphous structure.[43] Even though, hemicellulose is insoluble in water at low temperatures. By increasing temperature above 100 °C, hydrolysis of hemicellulose can be promoted in aqueous systems allowing to achieve solubility superior than cellulose. The lack of crystalline regions in hemicellulose structure constitutes weaker hydrogen bond network, thus disruption and subsequent dissolution of hemicellulose is facilitated.[44]

A diverse macromolecular composition of hemicellulose is a challenge but also opens a large window of opportunities in the exploitation of lignocellulosic biomass. For instance, furfural is one of the main pivot chemicals obtained through dehydration of hemicellulose-derived pentoses.[45] Xylitol and arabitol are other examples of products possible to be obtained from hemicellulose hydrolysates.[46] On the other hand, low extent of hemicellulose hydrolysis delivers another products such as oligosaccharides, which have potential in applications in nutraceutical and cosmetic products.[47] Furthermore, a growing interest has emerged in using native hemicellulose for various technological applications, *i.e.* in the synthesis of cationic polymers,[48] hydrogels,[49] or thermoplastic xylan derivatives.[50] However, production of native hemicellulose as pure fraction is a challenge for current biomass processing technologies.

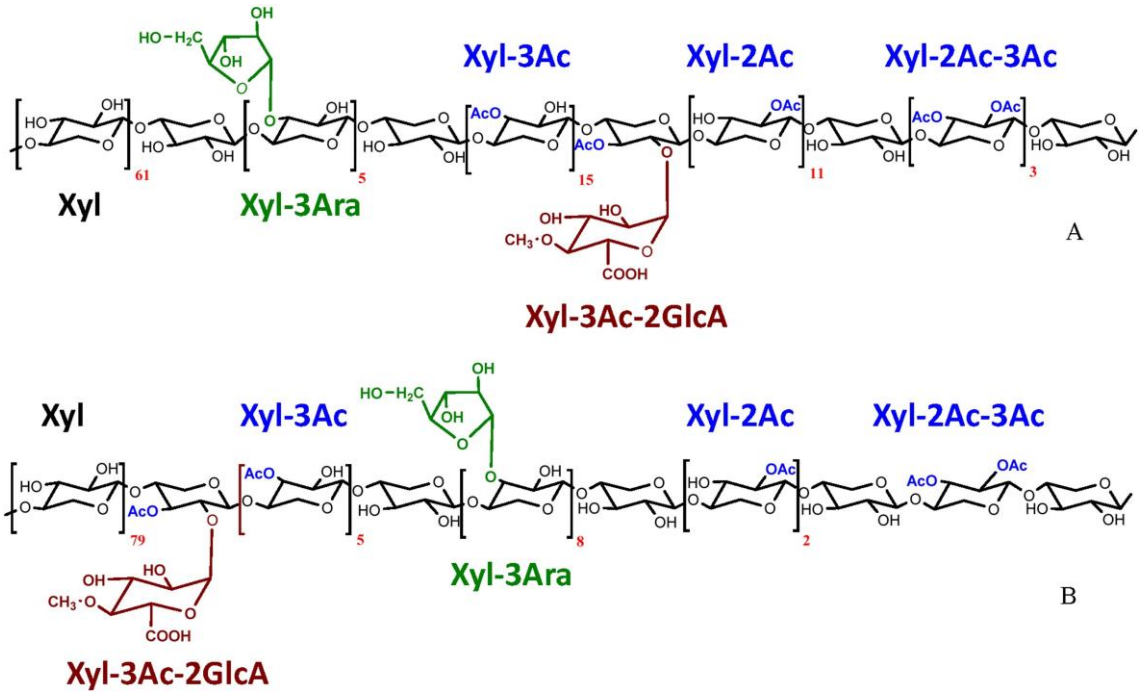

Figure 1.5. Empirical structure of xylans extracted from sugarcane bagasse (A) and sugarcane straw (B). The respective units containing xylose (Xyl), arabinose (Ara); acetyl group (Ac) and glucuronic acid (GlcA) are depicted. The repetition number of each unit in structures of extracted xylans are indicated in red. Reprinted from [42] with permission of Elsevier.

1.3.3. Lignin

Lignin is an amorphous branched polymer with phenylpropanoid building block units.[17] This aromatic macromolecule is formed by three monolignol precursors with different degrees of methoxylation (-OCH_3 groups), namely coniferyl alcohol, sinapyl alcohol, and *p*-coumaryl alcohol as shown in Figure 6. Lignin macromolecule is formed by a series of reaction between each of these lignols and once

incorporated they are identified as phenylpronaoid guaiacyl, syringyl and *p*-hydroxyphenyl units (Figure 6).[51]

Lignin polymerisation produces a macromolecule with a broad range of size and with irregular order of units. Therefore, identification and quantification of syringyl, guaiacyl and *p*-hydroxyphenyl units in lignin structure is of extreme importance to differentiate lignin composition between lignocellulosic materials.[52] For instance, softwood lignin is mostly composed by guaiacyl units, while hardwood lignin is constituted by both guaiacyl and syringyl units. For grasses and herbaceous crops, lignin composition is based on those three units.[53] Furthermore, softwood lignin reveals to be more condensed than hardwood lignin, as a consequence of the lower quantity of methoxyl groups in softwood lignin, which hampers the chemical conversion into desired aromatic products.[41]

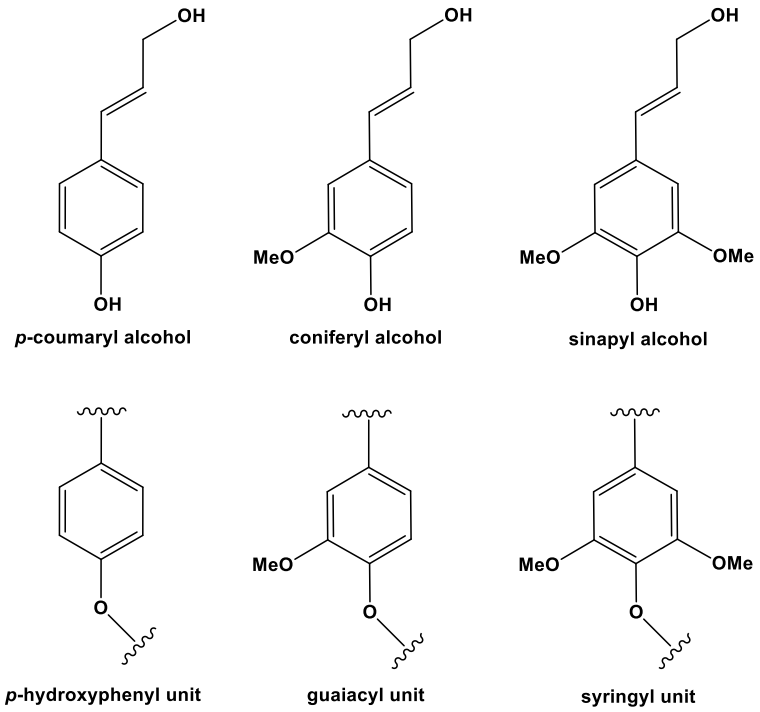

Figure 1.6. Chemical structure of three monolignol precursors and the respective phenylpropanoid units composing lignin macromolecule. Adapted from [51] with permission of The Royal Society of Chemistry.

A high complexity of lignin macromolecule arises from several combinations between free radicals of three monolignol units that form different chemical bonds and functional groups in lignin structure.[54] Two different linkages between monolignol units can be formed, namely C-C and C-O-C (ether) bonds. However, depending on monolignol carbons participating in linkages different nomenclature is provided. For example, β-β, β-O-4, α-O-4, 4-O-5, β-5, β-1 or 5-5 are identified as the main chemical linkages existing in lignin.[55] On the other hand, the variety of functional groups present in lignin has a great impact on its reactivity. The major functional group in lignin corresponds to methoxyl groups

attached to guaiacyl and syringyl units, but phenolic hydroxyl groups and a few terminal carbonyl groups also appear. Only a small part of the phenolic hydroxyl groups are free, once most of them mediates chemical linkages between neighbouring phenylpropanoid units.[56]

The nature of the lignification process results in the formation of a three-dimensional, highly-branched, interlocking matrix as depicted in Figure 7.

As a by-product of pulp and paper industry, lignin has been applied as a low-value heating fuel, binder, dispersant, emulsifier and sequestrant.[57] In the frame of a biorefinery approach, lignin as a source high-value aromatic chemicals has higher potential than those applications.[55] For instance, production of polyurethane and polyesters derived from lignin as a valuable renewable bioplastic resource has been demonstrated.[58] In other case, alkylated lignin derivatives exhibited tensile strength properties similar to polystyrene and were employed to prepare promising thermoplastic blends with aliphatic polyesters.[59, 60] Furthermore, there is a growing interest in developing new lignin-based products driven by the fact that lignin has the potential to substitute aromatic compounds currently produced from fossil resources.[61]

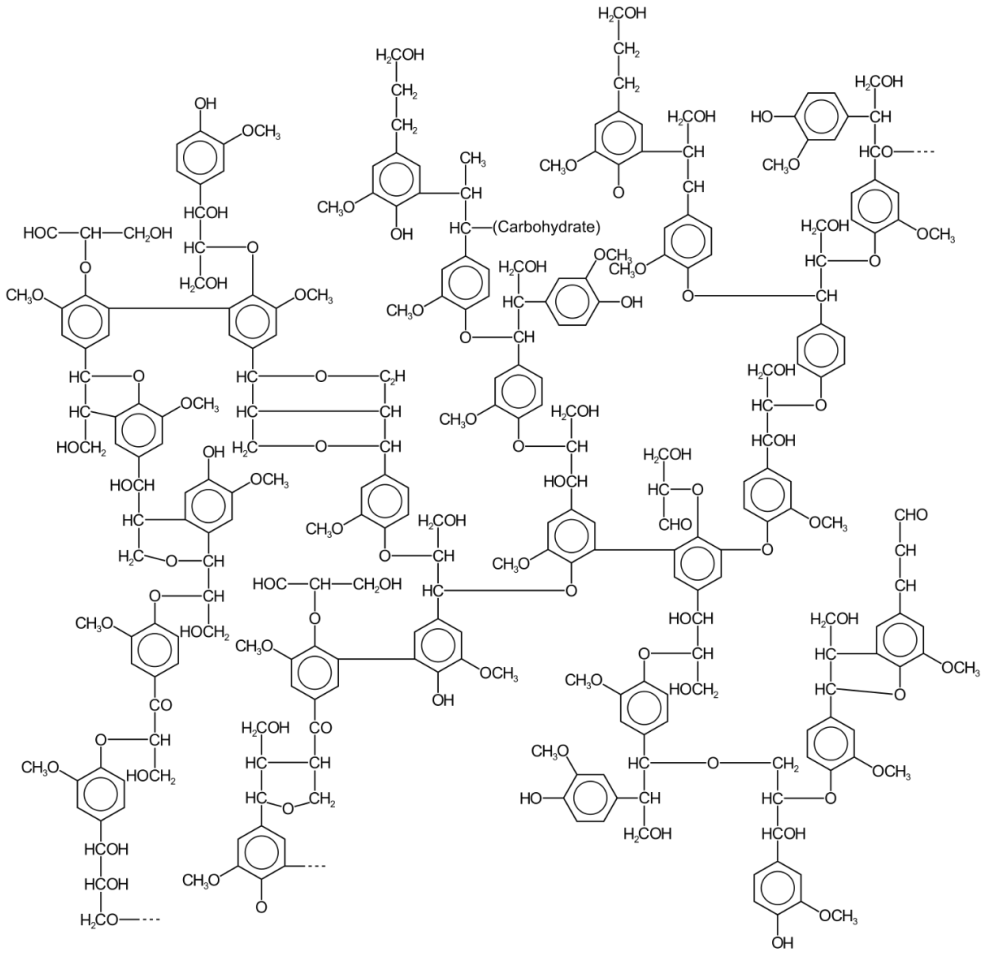

Figure 1.7. Representation of a possible lignin structure. Reprinted from [62].

1.4. Biomass pre-treatment technologies

The physicochemical properties of cellulose, hemicellulose and lignin as well as the strong molecular interactions between them makes lignocellulosic biomass as a very recalcitrant material.[63] Nowadays, research is focused on efficient separation of each biomass component. In this context, several deconstruction processes, also designated as pre-treatments, have been developed to overcome the complex and rigid structure of lignocellulosic biomass towards an efficient fractionation of main constituents.[63]

According to definition, pre-treatment aims at the removal of lignin and hemicellulose from the lignocellulosic biomass in order to expose cellulose fibres (Figure 8). Afterwards, acid or enzymatic hydrolysis are employed to cellulose fibres to produce glucose, which later can be fermented into final product(s).[63] Pre-treatment should alter the size, structure and chemical composition of biomass in a manner that hydrolysis of cellulose can be efficient without the extensive use of chemicals. Therefore, not only the impediments of hemicellulose and lignin present in biomass materials must be overcome, but also other factors, which enhance cellulose hydrolysis, such as the reduction of cellulose crystallinity, the increase of porosity and surface area of the material, must be accomplished.

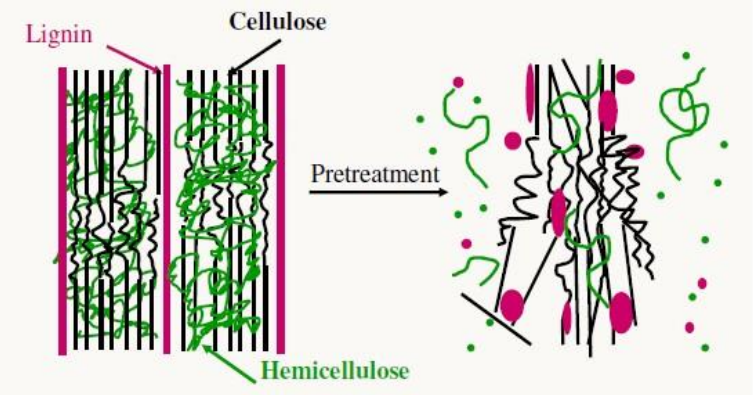

Figure 1.8. Representation of biomass pre-treatment. Hemicelluloses and lignin are removed from lignocellulosic complex exposing cellulose fibres. Adapted from [64] with permission of Creative Commons Attribution License 3.0 (Copyright © 2013 Z. Liu and B. Fei).

The ability of each of these pre-treatments in altering and fractionating biomass is distinct providing multiple options for biomass processing. The classification of current pre-treatments and a brief description of the most common and innovative technologies are given in the following sections.

1.4.1. Classification

Pre-treatments can be divided into physical, chemical, physicochemical and biological. The most fundamental are physical pre-treatments, such as chipping, milling and gridding, which are used to decrease the biomass particle size and often to reduce DP, making material easier to handle for subsequent processing steps.[65] Chemical pre-treatments associate the use of chemicals that disrupt interactions of lignocellulosic components. Among chemical pre-treatments exist those using acids (H_2SO_4, HCl, HNO_3, organic acids), alkali (NaOH, $Ca(OH)_2$, NaOH-urea, Na_2CO_3), oxidizing agents (H_2O_2 and ozone), organic solvents (ethanol, acetone, phenols), and more recent ionic liquids (*e.g.* 1-ethyl-3-methylimidazolium acetate).[66, 67] High-pressure processes, such as steam explosion, liquid hot water and supercritical carbon dioxide (CO_2) are main physicochemical pre-treatment technologies.[68-71] The least explored pre-treatments are the biological which action is governed by microorganisms, *e.g.* white and brown rot fungi.[72, 73] The biodegradation of lignocellulosic biomass performed by these microorganisms allows having a substrate more accessible to hydrolysis. Although this type of pre-treatment is environmentally friendly, the activity of the hydrolysis process is very slow making it time consuming and less efficient than other pre-treatments.[74]

1.4.2. Acid hydrolysis

The treatment of lignocellulosic materials with acid can efficiently improve the subsequent enzymatic hydrolysis. The most commonly used acid is sulphuric acid, while others such as hydrochloric and nitric acid were also reported.[75] These pre-treatments require dilute or concentrated acids and temperature in the range between 120 °C and 210 °C.[13] In the case of using dilute acids, hemicellulose undergoes depolymerisation and produces monomers and/or oligomers in a liquid phase, leaving cellulose as an accessible solid for the enzymatic treatment. The removal of hemicellulose increases porosity and enhances cellulose enzymatic digestibility.[76] Nevertheless, the resulting solid containing high lignin content might suffer a delignification process before enzymatic hydrolysis to increase the accessibility of cellulose to enzymes. In the case of concentrated acid processes, both cellulose and hemicellulose are hydrolysed to monomeric sugars. Therefore, a subsequent enzymatic hydrolysis step is not always required, being the key advantage of this type of pre-treatment. Due to a presence of concentrated acid, temperature of the process must be as low as possible and compensated by longer pre-treatment time. Nevertheless, it is difficult to attain 100 wt.% sugar yield due to the risk of extensive degradation of sugars occurring along the process.

1.4.3. Alkaline treatments

Sodium hydroxide (NaOH) and ammonia (NH_3) are mostly used for alkaline pre-treatments leading to an extensive removal of lignin from lignocellulose by breaking down the main interactions with polysaccharides. The alkaline hydrolysis mechanism is explained as a saponification of intermolecular

ester bonds linking lignin and hemicellulose fractions and also as a disruption of lignin structure.[66, 77] The remaining polysaccharides are much more accessible to hydrolysis, not only because of major lignin content is removed, but also, due to the removal of acetyl groups and uronic acids from hemicellulose.[78] However, this treatment appears to partially dissolve hemicellulose due to the degradation of glycosidic bonds by alkali agents.[79] Aqueous NaOH and NH_3 treatments are generally used at mild conditions, which prevent lignin condensation phenomena, resulting in improved lignin hydrolysis. Nevertheless, these treatments are especially effective for biomass with low lignin content such as softwood and grasses.[80]

1.4.4. Organosolv treatments

Organosolv processes use an organic solvent or mixtures of organic solvents with water for removal of lignin and partially hemicellulose. The most commonly used organic solvents are alcohols, esters, ketones, glycols, organic acids, phenols and ethers.[66, 81] The temperatures applied in these pre-treatments depend on the organic solvents chosen however normally are between 150-200 °C. The catalysts may be added either to reduce the operating temperature or to enhance the delignification process.[65] The main benefits of organosolv pre-treatment are the production of high-quality lignin and the potential of lowering the enzyme costs by separation of lignin before the enzymatic hydrolysis of cellulose. However, the use of organic solvents for lignocellulosic pre-treatment has some disadvantages because solvent itself can be an inhibitor for the subsequent enzymatic hydrolysis and fermentation steps. Therefore, removal and recovery of the solvent prior to these processes is required to enhance yields of desired products and to reduce operational costs and environmental impact.[81]

1.4.5. Ionic liquids

The application of ionic liquids in biomass processing has been characterised as green approach. Ionic liquids (ILs) are organic salts normally constituted by an asymmetric organic cation and a counterpart inorganic or organic anion. ILs possess a melting point below 100 °C and generally are in the liquid state at room temperature. The general physicochemical properties of ILs are: negligible vapour pressure, high thermal stability, large electrochemical window, high solvent power, non-flammability, high recyclability, among others.[82-89] These properties open the possibility for implementing ILs in industry processes[90] with potential to decrease the environmental footprint of developed technologies. ILs are also called "designed solvents" because of a wide range of possible anions and cations to be used to form IL with tailored properties according to the process needs.[91-94] Therefore, taking into account the promising solvent capabilities of ILs, they were examined in biomass pre-treatment.

A decade ago ILs were found to dissolve cellulose, where up to 25 wt.% cellulose was successfully solvated in 1-butyl-3-methylimidazolium chloride ([bmim][Cl]) at mild conditions (100-140 °C).[28] The same imidazolium-based IL, with other anions, *e.g.* [Br], [SCN], [PF_6], etc. were also used, although

lower or no solubility for cellulose was reported.[28] These results demonstrated the capacity of [Cl] to interact with cellulose allowing its dissolution. NMR studies demonstrated that the extensive hydrogen-bond network of cellulose structure is effectively disrupted during the dissolution in [bmim][Cl]. The formation of hydrogen bonds between chloride ions of the IL and hydroxyl protons of polysaccharides in 1:1 ratio is the major reason for the dissolution effect, despite the interaction of imidazolium cation.[95] During the dissolution in ILs the swelling of cellulose was also detected and after cellulose regeneration a decrease in crystallinity was observed.[96, 97] Apart from cellulose, lignin was also dissolved in some ILs demonstrating the wide range of molecules and compounds that ILs are able to dissolve.[98] Following the successful dissolution of cellulose and lignin study, the lignocellulosic biomass solubility in ILs was also extensively explored.[97, 99-102] All three macromolecular components of lignocellulose demonstrated to be soluble in several ILs, where 1-ethyl-3-methylimidazolium acetate, ([emim][OAc]), 1-butyl-3-methylimidazolium acetate ([bmim][OAc]), 1-ethyl-3-methylimidazolium chloride ([emim][Cl]) and [bmim][Cl] were observed to be the most efficient.[102, 103] Furthermore, other ILs allowed to selectively dissolve one of the macromolecules of lignocellulose, such as cellulose using phosphinate-based ILs,[104] or extracting lignin by 1-ethyl-3-methylimidazolium alkylbenzenesulfonate ([emim][ABS]),[105] 1,3-dimethylimidazolium methylsulphate ([mmim][$MeSO_4$]),[106] or amino acid-based ILs.[107, 108] Therefore, ILs are useful as pre-treatment and/or extraction agents being capable to modify the physicochemical properties of biomass with simultaneous extraction of macromolecules.[109]

On the other hand, recent advances showed that some ILs are capable to act as both solvent and catalyst in biomass processing.[110-112] ILs with acidic character demonstrated ability to selectively hydrolyse hemicellulose,[110] both cellulose and hemicellulose,[113, 114] or lignin.[115] The use of ILs for biomass processing is now a topical area of biomass processing as it includes processes focused on fractionation, hydrolysis, conversion and extraction processes.[100, 104, 116-118]Although ILs have been associated to be expensive solvents, the development of bulky low price ILs capable to efficiently pre-treat biomass were recently reported.[51, 111] Nevertheless, the recovery of IL is highly required to avoid technical hindrances in downstream processing and to not compromise the economic efficiency of the pre-treatment process.

1.4.6. High-pressure treatments

These type of pre-treatments have been raising acceptance to scale-up for industry and among the most common are hydrothermal processes, such as steam explosion and liquid hot water.[119, 120] In these processes no catalysts are added to the system making them cheaper in comparison to other pre-treatments. During steam explosion, biomass is treated by high-pressure saturated steam and temperature (160-240 °C).[66] Thereafter, the pressure is rapidly reduced and by this, material undergoes an explosive decompression aiming at drastic reduction of cellulose crystallinity. Moreover, a high temperature applied allows hemicellulose hydrolysis, although further degradation of hydrolysed sugars occurs after the explosive decompression. Furthermore, steam explosion causes the destruction of a

portion of the xylan fraction and leads to incomplete disruption of the lignin-carbohydrate matrix in a way that lignin is removed in a limited extent.[13] The selectivity of steam explosion is thus very low for any desired macromolecule of lignocellulose. Therefore, two stage processing can be performed in order to increase selectivity for either pentose or hexose yields.[121] As example, the first step involves temperatures of 180 °C in order to dissolve and to remove the hemicelluloses fraction. The second stage uses pressurisation at temperatures up to 210 °C (not exceeding 240 °C), in which the cellulose fraction is subjected to break down of its carbohydrate linkage.[121] This two-step process permits better accessibility of cellulose structure caused by the reduction of the hemicelluloses fraction content, increasing enzymatic hydrolysis yield and subsequent fermentative production of *e.g.* bioethanol. In this context, a decrease of operational costs can be achieved because less enzyme dosage is required.[121]

Liquid hot water, also often called autohydrolysis, is similar to steam explosion procedure but requires high temperature and auto-generated pressure to maintain water in the liquid state, on the contrary of gas state used in steam explosion. The disintegration of the lignocellulosic matrix is performed by liquid water, which is capable to penetrate through biomass cells. The acidity of hot water leads to subsequent auto-catalysed hydrolysis of hemicellulose to sugar oligomers and monomers, but also to further degradation into diverse products such as furans or even organic acids. Cellulose and lignin are almost unaffected and make a part of the resulting solid fraction.

Carbon dioxide either at gas or at supercritical conditions has been employed in the biomass processing.[71, 122] Carbon dioxide is an interesting solvent as it can be under supercritical conditions just at 31.1 °C and 73.8 bar. CO_2 is a sustainable solvent, readily available, non-toxic, non-flammable, inexpensive and leaves no residue in the reaction system. The great advantage of using CO_2 is the *in-situ* formation of carbonic acid in the presence of water (added in purpose or as biomass humidity), which acts as catalyst improving the hydrolysis rate of hemicellulose.[71, 122] Apart from the chemical action provided by CO_2 treatments, also physical behaviours are observed like biomass swelling. This physical effect is promoted by the high diffusivity of CO_2, because CO_2 is able to penetrate into biomass increasing the accessible surface area of the pre-treated biomass material.[123] During depressurisation, the equilibrium is shifted towards CO_2 and therefore, catalyst can be easily removed. In comparison to autohydrolysis process, the pre-treatment with $scCO_2$ is less aggressive. Actually, lower temperatures and pressures can be used for $scCO_2$ to achieve the same goal as hydrothermal treatment.[124] Furthermore, an enhanced selectivity for the production of value-added oligosaccharides from hemicellulose can be equally attained with CO_2 treatment.[122]

1.5. Benchmarking of conventional pre-treatment processes: technical and environmental challenges in the perspective of the biorefinery concept

Diverse types of pre-treatments provide a great portfolio of potential application of pre-treated biomasses. Therefore, depending on the specific requirements and goals of the lignocellulosic

processing to attain a final product, a determined pre-treatment can be chosen. A preceding evaluation of the advantages and disadvantages of each type of pre-treatment should be taken into account considering an individual requirement of the process. Table 1 intends to demonstrate the comparisons between the aforementioned pre-treatments. The evaluation encloses:

(i) the biomass fractionation ability into cellulose, hemicellulose and lignin towards the maximal exploitation of biomass within the biorefinery concept

(ii) the capacity of hemicellulose and lignin removal from biomass to obtained cellulose readily available for enzymatic hydrolysis;

(iii) the potential for enzymatic digestibility of cellulose fraction;

(iv) the capacity for the simultaneous production of monosaccharides (glucose and pentoses), furans (5-hydroxymethylfurfural and furfural) and/or organic acids that can be considered as pivot chemicals in biorefineries;

(v) the recovery of catalyst/solvent to evaluate the economic and environmental feasibility of the process.

If production of biofuels, such as ethanol, is a priority requirement of lignocellulosic biomass processing, lignin and hemicellulose should be removed from biomass to expose cellulose to enzymatic hydrolysis. In this context, high-pressure processes seem to be one of the most efficient because it improves enzymatic performances by causing the severe changes in cellulose morphology. A decrease of DP and increased surface area of cellulose are especially promoted with this type of pre-treatments. On the other hand, the fact that ILs are able to change crystalline structure of cellulose to amorphous morphology, it also allows enhanced depolymerisation of cellulose through enzymatic hydrolysis. More advantageous is the case of (concentrated) acid hydrolysis, which does not require enzymatic hydrolysis to produce fermentable sugars (glucose and pentoses). However, due to acidic environment used in this pre-treatment, the need of acid neutralisation and conditioning of hydrolysate is required for further processing, *e.g.* fermentation. Similar proceeding must be adopted for alkali pre-treatments.

One of the major restrictions of pre-treatments is the formation of compounds that inhibits enzymatic hydrolysis or growth and productivity of microorganisms during fermentation process. Those compounds are derived from carbohydrate degradation, such as furfural, 5-hydroxymethylfurfural and organic acids, or are lignin depolymerisation products as in case of phenolic compounds. The concentrate acid pre-treatment leads to the highest production of those inhibitory compounds decreasing the efficiency of the fermentation process. Therefore, to remove those compounds, previous detoxification of hydrolysate is required before fermentation. By different reasons less inhibitory products are formed with high pressure technologies and pre-treatment with ILs. In the first case, this is due to a low acidic medium, while in the second case biomass processing can be performed at mild conditions (<140 °C).

Table 1.1. Comparison of pre-treatment technologies for biomass processing and valorisation. Adapted from [125].

		Acid		Alkaline	Organosolv	Ionic Liquids[a]	High-pressure treatments		
		Dilute	Concentrated				Steam explosion	Autohydrolysis	Sub/supercritical CO_2
Removal	Lignin	↓	↓	↑	↑↑	↑	↓	↓	↓
	Hemicellulose	↑	↑	↓	↓↓	↑	↓	↑↑	↑↑
Fractionation	Cellulose	↓	↓	↓	↓	↑	↓	↑	↑
	Hemicellulose	↑	↓	↓	↓	↑	↑	↓	↓
	Lignin	↓	↓	↑	↑↑	↑	↓	↓	↓
Enzymatic digestibility		↑	N.A.	↑	↑	↑↑	↑↑	↑↑	↑↑
Production	Glucose	↓	↑	↓	↓	↓	↓	↓	↓
	Pentoses	↑	↑	↓	↓	↓	↓	↑	↑
	HMF/FUR	↑	↑↑	↓	↓	↓	↓	↓	↓
	LVA	↓	↑↑	↓	↓	↓	↓	↓	↓
Recovery	Catalyst/Solvent	↓	↓	↓	↑	↑	N.A.	N.A.	↑↑

[a] alkaline-based ILs; very high (↑↑), high (↑), low (↓), and very low (↓↓); N.A. – Not applicable; HMF – 5-hydroxymethylfurfural; FUR – furfural; LVA – levulinic acid.

Regarding to the equipment for biomass processing, special requirements, such as equipment resistant to corrosion, is needed for both acid and alkali processes. On the contrary, no corrosion is observed by high pressure pre-treatments, but expensive reactors able to sustain high pressures and temperatures are required. On the other hand, special equipment is avoided with organosolv and pre-treatments with ionic liquids.

Furthermore, pre-treatments cannot afford inefficient catalyst recovery (*e.g.* sulphuric acid) and the use of costly solvents, such as ionic liquids, when the goal is the production of large scale biofuel production. In this context, pre-treatment like steam explosion are advantageous to pre-treat wide amounts of lignocellulosic biomass to produce highly accessible cellulose for enzymatic hydrolysis and subsequent fermentation into large quantities of ethanol, in detriment of hemicellulose and lignin fractions.

However, the production of biofuels as major goal is not a solution for economically favourable lignocellulosic biomass valorisation. When following the biorefinery concept, hemicellulose and lignin must be valorised too in order to find the economical balance of the entire biomass processing. Therefore, the versatility in the fractionation of biomass to produce cellulose, hemicellulose and lignin as well-separated fractions is needed to accomplish the biorefinery processing goal. Although pre-treatment with ILs seem to be the most suitable for that purpose, it is clear that currently known processes lacks to provide highly selectivity and efficiency for the satisfactory and versatile use in biorefineries. Definitely, pre-treatments are one of the most important steps in biomass processing, but they are also main bottlenecks that extremely affect the efficiency and sustainability of the entire biorefinery.[126] The ideal pre-treatment must be dedicated to the maximal exploitation of lignocellulosic biomass respecting some criteria in terms of efficiency and sustainability. Therefore, research must be focused on developing novel and innovative technologies that address this vision.

Furthermore, currently where climate change and environmental issues are topical concerns any action in the development of green technologies is crucial. Therefore, valorising lignocellulosic biomass with new methods based on green chemistry and without biasing the aims of the biorefinery concept could be a solution. The use of green chemistry towards the efficient and sustainable fractionation of lignocellulosic biomass is a hot research topic that should be pushed forward in the next decades. That is why the use of the so called green solvents, such as ionic liquids and supercritical fluids, have been considered as promising to meet sustainability in biomass processing.[127]

1.6. References

1. E. de Jong and G. Jungmeier, in *Industrial Biorefineries & White Biotechnology*, eds. A. Pandey, R. Hofer, C. Larroche, M. Taherzadeh and M. Nampoothiri, Elsevier, 2015, pp. 3-33.
2. J. Rogelj, M. Den Elzen, N. Höhne, T. Fransen, H. Fekete, H. Winkler, R. Schaeffer, F. Sha, K. Riahi and M. Meinshausen, *Nature*, 2016, **534**, 631-639.
3. European Commission, *Innovating for Sustainable Growth: A Bioeconomy for Europe*, 2012.
4. European Commission, *Closing the loop-An EU action plan for the Circular Economy*, 2015.
5. K. McCormick and N. Kautto, *Sustainability*, 2013, **5**, 2589-2608.
6. N. Scarlat, J.-F. Dallemand, F. Monforti-Ferrario and V. Nita, *Env. Dev.*, 2015, **15**, 3-34.
7. B. Kamm and M. Kamm, *Adv. Biochem. Eng. Biotechnol.*, 2007, **105**, 175-204.
8. European Commission, *http://ec.europa.eu/research/bioeconomy/index.cfm*, 2012.
9. B. Kamm, P. R. Gruber and M. Kamm, *Biorefineries–industrial processes and products*, Wiley Online Library, 2006.
10. B. Kamm and M. Kamm, in *White Biotechnology*, eds. R. Ulber and D. Sell, Springer, 2007, pp. 175-204.
11. A. Azapagic, *Trends Biotechnol.*, 2014, **32**, 1-4.
12. P. T. Anastas and J. C. Warner, *Green chemistry: theory and practice*, Oxford university press, 2000.
13. P. Kumar, D. M. Barrett, M. J. Delwiche and P. Stroeve, *Ind. Eng. Chem. Res.*, 2009, **48**, 3713-3729.
14. M. Galbe and G. Zacchi, *Biomass Bioenerg.*, 2012, **46**, 70-78.
15. H. Lee, S. Hamid and S. Zain, *Sci. Wood J.*, 2014, **2014**.
16. P. Bajpai, in *Pretreatment of Lignocellulosic Biomass for Biofuel Production*, ed. P. Bajpai, Springer, 2016, pp. 7-12.
17. J. G. Linger, D. R. Vardon, M. T. Guarnieri, E. M. Karp, G. B. Hunsinger, M. A. Franden, C. W. Johnson, G. Chupka, T. J. Strathmann and P. T. Pienkos, *P. Natl. Acad. Sci. USA*, 2014, **111**, 12013-12018.
18. A. Kuila and V. Sharma, *Lignocellulosic Biomass Production and Industrial Applications*, John Wiley & Sons, 2017.
19. H. Kargarzadeh, I. Ahmad, S. Thomas and A. Dufresne, *Handbook of Nanocellulose and Cellulose Nanocomposites*, Wiley Online Library, 2017.
20. S. Rebouillat and F. Pla, *J. Biomater Nanobiotechnol.*, 2013, **4**, 165.
21. B. B. Hallac and A. J. Ragauskas, *Biofuels Bioprod. Biorefining*, 2011, **5**, 215-225.
22. A. Pinkert, K. N. Marsh, S. Pang and M. P. Staiger, *Chem. Rev.*, 2009, **109**, 6712-6728.
23. K. Ruel, Y. Nishiyama and J.-P. Joseleau, *Plant Sci.*, 2012, **193**, 48-61.
24. S. Zhang, W.-C. Wang, F.-X. Li and J.-Y. Yu, *Cellul. Chem. Technol.*, 2013, **47**, 671-679.
25. L. C. Fidale, N. Ruiz, T. Heinze and O. A. E. Seoud, *Macromol. Chem. Phys.*, 2008, **209**, 1240-1254.
26. T. Dawsey and C. L. McCormick, *J. Macromol. Sci. R. M. C.*, 1990, **30**, 405-440.
27. J. Cai, L. Zhang, S. Liu, Y. Liu, X. Xu, X. Chen, B. Chu, X. Guo, J. Xu and H. Cheng, *Macromolecules*, 2008, **41**, 9345-9351.
28. R. P. Swatloski, S. K. Spear, J. D. Holbrey and R. D. Rogers, *J. Am. Chem. Soc.*, 2002, **124**, 4974-4975.
29. H. Abou-Yousef and P. Steele, *J. Fuel Chem. Tech.*, 2013, **41**, 214-222.
30. L. N. Ding, A. Q. Wang, M. Y. Zheng and T. Zhang, *ChemSusChem*, 2010, **3**, 818-821.
31. C.-T. Buruiana, C. Vizireanu, G. Garrote and J. C. Parajó, *Energ. Fuel.*, 2014, **28**, 1158-1165.
32. N. Qureshi, S. Liu and T. Ezeji, in *Advanced Biofuels and Bioproducts*, ed. J. W. Lee, Springer, 2013, pp. 247-265.
33. G. Jiang, D. J. Hill, M. Kowalczuk, B. Johnston, G. Adamus, V. Irorere and I. Radecka, *Int. J. Mol. Sci.*, 2016, **17**.
34. M. A. Eiteman and S. Ramalingam, *Biotechnol. Lett.*, 2015, **37**, 955-972.
35. S. Y. Oh, D. I. Yoo, Y. Shin and G. Seo, *Carbohydr. Res.*, 2005, **340**, 417-428.

36. X. Chen, J. Liu, Z. Feng and Z. Shao, *J. Appl. Polym. Sci.*, 2005, **96**, 1267-1274.
37. Z. Chen, M. Deng, Y. Chen, G. He, M. Wu and J. Wang, *J. Membr. Sci.*, 2004, **235**, 73-86.
38. N. Reddy and Y. Yang, *Trends Biotechnol.*, 2005, **23**, 22-27.
39. J. K. Rose, *The plant cell wall*, CRC Press, 2003.
40. K. W. Waldron, *Bioalcohol production: biochemical conversion of lignocellulosic biomass*, Elsevier, 2010.
41. L. P. Ramos, *Quim. Nova*, 2003, **26**, 863-871.
42. D. M. de Carvalho, A. Martínez-Abad, D. V. Evtuguin, J. L. Colodette, M. E. Lindström, F. Vilaplana and O. Sevastyanova, *Carbohydr. Polym.*, 2017, **156**, 223-234.
43. N. S. Thompson, in *Kirk-Othmer Encyclopedia of Chemical Technology*, ed. Kirk-Othmer, John Wiley & Sons, Inc., 1991.
44. G. Brodeur, E. Yau, K. Badal, J. Collier, K. Ramachandran and S. Ramakrishnan, *Enzyme Res.*, 2011, **2011**.
45. J. B. Binder, J. J. Blank, A. V. Cefali and R. T. Raines, *ChemSusChem*, 2010, **3**, 1268-1272.
46. K. Dietrich, C. Hernandez-Mejia, P. Verschuren, G. Rothenberg and N. R. Shiju, *Org. Process Res. Dev.*, 2017, **21**, 165-170.
47. S. Patel and A. Goyal, *W. J. Microb. Biot.*, 2011, **27**, 1119-1128.
48. J. Ren, R. Sun, C. Liu, L. Lin and B. He, *Carbohydr. Polym.*, 2007, **67**, 347-357.
49. W. Zhao, K. Odelius, U. Edlund, C. Zhao and A.-C. Albertsson, *Biomacromolecules*, 2015, **16**, 2522-2528.
50. X. Zhang, H. Wang, C. Liu, A. Zhang and J. Ren, *Sci. Rep. UK*, 2017, **7**.
51. A. Brandt, J. Grasvik, J. P. Hallett and T. Welton, *Green Chem.*, 2013, **15**, 550-583.
52. R. El Hage, N. Brosse, L. Chrusciel, C. Sanchez, P. Sannigrahi and A. Ragauskas, *Polym. Degrad. Stab.*, 2009, **94**, 1632-1638.
53. L. J. Jönsson and C. Martín, *Bioresource Technol.*, 2016, **199**, 103-112.
54. R. Vanholme, B. Demedts, K. Morreel, J. Ralph and W. Boerjan, *Plant Physiol.*, 2010, **153**, 895-905.
55. M. P. Pandey and C. S. Kim, *Chem. Eng. Technol.*, 2011, **34**, 29-41.
56. A. J. Ragauskas, G. T. Beckham, M. J. Biddy, R. Chandra, F. Chen, M. F. Davis, B. H. Davison, R. A. Dixon, P. Gilna and M. Keller, *Science*, 2014, **344**.
57. F. S. Chakar and A. J. Ragauskas, *Ind. Crop. Product.*, 2004, **20**, 131-141.
58. C. Bonini, M. D'Auria, L. Emanuele, R. Ferri, R. Pucciariello and A. R. Sabia, *J. Appl. Polym. Sci.*, 2005, **98**, 1451-1456.
59. Y. Li and S. Sarkanen, *Macromolecules*, 2002, **35**, 9707-9715.
60. Y. Li and S. Sarkanen, *Macromolecules*, 2005, **38**, 2296-2306.
61. F. H. Isikgor and C. R. Becer, *Polym. Chem.*, 2015, **6**, 4497-4559.
62. A. N. Glazer and H. Nikaido, *Microbial biotechnology: fundamentals of applied microbiology*, Cambridge University Press, 2007.
63. M. H. L. Silveira, A. R. C. Morais, A. M. da Costa Lopes, D. N. Olekszyszen, R. Bogel-Lukasik, J. Andreaus and L. Pereira Ramos, *ChemSusChem*, 2015, **8**, 3366-3390.
64. Z. Liu and B. Fei, in *Sustainable degradation of lignocellulosic biomass-Techniques, applications and commercialization*, eds. A. K. Chandel and S. S. da Silva, InTech, 2013, pp. 3-14.
65. M. J. Taherzadeh and K. Karimi, *Int. J. Mol. Sci.*, 2008, **9**, 1621-1651.
66. Y. Sun and J. Cheng, *Bioresource Technol.*, 2002, **83**, 1-11.
67. G. Y. S. Mtui, *Afr. J. Biotechnol.*, 2009, **8**, 1398-1415.
68. L. P. Ramos, L. da Silva, A. C. Ballem, A. P. Pitarelo, L. M. Chiarello and M. H. L. Silveira, *Bioresource Technol.*, 2015, **175**, 195-202.
69. A. P. Pitarelo, C. S. da Fonseca, L. M. Chiarello, F. M. Gírio and L. P. Ramos, *J. Braz. Chem. Soc.*, 2016, **27**, 1889-1898.
70. F. Carvalheiro, T. Silva-Fernandes, L. C. Duarte and F. M. Gírio, *Appl. Biochem. Biotechnol.*, 2009, **153**, 84-93.
71. A. R. C. Morais, A. C. Mata and R. Bogel-Lukasik, *Green Chem.*, 2014, **16**, 4312-4322.
72. E. Rouches, S. Zhou, J. Steyer and H. Carrere, *Process Biochem.*, 2016, **51**, 1784-1792.

73. M. J. Ray, D. J. Leak, P. D. Spanu and R. J. Murphy, *Biomass Bioenerg.*, 2010, **34**, 1257-1262.
74. M. Saritha, A. Arora and Lata, *Indian J. Microbiol.*, 2012, **52**, 122-130.
75. M. J. Taherzadeh and K. Karimi, *BioResources*, 2007, **2**, 472-499.
76. Y. Chen, R. R. Sharma-Shivappa, D. Keshwani and C. Chen, *Appl. Biochem. Biotechnol.*, 2007, **142**, 276-290.
77. H. Tarkow and W. C. Feist, in *Cellulases and Their Applications*, eds. G. J. Hajny and E. T. Reese, American Chemical Society, 1969, pp. 197-218.
78. N. Beukes and B. I. Pletschke, *Bioresource Technol.*, 2010, **101**, 4472-4478.
79. S. McIntosh and T. Vancov, *Bioresource Technol.*, 2010, **101**, 6718-6727.
80. H. Xu, B. Li and X. Mu, *Ind. Eng. Chem. Res.*, 2016, **55**, 8691-8705.
81. X. Zhao, K. Cheng and D. Liu, *Appl. Microbiol. Biotechnol.*, 2009, **82**, 815-827.
82. C. Chiappe and D. Pieraccini, *J. Phys. Org. Chem.*, 2004, **18**, 275-297.
83. U. Domanska and R. Bogel-Lukasik, *J. Phys. Chem. B*, 2005, **109**, 12124-12132.
84. L. J. A. Conceiçao, E. Bogel-Lukasik and R. Bogel-Lukasik, *RSC Adv.*, 2012, **2**, 1846-1855.
85. A. Forte, E. Bogel-Lukasik and R. Bogel-Lukasik, *J. Chem. Eng. Data*, 2011, **56**, 2273-2279.
86. A. Forte, C. I. Melo, R. Bogel-Lukasik and E. Bogel-Lukasik, *Fluid Phase Equilib.*, 2012, **318**, 89-95.
87. Y. U. Paulechka, G. J. Kabo, A. V. Blokhin, O. A. Vydrov, J. W. Magee and M. Frenkel, *J. Chem. Eng. Data*, 2003, **48**, 457-462.
88. Y. U. Paulechka, A. V. Blokhin, G. J. Kabo and A. A. Strechan, *J. Chem. Thermodyn.*, 2007, **39**, 866-877.
89. R. D. Rogers and K. R. Seddon, *Science*, 2003, **302**, 792-793.
90. N. V. Plechkova and K. R. Seddon, *Chem. Soc. Rev.*, 2008, **37**, 123-150.
91. R. Bogel-Lukasik, *Monatsh. Chem.*, 2007, **138**, 1137-1144.
92. U. Domanska and M. Krolikowski, *J. Chem. Thermodyn.*, 2012, **53**, 108-113.
93. E. Bogel-Lukasik, S. Santos, R. Bogel-Lukasik and M. N. da Ponte, *J. Supercrit. Fluid.*, 2010, **54**, 210-217.
94. U. Domanska, A. Pobudkowska and P. Bochenska, *J. Chem. Eng. Data*, 2012, **57**, 1894-1898.
95. R. C. Remsing, R. P. Swatloski, R. D. Rogers and G. Moyna, *Chem. Commun.*, 2006, 1271-1273.
96. C. Li, B. Knierim, C. Manisseri, R. Arora, H. V. Scheller, M. Auer, K. P. Vogel, B. A. Simmons and S. Singh, *Bioresource Technol.*, 2010, **101**, 4900-4906.
97. S. Singh, B. A. Simmons and K. P. Vogel, *Biotechnol. Bioeng.*, 2009, **104**, 68-75.
98. Y. Pu, N. Jiang and A. J. Ragauskas, *J. Wood Chem. Technol.*, 2007, **27**, 23-33.
99. I. A. Kilpeläinen, H. Xie, A. King, M. Granstrom, S. Heikkinen and D. S. Argyropoulos, *J. Agric. Food Chem.*, 2007, **55**, 9142-9148.
100. N. Sun, M. Rahman, Y. Qin, M. L. Maxim, H. Rodriguez and R. D. Rogers, *Green Chem.*, 2009, **11**, 646-655.
101. H. T. Vo, C. S. Kim, B. S. Ahn, H. S. Kim and H. Lee, *J. Wood Chem. Technol.*, 2011, **31**, 89-102.
102. M. Zavrel, D. Bross, M. Funke, J. Buchs and A. C. Spiess, *Bioresource Technol.*, 2009, **100**, 2580-2587.
103. A. Brandt, J. P. Hallett, D. J. Leak, R. J. Murphy and T. Welton, *Green Chem.*, 2010, **12**, 672-679.
104. M. Abe, Y. Fukaya and H. Ohno, *Green Chem.*, 2010, **12**, 1274-1280.
105. S. S. Y. Tan, D. R. MacFarlane, J. Upfal, L. A. Edye, W. O. S. Doherty, A. F. Patti, J. M. Pringle and J. L. Scott, *Green Chem.*, 2009, **11**, 339-345.
106. A. A. Shamsuri and D. K. Abdullah, *Mod. Appl. Sci.*, 2010, **4**, 19-27.
107. N. Muhammad, Z. Man, M. A. Bustam, M. I. A. Mutalib, C. D. Wilfred and S. Rafiq, *Appl. Biochem. Biotechnol.*, 2011, **165**, 998-1009.
108. X. D. Hou, T. J. Smith, N. Li and M. H. Zong, *Biotechnol. Bioeng.*, 2012, **109**, 2484-2493.
109. A. M. da Costa Lopes, K. G. João, A. R. C. Morais, E. Bogel-Lukasik and R. Bogel-Lukasik, *Sustain. Chem. Process.*, 2013, **1**.

110. A. Brandt, M. J. Ray, T. Q. To, D. J. Leak, R. J. Murphy and T. Welton, *Green Chem.*, 2011, **13**, 2489-2499.
111. A. George, A. Brandt, K. Tran, S. M. N. S. Zahari, D. Klein-Marcuschamer, N. Sun, N. Sathitsuksanoh, J. Shi, V. Stavila and R. Parthasarathi, *Green Chem.*, 2015, **17**, 1728-1734.
112. P. Verdia, A. Brandt, J. P. Hallett, M. J. Ray and T. Welton, *Green Chem.*, 2014, **16**, 1617-1627.
113. C. Z. Li, Q. Wang and Z. K. Zhao, *Green Chem.*, 2008, **10**, 177-182.
114. A. S. Amarasekara and P. Shanbhag, *Bioenerg. Res.*, 2013, **6**, 719-724.
115. B. J. Cox and J. G. Ekerdt, *Bioresource Technol.*, 2012, **118**, 584-588.
116. A. M. da Costa Lopes and R. Bogel-Lukasik, *ChemSusChem*, 2015, **8**, 947-965.
117. S. P. Magalhães da Silva, A. M. da Costa Lopes, L. B. Roseiro and R. Bogel-Lukasik, *RSC Adv.*, 2013, **3**, 16040-16050.
118. S. Peleteiro, A. M. da Costa Lopes, G. Garrote, R. Bogel-Łukasik and J. C. Parajó, *Ind. Crop. Product.*, 2015, **77**, 163-166.
119. N. S. Mosier, R. Hendrickson, M. Brewer, N. Ho, M. Sedlak, R. Dreshel, G. Welch, B. S. Dien, A. Aden and M. R. Ladisch, *Appl. Biochem. Biotechnol.*, 2005, **125**, 77-97.
120. F. M. Oliveira, I. O. Pinheiro, A. M. Souto-Maior, C. Martin, A. R. Goncalves and G. J. Rocha, *Bioresource Technol.*, 2013, **130**, 168-173.
121. J. Soderstrom, L. Pilcher, M. Galbe and G. Zacchi, *Appl. Biochem. Biotechnol.*, 2002, **98**, 5-21.
122. S. P. Magalhães da Silva, A. R. C. Morais and R. Bogel-Lukasik, *Green Chem.*, 2014, **16**, 238-246.
123. M. Stamenic, I. Zizovic, R. Eggers, P. Jaeger, H. Heinrich, E. Roj, J. Ivanovic and D. Skala, *J. Supercrit. Fluid.*, 2010, **52**, 125-133.
124. G. P. van Walsum, *Appl. Biochem. Biotechnol.*, 2001, **91**, 317-329.
125. F. M. Gírio, C. Fonseca, F. Carvalheiro, L. C. Duarte, S. Marques and R. Bogel-Łukasik, *Bioresource Technol.*, 2010, **101**, 4775-4800.
126. V. B. Agbor, N. Cicek, R. Sparling, A. Berlin and D. B. Levin, *Biotechnol. Adv.*, 2011, **29**, 675-685.
127. L. Soh and M. J. Eckelman, *ACS Sustain. Chem. Eng.*, 2016, **4**, 5821-5837.

CHAPTER II

Scope of the thesis

2.1. Scope and aims

The work disclosed in this thesis refers to the development of novel technologies with ionic liquids (IL) focused on the maximal exploitation of lignocellulosic biomass in the frame of the biorefinery concept. Wheat straw is one of the principal lignocellulosic residues produced in European Union and due to its abundance was used as a feedstock for processing with ILs. The valorisation of wheat straw was examined using two distinct strategies that relies on the chemical properties of studied ILs, namely:

i) Basicity of 1-ethyl-3-methylimidazolium acetate ([emim][OAc]);
ii) Acidity of hydrogensulphate-based ILs ([bmim][HSO_4] and [emim][HSO_4]).

Very distinct chemical character of examined ILs influences biomass processing especially the biomass dissolution, fractionation, hydrolysis and conversion. All these stages were scrutinised in the proposed methodologies aiming at maximal separation and transformation of main macromolecular components of biomass, *i.e.* cellulose, hemicellulose and lignin. Depending on the IL employed, different fractionation steps were conducted. Among them are the use of anti-solvents, changes in pH, extraction processes (solid-liquid, adsorption, supercritical), enzymatic hydrolysis and preparative chromatography. These steps attempted the separation of cellulose, hemicellulose and lignin in their polymeric and/or depolymerised forms as demonstrated in Figure 2.1.

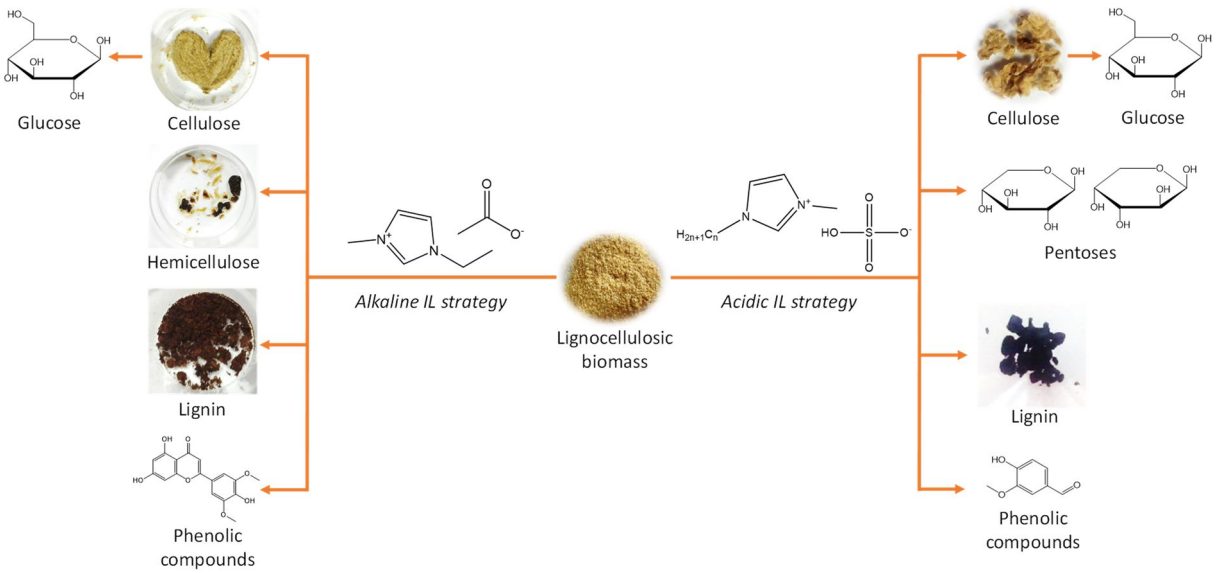

Figure 2.1. Two biomass valorisation approaches with alkaline and acidic ILs presented in this thesis.

The strategy with alkaline IL demonstrated potential in valorisation of lignocellulosic biomass by producing cellulose, hemicellulose, lignin and phenolic compounds as pure and separated fractions. On the other hand, the employment of acidic IL showed a different vision on lignocellulosic biomass

valorisation, where high-purity separated streams of glucose, pentoses, high quality lignin and phenolic compounds were obtained.

2.1.1. The alkaline ionic liquid strategy

The capacity of [emim][OAc] to modify the physicochemical properties of lignocellulosic biomass and to provide more susceptible fractions for further valorisation is presented in **CHAPTERS III** and **IV**. The work presented in **CHAPTER III** allowed understanding the key parameters governing the biomass dissolution, pre-treatment and fractionation processes with ILs and, consequently, a novel three-step fractionation process of wheat straw with alkaline [emim][OAc] was proposed. This developed process comprehends dissolution of biomass in [emim][OAc] with subsequent selective precipitation of three major components, namely cellulose, hemicellulose and lignin in their polymeric forms. The effect of temperature and time on the recovery of these fractions and their purities was examined in this work. Besides, the recovery of IL and its reuse was also attempted, as a way to achieve the economic and environmental sustainability of the process. In addition, an extended valorisation of wheat straw after the three-step fractionation process and recovery of IL was shown in **CHAPTER IV**. Recovered [emim][OAc] contained some phenolic compounds originated from lignin depolymerisation and these products were extracted by means of adsorption to polymeric resins and subsequently selective extraction with supercritical CO_2.

2.1.2. The acidic ionic liquid strategy

Rather than dissolve biomass, acidic ILs can act as catalysts by mediating chemical reactions with lignocellulosic biomass. Process intensification by integration of pre-treatment, hydrolysis and conversion of biomass into a one-pot reaction was accomplished with acidic ILs and this topic was explored in **CHAPTERS V, VI** and **VII**. The wheat straw hydrolysis with [bmim][HSO_4] at different reaction temperature and time was studied and resulted in the selective processing of hemicellulose fraction as demonstrated in **CHAPTER V**. The acidic character of [bmim][HSO_4] allowed achieving the hemicellulose hydrolysis to respective pentoses (xylose and arabinose), but also further dehydration of these monosaccharides into furfural was observed as well. A process of pentose and furfural production can be controlled by the presence of water in the reaction system. The optimisation of this phenomenon is presented in **CHAPTER VI**. The solid constituted by cellulose and lignin, resulting from the biomass hydrolysis with aqueous [emim][HSO_4], was also valorised in two different manners, namely: A) direct enzymatic hydrolysis of cellulose to glucose; or B) extraction of lignin and subsequent enzymatic hydrolysis of resulting cellulose-rich solid to glucose. Extracted lignin was recovered as a high purity fraction and aromatic compounds derived from lignin depolymerisation were also produced. A preliminary techno-economic analysis was also addressed to evaluate both scenarios in the context of biorefinery. The purification of pentose stream and recovery of IL was also accomplished through preparative chromatography, which optimisation procedure is given in **CHAPTER VII**.

2.2. Author contribution to the presented studies

The aforementioned chapters are based on information and data from scientific articles published with contributions from several authors. Therefore, for clarification my direct contributions are presented below:

CHAPTER III:

i) Development of the three-step fractionation process of wheat straw (patented process – PT106947);
ii) Extraction of phenolic compounds from recovered IL and analysis by capillary electrophoresis;
iii) Discussion of the obtained results and the manuscript preparation.

CHAPTER IV:

i) Scale-up of the three-step fractionation process of wheat straw with recovered IL;
ii) Study related to phenolic adsorption to polymeric resins and supercritical CO_2 extraction;
iii) Discussion of the obtained results and the manuscript preparation.

CHAPTER V:

i) Development and optimisation of capillary electrophoresis method for the analysis of monosaccharides;
ii) Analysis of the water role in the system aiming at higher yield of pentoses;
iii) Discussion of the obtained results and the manuscript preparation.

CHAPTER VI:

i) Development of scenarios for solid fractionation;
ii) Development of the preparative chromatography method for separation and recovery of pentoses and ionic liquid;
iii) Techno-economic analysis of developed biorefinery approach;
iv) Discussion of the obtained results and the manuscript preparation.

CHAPTER VII:

i) The ternary phase equilibrium determination;
ii) Study related to xylose and ionic liquid adsorption to alumina;
iii) Development of the preparative chromatography method for separation and recovery of xylose and ionic liquid;
iv) Discussion of the obtained results and the manuscript preparation.

CHAPTER III

Biorefinery approach for biomass valorisation with alkaline ionic liquid

---

This chapter is based on data and information of the following publication:

S. P. Magalhães da Silva, A. M. da Costa Lopes, L. B. Roseiro and R. Bogel-Lukasik, Novel pre-treatment and fractionation method for lignocellulosic biomass using ionic liquids, *RSC Adv.*, 2013, **3**, 16040-16050.

3.1. Introduction

Lignocellulosic biomass from agricultural residues, forestry wastes, waste paper, and energy crops has come under an intense research as an alternative to fossil resources, due to their potential as starting materials for the production of biofuels and other value-added products.[1] Moreover, lignocellulosic biomass is a renewable, relatively carbon-neutral source of energy and is readily available.[2, 3]

The lignocellulosic material is composed mainly of cellulose (35-50 wt.%), hemicellulose (20-35 wt.%) and lignin (5-30 wt.%),[4] wherein the composition's variation depends mostly on the species, age and origin of biomass. Cellulose is a water-insoluble homopolysaccharide. Cellulose chains are completely linear and have a strong tendency to form intra- and intermolecular hydrogen bonds, which make cellulose a highly crystalline polymer. In contrast, hemicellulose is a non-crystalline, highly branched, water-insoluble heteropolysaccharide. On the other hand, lignin is an amorphous three-dimensional polymer of phenylpropane units which are covalently linked to hemicellulose. Merely, cellulose forms a skeleton which is surrounded by other substances forming a matrix (hemicelluloses) and encrusting (lignin) materials.[5]

Due to the complex structure of lignocellulosic materials, several pre-treatment technologies are currently employed to overcome this recalcitrance against chemical and microbial attacks. Hence, the pre-treatment step is a key process in the biorefinery to convert lignocellulosic biomass into low-value high-volume fuels and high-value low-volume chemicals.[6] The pre-treatment methods can be divided according to various criteria.[7, 8] Among these criteria, pre-treatments can be conventional[9, 10] or alternative, such as the pre-treatment with ionic liquids.[11]

Ionic liquids (ILs) are salts usually composed of a large organic cation and an organic or an inorganic anion. The low lattice energy between cation and anion leads to low melting point usually below 100 °C.[12] These novel solvents possess interesting properties over molecular organic solvents, such as a negligible vapour pressure, high conductivity and thermal stability,[13] highly solvating capacity either for polar or nonpolar compounds.[14-17] Due to a large number of possible cationic and anionic structural combinations, desired physicochemical properties of ILs for a particular process can be easily tuned.[18]

Rogers and co-workers[19] demonstrated for the first time that imidazolium-based ILs can efficiently dissolve cellulose. More specifically, Sun *et al*.[20] reported 1-ethyl-3-methylimidazolium acetate ([emim][OAc]; Figure 3.1.) to be the best candidate for dissolution of cellulose due to its desirable properties such as low toxicity, viscosity, corrosiveness, low melting point (<-20 °C) and favourable biodegradability. The importance of a strong hydrogen bond basicity[21] that facilitates the breakdown of inter- and intramolecular hydrogen bonds is commonly known. Imidazolium acetate ILs exhibit a promising dissolution behaviour for cellulose, although there is a lack of thermal properties of these ILs. The calorimetric analyses of [emim][OAc]) were performed by Wendler *et al*.,[22] where a

significant mass loss was observed for temperatures close to 200 °C. From the TGA measurements it can be concluded that acetate generally decreases the thermal stability, which was reported by Ohno *et al*.[23]

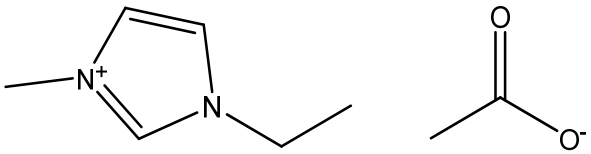

Figure 3.1. Chemical structure of 1-ethyl-3-methylimidazolium acetate.

Not only cellulose can be dissolved by ILs, but also lignin[24] or even wood.[25, 26] The major challenge of the wood pre-treatment is the recovery of all lignocellulosic fractions constituting biomass. Up to now only few literature reports show the complete fractionation of the biomass into the main constituents amongst the IL recovery at the final stage.[11, 27-30]

The aim of this work is to present a new methodology where a complete fractionation of the wheat straw biomass into cellulose, hemicellulose and lignin is accomplished. Moreover, the effect of temperature and processing time on the pre-treatment of the wheat straw with [emim][OAc] was studied. To evaluate the efficiency of a new method on the production of cellulose for further potential applications, the enzymatic hydrolysis of cellulose-rich fractions was performed. The dependency of cellulose-rich fractions from the applied conditions was evaluated by a regression analysis concerning the cellulose recovery %($w \cdot w^{-1}$) and the glucan content (wt.%). Additionally, the presence of phenolic compounds in the recovered ILs was investigated through a capillary electrophoresis (CE) methodology.

3.2. Materials and Methods

3.2.1. Materials

For the pre-treatment experiments [emim][OAc] IL was used (>95 wt.% purity, Iolitec GmbH, Heilbronn, Germany). The water content was measured to be 2800 ppm by a volumetric Karl – Fischer titration. Prior to use, [emim][OAc] was dried under vacuum (0.1 Pa) at room temperature for at least 24 hours. Wheat straw was the feedstock material, supplied by Estação Nacional de Melhoramento de Plantas (Elvas, Portugal). The material was ground with a knife mill (IKA® WERKE, MF 10 basic, Germany) to particles smaller than 0.5 mm, and stowed at room temperature. The wheat straw moisture was found to be 8 wt.%.

For the IL pre-treatment experiments the following reagents were used: 1 M and 4 M HCl aqueous solutions prepared from fuming 37 wt.% HCl bought from Merck – Darmstadt, Germany; 1 M and 3

wt.% NaOH aqueous solutions prepared from pure (99 wt.%) NaOH pellets supplied from Eka Chemicals/Akzonobel - Bohus, Sweden. To prepare HCl and NaOH aqueous solutions, distilled water (17 MΩ·cm^{-1}) produced by the PURELAB Classic of Elga system was used. From 4 M HCl aqueous solution, an acidic water solution (pH ≤ 2) was prepared. Ethanol (purity of 96 vol.%) and acetonitrile were bought from Carlo Erba Group - Arese, Italy. Paper filter membranes (Ø=47 mm, nº 1, 1.2 µm porosity) obtained from Whatman, GE Healthcare Life Generations - Buckinghamshire, United Kingdom, and nylon filters (Ø=47 mm, 0.45 µm porosity) from Merck Millipore, Country Cork, Ireland, were used. For FTIR analysis, all samples were prepared with KBr (≤ 99 wt.% trace metal basis) purchased from Sigma-Aldrich Co. (St. Louis, MO, USA). Deuterium oxide with an isotopic purity > 99.8 wt.% from Fluka, Sigma-Aldrich Quimica, S.L. Sintra, Portugal, was used to prepare IL samples for NMR analyses.

Enzymatic hydrolysis was performed using a 0.1 M sodium citrate buffer (pH 4.8) prepared from citric acid monohydrate (99.7 wt.% purity) and tris-sodium citrate (>99 wt.% purity), both bought from VWR International Ltd. - Leicester, England; a 2 wt.% sodium azide solution was prepared from sodium azide (99 wt.% purity; Merck - Darmstadt, Germany). Commercial enzymes Celluclast® 1.5 L (activity 60 FPU·g^{-1}, 105.89 FPU·mL^{-1}) and β-glucosidase Novozym 188 (activity 64 NPGU·g^{-1}, 797.25 pNPGU·mL^{-1}), both purchased from Novozymes - Bagsvaerd, Denmark, were used in this work.

Capillary electrophoresis (CE) analysis was performed using an electrolyte solution containing 15 mM of sodium tetraborate decahydrate (>99.5 wt.% from Sigma-Aldrich, Aldrich Co., St. Louis, MO, USA) in 10 vol.% methanol (>99.9 wt.% from Carlo Erba Group, Arese, Italy). This solution was adjusted to pH 9.13 using 0.1 M NaOH.

Nylon syringe filters (Ø=13 mm, 0.22 µm porosity), purchased from Red® analytical, Cambridgeshire, UK, were used to filtrate all the samples before running on HPLC and CE.

3.2.2. Pre-treatment of wheat straw using [emim][OAc]

A new methodology was developed based on our previous work dedicated to this subject.[27] Various pre-treatment times and temperatures were examined using a constant biomass/IL ratio of 5 %(w·w^{-1}). A schematic presentation of the described method is shown in Figure 3.2.

In a 15 mL vial [emim][OAc] was mixed with the wheat straw under a continuous stirring for a defined period of time and temperature. The pre-treatment times and temperatures used in this work are shown in Table 3.1. After dissolution, a 3 wt.% NaOH was added until the vial was filled up. Next, the mixture was transferred to a 100 mL Erlenmeyer flask and a vigorous agitation was applied during 1 h. To the formed solution 3 wt.% NaOH was added to promote the regeneration of cellulose. The resulting solution was subject to a centrifugation (Digicen 21R centrifuge, Orto Alresa, Madrid, Spain)

at 6000 rpm, 20 °C for 20 min. The supernatant was filtrated under vacuum and distilled water was used to wash the cellulose pellet. A new centrifugation step (6000 rpm, 20 °C for 20 min) was performed and both supernatant and cellulose pellet were filtrated. During the vacuum filtration, the cellulose pellet was washed with distilled water until the filtrate demonstrated neutral pH (measured with pH indicator strips from Merck Millipore, Country Cork, Ireland). Subsequently, cellulose was collected and dried in the oven at 60 °C for at least 24 h.

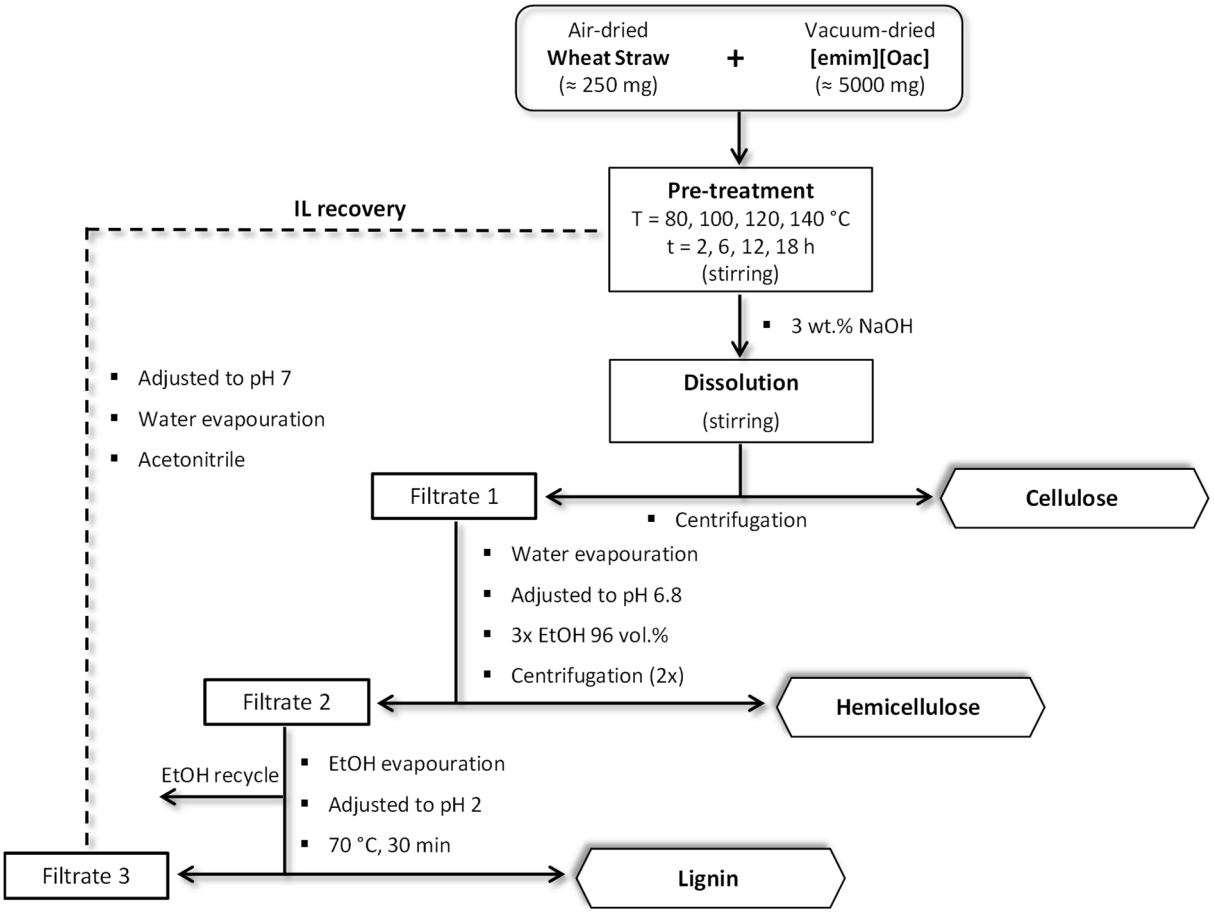

Figure 3.2. Schematic presentation of the optimised method.

Table 3.1. Pre-treatment temperature and time studied in this work.

T (°C)	**80**		**100**			**120**		**140**	
T (h)	12	18	6	12	18	2	6	2	6

Water was evapourated under reduced pressure (Rotavapour R-210/215, Büchi, Flawil, Switzerland) from the filtrate to a final volume of 30 mL. Then, the solution was adjusted to pH 6.8 (GLP 21 pH meter, Crison, Barcelona, Spain) with 4 M and 1 M HCl solutions, and hemicellulose was precipitated with 3 volumes of 96 vol.% EtOH with the continuous stirring. Once again, the resulting solution was

centrifuged at the conditions referred earlier. After the first centrifugation, the liquid fraction was filtrated while the solid fraction (hemicellulose) remained on the centrifugation flasks. This first liquid fraction was kept to further use. Distilled water was added to the centrifugation flasks in order to wash the hemicellulose precipitate and a last centrifugation step was performed. After that, using the same filter, the hemicellulose precipitate was filtrated and continuously rinsed with distilled water. The washing water was also kept to posterior use, and hemicellulose was dried at 60 °C for at least 24 h in the oven. Ethanol present in the first liquid fraction was evapourated under reduced pressure and the solution was acidified to pH 2, with a 4 M HCl solution, to precipitate the lignin material. The solution was heated up to 70 °C for 30 min and a subsequent filtration was performed without cooling. The lignin material was washed with 10 mL of acidified water (pH $\leq$ 2) and dried in the oven at 60 °C for at least 24 h. ·

For [emim][OAc] recovery, the washing water from the hemicellulose precipitation step was added to the remaining filtrate (from the lignin filtration) to guarantee that all the IL used is recovered. The solution was then neutralised with the NaOH pellets and water was removed under the reduced pressure resulting in a solid containing NaCl and IL. Subsequently, 130 mL of acetonitrile was added to dissolve IL and to precipitate the salt, that was removed by filtration. Acetonitrile was removed under reduced pressure and the recovered IL was dried for at least 24 h under vacuum.

All the pre-treatment experiments were at least duplicated and all the weighing was made using an XS205 DualRange analytical balance, Mettler Toledo, Ohio, USA.

3.2.3. Chemical analysis

3.2.3.1. FTIR characterisation of fractionated samples

Perkin Elmer BX Series Spectrum (San Jose, CA, USA) was used to scan all samples. This model features a temperature-stabilised DTGS detector and a KBr beam splitter and is capable of routine mid-IR work. The operating system used to analyse all the spectra was Spectrum Software Version 5.3.1, Perkin Elmer, Inc., San Jose, CA, USA). Thirty two scans were taken for each sample with a resolution of 4 cm^{-1} in an absorbance mode in the range of 4000-400 cm^{-1}. For each spectrum the air background spectrum was subtracted.

For the composition analysis two calibration curves were built – carbohydrates and lignin – using an acid hydrolysed wheat straw with known composition as a standard.[31] For the preparation of these curves, bands with a maximum linearity were selected. Specifically, 898 cm^{-1} band for carbohydrates and the range at 1503-1537 cm^{-1} for lignin were used. All samples were scanned at least three times and the average number was used. For each series of analyses calibration curves were validated.

3.2.3.2. NMR analysis of recovered ionic liquid

Bruker ARX-400 spectrometer was used to analyse ^{1}H NMR and ^{13}C NMR spectra of all the recovered ILs using deuterium oxide solution as a solvent.

3.2.3.3. Capillary electrophoresis of recovered ionic liquid

Electrophoretic analyses for the presence of phenolic compounds in each recovered IL were carried out using an Agilent Technologies CE system (Waldbronn, Germany) equipped with a diode array detector (UV-DAD). An uncoated fused silica extended light-path capillary from Agilent, i.d.=50 μm, total length 62 cm (56 cm to the detector) was also used. The Agilent 3D-CE ChemStation data software (Rev B.04.01) was used to perform qualitative analysis of the electropherograms. The temperature in capillary was kept constant at 30 °C and it was preconditioned by rinsing sequentially a 1 M sodium hydroxide, 0.1 M sodium hydroxide and Milli-Q water, for 20 min each solution. Between runs, the capillary was washed with 0.1 M NaOH followed by buffer solutions. Electropherograms were recorded at 200, 280, 320 and 375 nm, and phenolic compounds were identified by electrophoretic comparisons (migration times and UV spectra) with authentic phenolic standards. Before performing CE, all the IL samples were subjected to a solid phase extraction (SPE) to concentrate and separate the phenolic compounds from the IL solution through a non-polar surface. The SPE was performed to remove polar non-phenolic compounds such as sugars and salts, thus reducing the absorption of [emim][OAc] in the selected UV wavelengths. Separation columns SPE cartridge (C18 ec, 6 mL, 1000 mg) from Chromabond®, (Macherey-Nagel GmbH&Co. KG, Düren, Germany) were used. The columns were preconditioned with methanol, and then neutralised with ultrapure water (18.2 $M\Omega \cdot cm^{-1}$, PURELAB) using a high vacuum system (VacElut 20 Manifold Tall Glass Basin from Agilent Technologies, Santa Clara, CA, USA). The recovered ILs were loaded in the columns, and ultrapure water was used to the water-soluble constituents and simultaneously to remove the IL. The phenolic compounds were then eluted with absolute methanol and concentrated under vacuum prior to CE analysis.

3.2.4. Enzymatic hydrolysis

Cellulose-rich samples obtained from all the pre-treatments at different conditions were subjected to enzymatic hydrolysis, in order to determine the glucan content. The adopted procedure was based on the standard NREL protocol.[32] The Optic Ivymen® System (Spain) incubator shaker was used to perform the enzymatic hydrolysis at 150 rpm and 50 °C for 72 h. After hydrolysis all vials were placed in a hot bath (approximately 95 °C) for 5 min for enzymes denaturation. The concentration of reducing sugars was then analysed by an HPLC system (Agilent 1100 series HPLC system, Santa Clara, CA, USA) using a Bio-Rad Aminex HPX-87H column (Hercules, CA, USA). A 5 mM sulphuric acid was used as a mobile phase. Before running HPLC, all samples were filtrated. The set conditions of the

column were: 50 °C, 0.6 mL·min^{-1} flow rate 5 µL injection volume and the acquisition time of 15 min for standards and 30 min for samples. Glucose standards with concentrations of 0.25, 0.50, 1.00, 1.75, 2.50 and 5.00 g·L^{-1} were used to construct the calibration curve. The determination of glucan content was made by multiplying glucose with a conversion factor of 0.90.[33]

3.2.5. Experimental errors

Standard deviation error (u) was determined for all the obtained results. All weighing was made considering a u(m)=0.1 mg. For all different dissolution conditions in the wheat straw pre-treatment, the applied temperature demonstrated a u(T)=1 °C. An arbitrary error of 5 % was defined to all the FTIR measurements.

3.3. Results

3.3.1. Wheat straw pre-treatment with [emim][OAc]

This work was devoted to the fractionation of the wheat straw from the pre-treatment with [emim][OAc] using a new fractionation pathway based on previously developed methodology.[27] The results of the wheat straw pre-treatment with [emim][OAc] at settled conditions, as well as the yield of IL recovery, are presented in Table 3.2.

Table 3.2. Results of the wheat straw pre-treatment with [emim][OAc]: fractionation at various pre-treatment temperatures and times. The yield of IL recovery after each pre-treatment is depicted.

T/°C	t/h	Lignocellulosic materials %(w·w^{-1})[a]			IL recovery %(w·w^{-1})
		Cellulose-rich	Hemicellulose-rich	Lignin-rich	
Native		38.9[b]	23.5[b]	18.0[b]	-
80	12	57.4	17.4	10.1	91.3
	18	50.4	17.6	8.9	95.5
100	6	44.2	19.7	8.9	86.7
	12	48.0	18.7	8.5	94.9
	18	42.1	17.4	10.2	93.2
120	2	45.4	18.8	10.9	91.4
	6	44.5	19.8	11.6	85.9
140	2	38.4	20.8	6.9	95.8
	6	37.1	18.2	7.6	90.3

[a] on the basis of dry weight, [b] Wheat straw macromolecular composition.[31]

Considering the temperature effect, it can be stated that temperature is more important parameter regarding the recovery of cellulose-rich fractions. At 140 °C the amount of cellulose-rich fractions obtained (38.4 %(w·w^{-1}) and 37.1 %(w·w^{-1})) were equivalent to the content of the cellulose fraction in the native biomass (38.9 %(w·w^{-1})). An irrelevant effect in the recovery of hemicellulose-rich fractions was verified, where no clear trend was observed at different temperatures (80-140 °C). The obtained recovery of hemicellulose varied between 17.4 %(w·w^{-1}) and 20.8 %(w·w^{-1}) of the initial biomass. A similar effect was also observed for lignin fractions recovery, except those performed at the higher studied temperature. At 140 °C, the amount of lignin-rich fractions decreased from ≈10 %(w·w^{-1}) (average observed for the other studied temperatures) to ≈7 %(w·w^{-1}). Regarding the effect of the pre-treatment time, its increase did not affect significantly the amount of lignocellulosic materials recovered. Only at 80 °C, a minor effect of the pre-treatment time was verified, where an additional 6 h pre-treatment up to18 h led to a decrease by 7 %(w·w^{-1}) of the cellulose recovery.

Concerning the IL recovery at the different conditions, the attained results were at a similar level ranging from 85.9 %(w·w^{-1}) to 95.8 %(w·w^{-1}). However, a noteworthy effect of temperature can be observed in the colour of the recovered ILs after pre-treatment. Figure 3.3 shows the colour of the fresh [emim][OAc] and ILs recovered from the pre-treatment at various temperatures. The colour of the recovered [emim][OAc] became deeper with an increase of the pre-treatment temperature comparatively with the colour of the fresh IL, probably due to temperature effect on the lignin degradation products.

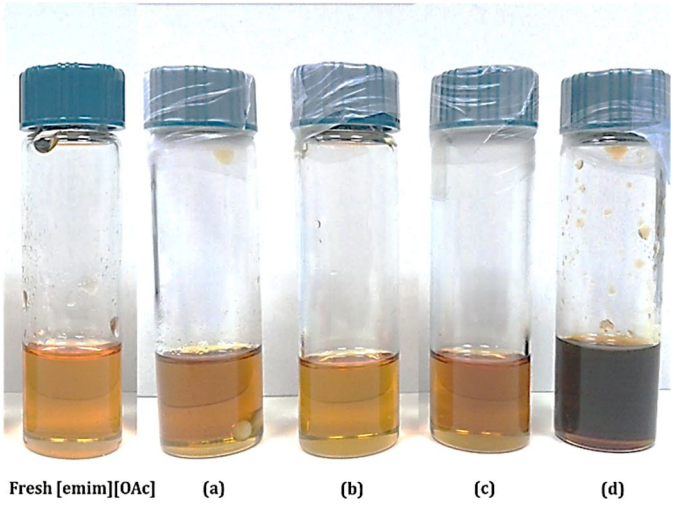

Figure 3.3. Colour of the fresh [emim][OAc] and recovered ILs after the wheat straw pre-treatment at different temperatures: (a) 80 °C; (b) 100 °C; (C) 120 °C and (d) 140 °C.

3.3.2. FTIR characterisation

3.3.2.1. Qualitative analysis

Fourier Transform Infrared (FTIR) technique was selected to analyse the chemical characterisation of the solid materials recovered from pre-treatments. The main chemical bond vibrations of lignocellulosic materials are identified in the region of 1800-800 cm^{-1}. The characteristic absorption bands attributed to carbohydrates – cellulose and hemicellulose – are 1161, 1112-1120 and 897 cm^{-1}. Absorption bands at 1376, 1061 and 1025 cm^{-1} are also recognised as cellulose characteristic bands. Characteristic bands of hemicellulose are observed at 1251, 1046 and 990-996 cm^{-1}.[34-36] The lignin characteristic absorption bands are displayed at 1718, 1702, 1654, 1508, 1597, 1458, 1420, 1261, 1242, 1224, 1127, 1033 and 840 cm^{-1}.[37, 38] An absorption band at 1734 cm^{-1}, which is characteristic for untreated lignocellulosic biomass, is associated to ester-linked acetyl, feruloyl and p-coumaroyl groups between hemicellulose and lignin.[39] All the above-mentioned bands are characterised in detail elsewhere.[27]

The FTIR spectra of lignocellulosic materials obtained after the pre-treatment of the wheat straw in [emim][OAc] at different conditions were analysed.

All spectra of cellulose-rich fractions presented the characteristic vibration bands of cellulose in the region of 1250-850 cm^{-1}. The obtained samples using temperatures at 100, 120, 140 °C presented well-defined vibrations bands at 897, 1025, 1061, 1161 cm^{-1}. However, the experiments at 80 °C demonstrated a slight difference in the shape of cellulose characteristics bands that were not well-defined. Additionally, a vibration band at 1376 cm^{-1} assigned to bending of C-H group in cellulose of the native wheat straw was also observed. Furthermore, the band at 1112 cm^{-1} is detected in all the cellulose-rich samples, but with low intensity. Pre-treatment at 140 °C for a 2 h cellulose-rich fraction exhibits a pronounced band at 996 cm^{-1} which indicates the presence of arabinosyl side chains (arabinose). Insignificant bands at 1420, 1508, 1654 cm^{-1} are observed in all cellulose spectra indicating the presence of lignin. Moreover, the band at 1734 cm^{-1} which is related to ester-linked groups between hemicellulose and lignin appears only in spectra of cellulose-rich fractions recovered from both pre-treatments at 80 °C. Besides, absorption bands at 2850 and 2920 cm^{-1} that are attributed to asymmetric and symmetric C-H stretching of CH, CH_2 and CH_3 are present in all the spectra.

FTIR spectra of hemicellulose-rich fractions presented characteristic absorption bands at 1251, 1046 and 990-996 cm^{-1}. The various hemicellulose-rich samples recovered from the pre-treatments at different conditions exhibited a great similarity. Moreover, a vibration band at 2918 cm^{-1} is visualised in all the spectra.

The lignin-rich samples' spectra displayed numerous vibration bands owing to the complex structure of lignin. All the recovered lignin materials were successfully fractionated revealing all the lignin

characteristic bands. Absorption bands are observed at 1127, 1508, 1597 and 1654 cm^{-1} in all the recovered lignin-rich samples. Also, an absorption band at 1033 cm^{-1} which is related to the aromatic C-H bond in the plane deformation for guaiacyl units is clearly identified in all the lignin samples. Vibration bands at 2850 and 2920 cm^{-1} are present in lignin-rich samples, except in samples recovered at 120 °C and 140 °C both for 6 h. The absence of carbohydrates is plainly observed in all the lignin-rich samples.

3.3.2.2. Quantitative analysis

Following the successful examples of the use of FTIR analysis in the biomass fraction quantitative analysis, the mentioned technique was used in this work.[27, 40, 41] Based on FTIR measurements, a quantitative analysis was performed for each recovered solid fraction in order to evaluate the efficiency of the new method to fractionate lignocellulose. The quantification was made for carbohydrate and lignin contents following the same technique presented elsewhere.[27, 42] The composition determined for the recovered solid fractions at different pre-treatment conditions is presented in Table 3.3. A general overview indicates that different temperatures and times applied in the pre-treatment of the wheat straw with [emim][OAc] had a significant effect on the purity of the fractionated materials.

Table 3.3. Results of the FTIR quantitative analysis of the fractionated samples obtained at different pre-treatment temperatures and times.

T/°C	t/h	Purity (wt.%)					Carbohydrate yield/ %(w·w^{-1})
		Cellulose		Hemicellulose		Lignin*	
		Carbohydrates	*Lignin*	*Carbohydrates*	*Lignin*		
80	**12**	64	6	78	6	67	81
	18	79	7	83	7	61	87
100	**6**	80	9	80	6	63	82
	12	80	7	88	6	78	88
	18	90	8	92	7	65	86
120	**2**	67	8	80	7	69	73
	6	86	8	96	6	92	92
140	**2**	84	8	73	7	72	76
	6	91	6	96	8	97	82

*Lignin samples were free from carbohydrates.

The recovered carbohydrate fractions – cellulose and hemicellulose – showed that for each temperature, the prolonged pre-treatment time resulted in higher carbohydrate content. Likewise, higher temperatures led to the higher carbohydrate content. For instance, the pre-treatment at 80 °C for 18 h gave the carbohydrate content of 79 wt.% in cellulose-rich samples, while in the pre-treatment at 140 °C during 6 h a 91 wt.% carbohydrate content was obtained. Following the same line for hemicellulose-rich samples, pre-treatment at 80 °C for 18 h gave the carbohydrate content of 83 wt.%, while at 140 °C during 6 h a 96 wt.% carbohydrate content was attained. The lignin content of both cellulose and hemicellulose fractions was relatively low varying from ≈6 wt.% to ≈9 wt.%. On the other hand, the temperature seemed not to have a pronounced effect on the purity of the recovered lignin-rich solid fractions in the pre-treatments performed at 80 °C and 100 °C**.** However, at 120 °C and 140°C, longer time such as 6 h, resulted in high pure solid lignin-rich fractions with 92 wt.% and 97 wt.% of purity, respectively. One of the greatest accomplishes was that all the lignin-rich fractions obtained were free from carbohydrates. Additionally, it can be assumed that dissolution times superior to 12 h led to a decrease in the lignin purity.

3.3.3. Enzymatic hydrolysis

After FTIR analysis of cellulose-rich samples enzymatic hydrolysis was performed in order to investigate the amount of the glucan present in cellulose-rich samples. Glucan yields (wt.%) and the amount (mg) of pure cellulose recovered after each pre-treatment, as well as the quantity of other compounds present on cellulose-rich fractions, are displayed in Table 3.4.

Table 3.4. Glucan yields (wt.%) and the amounts (mg) of pure cellulose and other compounds present on the recovered cellulose after pre-treatment at different conditions.

T/°C	t/h	Glucan (wt.%)	Cellulose (mg)	Other compounds* (mg)
80	12	59.8	79.0	53.1
	18	60.9	70.7	45.3
100	6	67.9	69.1	32.7
	12	67.5	74.6	35.9
	18	71.9	69.5	27.2
120	2	73.8	77.1	27.2
	6	78.2	79.9	22.4
140	2	74.8	66.1	22.3
	6	81.1	69.2	16.2

*Other compounds are mainly hemicellulose and lignin.

The amount of pure cellulose was determined by equation 1.

$$Cellulose_{mg} = Recovered\ Cellulose_{mg} \times Glucan_{wt.\%} \quad (1)$$

Considering the results presented in Table 3.4, it can be noticed that with the pre-treatment temperature increase, an enrichment of the glucan content from 59.8 to 81.1 wt.% is observed. The same trend is visualised with the increase of pre-treatment time at one fixed temperature. Furthermore, it can be also observed that higher temperatures (120 °C and 140 °C) resulted in a more efficient fractionation by the lower amount of other compounds present in cellulose fractions. However, in the experiments using 140 °C, a lower amount of pure cellulose was achieved in comparison to pre-treatments at 120 °C.

3.3.4. NMR analysis

The purity of the recovered ILs after pre-treatments was verified using ^{1}H- and ^{13}C-NMR techniques. The determined chemical shifts of pure [emim][OAc] were as follows: ^{1}HNMR (400 MHz; D_2O) δ(ppm): 1.34 (t, 3H, NCH_2CH_3); 1.77 (s, 3H, CH_3COO); 3.76 (s, 3H, NCH_3); 4.10 (q, 2H, NCH_2CH_3); 7.32 (d, 2H, NCHCHN); 8.58. (s, 1H, CH_3COOH). ^{13}CNMR (D_20) δ(ppm): 14.44 (NCH_2CH_3); 23.26 (CH_3COO); 35.55 (NCH_3); 44.73 (NCH_2CH_3) 121.81 (NCHCHN); 123.37 (NCHCHN); 135.52 (NCHN) and 181.21 (CH_3COO).

3.3.5. Capillary electrophoresis analysis

The change in the IL colour after the pre-treatment with an increase of the pre-treatment temperature coupled to the loss of almost ≈50 %($w \cdot w^{-1}$) of lignin present in the wheat straw led to investigate the presence of phenolic compounds associated to the delignification process during the pre-treatment with IL. Coupling SPE with CE it was possible to identify the presence of phenolic compounds in the IL solutions. As an example, Figure 3.4 shows the electropherogram recorded at 320 nm for the phenolic profile of the recovered IL after the pre-treatment at 100 °C during 18 h.

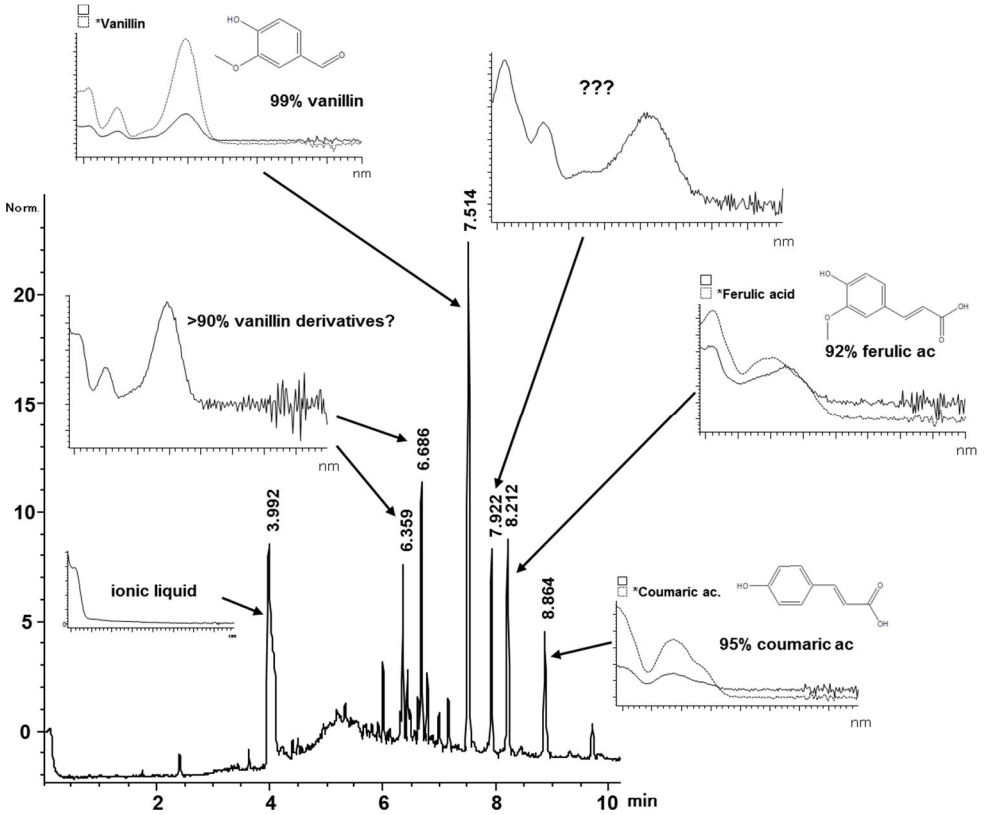

Figure 3.4. Electropherogram recorded at 320 nm showing the phenolic profile of the recovered IL after pre-treatment at 100 °C during 18 h. Refer to text for CE conditions.

By comparison with electrophoretic data obtained with authentic standards, it was possible to identify vanillin, erulic acid and coumaric acid with >90 % matching. Another unidentified phenolic compound (migration time 7.9 min) with a characteristic flavonoid spectrum[43] was also detected. Between the four studied temperatures the phenolic compounds identified were the same. However, it was verified that the most abundant compound differs according to the pre-treatment temperature. Vanillin was a major compound in the recovered ILs from the pre-treatments occurred at 100 °C and 120 °C, but at 140 °C, the unidentified phenolic compound was the main component present. This was probably due to some degradation caused by the effect of temperature.

3.4. Discussion

3.4.1. A three-step fractionation process

A novel three-step fractionation process was developed. Comparatively to previous work,[27] the increase of NaOH concentration from 0.1 M to 3 wt.% (≈ 0,75 M) leads to a more effective fractionation of wheat straw into cellulose, hemicellulose and lignin-rich fractions. In this work, the cellulose-rich material is obtained directly by the addition of an anti-solvent. Obtained results show that the increase of the hydroxyl group concentration leads to higher solubility of lignin and

hemicellulosic fractions, therefore, the fractionation process of the carbohydrate-rich material is eliminated. This is contrary to the previous work where the carbohydrate-rich fraction was obtained and subsequently fractionated into cellulose and hemicellulose was needed.[27]

3.4.2. Effect of temperature and time on the pre-treatment of biomass

The effect of the pre-treatment temperature (80-140 °C) and time (2-18 h) was studied regarding the recovery and purity of the separated lignocellulosic materials. As it is presented in Tables 3.2 and 3.3, at higher temperatures lower amounts of cellulose-rich fractions were recovered, although purer fractions were achieved. Likewise, longer times at a set temperature gave higher purity cellulose-rich fractions. On the other hand, by changing the conditions on the pre-treatment, approximately the same amount of hemicellulose-rich fractions was obtained. Therefore, the temperature and time have no significant effect on hemicellulose recovery. Notwithstanding, the pre-treatments at 120 °C and 140 °C during 6 h gave high pure hemicellulose-rich fractions attaining a 96 wt.% carbohydrate content. The same trend was observed in the purity of lignin-rich fractions, where at 120 °C and 140 °C during 6 h the fractions with higher purities (92 wt.% and 97 wt.%, respectively), were obtained. Additionally, close to a 4 %($w \cdot w^{-1}$) mass loss of the lignin-rich fraction was noticed with increasing temperature from 120 °C to 140 °C. This can be justified by the fact that the recovery of lignin can be hampered due to stronger interactions between lignin and [emim][OAc] at higher temperatures, and 140 °C is closeness to the glass transition temperature of lignin (165 °C).[11]

The temperature affects the viscosity as well as the conductivity of ILs. The [emim][OAc] IL exhibits a relatively low viscosity that facilitates dissolution of cellulose at lower temperatures. The increase in the dissolution temperature increases the diffusivity, both adding thermal energy to the system. However, at higher temperatures thermal degradation of cellulose can occur.[44] Longer times allow the IL to penetrate further into the biomass.

The pre-treatment efficiency of the new method at different pre-treatment conditions was also evaluated by enzymatic hydrolysis of the cellulose-rich fractions. The results of enzymatic hydrolysis (Table 3.4) followed the same trend exhibited by FTIR results (Table 3.2). It is clearly visible that at lower temperatures not only glucan is present in cellulose-rich fractions. A larger amount of other compounds, mainly hemicellulose and lignin, are also present. With the temperature increase, enrichment in the glucan content is observed. At the highest temperature studied, an 81.1 wt.% content of glucan was obtained, comparatively to only 59.8 wt.% of the glucan content obtained from the pre-treatment at 80 °C (for 6 h process). Concerning the amount of pure cellulose present in each cellulose-rich fraction (Table 3.4), the higher values obtained for samples recovered at lower temperatures are a consequence of the increase amount of the cellulose-rich material recovered. The selection of the best set of conditions should have in consideration the final use of these fractions. For example, for biofuel production it will probably be more feasible to obtain higher mass of cellulose,

even with lower purity, as long as the contamination compounds will not interfere with the rate and performance of enzymatic hydrolysis process. In this way, higher yield of glucose can be accessed for fermentation. On the other hand, high purity cellulose is desirable to produce value added derivative products. Thus, pre-treatment with ILs can be perfectly tuned for biomass processing in biorefinery.

Since the different conditions studied had a direct effect on cellulose recovery, a multiple linear regression with an interaction factor (Equation 2) was made to describe the dependency of cellulose recovery on pre-treatments temperature and time.

$$y = \beta_0 + \beta_1 T + \beta_2 t + \beta_{12} Tt \quad (2)$$

where y is the desired response, T and t correspond to temperature and time and ($\beta_0, \beta_1, \beta_2$ and β_{12}) are the regression coefficients. Matlab® software (version 7.12.0.635) was used to determine the regression coefficients by minimizing the sum of the squares of the deviations of the data from the model (least-squares fit). Regression coefficients were calculated with a 95 % level of confidence. The obtained and adjusted models are $\%CR = 79.32 - 0.2753T + 0.3138t - 0.0077Tt$ with R^2 = 0.96 and $\%C = 48.49 + 0.1857T - 2.0157t + 0.0226Tt$ with R^2 = 0.97, where RC – cellulose recovery (%($w \cdot w^{-1}$); %C - glucan yield from the enzymatic hydrolysis (wt.%); T – temperature (°C); t – time (h). From the analysis of the results, it can be assumed a strong dependency between the different pre-treatment conditions and the recovery of cellulose-rich fractions – in terms of the quantity recovered as well as of the enhancement of the enzymatic hydrolysis (Figure 3.5).

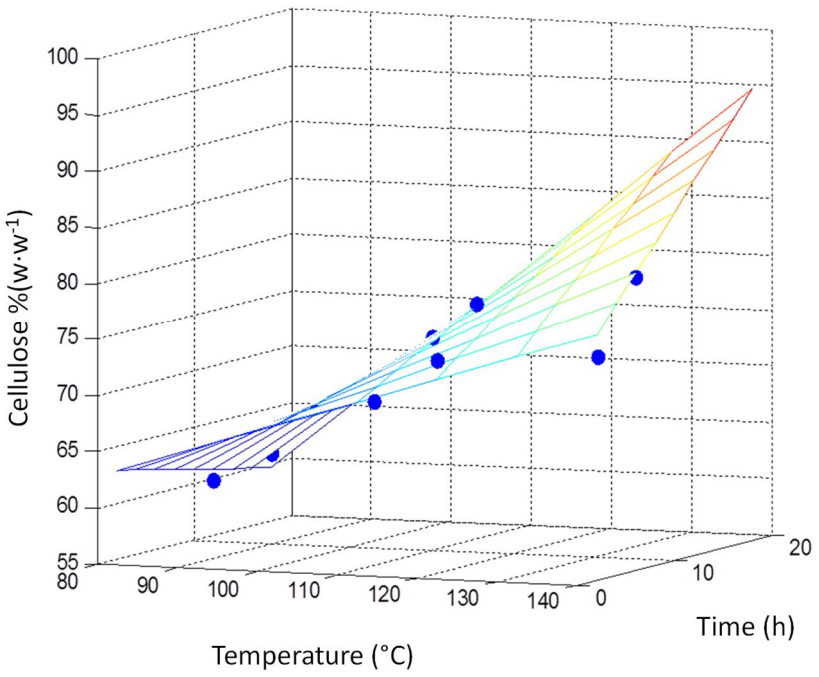

Figure 3.5. Representation of the adjusted model for cellulose %($w \cdot w^{-1}$) obtained from the enzymatic hydrolysis. (●) experimental data.

The optimal result achieved in this work for the recovery of cellulose-rich fractions (37.1 % ($w \cdot w^{-1}$)) was obtained at 140 °C during 6 h. Furthermore, the same conditions gave the optimal result in terms of higher amount of the glucan present (81.1 wt.%) in cellulose-rich fractions. At such conditions a recovery of 18.2 %($w \cdot w^{-1}$) was obtained for hemicellulose-rich fractions (purity of 96 wt.%), and for lignin-rich fractions a recovery of 7.6 %($w \cdot w^{-1}$) was attained (purity of 97 wt.%). Also, at the end of process it was recovered 90.3 %($w \cdot w^{-1}$) of [emim][OAc] from the initial load. Nevertheless, the choice of the optimal pre-treatment conditions has to be optimised according to the biomass and the IL used.

An interesting association can be performed on the relation between the amount of energy required for the pre-treatment process and the purity of the fractionated lignocellulosic materials. An estimation of the energy spent was calculated according to Equation 3. The molar heat capacity (Cp_m) of [emim][OAc] for each dissolution temperature was estimated from the results reported for [bmim][OAc][45] which were adjusted for the temperatures examined in this work taking into account the difference between the literature data for [bmim][OAc][45] and for [emim][OAc].[15] The estimated energy values obtained are illustrated in Figure 3.6.

$$E = Cp_{m,T} \times m_{IL} \times (T - T_{room}) \times t \quad (3)$$

Considering the cellulose-rich fraction recovered from the pre-treatment at 100 °C for 18 h (purity of 90 wt.%) and those recovered from the pre-treatment at 120 °C during 6 h (purity of 86 wt.%), a slight difference is observed in the purity of cellulose samples, but in terms of the energy required a significant increase of ≈47 $kJ \cdot h^{-1}$ is noticed. On the other hand, an increase of 20 °C (140 °C) in the pre-treatment temperature gave an increase of 5 wt.% in purity (from 86 wt.% to 91 wt.%), with a small noticeable increase in the energy demand (from 27.1 $kJ \cdot h^{-1}$ to 29.9 $kJ \cdot h^{-1}$). Concerning the purity of hemicellulose-rich fractions, an identical result was obtained for the experiments at 120 °C and 140 °C during 6 h (96 wt.%). However, a demand of an extra 2.8 $kJ \cdot h^{-1}$ is required. The same tendency can be observed in the case of the purity of lignin-rich fractions recovered at the same conditions referred earlier. Also, a difference of ≈5 wt.% between purity of lignin-rich fractions from 120 °C and 140 °C was attained. Once again, the selection of the best pre-treatment conditions in terms of energetic consumption should be taken into account according to the final use of the processed lignocellulosic materials.

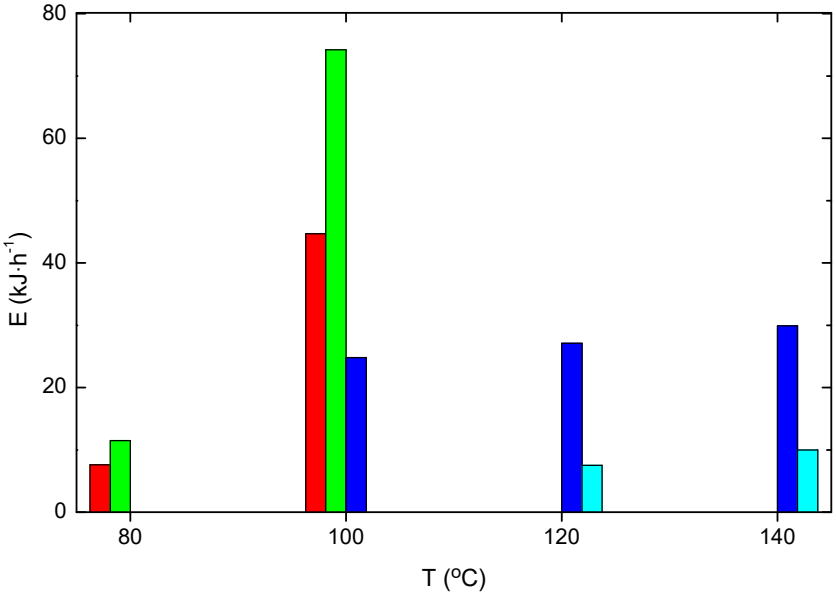

Figure 3.6. Graphical presentation of the amount of energy spent in the pre-treatments at the different dissolution conditions. The vertical bars present various pre-treatment time in the following manner: light blue – 2 h, dark blue – 6 h, red – 12 h, green – 18 h.

3.4.3. Ionic liquid recovery

The [emim][OAc] recovery obtained in the presented method at different dissolution conditions was mainly superior to 90 %(w·w^{-1}) from the original IL load (Table 3.2). The presence of impurities within the recovered ILs was analysed by ^{13}C and ^{1}H NMR analysis. Although negligible differences in chemical shifts are visualised between all recovered ILs and the pure [emim][OAc], the intensity of the chemical shifts related to carbons in position 9 and 10 decreases significantly. According to ^{1}H NMR analysis, the same difference in chemical shift is observed to hydrogen in position 10. The aforementioned chemical shifts are associated with the acetate anion (Figure 3.7.). Therefore, this can suggest the substitution of the acetate anion by hydroxide anion, for instance, due to the use of NaOH as the antisolvent and a pH neutraliser in the IL recovery step.

From Figure 3.3. it is clearly visible that ILs' colour became increasingly darker with the temperature increase. Currently, very limited information concerning the chemical analysis of the recovered ILs is available. Due to the similarity of the colour revealed by the recovered ILs with that exhibited by the lignin material, and a loss of ≈36-62 %(w·w^{-1}) of the lignin material from the theoretical lignin,[31] it was found crucial to study the presence of phenolic compounds in the recovered ILs. Additionally, a few papers also refer that the dark colour exhibited by the recovered ILs is due to the presence of lignin materials.[46-48] In fact, Lee *et al.* [46] reported that the accumulation of lignin in [emim][OAc] is given by the high solubility of lignin in this IL.

In fact, after SPE-CE analysis (Figure 3.4.), the presence of phenolic compounds, namely vanillin and phenolic acids, in the recovered ILs suggests the presence of lignin degradation products. Thus, the change in colour intensity with increased temperatures could indicate the existence of other compounds in the recovered IL.

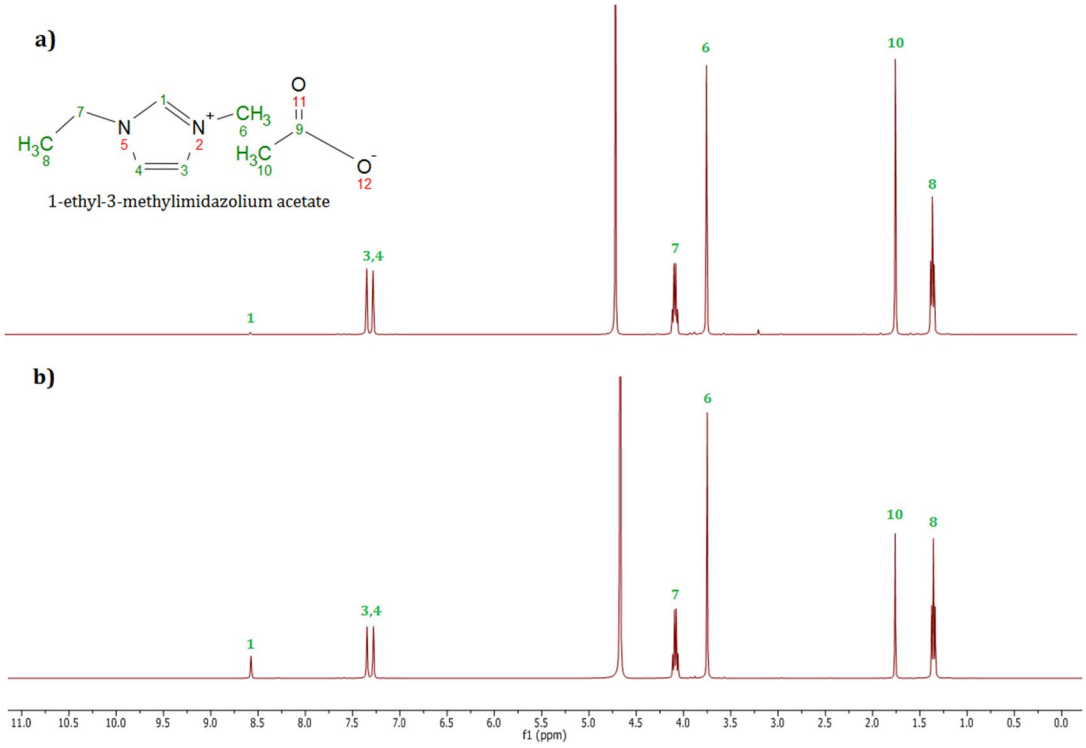

Figure 3.7. ^{1}H NMR spectra of the a) pure [emim][OAc]; b) recovered [emim][OAc] from pre-treatment at 140 °C, 6 h.

3.5. Conclusion

A new methodology of fractionation of the wheat straw into cellulose, hemicellulose and lignin-rich fractions at different temperatures and times of the pre-treatment using [emim][OAc] was developed. The [emim][OAc] recovery at different dissolution conditions was mainly superior to 90 %(w·w^{-1}) from the initial IL load. Within the different pre-treatment temperatures (80-140 °C) and times (2-18 h) studied, higher temperatures and longer times favour obtaining higher purity of the fractionated lignocellulosic materials, as well as the release of glucose from cellulose-rich fractions. Specifically, the wheat straw pre-treatment at 140 °C for 6 h gave the highest purity values for lignocellulosic materials (91 wt.% cellulose, 96 wt.% hemicellulose and 97 wt.% lignin), and a glucan content of 81.1 wt.%.

Delignification of lignocellulosic biomass by ILs is a potential technique for further application of carbohydrate fractions for biofuel production and carbohydrate derivative products, within a

biorefinery approach. Moreover, considering the biorefinery concept, this work can prove that the presence of value-added phenolic compounds (*e.g.* vanillin) in the recovered ILs, followed by their extraction, could make this process more economically efficient. Nevertheless, further studies are required for the purification of the recovered ILs and the extraction of phenolic compounds from ILs.

Furthermore, it should be stated that the optimal set of pre-treatment conditions is dependent on the type of biomass and the IL used. The final use of the fractionated lignocellulosic materials and the amount of energy required are also important aspects needed to be consider for the sustainability of pre-treatment processes using ILs.

3.6. References

1. G. Y. S. Mtui, *Afr. J. Biotechnol.*, 2009, **8**, 1398-1415.
2. M. Zavrel, D. Bross, M. Funke, J. Büchs and A. C. Spiess, *Bioresource Technol.*, 2009, **100**, 2580-2587.
3. D. Fu, G. Mazza and Y. Tamaki, *J. Agr. Food Chem.*, 2010, **58**, 2915-2922.
4. J. Van Spronsen, M. A. T. Cardoso, G. Witkamp, W. Jong and M. C. Kroon, *Chem. Eng. Process.*, 2011, **50**, 196-199.
5. E. Sjöström, *Wood chemistry: fundamentals and applications*, Academica Press, 1993.
6. L. Costa Sousa, S. P. S. Chundawat, V. Balan and B. E. Dale, *Curr. Opin. Biotech.*, 2009, **20**, 339-347.
7. M. Galbe and G. Zacchi, *Biomass. Bioenerg.*, 2012.
8. P. Alvira, E. Tomás-Pejó, M. Ballesteros and M. Negro, *Bioresource Technol.*, 2010, **101**, 4851-4861.
9. M. J. Taherzadeh and K. Karimi, *Int. J. Mol. Sci.*, 2008, **9**, 1621-1651.
10. C. Conde-Mejía, A. Jiménez-Gutiérrez and M. El-Halwagi, *Process Saf. Environ.*, 2012, **90**, 189-202.
11. A. da Costa Lopes, K. João, R. Morais, E. Bogel-Lukasik and R. Bogel-Lukasik, *Sustain. Chem. Process.*, 2013, **1:3**.
12. M. G. Freire, Carvalho, P. J., Fernandes, A. M., Marrucho, I. M., Queimada, A. J. and Coutinho, J. A. P., *J. Colloid Inter. Sci.*, 2007, **314**, 621-630.
13. U. Domanska and R. Bogel-Lukasik, *J. Phys. Chem. B*, 2005, **109**, 12124-12132.
14. M. G. Freire, L. M. N. B. F. Santos, A. M. Fernandes, J. A. P. Coutinho and I. M. Marrucho, *Fluid Phase Equilibr.*, 2007, **261**, 449-454.
15. M. G. Freire, A. R. R. Teles, M. A. A. Rocha, B. Schröder, C. M. S. S. Neves, P. J. Carvalho, D. V. Evtuguin, L. M. Santos and J. A. P. Coutinho, *J. Chem. Eng. Data*, 2011, **56**, 4813-4822.
16. C. Reichardt, *Green Chem.*, 2005, **7**, 339-351.
17. R. D. Rogers and K. R. Seddon, *Science*, 2003, **302**, 792-793.
18. M. J. Earle and K. R. Seddon, *Pure Appl. Chem.*, 2000, **72**, 1391-1398.
19. R. P. Swatloski, S. K. Spear, J. D. Holbrey and R. D. Rogers, *J. Am. Chem. Soc.*, 2002, **124**, 4974-4975.
20. N. Sun, M. Rahman, Y. Qin, M. L. Maxim, H. Rodríguez and R. D. Rogers, *Green Chem.*, 2009, **11**, 646-655.
21. F. M. Girio, C. Fonseca, F. Carvalheiro, L. C. Duarte, S. Marques and R. Bogel-Lukasik, *Bioresource Technol.*, 2010, **101**, 4775-4800.
22. F. Wendler, L. N. Todi and F. Meister, *Thermochim. Acta*, 2012, **528**, 76-84.
23. H. Ohno and Y. Fukaya, *Chem. Lett.*, 2009, **38**, 2-7.
24. Y. Pu, N. Jiang and A. J. Ragauskas, *J. Wood Chem. Technol.*, 2007, **27**, 23-33.
25. I. Kilpeläinen, H. Xie, A. King, M. Granstrom, S. Heikkinen and D. S. Argyropoulos, *J. Agr. Food Chem.*, 2007, **55**, 9142-9148.
26. D. A. Fort, R. C. Remsing, R. P. Swatloski, P. Moyna, G. Moyna and R. D. Rogers, *Green Chem.*, 2007, **9**, 63-69.
27. A. da Costa Lopes, K. João, D. Rubik, E. Bogel-Lukasik, L. C. Duarte, J. Andreaus and R. Bogel-Lukasik, *Bioresource Technol.*, 2013, **142**, 198-208.
28. W. Lan, C. F. Liu and R. C. Sun, *J. Agr. Food Chem.*, 2011, **59**, 8691–8701.
29. D. Yang, L.-X. Zhong, T.-Q. Yuan, X.-W. Peng and R.-C. Sun, *Ind. Crop. Prod.*, 2013, **43**, 141-149.
30. J. G. Lynam, M. Toufiq Reza, V. R. Vasquez and C. J. Coronella, *Bioresource Technol.*, 2012, **114**, 629-636.
31. F. Carvalheiro, T. Silva-Fernandes, L. C. Duarte and F. M. Gírio, *Appl. Biochem. Biotechnol.*, 2009, **153**, 84-93.
32. M. Selig, N. Weiss and Y. Ji, *Enzymatic Saccharification of Lignocellulosic Biomass: Laboratory Analytical Procedure (LAP),* Report NREL/TP-510-42629*,* National Renewable Energy Laboratory, Colorado, USA, 2008.

33. L. Zhu, J. P. O'Dwyer, V. S. Chang, C. B. Granda and M. T. Holtzapple, *Bioresource Technol.*, 2008, **99**, 3817-3828.
34. R. C. Sun and J. Tomkinson, *Carbohyd. Polym.*, 2002, **50**, 263-271.
35. M. Sain and S. Panthapulakkal, *Ind. Crop. Prod.*, 2006, **23**, 1-8.
36. R. Liu, H. Yu and Y. Huang, *Cellulose*, 2005, **12**, 25-34.
37. Q. Yang, S. Wu, R. Lou and G. LV, *Wood Sci. Technol.*, 2011, **45**, 419-431.
38. S. Kubo and J. F. Kadla, *Biomacromolecules*, 2005, **6**, 2815-2821.
39. B. Wang, H. Feng, X. Wang, B. Zhou and J. A. de Frias, US8173406, 2012.
40. M. P. Tucker, R. K. Mitri, F. P. Eddy, Q. A. Nguyen, L. M. Gedvilas and J. D. Webb, *Appl. Biochem. Biotechnol.*, 2000, **84**, 39-50.
41. M. P. Tucker, Q. A. Nguyen, F. P. Eddy, K. L. Kadam, L. M. Gedvilas and J. D. Webb, *Appl. Biochem. Biotechnol.*, 2001, **91-93**, 51-61.
42. Q. Li, Y. C. He, M. Xian, G. Jun, X. Xu, J. M. Yang and L. Z. Li, *Bioresource Technol.*, 2009, **100**, 3570-3575.
43. B. Naseem, S. W. H. Shah, A. Hasan and S. Sakhawat Shah, *Spectrochim. Acta A*, 2010, **75**, 1341-1346.
44. P. Maki-Arvela, I. Anugwom, P. Virtanen, R. Sjoholm and J. Mikkola, *Ind. Crop. Prod.*, 2010, **32**, 175-201.
45. A. A. Strechan, Y. U. Paulechka, A. V. Blokhin and G. J. Kabo, *J. Chem. Thermodyn.*, 2008, **40**, 632-639.
46. S. H. Lee, T. V. Doherty, R. J. Linhardt and J. S. Dordick, *Biotechnol. Bioeng.*, 2009, **102**, 1368-1376.
47. H. Wu, M. Mora-Pale, J. Miao, T. V. Doherty, R. J. Linhardt and J. S. Dordick, *Biotechnol. Bioeng.*, 2011, **108**, 2865-2875.
48. K. Shill, S. Padmanabhan, Q. Xin, J. M. Prausnitz, D. S. Clark and H. W. Blanch, *Biotechnol. Bioeng.*, 2011, **108**, 511-520.

CHAPTER IV

Extraction of phenolic compounds from recovered alkaline ionic liquid

---

This chapter is based on data and information of the following publication:

A. M. da Costa Lopes, M. Brenner, P. Fale, L. B. Roseiro and R. Bogel-Lukasik, Extraction and purification of phenolic compounds from lignocellulosic biomass assisted by ionic liquid, polymeric resins and supercritical CO_2, *ACS Sustain. Chem. Eng.*, 2016, **4**, 3357-3367.

4.1. Introduction

Lignocellulose is an abundant and renewable carbon source, which still nowadays is barely exploited in industry. The complete valorisation of lignocellulosic feedstock lies in the efficient pre-treatment and further fractionation of biomass into main fractions, namely cellulose, hemicellulose and lignin. The subsequent processing of these fractions gives an array of chemicals, fuels and bioproducts raising the value of lignocellulose feedstock.[1] However, up to now, a scant regard has been given to phenolic compounds that are also present in lignocellulosic biomass. Although, the content of phenolic compounds is much smaller than other fractions in biomass and due to their bioactive properties, they are characterised by a very high commercial value[2] that may contribute significantly to economic revenues of lignocellulosic biorefineries.

Phenolic compounds encompass different families of aromatic secondary plant metabolites, being responsible for structural and protective functions in plants. Furthermore, due to the aromatic content of lignin, several phenolic compounds could be produced by lignin transformation, mainly with chemical processes.[3] The main property attributed to phenolic compounds is the antioxidant activity against reactive molecule species involved in provoking diverse human diseases.[4] Promising results have been achieved in the human disease prevention studies increasing, for instance, the demand on food commodities with functional properties.[5]

Studies tackling the extraction of phenolic compounds from lignocellulosic biomass have been presented elsewhere.[6, 7] However, extraction of phenolic compounds from lignocellulosic biomass is needed along the valorisation of other major constituents. The main challenge is to surpass the recalcitrance of lignocellulose. It can be accomplished by the development of efficient processes able to deconstruct biomass into main components. To meet this aim, pre-treatments based on thermal, catalytic and/or high pressure processing are normally applied to biomass.[8-15] Although some of the conventional pre-treatment processes are effective on dismantling biomass and transforming it into desired products, the fractionation efficiency of these technologies is still the foremost limitation. It is very common that conventional processes are effective to process only one of biomass fractions, but does not exploit appropriately (or even degrades) other fractions.[16, 17] This lack of efficiency leads to explore novel methodologies aiming more efficient fractionation of biomass to maximise valorisation of this feedstock.

Two of the ground-breaking methodologies of biomass pre-treatment are the use of ionic liquids (ILs) and supercritical CO_2 ($scCO_2$) as tools for biomass dissolution, pre-treatment, fractionation and catalytic conversion.[11, 18-20] The employment of ILs and $scCO_2$ in chemical processes has been considered as green approaches, being excellent alternatives to volatile organic compounds and hazardous chemicals.

In the last decade, ILs have been used in processing of lignocellulosic biomass demonstrating the ability to dissolve all fractions. Furthermore, ILs alter the physicochemical properties of biomass allowing fractionation superior to conventional pre-treatment processes.[21] Recently, novel methodologies using ILs for the pre-treatment and fractionation of lignocellulosic biomass were developed.[22-24] For instance, protic ILs, such as pyrrolidinium acetate ([pyrr][OAc]), were able to efficiently separate lignin from the carbohydrate fraction of biomass.[23] On the other hand, a cellulose-rich fraction was easily collected as solid material after treating biomass with switchable ILs, such as 1,8-diazabicyclo-[5.4.0]-undec-7-ene-glycerol carbonate, which is capable to dissolve hemicellulose and lignin.[24] Other work showed a complete biomass fractionation into high purity cellulose, hemicellulose and lignin in a three-step process using 1-ethyl-3-methylimidazolium acetate ([emim][OAc]) IL.[25] Furthermore, this IL was recycled and successfully reused up to seven run pre-treatments without efficiency losses.[26] Particularly, [emim][OAc] has been considered to be one of the most efficient ILs in dismantling biomass at moderate temperatures, without simultaneously destroying biomass macromolecular fractions. This feature is one of the main reasons of such an interest in using [emim][OAc] to process biomass.[21, 26]

In this work, an integrated process of biomass fractionation with a focus on the extraction and separation of phenolic compounds is presented. Pre-treatment and fractionation of wheat straw into cellulose, hemicellulose and lignin assisted by [emim][OAc] was performed at first[25] and finally the examined IL was regenerated. The recovered IL, containing a phenolic rich-fraction, was then used to scrutinise the extraction of phenolic compounds by resin adsorption. The physico-chemical nature of polymeric resins determined large differences in the selectivity of adsorption of IL and phenolic compounds. Finally, for the first time, $scCO_2$ extraction was used to purify biomass originated phenolic compound extract from the residual IL.

4.2. Experimental

4.2.1. Materials

Wheat straw was received from Estação Nacional de Melhoramento de Plantas (Portugal) and its composition was determined and is as follows: 38.5 wt.% cellulose, 24.9 wt.% hemicellulose, 17.7 wt.% lignin and 18.9 wt.% other compounds.[27] The moisture of the raw material was determined to be 8 wt.%. The reagents including [emim][OAc] (Iolitec GmbH, Germany - ≥ 95 wt.%), 3 wt.% NaOH solution prepared from NaOH pellets (EKA, Sweden), 4 M HCl solution prepared from HCl fuming 37 wt.% (Merck, Germany) and ethanol 96 vol.% (Merck, Germany) were used for biomass pre-treatment and fractionation process. After pre-treatment, IL was recovered using acetonitrile (99.9 wt.% CARLO ERBA reagents, Italy).

PVPP (Polyclar AT, Biochemical BDH, England) with ≈110 µm particle size; Amberlite XAD-2 (Fluka, Switzerland) with 20/60 mesh, 330 $m^2 \cdot g^{-1}$ surface area and 90 Å pore size; Amberlite XAD-7 (Rohm & Haas Company, USA) with 20/60 mesh, 450 $m^2 \cdot g^{-1}$ surface area and 90 Å pore size; and Silica C18 (LiChroprep®, Merck, Germany) with 25/40 mesh, 320 $m^2 \cdot g^{-1}$ surface area and 100 Å pore size; were used for the extraction of phenolic compounds.

The CO_2 employed in the extraction experiments was purchased from Air Liquid, AlphaGaz™ gamma, Paris, France with ≥ 99.9 wt.% purity. A borate buffer was used for detection of phenolic compounds (in capillary electrophoresis) consisting of 15 mM disodium tetraborate decahydrate (≥99.5 wt.% Merck, Germany) dissolved in 10 vol.% methanol (99.9 wt.%, CARLO ERBA reagents, Italy) aqueous solution (18 $M\Omega \cdot cm^{-1}$ Milli-Q, ELGA Purelab Classic, Portugal) and pH was adjusted to 9. Furthermore, two different stock solutions of phenolic standards with 0.5 $g \cdot L^{-1}$ concentration of each were performed. The first standard stock solution contained vanillin (≥98 wt.% Fluka, Switzerland), vanillic acid (97 wt.% Aldrich, Germany) and syringaldehyde (≥97 wt.% Fluka, Switzerland). The second standard stock solution contained catechol (99 wt.% Sigma, Germany), syringic acid (≥97 wt.% Fluka, Switzerland) and *p*-coumaric acid (≥98 wt.% Fluka, Germany). Gallic acid (≥97.5 wt.% Sigma, Germany) and [emim][OAc] IL were introduced in both stock solutions as internal standards.

4.2.2. Wheat straw pre-treatment and fractionation using [emim][OAc]

The adopted methodology for the pre-treatment and fractionation of wheat straw using [emim][OAc] was presented elsewhere.[25] Briefly, wheat straw (3.5 g) was mixed with [emim][OAc] (70.0 g) in a 100 mL flask and heated up at 120 °C during 6 h under continuous stirring. Afterwards, 3 wt.% NaOH solution (0.56 L) was added to precipitate cellulose-rich fraction. The obtained solid was centrifuged, filtrated and rinsed with distilled water. The filtrate 1 was then concentrated by evapouration and pH was adjusted to 6.8. The resulting solution (approximately 400 mL) was mixed with 3-times volume ethanol 96 vol.% to precipitate hemicellulose rich-fraction. The obtained fraction was centrifuged, filtrated and washed with water. Ethanol was evapourated under reduced pressure from such produced filtrate 2. The resulting solution was acidified by adding HCl solution (4 M) to precipitate lignin-rich fraction. The solution was then placed at 70 °C for 30 min, which increased the efficiency of lignin precipitation. The solution was filtered and the recovered lignin powder was washed with acidified water (pH 2.0) using HCl. The resulting filtrate 3 was used for IL recovery.

4.2.3. Ionic liquid recovery process

The filtrate 3 was neutralised using NaOH pellets and subsequently water was totally evapourated under reduced pressure resulting in precipitation of a solid residue. This residue consisted of formed NaCl salt, IL entrapped in NaCl and biomass which was lost in pre-treatment and fractionation

process. Subsequently, acetonitrile was added in order to extract IL from NaCl. The solid was filtered and the extracted IL was recovered in the filtrate. Acetonitrile was evapourated under reduced pressure leaving IL, which was later dried under vacuum. Finally, after a drying step the recovered IL sample was used to study the extraction of phenolics.

4.2.4. Extraction of phenolic compounds by resin adsorption from ionic liquid sample

Four previously listed resins were examined in the extraction of phenolic compounds from the recovered IL phase. For each adsorption trial, 0.5 g of resin was washed and activated by stirring it with 3.0 mL of acidified water (pH 2.0) for 30 min in a 15 mL vial. Specifically, in case of Silica C18, 3.0 mL methanol was firstly used to activate resin and then 3.0 mL water was added. Afterwards, in case of all resins 2.0 mL solution was removed and 3.0 g of IL sample was placed in the vial. The extraction was then performed by stirring for 30 min at room temperature. Subsequently, the solution was filtered (0.45 μm nylon membrane) and resin was washed 3 times with 15 mL water each. The filtration system was transferred to the oven at 60 °C for 1 h to dry the collected resin to have an effective and equal desorption performance for each examined resin. The dried resin was transferred to a glass flask and 3 mL of methanol 96 vol.% was added under stirring to perform desorption of phenolic compounds from resin. To improve the desorption efficiency, the flask was placed into ultrasound bath (Elma Transsonic T700) for 1 min. Afterwards, the methanol extract was collected and filtered using polypropylene syringe filters (Ø 25 mm, 0.45 μm, FILTER-LAB, Spain). Desorption step was repeated 3 times with 2 mL of methanol corresponding to 9 mL of total methanol extract. Methanol was totally evapourated in the oven to obtain the extract as solid material.

4.2.5. Optimisation methodology for the extraction of phenolic compounds with Amberlite XAD-7 resin

The optimisation methodology was based on Doehlert experimental design[28] considering an experimental distribution for two factors. Fourteen experiments (Table 4.1. - A to H trials, including replicates) were carried out with the independent variables being "adsorption time" (X_1) between 2.0 and 60.0 min and "water content" (X_2) varying between 0 and 5.0 mL. Coded representation of the factors was used for calculation purposes and respective values are presented in Table 4.1.

The analysis was made considering two different responses: Y_1 = total phenolic extraction yield (%); and Y_2 = vanillin extraction yield ($\mu g \cdot g_{biomass}^{-1}$). The model used to express the responses was a second order polynomial model according to following equation $Y = \beta_0 + \beta_1 X_1 + \beta_2 X_2 + \beta_{12} X_1 X_{12} + \beta_{11} X_1^2 + \beta_{22} X_2^2$, where Xs are the experimental factor levels (independent variables - coded units); Y is the experimental response; and βs are parameters of the model (regression coefficients). The β parameters of the polynomial models utilised to estimate the responses have precise meanings: β_0

represents the analysed response in the centre of the experimental domain; β_1 and β_2 indicates the importance of the respective factors (adsorption time and water content, respectively) on the responses; β_{12} is the interaction parameter that indicates how the effect of one factor depends on the level of another factor; β_{11} and β_{22} determine how the response surface folds downward (negative values) or upward (positive values) quadratically, more or less rapidly, depending on the magnitude of the absolute value. SigmaPlot® Systat Software Inc. was used as tool to perform 3D response surface plots to demonstrate the correlation between the independent variables (*X*) and the response variable (*Y*). More details about Doehlert methodology are given in Appendix A (Tables A.1.and A.2.).

Table 4.1. Independent variables studied in this work for phenolic extraction with Amberlite XAD-7 resin and respective coded levels for statistical modelling.

Entry	X_1		X_2	
	Adsorption time (min)	**Coded level**	**Water content (mL)**	**Coded level**
A	30.0	-0.03	1.5	-0.40
B	55.0	0.83	1.5	-0.40
C	5.0	-0.90	1.5	-0.40
D	42.5	0.40	2.8	0.12
E	17.5	-0.47	0.2	-0.92
F	42.5	0.40	0.2	-0.92
G	17.5	-0.47	2.8	0.12
H	5.0	-0.90	4.5	0.80
I	120.0	[a]	0.2	[a]
J	120.0	[a]	4.5	[a]

[a] Not used for Doehlert experimental design

4.2.6. Separation of phenolic compounds using supercritical carbon dioxide

The CO_2 extraction apparatus used in this work is shown in Figure 4.1. Approximately 1.0 mL of phenolic extract obtained from Amberlite XAD-7 was transferred to 6.0 mL high pressure vessel equipped with sapphire window (5 in Figure 4.1.). The extraction vessel was then placed and maintained in water bath (6 in Figure 4.1.) at constant temperature (35 °C). Subsequently, the vessel was pressurised by adding CO_2 to reach 140 bar pressure. The extraction was performed with the CO_2 flowrate of 7.7 x 10^{-3} mol·min^{-1}. The extracted phenolics were collected in a methanol solution (9 in Figure 4.1.). After the extraction, methanol was totally evapourated in oven (60 °C) and the resulting

solid extract was re-dissolved in precisely known volume of methanol (0.5 mL). The resulting sample was then analysed by capillary electrophoresis (CE).

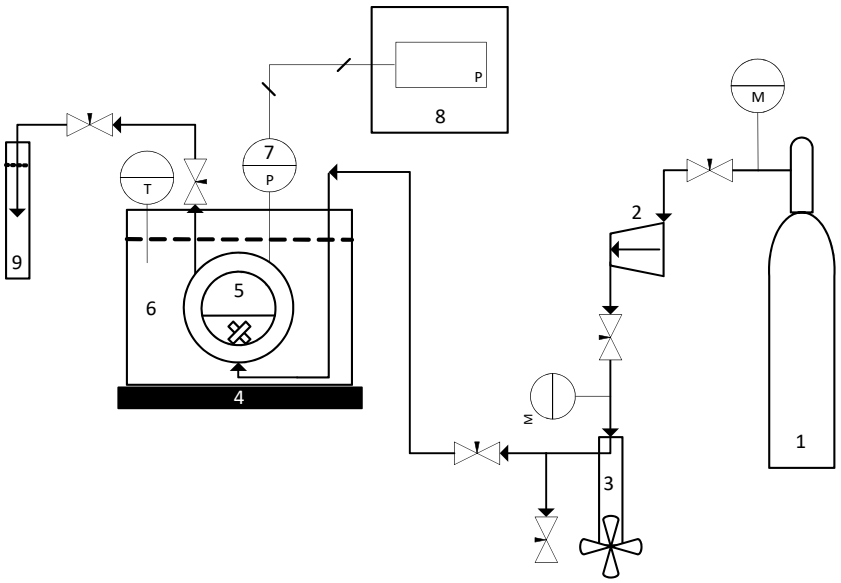

Figure 4.1. Scheme of CO_2 extraction apparatus: 1 - CO_2 cylinder; 2 - condenser (-10 ºC); 3 - manual screen injector; 4 - magnetic stirrer and hot plate; 5 - high pressure vessel with IL phenolic-rich sample and stirrer; 6 - water bath; 7 - pressure transducer; 8 - pressure PID controller; and 9 – phenolic extract collecting vial with methanol solution. M – manometer; P - pressure; and T - temperature.

4.2.7. Analysis of phenolic extracts by capillary electrophoresis (CE)

Capillary electrophoresis technique was used to perform quantitative and qualitative analyses of the phenolic extracts. Separation of standards and extract samples were performed with an Agilent Technologies CE system (Waldbronn, Germany), equipped with a diode array detector (DAD). The Agilent 3D-CE ChemStation data software (Rev B.04.01) was used to perform qualitative and quantitative analyses. An uncoated fused-silica extended light path capillary from Agilent with i.d. 50 µm and 56/64.5 cm length was also used. Between runs the capillary was pre-conditioned by flushing with 1.0 M NaOH and 0.1 M NaOH 3 min each and finally the electrolyte solution (15 mM borate buffer) for 5 min. Samples were filtered through a 0.45 µm membrane filter and were injected directly for 5 s under the pressure of 50 mbar at the anode of the CE system. The separation voltage applied was +30 kV producing approximately 25 µA current. The product monitoring was carried out using direct UV detection. Electropherograms were recorded at wavelengths 200, 280, 320 and 375 nm with a bandwidth of 10 nm.

A quantitative analysis was made using standards of phenolic compounds. The stock solution concentration of phenolic compounds was established as 0.5 $g \cdot L^{-1}$ in 50 vol.% methanol. For

calibration curves, dilutions of stock solutions including 1/2, 1/4, 1/8, 1/16 and 1/32 were performed and analysed in duplicate. For sample analysis, the solid extracts previously obtained were re-dissolved in 1.0 mL of 50 vol.% methanol, filtered, treated with ultrasound and readily analysed in duplicate. Standards and samples were run in parallel to provide the same analysis conditions.

4.2.8. Analysis of phenolic extracts by liquid chromatography coupled with mass spectroscopy (LC/MS)

LC–MS and LC–MS/MS analysis were carried out using a liquid chromatograph Surveyor Plus Modular LC system connected to a LCQ Duo ion trap mass spectrometer equipped with an electrospray ionisation source, from Thermo Scientific (Bremen, Germany). The column used for LC was a LiChroCART® 250-4 LiChrospher® 100 RP-8 column (Merck, Darmstadt, Germany). The extracts were analysed by injection of 25 µL at a concentration of 10 $mg \cdot mL^{-1}$ using a linear gradient composed of solution A (1.0 vol.% formic acid), and solution B (methanol) as follows: 0 min, 70 vol.% A, 30 vol.% B; 20 min, 20 vol.% A, 80 vol.% B; 25 min, 20 vol.% A, 80 vol.% B. The flow was 1.0 $mL \cdot min^{-1}$ and the detection was carried out between 200 nm and 500 nm with a diode array detector (DAD). After the DAD, the flow was split in half before undergoing mass spectrometry analysis. The mass spectrometer was operated in both positive and negative ion modes in the range m/z = 120–1000 and the parameters were adjusted in order to optimise the signal-to-noise ratios for the ions of interest. Briefly, the nebulising and auxiliary gas (nitrogen) flow rates were 40 and 20 (arbitrary units) and the capillary temperature was set to 250 °C. Collision induced dissociation (CID) experiments were performed by isolating the ions within the ion trap and accelerating them in order to suffer multiple collisions with the background gas present in the ion trap (helium) using a data dependent acquisition mode. The ions of interest were activated by applying a percentage of a supplementary a.c. potential in the range of 0.75–1.75 V_{p-p} (peak-to-peak) to the end cap electrodes of the ion trap at the resonance frequency of the selected ion (referred to as the Normalized Collision Energy, NCE). The injection times were 50 ms in a full scan and 200 ms in an MS/MS scan Xcalibur® software from Thermo Scientific was used to acquire and process the data.

4.2.9. Experimental error analysis

Standard uncertainty errors (u) were determined for all performed results. The applied temperature in pre-treatment experiments demonstrated a u(T)=1 °C. All mass determinations were performed using a Mettler Toledo, XS205 dual range scale (Germany) with a given u(m)=0.1 mg. Phenolic extraction experiments were performed in duplicate.

4.3. Results and Discussion

4.3.1. Pre-treatment and fractionation of wheat straw and [emim][OAc] recovery

The process developed in this work aimed the maximal exploitation of biomass in a biorefinery frame. The proposed approach encompassed a production of high purity fractions of cellulose, hemicellulose, lignin and a valorisation of the fraction of phenolic compounds originated from biomass feedstock processing. One of the main advantages of this process is the successful selective fractionation of three main fractions of biomass assisted by [emim][OAc]. In this work, complete dissolution of wheat straw in [emim][OAc] was reached using specific conditions (temperature: 120 °C, reaction time: 6 h, solid/liquid mass ratio: 1/20), confirming the achievements reported in previous works.[26, 29] Furthermore, successful scaling-up of wheat straw fractionation into cellulose, hemicellulose and lignin was achieved and results presented in Table 4.2. are in agreement with those obtained in small scale presented elsewhere.[25]

Table 4.2. Mass balance of wheat straw fractionation process and [emim][OAc] recovery yield.

Entry	Mass input (g)	Mass output (g)	Recovery yield %(w·w^{-1})
Wheat straw	3.20	-	
Cellulose	1.23	1.40	114
Hemicellulose	0.80	0.70	86
Lignin	0.57	0.24	42
[emim][OAc]	70.0	63.8	91

Cellulose was recovered with a yield superior to 100 %(w·w)$^{-1}$, while recovery yields of hemicellulose and lignin fractions were 86 %(w·w)$^{-1}$ and 42 %(w·w)$^{-1}$, respectively. The obtained amount of cellulose fraction was slightly superior to cellulose in the native biomass due to the presence of impurities, such as hemicellulose and lignin. On the other hand, it is noticeable the high amount of lignin that was lost over the process. At the end of the fractionation process, IL was recovered at the level of 91 %(w·w)$^{-1}$. The obtained IL recovery yield demonstrated to be at the same level of those recorded in other work using the same process.[25] Even though, we believe that IL recovery can be enhanced to values near 100 %(w·w)$^{-1}$ by improvements of IL removal from NaCl formed in the last recovery step (section 4.2.3.) that should be addressed in future works. Although it was not the core of the present work, [emim][OAc] could be reused without losing efficiency on biomass pre-treatment as it has been showed elsewhere.[26, 30]

Approximately 250 mL recovered [emim][OAc] was obtained after performing four pre-treatment/fractionation runs, always with fresh IL. However, the original light yellow colour of [emim][OAc] turned to dark brown, as shown in Figure 4.2., suggesting that some biomass components were still present in IL. Actually, it has been stated that accumulation of lignin in IL occurs after IL recycling,[31] which corroborates the fact of reduced mass balance of lignin observed in this work. The main reason could lie in lignin reactions with [emim][OAc] recently revealed.[32, 33] At temperatures higher than 110 °C, in the presence of this IL, lignin undergoes a series of specific cleavages, *e.g.* β-O-4', β-β' and β-5',[33] or methoxyl groups (-OCH_3).[32] Therefore, several lignin-derived compounds with small molecular weight could be produced which are strongly solvated by IL, making difficult the self-aggregation of lignin to recover it as solid material. Due to this phenomenon, the aromatic-based composition of lignin allows the formation of several phenolic compounds, which remain soluble in IL after the recovery process. Additionally, other phenolic compounds naturally present in wheat straw could also remain soluble in IL. The addition of specific anti-solvents in previous biomass fractionation does not allow the precipitation of phenolic compounds, due to their small molecular weight and strong specific interactions with IL. Thus the presence of phenolic compounds in the recovered IL opens the opportunity to scrutinise in this work the extraction and further purification of these value added compounds.

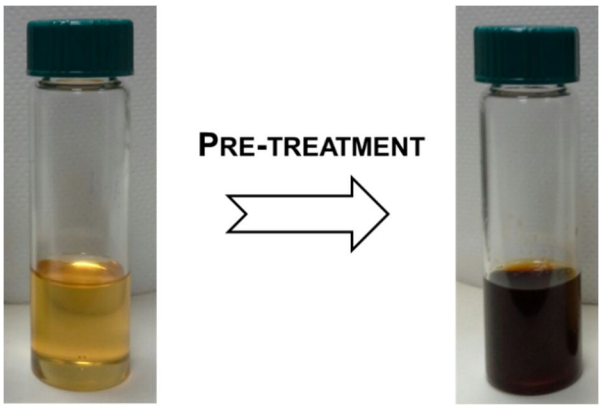

Figure 4.2. [emim][OAc] colour change from yellow (fresh IL before pre-treatment) to dark brown (recovered IL after pre-treatment).

4.3.2. Adsorption of phenolic compounds to polymeric macroporous resins and semi-quantitative analysis

Polymeric resins Amberlite XAD-2 and XAD-7, PVPP and Silica C18 were white after activation and washing. However, as it can be seen in Figure 4.3., the extraction turned resins to a brownish, from dark to light.

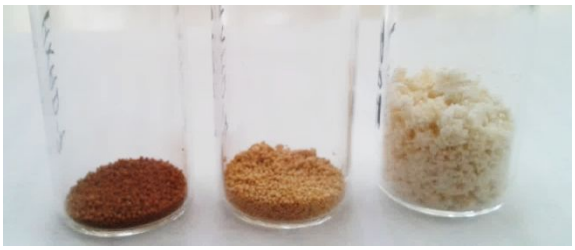

Figure 4.3. Amberlite XAD-7, Amberlite XAD-2 and PVPP resins (from left to right) after the extraction step (Silica C18 is not shown).

Desorption of phenolic compounds from polymeric resins was performed and the extracts were analysed by capillary electrophoresis (CE). The qualitative results obtained for Amberlite XAD-7 extract are demonstrated in Figure 4.4. These results are also representative for extracts obtained with XAD-2 and Silica C18, as the same phenolic profile was observed. The approached CE method showed an efficient detection and separation of phenolic compounds in only 12 min run. Depending on the selected wavelength in CE analysis, different phenolic compounds can be identified. It is possible to observe that at 200 nm the highest absorbance was found, which corresponds to major molar absorptivity of phenolic compounds. Nonetheless, other examined wavelengths allowed better detection of specific phenolic compounds. At 280 nm, catechins with diverse molecular mass produce a characteristic region on the recorded electropherogram. Furthermore, at the same wavelength, *p*-coumaric and vanillic acids were also identified. For other wavelengths, such as 320 and 375 nm, vanillin was detected. Unavoidable is the presence of IL in all extracts obtained for each examined resin. The detection of IL is considerably high at 200 nm wavelength as observed in both Figures 4.4. and 4.5.

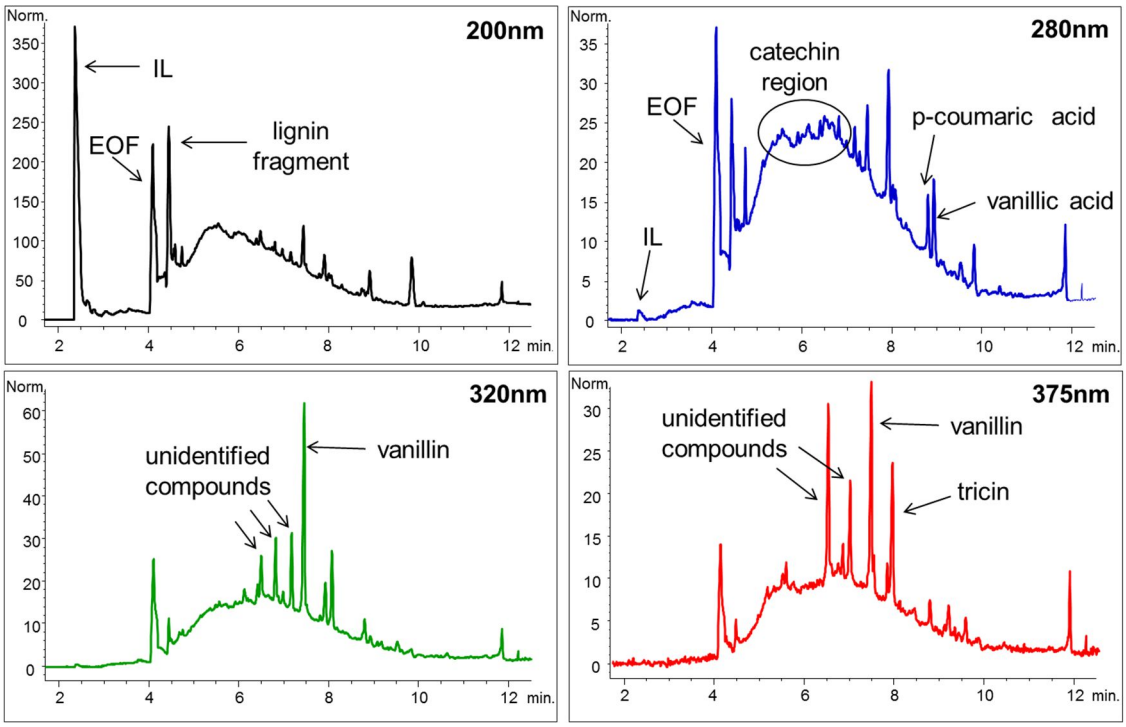

Figure 4.4. The phenolic adsorption profiles after the use of Amberlite XAD-7 depicted on electropherograms recorded at 200, 280, 320 and 375 nm. The identification of all listed compounds was done by electrophoretic comparison (migration times and spectra) with authentic standards except for lignin fragment and tricin detected as mentioned above.

In case of PVPP resin, an impressive selectivity for only two compounds, namely tricin and a lignin fragment was observed as it is depicted in Figure 4.5. The identification of such compounds was accomplished with LC-MS/MS analysis using negative ionisation mode ($[M-H]^-$), which allowed the detection of two main ions. The first product ion at m/z = 329 was associated to tricin (M=330). MS^2 and MS^3 analysis showed a fragmentation pathway with consecutive removal of two methyl groups (m/z = 314 and m/z = 299)[34] derived from methoxyl groups present in tricin structure (Figure 4.5.). Furthermore, the UV/VIS spectrum of this compound confirmed to be the fingerprint of the aglycone form of tricin.[35] The second product ion at m/z = 723 demonstrated complex fragmentation after performing MS^2 and MS^3 analysis. Nevertheless, MS fragmentation (m/z = 677/451/225 $[M-H]^-$) indicates a possible trimer phenolic compound derived from tricaffeoylquinic acid.[36] The relative high molecular mass and the MS fragmentation pathway led to associate this compound to a specific lignin fragment generated from biomass processing with IL. Notwithstanding of the high selectivity of PVPP resin for tricin and lignin fragment, these two compounds were also extracted by the other resins (Figure 4.4.).

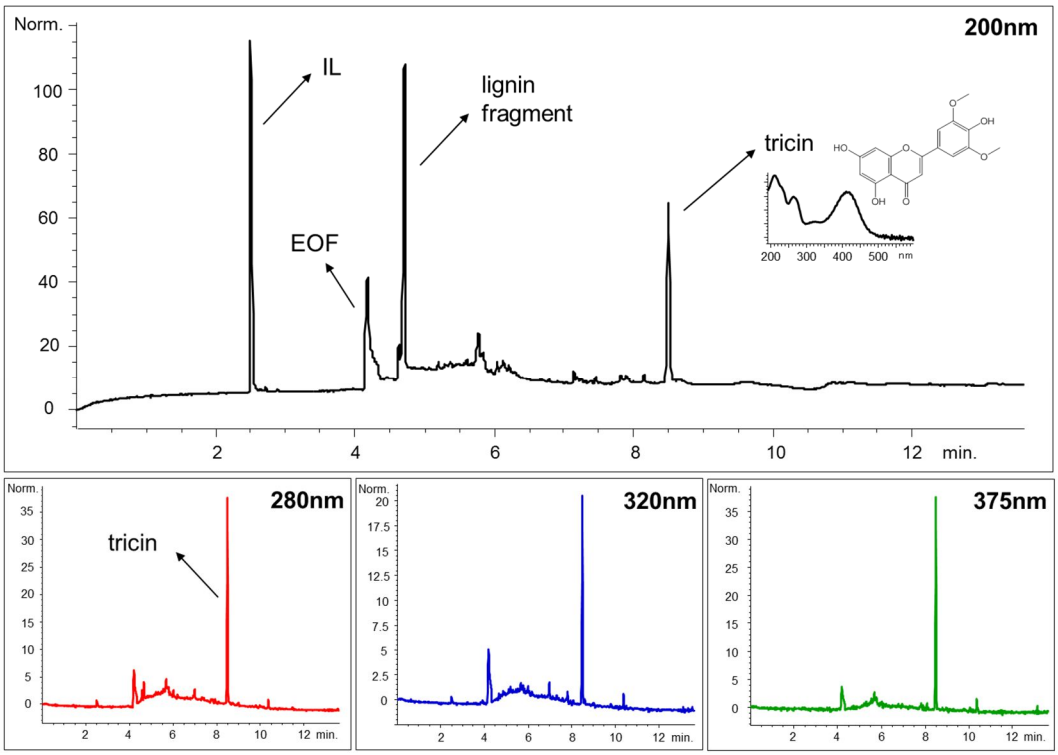

Figure 4.5. The phenolic adsorption profile after the extraction with PVPP registered on electropherograms recorded at 200, 280, 320 and 375 nm. Tricin and lignin fragment were identified by LC-MS.

A semi-quantitative analysis was performed to evaluate the efficiency and selectivity of each resin for the extraction of phenolic compounds from the recovered IL. The analysis of IL waste stream would support the evaluation of real adsorption ability of resins by determining the amount of phenolic compounds that were not adsorbed to the polymeric material. Nevertheless, quantification of phenolic content by standard methods, such as Folin-Ciocalteau colorimetric method,[37] was unsuccessfully approached in this work. The presence of [emim][OAc] create a complex with Folin-Ciocalteau reagent constituted by phosphomolybdate and phosphotungstate guiding to its precipitation. FTIR analysis of precipitate demonstrated a possible complexation between imidazolium ring of imidazolium-based ILs and Folin-Ciocalteau composing acids as reported elsewhere.[38] Even CE analysis of IL waste stream was unsuccessful due to high ionic strength of the sample. Therefore, evaluation of resin efficiency was based on the data obtained after desorption of phenolic compounds from resins (extracts). Particularly, the absorption areas of total phenolic compounds detected at the examined wavelengths (200, 280, 320 and 375 nm) was compared between each extract as shown in Figure 4.6. On the other hand, the selectivity was studied comparing the absorption area of total phenolic compounds at 200 nm with the absorption area of residual IL at the same wavelength.

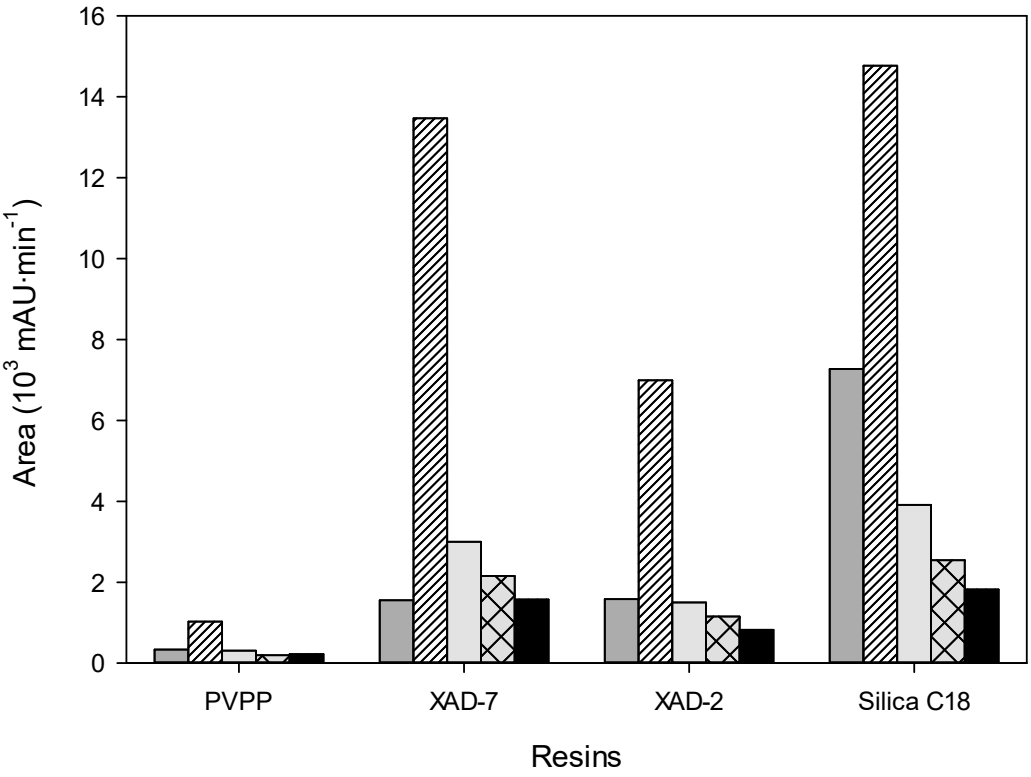

Figure 4.6. Extraction performance of phenolic compounds for the examined resins. Absorption area of IL at 200 nm (▭), and total phenolic compounds at 200 nm (▨), 280 nm (▭), 320 nm (▨) and 375 nm (■) obtained with CE analysis.

The efficiency of phenolic compound adsorption was the highest in Silica C18 and reduced in the following order: Silica C18> Amberlite XAD-7 > Amberlite XAD-2 > PVPP. The strong nonpolar character of long carbon chains in Silica C18 is the main factor to obtain higher amount of extracted phenolic compounds. Essentially, adsorption is made by strong nonpolar interactions established between the hydrophobic surface of Silica C18 with π-systems (aromatic rings) of phenolic compounds and with nonpolar methoxyl groups present in most of them, *e.g.* vanillin and tricin. Furthermore, silanol groups of Silica C18 could be responsible for hydrogen bond interactions with polar phenolic compounds.[39] On the other hand, Silica C18 resin is poorly selective and in comparison to other resins, the highest amount of phenolic compounds present was accompanied by the highest quantity of residual IL extracted.

Among examined Amberlite type resins, XAD-7 demonstrated higher efficiency than XAD-2 for phenolic adsorption. Amberlite XAD-2 favours π-π interactions between aromatic rings of nonpolar phenolic compounds and benzene rings of polystyrene cross-linked resin,[40] while the polyacrylic ester structure of Amberlite XAD-7 allows not only the interaction with non-polar phenolic compounds but also with moderate polar ones. As an example of the last ones can be given a formation of strong

hydrogen bonds between the ester groups on the surface of XAD-7 resin beads and hydroxyl groups of phenolic molecules.[41] Actually, Amberlite XAD-7 presented an overall better performance among the examined resins considering the efficiency and selectivity studied parameters. Albeit higher amount of phenolic compounds were recovered with Silica C18 resin, Amberlite XAD-7 demonstrated lower interaction with IL, which means higher selectivity for the recovery of phenolic compounds. For instance, the ratio of absorption areas between phenolic compounds and IL, both at 200 nm, is much higher for Amberlite XAD-7 (8.7) than for Silica C18 (2.0). This can be explained by the physical nature of long carbon chains in Silica C18 that helps to retain higher amount of IL than the acrylic ester resin. Therefore, Amberlite XAD-7 was chosen for the optimisation of phenolic compound extraction as presented below.

PVPP was clearly the most ineffective resin among all examined resins (Figure 4.6.). According to other works, PVPP has the ability to form strong interactions with polyphenolic compounds (higher molecular weight phenolic compounds), such as tannins,[42] which may justify this selectivity only towards tricin and the lignin fragment. Fundamentally, the interactions between phenolic compounds and PVPP have been associated to hydrogen bonds of phenolic compounds' OH groups and carbonyl group of pyrrolidone, but also π system overlap between aromatic rings of phenolic compounds and pyrrolidone rings could be established.[43] Indeed, it was verified that PVPP ineffectively recovers lower molecular weight phenolic compounds, such as several types of catechins and phenolic acids from brewery waste stream.[44]

4.3.3. Optimisation of phenolic compound extraction using Amberlite XAD-7 resin

In order to optimise the extraction of phenolics, the best performer Amberlite XAD-7 resin was employed. Adsorption time and water content present in the extraction system were evaluated following the Doehlert experimental design as described in section 4.2.5. After the extraction trials, produced samples were analysed by CE. For all applied extraction conditions, the determined absorption areas for each detection wavelength showed similar behaviours. To demonstrate it, the absorption area of total phenolic compounds acquired at 200 nm wavelength for each extraction trial (A to J) is shown in Figure 4.7.

Among the performed experiment, the lowest extraction yields were observed for trials at 5 min adsorption time (C and J). The increase in time allowed to attain higher phenolic adsorption reaching 79 % extraction yield at 42.5 min (D). Furthermore, it can be observed that the amount of extracted phenolic compounds remained constant up to 120.0 min (H and I).

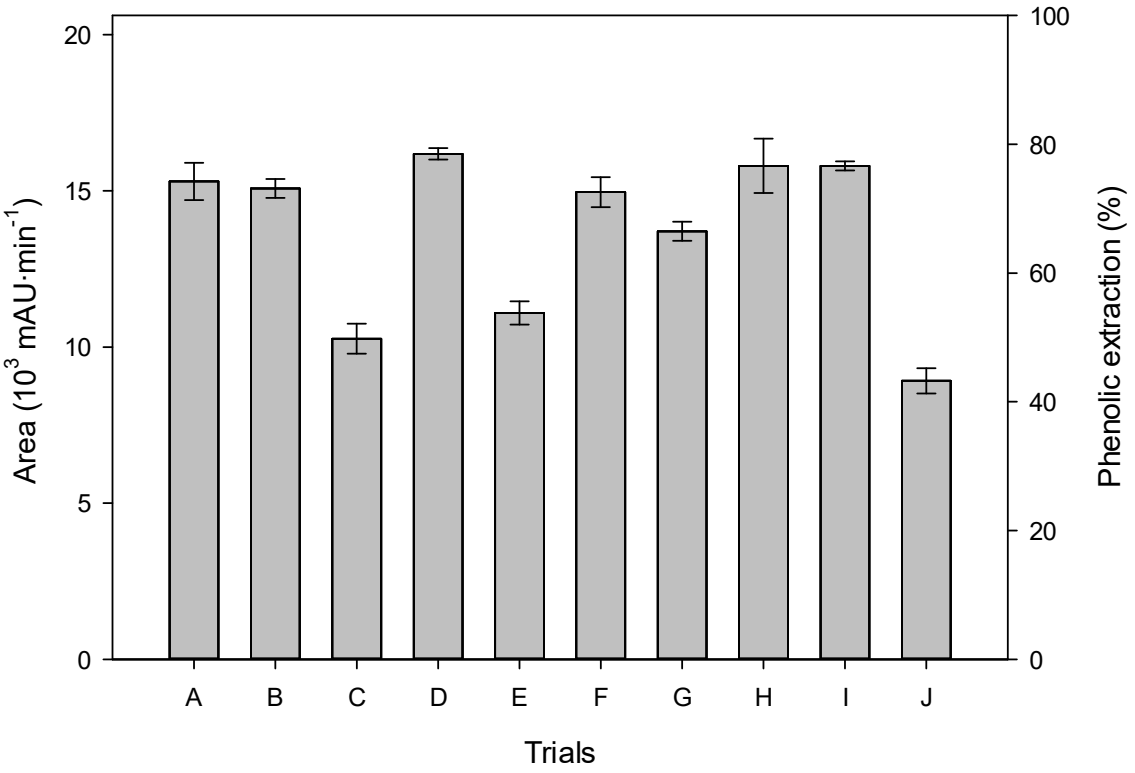

Figure 4.7. The dependence of the absorption area of total phenolic compounds at 200 nm and corresponding extraction yield on the extraction condition trials. The calculation of extraction yield was based on a trial with 3 times more resin (1.5 g) using the best extraction conditions found. In this specific trial the adsorption area of total phenolic compounds was considered as maximal.

On the other hand, comparing data of trials with the same adsorption time (*e.g.* 17.5 min) but different water content, E (0.2 mL) and G (2.8 mL), the adsorption of phenolic compounds raised with an increase of water content, from 54 % to 66 % of extraction yield. However, at reduced adsorption time (5.0 min), the increase in water content from C (0.2 mL water) and J (4.5 mL water) trials had a negative impact because the phenolic extraction yield decreased from 50 % to 43 %. These results indicate that low water content (0.2 mL – 28.5 wt%) allow to generate stronger interaction between IL and phenolic compound is stronger, reducing the adsorption efficiency of resin. On the contrary, at higher water contents (2.8 mL – 55.8 wt%) the interaction between phenolic compounds/resin is favoured due to the diluting effect of water that weakens IL/phenolic compound interactions. However, at some point, high dilution of the sample (4.5 mL – 64.7 wt%) reduces the efficiency of resin to adsorb the desired compounds. Therefore, the presence of water highly influences the adsorption process by changing the interactions established between IL/phenolic compounds and phenolic compounds/resin. It has been stated that water could decrease the solubility of phenolic compounds increasing the adsorption efficiency of resins.[45] The presence of water alters the physical

properties of solution, such as density, dynamic viscosity and dielectric constant, which in turn change the diffusion, activity coefficient and solvation of phenolic molecules in IL.[45]

In order to optimise the effect of the principal independent variables (adsorption time (X_1) and water content (X_2)) on the efficiency of total phenolic (Y_1) and vanillin (Y_2) extractions, the Doehlert experimental design was employed as presented in Table 4.1. The statistical data obtained after performing a multiple linear regression analysis is shown in Figure 4.8. as response surface models.

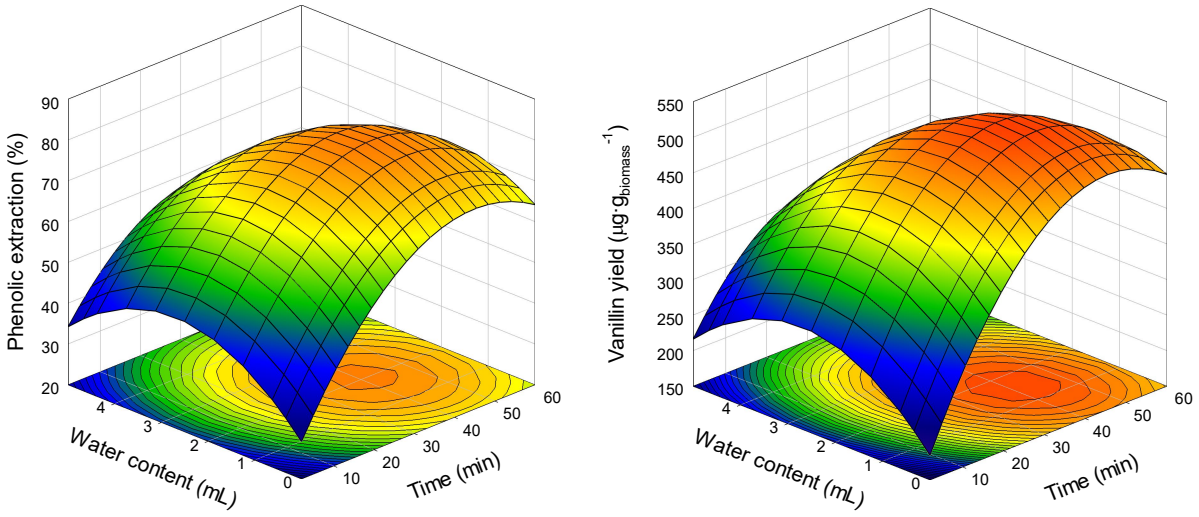

Figure 4.8. 3D response surfaces and contour plots of modelled phenolic extraction (left) and vanillin yields (right) using Amberlite XAD-7 resin as a function of water content and adsorption time.

The optimum condition set obtained after the statistical modelling analysis for Y_1 was 40.9 min adsorption time and 2.0 mL water content within the system. At this condition, the estimated total phenolic extraction yield is as high as 78.8 %. The optimal conditions for the response Y_2 were 41.3 min adsorption time and 1.6 mL water content, which give 518 $\mu g \cdot g_{biomass}^{-1}$ vanillin.

The model was validated by performing the adsorption experiments at the optimal conditions with Amberlite XAD-7 resin. The experimental value for the total phenolic extraction was 75.5 %, while in case of vanillin, extraction the experimental validations allowed to obtain 593 $\mu g \cdot g_{biomass}^{-1}$ confirming the theoretical values obtained from Doehlert experimental design. The obtained vanillin extraction yield is almost 17 times higher than that obtained in the pre-treatment of eucalyptus with [emim][OAc] at 160 °C for 3 h (approximately 35 $\mu g \cdot g_{biomass}^{-1}$).[46] In this case, high temperature negatively affected vanillin yield, once it promotes the cleavage of the methyl ketone of vanillin to produce guaiacol.[46] However, the value of vanillin yield achieved in the present work is considerably low when compared to the extraction of natural vanillin from vanilla pods.[47, 48] For instance, microwave treatment of vanilla pods with ethanol/water solutions resulted in almost 30-fold vanillin

yield in comparison to that obtained herein.[47] One of the most obvious reason is the fact that vanillin is not naturally present in wheat straw in contrary to vanilla pods. However, the obtained results show that vanillin can be generated in the course of lignin transformation during wheat straw pre-treatment with [emim][OAc]. It is also important to stress that, the employed biomass pre-treatment with IL allowed to obtain several other bioactive phenolic compounds from lignin.

Although Amberlite XAD-7 provided the best extraction performance among the examined resins in this work, tailor-made resins could be an alternative to enhance the extraction of phenolic compounds from IL stream. The literature results show[49, 50] that specific post-cross-link processing allows to create hyper-cross-linked resins which present specificity to adsorb aromatic compounds. These types of resins are known to have controllable chemical structure, adequate pore definition and outstanding regeneration performance.[51-54]

4.3.4. Carbon dioxide as tool for separation of phenolic compounds from ionic liquid

As mentioned before, the application of polymeric resins allowed the extraction of phenolic compounds and a residual quantity of IL. Therefore, a demand for further purification of phenolic compounds from IL was required in the virtue of future applications in food/feed or pharmaceutical industries. The extraction of phenolic compounds with CO_2 has been demonstrated elsewhere either when phenolic compounds were present in aqueous[55] or methanol[56] solutions or in natural solid matrixes, such as seeds[57] and plant leaves.[58] Given the practically unmeasurable solubility of ILs in CO_2, a first attempt of phenolic compound separation from ILs, specifically [emim][OAc], assisted by CO_2 was demonstrated in this work. After using 15.1 mol CO_2, a succeeded extract enriched in phenolic compounds without any trace of [emim][OAc] was attained as demonstrated by CE analysis data in Figure 4.9. Vanillin appeared to be main phenolic compound in the resulting extract. This can be justified by the highest solubility of vanillin in CO_2 ($\approx 2.0 \cdot 10^{-2}$ mol%)[59] in comparison to other phenolic compounds, for instance, vanillic acid ($8.5 \cdot 10^{-6}$ mol%)[60] and *p*-coumaric acid (1.5×10^{-7} mol%)[61] under conditions similar to those used in this work. Furthermore, CO_2 extraction allowed identifying other phenolic compounds, such as *p*-hydroxybenzaldehyde, syringaldehyde and vanillin derivatives that were not detected in the initial phenolic extract obtained with resins. Therefore, it can be stated that CO_2 at 140 bar and 35 ºC presents physicochemical properties that are useful for the extraction of vanillin, vanillin derivatives (vanillic acid) and other compounds with similar chemical structure (*p*-hydroxybenzaldehyde, syringaldehyde, *p*-coumaric acid). On the contrary, flavonoids like tricin and catechins were barely extracted by CO_2, but this can be explained by relatively higher polarity of catechins than vanillin-like compounds. On the other hand, some small amount of catechins detected in extract could be an effect of the methanol content in the initial sample that slightly increases the polarity of CO_2 as extraction solvent. Additionally, it is important to observe that the

lignin fragment detected by CE was extracted by CO_2 also, suggesting that this fraction has strong affinity to CO_2. Other important aspect is that after extraction with CO_2 the amount of IL was still intact in the remaining solid residue as can be observed in Figure A.1. in Appendix A.

At last, it is important to point out that application of CO_2 as extracting solvent of phenolic compounds is viable if high concentration of phenolic compounds is present in the starting solution. This was accomplished with the application of polymeric resins that allowed pre-concentration of phenolic compounds out of the IL stream.

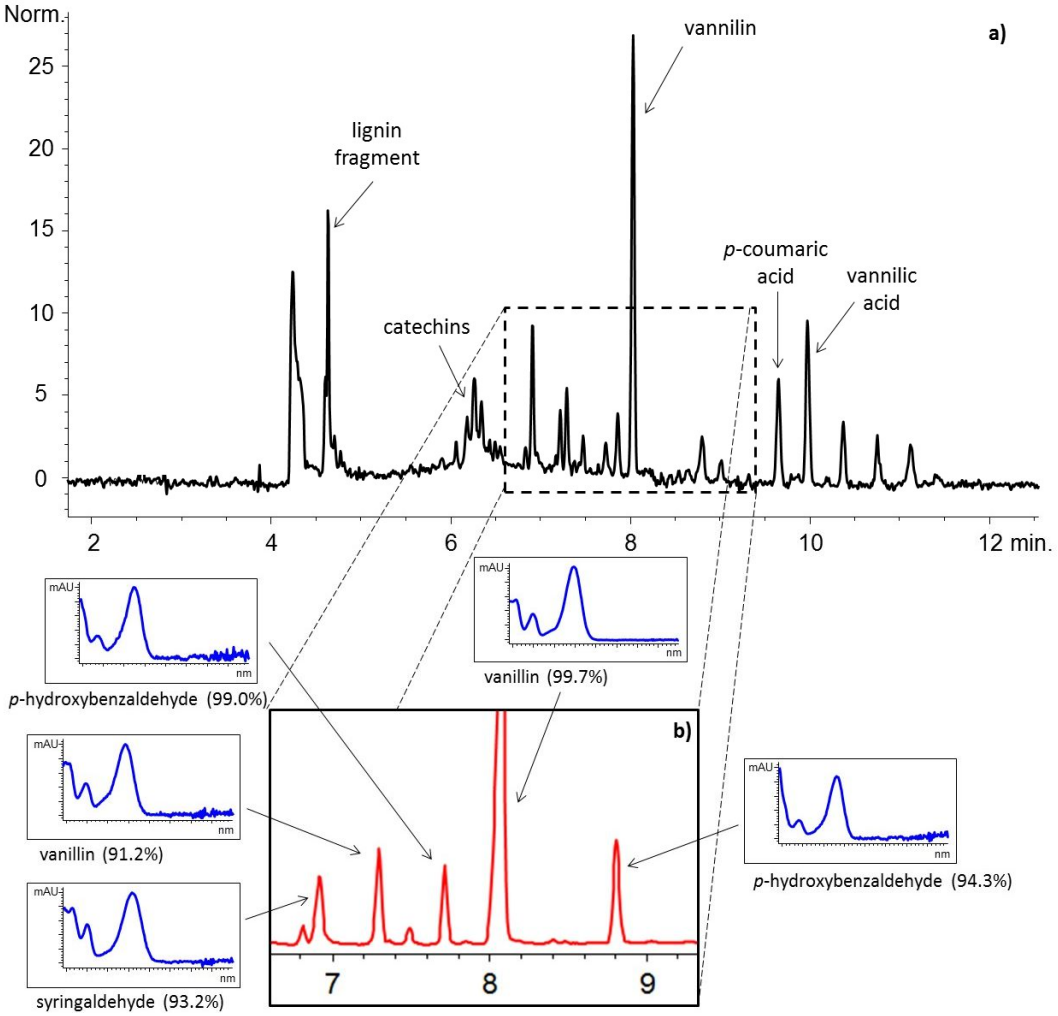

Figure 4.9. a) Phenolic adsorption profile of the extract obtained after CO_2 extraction recorded at 200 nm wavelength. b) Amplification of CE electropherogram recorded at 320 nm, showing the identification of vanillin, *p*-hydroxybenzaldehyde and other vanillin derivatives. Identification of all compounds, except lignin fragment, was done by electrophoretic comparison (migration times and spectra) with authentic standards.

4.4. Conclusion

An integrated process including biomass pre-treatment, fractionation and extraction of phenolic compounds was developed herein. The use of ionic liquids, application of polymeric resins and subsequent CO_2 extraction technology demonstrates novel, sustainable and green approach of biomass processing.

The production of phenolic compounds as high valuable products has a positive impact on this type of processing. The employment of polymeric resins demonstrated to be efficient in the recovery of phenolic compounds from IL. Amberlite XAD-7 resin presented the best performance in the adsorption process, while PVPP resin confirmed high selectivity for higher molecular weight phenolic compounds. Nevertheless, polymeric resins do not avoid minimal contamination by IL in the extracted samples. This limitation was successfully overcome by applying supercritical CO_2 to the extracted samples. This approach allowed to purify the extract of phenolic compounds without co-extraction of IL.

The integrated process developed in this work shows a new pathway of more sustainable and green valorisation of biomass in the frame of the biorefinery concept by producing cellulose, hemicellulose, lignin and bioactive phenolic compounds as high purity fractions. This poses an exploitation of green solvents (ILs and CO_2) as promising alternative to the conventional biomass processing.

4.5. References

1. F. M. Girio, C. Fonseca, F. Carvalheiro, L. C. Duarte, S. Marques and R. Bogel-Lukasik, *Bioresource Technol.*, 2010, **101**, 4775-4800.
2. S. K. Brar, G. S. Dhillon and C. R. Soccol, *Biotransformation of waste biomass into high value biochemicals*, Springer, 2014.
3. J. Zakzeski, P. C. Bruijnincx, A. L. Jongerius and B. M. Weckhuysen, *Chem. Rev.*, 2010, **110**, 3552-3599.
4. J. Dai and R. J. Mumper, *Molecules*, 2010, **15**, 7313-7352.
5. F. Shahidi and M. Naczk, *Phenolics in food and nutraceuticals*, CRC press, 2003.
6. O. Pourali, F. S. Asghari and H. Yoshida, *Chem. Eng. J.*, 2010, **160**, 259-266.
7. S. Sarkar, V. H. Alvarez and M. D. A. Saldana, *J. Supercrit. Fluid.*, 2014, **93**, 27-37.
8. T. Y. Nguyen, C. M. Cai, R. Kumar and C. E. Wyman, *ChemSusChem*, 2015, **8**, 1716-1725.
9. V. B. Agbor, N. Cicek, R. Sparling, A. Berlin and D. B. Levin, *Biotechnol. Adv.*, 2011, **29**, 675-685.
10. A. George, A. Brandt, K. Tran, S. N. S. M. S. Zahari, D. Klein-Marcuschamer, N. Sun, N. Sathitsuksanoh, J. Shi, V. Stavila, R. Parthasarathi, S. Singh, B. M. Holmes, T. Welton, B. A. Simmons and J. P. Hallett, *Green Chem.*, 2015, **17**, 1728-1734.
11. C. Zetzl, K. Gairola, C. Kirsch, L. Perez-Cantu and I. Smirnova, *Chem. Ing. Tech.*, 2011, **83**, 1016-1025.
12. P. Pollet, E. A. Davey, E. E. Urena-Benavides, C. A. Eckert and C. L. Liotta, *Green Chem.*, 2014, **16**, 1034-1055.
13. D. A. Cantero, M. D. Bermejo and M. J. Cocero, *J. Supercrit. Fluid.*, 2015, **96**, 21-35.
14. S. P. Magalhães da Silva, A. R. C. Morais and R. Bogel-Lukasik, *Green Chem.*, 2014, **16**, 238-246.
15. S. Hyvarinen, J. P. Mikkola, D. Y. Murzin, M. Vaher, M. Kaljurand and M. Koel, *Catal. Today*, 2014, **223**, 18-24.
16. M. H. L. Silveira, A. R. C. Morais, A. M. da Costa Lopes, D. N. Olekszyszen, R. Bogel-Lukasik, J. Andreaus and L. Pereira Ramos, *ChemSusChem*, 2015, **8**, 3366-3390.
17. Y. Sun and J. Y. Cheng, *Bioresource Technol.*, 2002, **83**, 1-11.
18. A. R. C. Morais, A. C. Mata and R. Bogel-Lukasik, *Green Chem.*, 2014, **16**, 4312-4322.
19. A. M. da Costa Lopes and R. Bogel-Lukasik, *ChemSusChem*, 2015, **8**, 947-965.
20. A. R. C. Morais, A. M. da Costa Lopes and R. Bogel-Lukasik, *Chem. Rev.*, 2015, **115**, 3-27.
21. A. Brandt, J. Grasvik, J. P. Hallett and T. Welton, *Green Chem.*, 2013, **15**, 550-583.
22. A. M. da Costa Lopes, K. G. João, E. Bogel-Lukasik, L. B. Roseiro and R. Bogel-Lukasik, *J. Agric. Food Chem.*, 2013, **61**, 7874-7882.
23. E. C. Achinivu, R. M. Howard, G. Li, H. Gracz and W. A. Henderson, *Green Chem.*, 2014, **16**, 1114-1119.
24. I. Anugwom, P. Maki-Arvela, P. Virtanen, S. Willfor, P. Damlin, M. Hedenstrom and J. P. Mikkola, *Holzforschung*, 2012, **66**, 809-815.
25. S. P. Magalhães da Silva, A. M. da Costa Lopes, L. B. Roseiro and R. Bogel-Lukasik, *RSC Adv.*, 2013, **3**, 16040-16050.
26. A. M. da Costa Lopes, K. G. Joao, D. F. Rubik, E. Bogel-Lukasik, L. C. Duarte, J. Andreaus and R. Bogel-Lukasik, *Bioresource Technol.*, 2013, **142**, 198-208.
27. F. Carvalheiro, T. Silva-Fernandes, L. C. Duarte and F. M. Gírio, *Appl. Biochem. Biotechnol.*, 2009, **153**, 84-93.
28. D. H. Doehlert, *Roy. Stat. Soc. C*, 1970, **19**, 231-239.
29. N. Sun, M. Rahman, Y. Qin, M. L. Maxim, H. Rodriguez and R. D. Rogers, *Green Chem.*, 2009, **11**, 646-655.
30. H. Wu, M. Mora-Pale, J. J. Miao, T. V. Doherty, R. J. Linhardt and J. S. Dordick, *Biotechnol. Bioeng.*, 2011, **108**, 2865-2875.
31. S. H. Lee, T. V. Doherty, R. J. Linhardt and J. S. Dordick, *Biotechnol. Bioeng.*, 2009, **102**, 1368-1376.
32. Y. Qu, H. Luo, H. Li and J. Xu, *Biotechnol. Rep.*, 2015, **6**, 1-7.
33. J.-L. Wen, T.-Q. Yuan, S.-L. Sun, F. Xu and R.-C. Sun, *Green Chem.*, 2014, **16**, 181-190.

34. J. M. Duarte-Almeida, G. Negri, A. Salatino, J. E. de Carvalho and F. M. Lajolo, *Phytochemistry*, 2007, **68**, 1165-1171.
35. M. Estiarte, J. Penuelas, S. Canigueral and I. Casals, *Cereal Chem.*, 1997, **74**, 495-496.
36. R. Jaiswal and N. Kuhnert, *J. Agric. Food Chem.*, 2011, **59**, 4033-4039.
37. V. L. Singleton, R. Orthofer and R. M. Lamuela-Raventos, *Methods Enzymol.*, 1999, 152-178.
38. T. Aid, M. Kaljurand and M. Vaher, *Anal. Methods*, 2015, **7**, 3193-3199.
39. F. Gritti and G. Guiochon, *J. Chromatogr. A*, 2004, **1028**, 75-88.
40. A. M. Li, Q. X. Zhang, J. L. Chen, Z. G. Fei, L. Chao and W. X. Li, *React. Funct. Polym.*, 2001, **49**, 225-233.
41. X. Qiu, N. Li, X. Ma, S. Yang, Q. Xu, H. Li and J. Lu, *J. Environ. Chem. Eng.*, 2014, **2**, 745-751.
42. M. Schubert and M. A. Glomb, *J. Agric. Food Chem.*, 2010, **58**, 8300-8304.
43. P. J. Magalhaes, J. S. Vieira, L. M. Goncalves, J. G. Pacheco, L. F. Guido and A. A. Barros, *J. Chromatogr. A*, 2010, **1217**, 3258-3268.
44. L. Barbosa-Pereira, I. Angulo, P. Paseiro-Losada and J. M. Cruz, *Food Res. Int.*, 2013, **51**, 663-669.
45. E. M. Silva, D. R. Pompeu, Y. Larondelle and H. Rogez, *Sep. Purif. Technol.*, 2007, **53**, 274-280.
46. P. Varanasi, P. Singh, M. Auer, P. D. Adams, B. A. Simmons and S. Singh, *Biotechnol. Biofuels*, 2013, **6**, 14.
47. Z. Z. Dong, F. L. Gu, F. Xu and Q. H. Wang, *Food Chem.*, 2014, **149**, 54-61.
48. A. Sharma, S. C. Verma, N. Saxena, N. Chadda, N. P. Singh and A. K. Sinha, *J. Sep. Sci.*, 2006, **29**, 613-619.
49. X. Jiang and J. Huang, *J. Colloid Interface Sci.*, 2016, **467**, 230–238.
50. X. Ling, H. Li, H. Zha, C. He and J. Huang, *Chem. Eng. J.*, 2016, **286**, 400-407.
51. H. Li, Z. Fu, C. Yan, J. Huang, Y.-N. Liu and S. I. Kirin, *J. Colloid Interface Sci.*, 2016, **463**, 61-68.
52. K. Li, Y. Wang, M. Huang, H. Yan, H. Yang, S. Xiao and A. Li, *J. Colloid Interface Sci.*, 2015, **455**, 261-270.
53. Z. Zhang, F. Wang, W. Yang, Z. Yang and A. Li, *Chem. Eng. J.*, 2016, **283**, 1522-1533.
54. X. Wang, Z. Fu, N. Yu and J. Huang, *J. Colloid Interface Sci.*, 2016, **466**, 322-329.
55. C. Boukouvalas, V. Louli and K. Magoulas, *Sep. Sci. Technol.*, 2001, **36**, 2279-2291.
56. M. D. A. Saldana, B. Tomberli, S. E. Guigard, S. Goldman, C. G. Gray and F. Temelli, *J. Supercrit. Fluid.*, 2007, **40**, 7-19.
57. M. Palma and L. T. Taylor, *J. Chromatogr. A*, 1999, **849**, 117-124.
58. J. L. Mau, P. T. Ko and C. C. Chyau, *Food Res. Int.*, 2003, **36**, 97-104.
59. M. Skerget, L. Cretnik, Z. Knez and M. Skrinjar, *Fluid Phase Equilib.*, 2005, **231**, 11-19.
60. R. Murga, M. T. Sanz, S. Beltran and J. L. Cabezas, *J. Chem. Eng. Data*, 2004, **49**, 779-782.
61. R. Murga, M. T. Sanz, S. Beltran and J. L. Cabezas, *J. Supercrit. Fluid.*, 2003, **27**, 239-245.

CHAPTER V

Selective processing of biomass by an acidic ionic liquid

This chapter is based on data and information of the following publication:

A. V. Carvalho, A. M. da Costa Lopes and R. Bogel-Lukasik, Relevance of the acidic 1-butyl-3-methylimidazolium hydrogen sulphate ionic liquid in the selective catalysis of biomass hemicellulose fraction, *RSC Adv.*, 2015, **5**, 47153-47164.

5.1. Introduction

The increasing demands for energy, fuels and chemicals force to seek for alternative sources of these commodities. Accordingly, finding new technologies and development of novel processes to bring this growth in line with the social demand for sustainability are major challenges for current and future generations. A biorefinery might be one of the ways to achieve this goal. A biorefinery aims to use biomass which is a readily available and low-cost feedstock and is one among a few resources that can facilitate the large-scale and sustainable production of the substantial volumes of energy and materials.[1] Normally, biomass referred to lignocellulosic feedstock is constituted by three major biopolymers: cellulose, hemicellulose and lignin which have specific and diverse properties. The strong intra- and intermolecular interaction established between these biomacromolecular components make lignocellulosic biomass a recalcitrant material, thus a pre-treatment process is required.

The major purpose of biomass pre-treatment is to process lignocellulosic feedstocks to make it more subjectable for further processing.[2,3] The pre-treatment exposes biomass fractions to biological and/or chemical treatments aiming further valorisation towards particular products or pivot chemicals.[4] However, to achieve this goal various challenges must be addressed. Furthermore, depending on the expected results, the most adequate pre-treatment method can be selected. In addition, the choice of pre-treatment should consider the overall compatibility of feedstocks, enzymes and organisms to be applied, overall economic assessment and environmental impact.[5] Up to now, several methodologies have been used to develop low cost pre-treatments to generate cellulose- and hemicellulose-originated sugar-rich liquors.[5] One of the approaches is the use of more sustainable solvents such as ionic liquids[6-19] and supercritical fluids.[20-24]

Ionic liquids (IL) are known as organic salts with melting points below 100 ºC composed solely of cations and anions. The possible choices of cations and anions allow to produce numerous ILs with various physicochemical properties.[25,26] One of the dominant applications of ILs are separation and extraction processes.[27-34] Dissolution of lignocellulosic biomass with ILs has been referred as an innovative process where the physicochemical properties of the original biomass are altered in a way not observed before by other solvents.[35-38] Interactions between lignocellulosic biomass and ILs are intricate due to the presence of lignin and extractives, as well as because of the recalcitrance inherent to these materials.[10,39] The efficiency of lignocellulosic biomass pre-treatment in ILs is associated to the hydrogen bond basicity which is generally governed by the IL anion behaviour. Generally, anions with strong hydrogen bond basicity can effectively weaken the hydrogen bond network of the biomass polymers.[17] Thus, pre-treatment of biomass with ILs offers advantages over conventional methods allowing to alter physicochemical properties of the biomass macromolecular components, such as reduction of the cellulose crystallinity, extraction of specific macromolecules, such as lignin and hemicellulose and execution of different fractionation approaches after biomass dissolution in ILs.[10]

However, rather than to dissolve and to pre-treat biomass, some ILs were found to be able to directly catalyse biomass conversion, mainly by hydrolysing and processing of the polysaccharides without presence of any other catalyst. Acidic ILs can behave as both solvents and catalysts because they combine the advantages of mineral acid and IL.[40] Therefore many kinds of acidic ionic liquids have been gaining interest as integrated solvents and catalysts for the biomass pre-treatment.[40-43] Acidic ILs functionalised with SO_3H greatly increase the reaction rate of the cellulose hydrolysis and have a higher catalytic activity for the cleavage of glycosidic bonds.[44] Nevertheless, no selectivity between cellulose and hemicellulose hydrolysis is observed and strong acidic character of these ILs leads to increase of biomass degradation. In case of $[HSO_4]$-based ILs, another example of acidic ILs able to catalyse biomass, a selective hemicellulose hydrolysis could be achieved.[18,45] Furthermore, $[HSO_4]$-based ILs have been procured increasingly not only because of their acidic properties, but also due to their low cost when compared to other ILs.[46] The 1-butyl-3-methylimidazolium hydrogen sulphate ([bmim][HSO_4]) IL has been found as an alternative to more exploited ILs such as 1-butyl-3-methylimidazolium chloride ([bmim][Cl]), and 1-ethyl-3-methylimidazolium acetate [emim][CH_3COO], among others.

5.2. Materials and Methods

5.2.1. Materials and chemicals

Wheat straw was kindly supplied by Estação Nacional de Melhoramento de Plantas (Elvas, Portugal) and was used as feedstock. The milling of raw material was done using a knife mill IKA® WERKE, MF 10 basic, Germany, to get <0.5 mm particles.

The moisture content in the biomass and processed solids was determined at the level of 8.3 wt.%. To perform the water content analysis a nickel plate was placed in oven at 100 ºC for at least 5 h to remove humidity. The known amount of pre-treated sample (0.1 g) was placed in each plate, heated up in oven for at least 18 h and then the dried sample was weighted.

The chemical analysis of the raw material (dry weight basis) was taken from literature[21] and was as follows: 38.8 wt.% glucan, 19.5 wt.% xylan, 2.9 wt.% arabinan, 2.7 wt.% acetyl groups, 17.6 wt.% Klason lignin, 9.7 wt.% protein and 4.5 wt.% ash.

For the pre-treatment experiments, the [bmim][HSO_4] IL (99 wt.% purity) acquired from Iolitec GmbH, Heilbronn, Germany was used. The [bmim][HSO_4] IL was used as received without further purification. The water content in the examined IL was measured by a volumetric Karl – Fischer titration and was 5385 ppm. For the pre-treatment experiments, 4 M HCl aqueous solution was prepared from fuming 37 wt.% HCl bought from Merck (Darmstadt, Germany) and ultra-pure water (18.2 $M\Omega \cdot cm^{-1}$) produced by Purelab Classic Elga. Nylon filters (Ø=47 mm, 0.45 µm porosity) from Merck Millipore (Billerica, MA, USA) were also used. The 4 M HCl was later used to prepare the HCl

aqueous solution with pH 2 by diluting the acid with water. Basylone M-350 oil purchased from Bayer (Leverkursen, Germany) was used as the heating medium for pre-treatment experiments. Nylon syringe filters (Ø=13 mm, 0.22 µm porosity), purchased from Red® analytical (Cambridgeshire, UK), were used to filtrate all samples before running on CE (Capillary Electrophoresis) and HPLC. For the solid analysis, H_2SO_4 wt.% by Panreac Química, (Barcelona, Spain), Nylon syringe filters (Ø=13 mm, 0.22 µm porosity) and filtering crucibles with fritted disc, Gooch with porosity grade 4 from SciLabware (Stone, Staffordshire) were used.

5.2.2. Pre-treatment method

A 4 g of [bmim][HSO_4] was placed into a 15 mL vial and mixed with wheat straw in 1/10 ($w \cdot w^{-1}$) solid/liquid ratio. The mixture was submitted to continuous magnetic stirring for a defined period of time and temperature. After pre-treatment, 10 mL of ultra-pure water was added to the flask under continuous agitation. The mixture was next filtrated under vacuum and 90 mL of HCl aqueous solution (pH 2) was used to wash the recovered biomass. The use of acidic solution of HCl with pH 2 allows to maintain the lignin in the solid phase as the processed lignin is insoluble in acidic solution with pH 2.[16] Furthermore, at the same time aqueous solution of HCl allows to wash out the hydrolysed sugars produced from hemicellulose fraction. In other words the HCl aqueous solution (pH 2) was used to achieve high selectivity for hemicellulose-derived products recovery in the liquid stream. The obtained liquor was collected and stored in freezer. The solid phase was dried in oven at 50 °C for 24 h. Subsequently, the recovered biomass was left for a minimum of 1 h at room temperature, and then the recovered mass was measured. The liquor obtained from each pre-treatment trial was subjected to CE and HPLC analyses while the recovered biomasses (solid phase) were submitted to chemical characterisation.

5.2.3. Chemical characterisation of the recovered solids

The solid phase resulting from the pre-treatment was washed with ultra-pure water and oven-dried at 50 ºC for at least 48 h. Subsequently, the solids were left at room conditions for a minimum of 12 h. After that, the solids were subjected to quantitative acid hydrolysis to determine the sugar content (both cellulose and hemicellulose) according to the protocol of National Renewable Energy Laboratory (NREL).[47]

5.2.4. Analytical techniques

The processes examined in this work resulted in the liquid phase containing mainly hemicellulose hydrolysis products and processed solids constituted by cellulose and lignin. After each pre-treatment both liquid and solid fractions were duly processed using CE and HPLC. The analysis was focused on the detection and quantification of compounds that are directly obtained from the hydrolysis and/or conversion of wheat straw. Therefore, CE was employed to analyse monosaccharides (xylose,

arabinose and glucose) and furans (furfural and HMF), while HPLC allowed to identify the organic acids found in the sample. The reason to use CE is the capacity of this technique to detect and separate analytes in the sample with higher tolerance for IL concentration than HPLC.[48] Unfortunately, CE could not be used for the organic acid analysis, due to the direct interference of the IL with the separation of organic acids.

5.2.4.1. Capillary electrophoresis (CE)

The method applied for sugar and furan determination was based on methodology described in literature.[49] Furthermore, [bmim][HSO_4] was also added to solution with concentration of 200 mM to mimic concentration of IL in samples obtained from the pre-treatment. At this IL concentration the linearity of calibration curves of sugars, furfural and HMF was observed.[48] A solution containing 130 mM NaOH (EKA, Funchal, Portugal) and 36 mM $Na_2HPO_4 \cdot 2H_2O$ (Sigma-Aldrich Laborchemikalien GmbH, Germany) was prepared as the electrolyte solution. The analyses were carried out using Agilent Technologies CE instrument (Waldbronn, Germany), equipped with a diode array detector. The detection was recorded at a wavelength of 270 nm and 200 nm, both with 10 nm bandwidth. Agilent 3D-CE ChemStation data software (Rev B.04.01) was used to perform qualitative and quantitative analysis. An uncoated fused-silica extended light path CE capillary with 50 μm i.d. and 56/64.5 cm total length was used. Between runs the capillary was pre-conditioned by rising sequentially acetic acid 1mM (3 min), sodium hydroxide 1 M (3 min), water (3 min) and the electrolyte solution (5 min) at 17 ºC. The samples were filtered with nylon syringe filters (Ø=13 mm, 0.22 μm porosity) and injected with a pressure of 35 mbar for 10 s. The separation voltage was fixed at +18 kV for run of 27 min.

For the preparation of standard sugar samples, D(+)-sucrose, D(+)-xylose, D(+)-cellobiose, D(+)-glucose and D(+)-arabinose were used and were acquired from Merck (Darmstadt, Germany). Furfural and HMF obtained from Sigma-Aldrich (St. Louis, USA) were also used as standards. The standard solutions were prepared using ultra-pure water and contained HMF (0.5-0.03 mM), furfural (3-0.05 mM) and sugars: sucrose, cellobiose, cellulose, arabinose and xylose (4-0.2 mM). The example of electropherogram is shown in Figure B.1. of Appendix B.

5.2.4.2. High-performance liquid chromatography (HPLC)

The organic acids (acetic, formic and levulinic acids) from the collected liquor samples were analysed by an Agilent 1100 Series HPLC equipped with Aminex HPX-87H (Bio-Rad, EUA) column and a refractive index detector (RID). All samples were filtrated using a 0.22 μm syringe filter. The quantification was made by calibration curves using standard samples of acetic acid, formic acid and levulinic acid from Panreac (Barcelona, Spain) with known concentrations. Sulphuric acid (Panreac Química, Barcelona, Spain) with 5 mM concentration with 0.6 $mL \cdot min^{-1}$ (sample volume 5 μL) flow

rate for liquor analysis and 0.4 mL·min^{-1} (sample volume 5 μL) for solid samples was used as mobile phase. Column temperature was 50 ºC and detector temperature of 45 ºC was employed. The example of chromatogram is depicted in Figure B.2. of Appendix B.

5.2.5. Statistical modelling

A methodology based on Doehlert experimental design[50] was performed for two different optimisation responses, namely xylose and furfural production from wheat straw hemicellulose. The experimental distribution was considered for two independent variables: temperature (X_1) and residence time (X_2). Two different experimental distributions were made. The first for xylose production, where 70 °C < X_1 < 160 °C and 20.0 min < X_2 < 120.0 min were considered while the second for furfural production by using 115 °C < X_1 < 175 °C and 63.3 min < X_2 < 163.3 min. The conditions of pre-treatment and respective coded factors, which were used for calculation purposes of two inspected optimisations, are presented in Table B.1. of Appendix B.

The responses studied were xylan hydrolysis to xylose (Y_1) and hemicellulose sugars (sum of xylan and arabinan) conversion to furfural (Y_2). The model used to express the responses was a second order polynomial represented by the following equation: $Y = \beta_0 + \beta_1 X_1 + \beta_2 X_2 + \beta_{12} X_1 X_2 + \beta_{11} X_1^2 + \beta_{12} X_2^2$, where X_1 and X_2 represents the independent variables, Y is the response obtained from experimentations and βs are parameters of the polynomial model. The β parameters utilised to estimate the responses have precise meanings: β_0 represents the analysed response in the centre of the experimental domain; the magnitude of β_1 and β_2 indicates the importance of the respective factors (temperature and time, respectively) on the responses; the interaction parameter, β_{12}, indicates how the effect of one factor depends on the level of the other factor. The values of β_{11} and β_{12} determine how the response surface folds downward (negative values) or upward (positive values) quadratically, depending on the magnitude of the absolute value. The relationship between the dependent variables and the response variables was demonstrated by the response surfaces and contour plots obtained using *SigmaPlot*®, Systat Software Inc. The adequacy of the models to fit the sets of data was performed using the statistical *F*-test for the effectiveness of the factors, which detects whether the source of variance included in the residuals is due to the inadequacy of the models to reproduce experimental data. The adequacy of the model was predicted through the regression analysis (R^2) and the ANOVA analysis (p< 0.05), using Microsoft Office Excel 2010 software.

5.2.6. Experimental errors

Standard deviation error (u) was determined for all the obtained results. All weighing was made considering a $u(m)$ = 0.1 mg. For all wheat straw pre-treatment, the applied temperature demonstrated error of $u(T)$ = 1 °C. An arbitrary error of 10 % of measured value was defined to all the CE measurements and HPLC analyses. All experiments were performed in duplicate.

5.3. Results

Wheat straw was subjected to processing with acidic [bmim][HSO_4] IL in temperature range from 70 to 175 °C and residence times from 20.0 to 163.3 min at fixed biomass/IL ratio of 10 ($w \cdot w^{-1}$) and water content equals to 1.24 wt.%. Pre-treatments with [bmim][HSO_4] were made focusing on the hydrolysis of hemicellulose fraction from wheat straw to produce xylose as the main product. Based on the literature report[16] the experimental conditions were settled using Doehlert experimental design (Table B.1. of Appendix B).

5.3.1. Production of xylose

The conditions of xylose production initially studied were: 85 °C/113.3 min, 100 °C/70.0 min, 115 °C/26.7 min, 115 °C/113.3 min and 130 °C/70.0 min. For the highest pre-treatment temperature (130 °C/70.0 min), among all examined conditions, the highest hydrolysis of xylan to xylose was found. Therefore, following the pattern of Doehlert experimental design, pre-treatments with higher temperatures were studied, namely at 145 °C/26.7 min and 145 °C/113.3 min. The results obtained for all performed experiments are given in Table 5.1. The data shows that xylose yield in liquor increases with temperature and residence time up to 130 °C/70.0 min up to 18.8 mol%, while for higher temperature (145 °C) the xylose yield decreases to less than 1/4 of the maximal one. This decrease is counterbalanced by increase of furfural yield to 26 mol%. In case of arabinose, a constant decrease of arabinose yield was found with an increase of reaction time and temperature. Analysing the glucose yield it can be stated that concentration of glucose remains constant in the range of experimental error for all experiments. Similar conclusion can be drawn for glucose degradation product such as HMF, which concentration remains constant in the range of studied parameters. Similar to furfural, the yield of acetyl groups' hydrolysis to acetic acid increases, leading to 83.3 mol% of the initial acetyl groups content. Two most common organic acids, such as formic and levulinic, were not found in the examined samples.

The results of solid produced during the wheat straw processing with [bmim][HSO_4] are summarised in Table 5.2. The solid yield varies from 89.4 %($w \cdot w^{-1}$) to 58.8 %($w \cdot w^{-1}$) for 85 ºC/113.3 min and 145 ºC/113.3 min respectively. Characterisation of obtained solids was necessary to determine the amount of each fractions which was not hydrolysed by [bmim][HSO_4]. The obtained data shows that xylan is still present in the recovered solids and its content decreases from 24.3 wt.% of produced solid to 5.6 wt.% for the lowest and the most severe conditions, respectively. Similar behaviour was observed for arabinan and acetyl groups found in the processed solids. The decrease of xylan, arabinan and acetyl group contents in the produced solids is counterbalanced by significant increase of glucan and lignin content. For the highest temperature examined, the glucan content was above 50 wt.% and lignin reached a maximum of 32.6 wt.% of produced solid sample.

The partition of cellulose and hemicellulose fraction between liquid and solid phases is depicted in Figure 5.1. Analysis of this figure reveals that hemicellulose recovery for the lowest temperature is quantitative, while for more severe conditions the recovery of hemicellulose fraction decreases significantly reaching only a 49.4 %($w \cdot w^{-1}$) for the most severe conditions. Furthermore, most of the hemicellulose can be found in liquor as hydrolysis and degradation products. In case of cellulose recovery, an analogous decrease is attained, however decline is much less pronounced than that of hemicellulose.

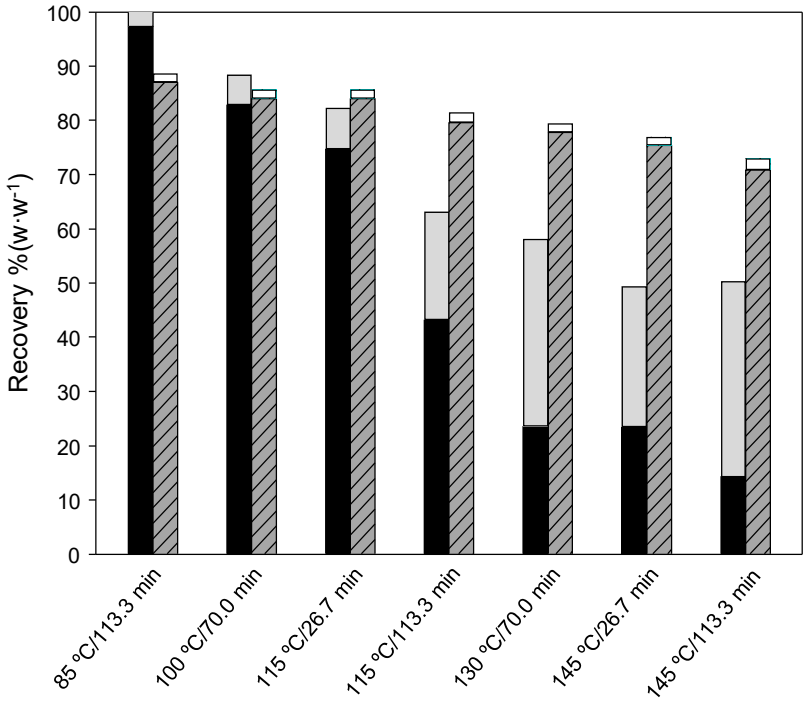

Figure 5.1. Total recovery of hemicellulose (black – in solid, grey – in liquor) and cellulose (dashed grey – in solid, white – in liquor) in pre-treatment of wheat straw with [bmim][HSO_4] for xylose production.

5.3.2. Production of furfural

The previously performed pre-treatments demonstrated that xylose is rapidly converted into furfural mostly at higher temperatures. Therefore, the extent of wheat straw pre-treatment and hydrolysis with the aim of hemicellulose conversion to furfural was also studied at more severe conditions. The conditions chosen by Doehlert experimental design (Table B.1. of Appendix B) to study and to optimise the production of furfural with [bmim][HSO_4] were as follows: 130 °C/70.0 min, 130 °C/156.6 min, 145 °C/113.3 min, 160 °C/70.0 min, 160 °C/156.6 min and 175 °C/113.3 min.

Furthermore, two additional set of conditions namely 175 °C/163.3 min and 175 °C/63.3 min were also taken into account for the optimisation of furfural production.

Table 5.1. presents the data obtained from the liquor analysis for new conditions regarding furfural production.

Table 5.1. Liquid phase composition obtained after wheat straw pre-treatment with [bmim][HSO_4] at examined temperatures and residence times.

T **(°C)**	***t*** **(min)**	**Yield (mol%)**							
		xylose[a]	**arabinose[b]**	**furfural[c]**	**glucose[d]**	**HMF[e]**	**acetic acid[f]**	**formic acid[g]**	**levulinic acid[h]**
85	113.3	0.0	20.3	0.1	1.0	0.6	9.5	0.0	0.0
100	70.0	2.1	20.0	0.2	0.8	0.8	12.4	0.0	0.0
115	26.7	4.6	15.2	0.3	0.9	0.8	17.8	0.0	0.0
115	113.3	15.3	11.3	3.1	1.0	0.9	38.3	0.0	0.0
130	70.0	18.8	10.3	14.3	0.8	0.7	57.9	0.0	0.0
145	26.7	12.5	4.5	10.9	0.7	0.8	56.6	0.0	0.0
145	113.3	4.4	4.1	26.1	1.1	1.0	83.3	0.0	0.0
130	156.6	16.0	7.8	23.4	1.1	1.1	69.5	0.0	0.0
160	70.0	1.3	0.0	30.7	1.0	1.6	89.7	0.0	0.0
160	156.6	0.0	0.0	36.2	0.9	2.6	106.4	0.8	1.7
175	63.3	0.6	0.0	30.6	0.9	1.8	95.9	1.0	1.5
175	113.3	0.0	0.0	34.4	0.9	3.0	95.1	0.3	2.0
175	163.3	0.0	0.0	15.6	0.0	1.6	108.8	2.1	2.1

a) $\frac{m_{xylose}}{m_{xylan_{native}}} \times \frac{132}{150} \times 100$; b) $\frac{m_{arabinose}}{m_{arabinan_{native}}} \times \frac{132}{150} \times 100$ c) $\frac{m_{glucose}}{m_{glucan_{native}}} \times \frac{162}{180} \times 100$; d) $\frac{m_{furfural}}{m_{(xylan+arabinan)_{native}}} \times \frac{132}{96} \times 100$; e) $\frac{m_{HMF}}{m_{glucan_{native}}} \times \frac{162}{126} \times 100$; f) $\frac{m_{acetic\ acid}}{m_{acetyl\ groups_{native}}} \times \frac{59}{60} \times 100$; g) $\frac{m_{formic\ acid}}{m_{(xylan+arabinan)_{native}}} \times \frac{132}{46} \times 100$; h) $\frac{m_{levulinic\ acid}}{m_{glucan_{native}}} \times \frac{162}{116} \times 100$.

The hemicellulose-originated monosaccharides present in the liquor clearly disappeared for more severe conditions. Xylose and arabinose were observed only for the less severe conditions (130 °C/156.6 min, 160 °C/70.0 min and 175 °C/63.3 min), and arabinose was only detected in the liquor obtained from the process at 130 °C/156.6 min, but even so in a negligible concentration. The xylose and arabinose disappearance was counterbalanced by the increase of furfural yield, in which a maximum yield of 36.2 mol% for pre-treatment at 160 °C/156.6 min was reached. However, for

higher temperature and longer pre-treatment time, its yield decreased significantly. It is worth mentioning that the increase of reaction time from 113.3 to 163.3 min at 175 °C leads to a significant decrease in furfural content compensated by a significant rise of formic acid production. Another product obtained from hemicellulose is acetic acid. The acetyl group hydrolysis is quantitative in all reactions showing that conditions more severe than 160 °C/70 min are harsh enough to convert acetyl groups present in the hemicellulose into acetic acid. Glucose, HMF and levulinic acid shows similar trends to those observed for xylose and its degradation products. Although the yields are much lower than in case of hemicellulose-based products it can be found that the glucose and HMF yields are virtually constant irrespectively on the examined reaction conditions.

As presented in Table 5.2., the solid yield obtained from pre-treatments was in the range of 59.7 to 68.6 %(w·w^{-1}). Arabinan and acetyl groups were not found in the solid residue. Also xylan was found only in samples produced at the less severe reaction conditions. The major fractions of produced solid are glucan and lignin. Along with the increase of reaction severity, the glucan content decreases by 1/3 to 38.6 wt.%. At the same time, an increase of lignin content was doubled and at the most severe conditions lignin constituted more than an half of the produced solids.

Table 5.2. Results of solid phase analysis obtained from wheat straw pre-treatment with [bmim][HSO_4] at various temperatures and residence times.

T **(°C)**	***t*** **(min)**	**Solid phase composition (wt%)**						**SY %(w·w^{-1})**
		Xylan	**Arabinan**	**Acetyl**	**Glucan**	**Lignin**	**Ash**	
untreated biomass		19.1	3.0	2.7	38.5	17.7	10.7	-
85	113.3	24.3	2.6	2.4	40.7	18.6	2.8	89.4
100	70.0	23.3	2.1	2.1	43.1	20.8	3.5	82.8
115	26.7	21.4	2.0	2.3	44.9	20.0	3.6	78.2
115	113.3	14.5	0.9	2.3	50.3	18.7	4.3	66.1
130	70.0	10.5	1.1	1.1	58.2	20.6	5.8	58.8
145	26.7	9.6	0.8	1.0	54.6	22.1	5.5	58.7
145	113.3	5.6	1.4	1.0	50.9	32.6	5.4	58.1
130	156.6	6.8	0.0	0.0	56.7	26.0	6.2	59.7
160	70.0	0.0	0.0	0.0	52.4	36.7	6.2	61.5
160	156.6	0.0	0.0	0.0	48.6	46.0	4.9	63.3
175	63.3	0.0	0.0	0.0	45.5	43.7	7.4	63.2
175	113.3	0.0	0.0	0.0	45.5	47.8	5.7	65.5
175	163.3	0.0	0.0	0.0	38.6	52.6	6.6	68.6

a) The oven-dried solid phase composition; SY solid yield

Analysing the recovery of polysaccharide fractions it can be stated that in case of hemicellulose a continuous decrease of recovery yield with an increase of temperature is observed. Hence cellulose recovery yield is less susceptible for examined reaction conditions and thus, the recovery yield decreases much slower than that for hemicellulose as observed in Figure 5.2.

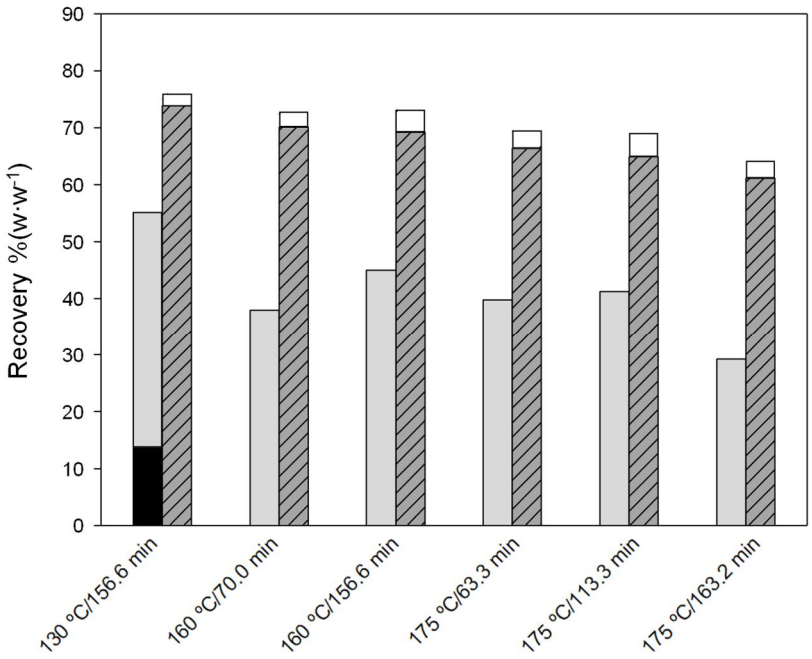

Figure 5.2. Total recovery of hemicellulose (black – in solid, gray – in liquor) and cellulose (dashed dark gray – in solid, white – in liquor) in pre-treatment of wheat straw with [bmim][HSO_4] for furfural production conditions.

5.3.3. Optimisation of xylose and furfural production

The pre-treatment reaction conditions for production of xylose and furfural were determined based on the Doehlert experimental designs according to data shown in Tables B.1.-B.4. of Appendix B. The 3D response surfaces based on the statistical modelling are depicted in Figure 5.3.

The optimum condition set obtained after the statistical modelling analysis for Y_1 was 125 °C/82.1 min with a statistical response estimated at the level of 17.1 mol% of xylose. The optimum condition for the response Y_2 was 161 °C/104.5 min with 33.3 mol% of conversion to furfural. The model was validated by performing the pre-treatment at the optimised conditions and results are presented in Appendix B (Tables B.5. and B.6.). The experimental value for the xylose production obtained was 16.7 mol% while in case of xylan to furfural conversion the experimental validations allowed to obtain 32.2 mol% of conversion to furfural.

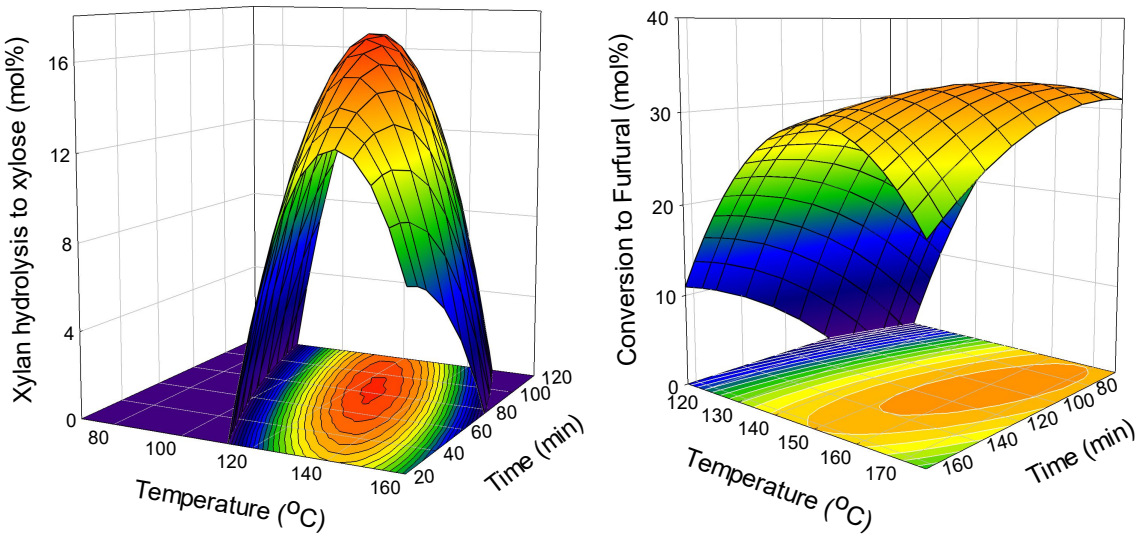

Figure 5.3. Response surface and contour plot of modelled xylan hydrolysis into xylose (left figure), and hemicellulose conversion to furfural (right figure) as a function of reaction time (min) and temperature (°C).

5.4. Discussion

In the last few years various studies about the pre-treatment and fractionation of biomass using ILs have been reported. [6-19,40] Recently, the ILs containing [HSO_4] anion became an appealing option to be used in the biomass pre-treatment, once the acidic properties of this IL allows the catalytic conversion of biomass.[6,45,51-53] In fact, the acidity of this IL not only allows the hydrolysis of hemicellulose into monosaccharides, such as xylose and arabinose, but also converts those monosaccharides into further degradation products such as furfural.[18] In this work, this approach was deeply scrutinised by the wheat straw pre-treatment with [bmim][HSO_4] focusing the selective catalysis of hemicellulosic fraction for the production of xylose and furfural.

5.4.1. Combined severity factor (CSF) as the comparison parameter

The analysis of the obtained results based on two independent parameters (temperature and time of the pre-treatment) does not allow for direct analysis of the influence of these parameters on the reaction results. Thus, for comparison purposes a severity factor ($logR_o$) defined by Overend and Chornet[54,55] was applied. A severity factor is described by the following equation $R_o = \int_0^t e^{\frac{T(t)-100}{14.75}} dt$, where t is time expressed in minutes, T relates to temperature in °C, 100 is the reference temperature (100 °C) and 14.75 is an empirical constant. Furthermore, considering a strongly acidic character of some pre-treatments the combined severity factor described by the following equation $CSF = log(R_0) - pH$

should be considered. A close inspection of the equation depicting the severity factor reveals that the reference temperature and empirical factors are related to temperature at which water starts to act as a catalyst. This approach is valid for classical pre-treatment processes (*e.g.* autohydrolysis or acid catalysis)[56], however this is not the case for pre-treatments occurring in non-aqueous media, such as ILs. Thus, new parameters are needed to be established following the methodology presented by Chum *et al.*[57] Hence, the severity factor, R_o, expressed by the aforementioned equation can be also presented in more general form such as $R_o = e^{\left(\frac{T_r - T_b}{\omega}\right)} \times \Delta t$, where, T_r and T_b are absolute reaction temperature and reference temperature when hydrolysis initiates, respectively expressed in °C, and ω is an adimensional constant that translates the effect of the temperature in the conversion. Yields of hemicellulose hydrolysis with [bmim][HSO_4] attained in this work were used to estimate the values of T_b and ω. The value of T_b was attained by applying the Doehlert design for all the hemicellulose hydrolysis experiments examined. The point (x,0,0) represents the value of T_b and as such, by resolving the equation obtained from experimental design in the form of $Y = 64.0048 + 74.5027X_1 + 19.4424X_2 - 19.9022X_1X_2 - 36.3594{X_1}^2$, where, Y is the percentage of hemicellulose hydrolysis; and X_1, X_2 are the temperature (°C) and pre-treatment time (min), respectively gave $T_b = 88.28$ °C. The value of ω was attained by representation of the equation $Y = mX + B$, where $Y = ln(-ln(1-\alpha))$, and α is the hydrolysis of hemicellulose, X is the combined severity factor calculated in the following manner: $X = CSF = log_{10}\left(R_{o_{heating}} - R_{o_{isothermal}}\right) - pH$, where $R_{o_{heating}}$ is the severity factor for heating and $R_{o_{isothermal}}$ is the severity factor for isothermal condition process, and pH is the pH of the [bmim][HSO_4] and is equal to 1.0. Hence the value of ω was obtained by maximisation of R^2 and for $R^2 = 0.99$ ω is equal to 6.47. Finally, the CSF used in this work has the following formula $CSF = log_{10}\left(e^{\left(\frac{T_r - 88.28}{6.47}\right)} \times \Delta t\right) - pH$. All CSF for examined conditions are depicted in Table 5.3.

Table 5.3. Combined severity factor for all conditions performed.

T (°C)	85	100	115	115	145	130	130	145	160	160	175	175	175
t (min)	113.3	70.0	26.7	113.1	26.7	70.0	156.6	113.3	70	156.6	63.3	113.3	163.3
CSF	0.80	1.56	1.89	2.79	3.52	3.52	3.94	4.77	5.46	5.93	6.34	6.74	6.95

5.4.2. Catalysis performance of [bmim][HSO_4]

Among all examined pre-treatment conditions, the hydrolysis of hemicellulose occurred, even at the lowest temperature examined. At CSF =0.80 (85 °C/ 113.3 min) the presence of arabinose in the liquid phase (20.3 mol%) without xylose indicates that arabinan is the first and the most susceptible fraction

for hydrolysis. Similar behaviour was found in literature for other types of pre-treatments. For instance, Carvalheiro *et al*. studied the kinetics of brewery's spent grain autohydrolysis and verified that the highest concentrations of arabinose oligomers were obtained firstly and for shorter reaction times than xylose oligomers.[58] This phenomenon finds also an explanation in the chemical structure of hemicellulose, which consists of arabinan branches in xylopyranosyl backbone that makes arabinan more susceptible to the hydrolysis than xylan polymer. Furthermore, it is important to notice that arabinose content in the liquid phase decreases with an increase of pre-treatment severity. On the contrary, yield of xylose increases and reaches maximum at CSF=3.52 (130 °C/70 min). Further increase of severity (CSF > 3.94) guides to complete disappearance of xylose observed in case of pre-treatments performed at CSF = 5.46 or in other words for temperatures equal or higher than 160 °C. As expected, the discussed decrease of monosaccharide yields is accompanied by the increase of furfural content in the liquid phase. The achieved results permit to conclude that temperature seems to be a key parameter in favouring the hydrolysis of hemicellulose,[20,56] which for more severe conditions (CSF > 3.52) guides the conversion of monosaccharides into furfural. These results are coherent with literature data for the pre-treatment of Miscanthus biomass by the same IL.[45]

As mentioned before arabinose is firstly formed, but next is rapidly converted into furfural. Xylose follows this pathway and undergoes a quick conversion to furfural too. Nonetheless, for CSF = 6.34 degradation of furfural was observed, suggesting that the used conditions were too much severe and furfural may suffer further degradation.[59,60] Similarly to both hemicellulosic saccharides, the increase of acetic acid production was observed in the liquid phase meaning a continuous hydrolysis of acetyl groups attached to hemicellulose structure. In respect to cellulose hydrolysis and conversion with [bmim][HSO_4], the results show that glucose is barely produced and the same time occurs its conversion into HMF. This is a unique characteristic of [bmim][HSO_4], which demonstrates to selectively hydrolyse hemicellulose and obtain its derivative products as depicted in Figure 5.4.

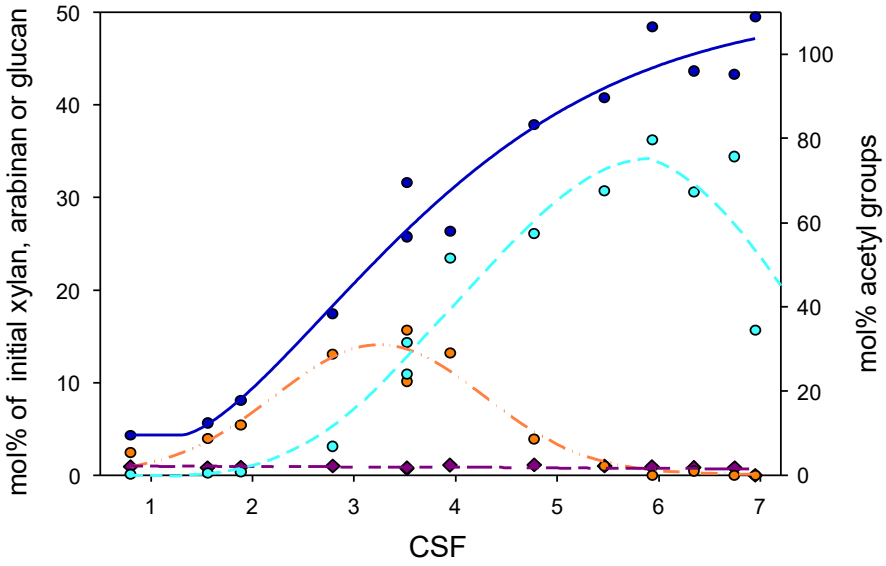

Figure 5.4. Glucose (♦), arabinose and xylose (●), furfural (●) (left scale) and acetyl groups (●) (right scale) found in liquors after pre-treatment carried out with [bmim][HSO_4]. Solid/dashed/dashed-dot-dot and short-long-short dashed lines are designed by polynomial adjustment to the experimental points and serve as guide for the eye.

The chemical characterisation of the pre-treated solids (Table 5.2.) shows an enrichment of glucan and lignin contents along the increase of severity of the performed reactions caused by the extensive hydrolysis of hemicellulose. Actually, total hemicellulose hydrolysis was achieved for pre-treatments with CSF > 4.77 (temperature above 145 °C). The main fractions constituting the processed solids are cellulose and lignin. The maximum cellulose content (58.2 wt.%) in the solid was reached at CSF = 3.52 (130 °C/70.0 min), but for more severe conditions, a cellulose content decreases and the lowest (38.6 wt.%) was found after the reaction at the most severe conditions (CSF = 6.95). Surprisingly, this decrease was not reflected in the liquid phase, where glucose, HMF and levulinic acid contents are very low (4.9 mol% on the glucan basis). Actually, analysing the mass balance of the process, close to 34.0 %($w \cdot w^{-1}$) cellulose was lost for the most severe reaction conditions (Figure 5.2.). In spite of high cellulose lost, the hemicellulose mass loss is even higher. Hemicellulose had the lowest recovery of 29.3 %($w \cdot w^{-1}$) at CSF = 6.95. Equally to cellulose, the total mass of hemicellulose quantified in the liquid phase does not correspond to the mass removed from the solid. The explanation of the cellulose and hemicellulose disappearance is the possibility to form humins (pseudo-lignin).[59,60] The literature reports state that released sugars and produced furans may react in the liquid phase and form polymeric insoluble carbon-enriched compounds called chars or pseudo-lignin (humins). The method for compositional analysis of lignocellulosic biomass, developed by the NREL and presented above, does not distinguish between Klason lignin, naturally present in the biomass, and pseudo-lignin resulting from sugar degradation.[60] Therefore, the disappearance of saccharide fractions and lignin

recovery higher than 180 %(w·w^{-1}) obtained in this work, shown in Figure 5.5., may justify cellulose and hemicellulose mass loss.

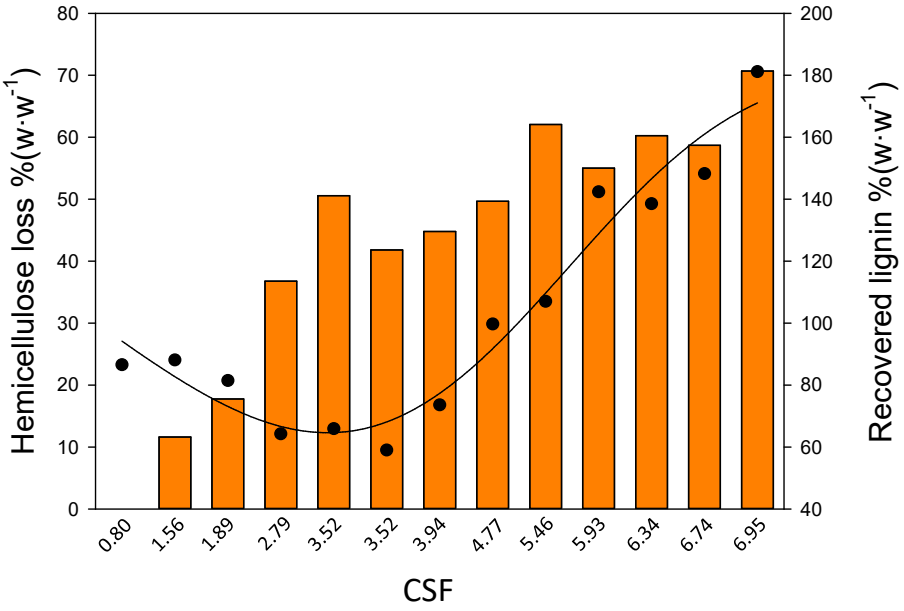

Figure 5.5. Total hemicellulose loss (bars) and recovered lignin (●) in the course of the pre-treatments executed. Solid line is designed by polynomial adjustment to the experimental data and does not have any physical meaning and serves as guide for the eye.

The creation of humins normally occurs for temperature superior to 160 ºC[60] and following the literature reports at more severe pre-treatment temperatures (180 °C) carbohydrate-derived pseudo-lignin can achieve even 94.4 %(w·w^{-1}).[60] Besides, the phenomenon of humin formation can be confirmed looking at the solid yield presented in Table 5.2. For less severe reaction conditions, especially those performed at lower temperature, the solid yield decreases with an increase of reaction severity, which is normal behaviour as a great part of hemicellulosic fraction became hydrolysed.[20,21,56] However, processes carried out at high temperatures show an increase of solid yield with the increase of reaction temperature which might be explained by the aforementioned formation of pseudo-lignin.

5.4.3. Optimisation of xylose and furfural production

Optimisation of hemicellulose hydrolysis to sugars, in particular to xylose, was one of the goals of this work. The collected data for xylose production was submitted to statistical modelling (data in Appendix B) and using the statistically significant regression coefficients (p<0.05) the following model equation was found: $Y_1 = 13.82 + 19.77X_1 + 7.04X_2 - 18.29X_1X_2 - 32.00{X_1}^2$. According to the positive linear coefficient for X_1 and X_2, it can be concluded that the amount of xylose obtained

increases with an increase of temperature and reaction time. The absolute values of the coefficients β_1 and β_2 show that the temperature (X_1) has stronger influence (almost 3-fold) on xylose production than time (X_2). On the other hand, the negative value for β_{11} implies that the quadratic interaction of X_1 effects negatively the production of xylose. The negative value of β_{12} coefficient indicates that the interaction of X_1 and X_2 is not proportional and the increase of temperature and, subsequent, reaction time has a negative effect on xylose yield.

The optimum conditions to attain maximal xylose yield was identified to be at 125 °C/82.1 min. The xylose yield obtained was 16.7 mol% and 7.6 mol% conversion to furfural. The TRS (total reducing sugar) yield, for this condition was 12.5 mol%. Li et. al also explored the use of [HSO_4] based ILs on the pre-treatment of corn stalk.[53] They attained a maximum 23 % and 15 % TRS yield at 5 and 2 min using [bmim][HSO_4] and [C_4SO_3Hmim][HSO_4], correspondingly for 100 ºC. Nevertheless, longer reaction times produced even lower TRS yield.[53]

The chemical analysis of solid fraction obtained for optimum conditions, demonstrated that xylan was still present in the recovered biomass (Table 5.2). In other words, at these conditions an incomplete hydrolysis of hemicellulose was attained. However, as it was found for other conditions, more severe conditions favour furfural production, thus it can be stated that [bmim][HSO_4] converts xylan to xylose and next a sudden conversion to furfural occurs. Therefore, the production of furfural with [bmim][HSO_4] was also studied considering higher biomass conversion provoked by this IL. The experimental data submitted to Doehlert model design presented low statistical significance after evaluating statistically significant regression coefficients (p<0.05). The following equation was obtained $Y_2 = 30.16 + 12.89X_1 - 13.70{X_1}^2$. This equation shows that only the variation of temperature has statistical significance (linear and quadratic) and as such, it can be concluded that variation of time is statistically insignificant for furfural production. Nevertheless, the negative value of the β_{11} coefficient translates into a decrease of furfural for more severe processes. This can be observed at CSF = 6.95 (175 °C/163.3 min) were a pronounced decrease of furfural concentration was observed. The optimum condition for furfural formation was found to be at 161 °C/104.5 min. At this condition, the conversion of hemicellulose to furfural was 30.7 mol% and xylose was not present in the pre-treatment liquor. Brandt *et al*. verified that at 120 ºC, using 80 vol.% of the IL [bmim][HSO_4] and 20 vol.% water in the pre-treatment of Miscanthus for 22 h, the resulting liquor contained approximately 33 mol% of furfural.[45] They also reported that using [bmim][$MeSO_3$] at the same conditions 14.8 mol% furfural yield was accomplished. Thus, comparing of the obtained results to these presented in this work, it can be stated that similar conversion to furfural 30.7 mol% vs 33 mol% was achieved for shorter pre-treatment processes without excessive amounts of water within the system.

5.4.4. Effect of water content on the biomass pre-treatment

As it has been reported water has a great influence on the efficiency of the biomass pre-treatments by ILs.[36,37,61-63] Generally, water acting as an anti-solvent affects negatively cellulose and lignocellulose dissolution in ILs.[35,36] Furthermore, considering the discussed above selectivity aspect, it is important to understand the mechanism driving the xylose conversion to furfural.[64-66] The mechanism proposed in literature assumes the formation of furfural by the dehydration of xylose molecule. Therefore, it can be assumed that equilibrium of this reaction should be sensitive on the water content in the reaction mixture. Considering that in the examined system only 1.24 wt.% (5385 ppm of water in IL and 8.3 wt.% humidity of biomass) is present, it can be understood why in the presence of hydrophilic ionic liquid such as [bmim][HSO_4], the hemicellulose undergoes hydrolysis to xylose and arabinose and later both rapidly, and kinetically favoured, are converted to furfural liberating water. Following this hypothesis and analysing the hemicellulose hydrolysis reaction chain shown in Figure 5.6., it can be expected that addition of water should have a positive "protecting" effect on inhibition of xylose and arabinose dehydration to furfural. Moreover, the additional amount of water could enhance the hydrolysis of hemicellulose to monosugars.

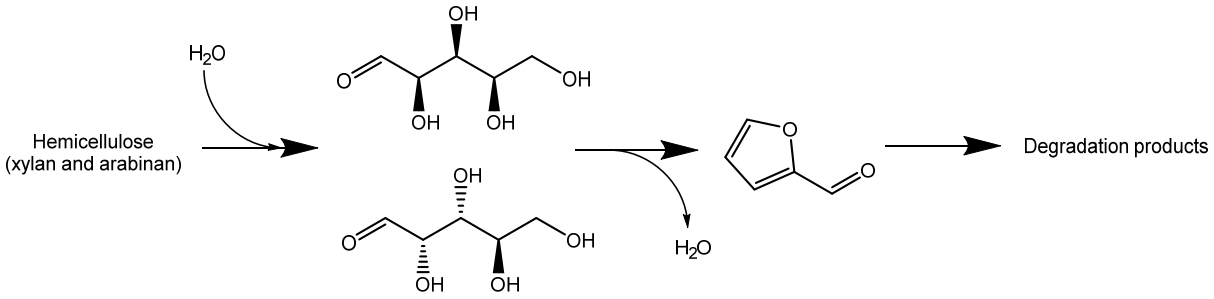

Figure 5.6. Schematic hemicellulose hydrolysis reaction chain.

To validate the veracity of this hypothesis, additional experiments were performed. Two additional pre-treatments at the optimum conditions achieved for xylose production (125 °C/82.1 min) were performed using 4.84 wt.% and 9.22 wt.% water content in the pre-treatment system. Liquid phase analysis demonstrated that by increasing the water content from 1.24 wt.% to 4.84 wt.% the sum of xylose and arabinose concentrations increase by 70 %. In the initial pre-treatment at 1.24 wt.% the sum of concentration of both monosaccharides was 21.4 mol% and at 4.84 wt.% water content the value increased to 36.4 mol% (Figure 5.7). For 9.22 wt.% water content in the pre-treatment system another increase of sum of xylose and arabinose concentrations (Figure 5.7) to 40.1 mol% was observed. It is also important to underpin that the amount of water does not alter significantly the furfural presence in the liquor, thus furfural yield was observed to be constant. On the other hand, the amount of degradation products shown on Figure 5.7. as hemicellulose loss is significantly reduced

and is well correlated with the abovementioned increase of arabinose and xylose concentrations especially that there is no increase of xylan and arabinan disappearance in solid.

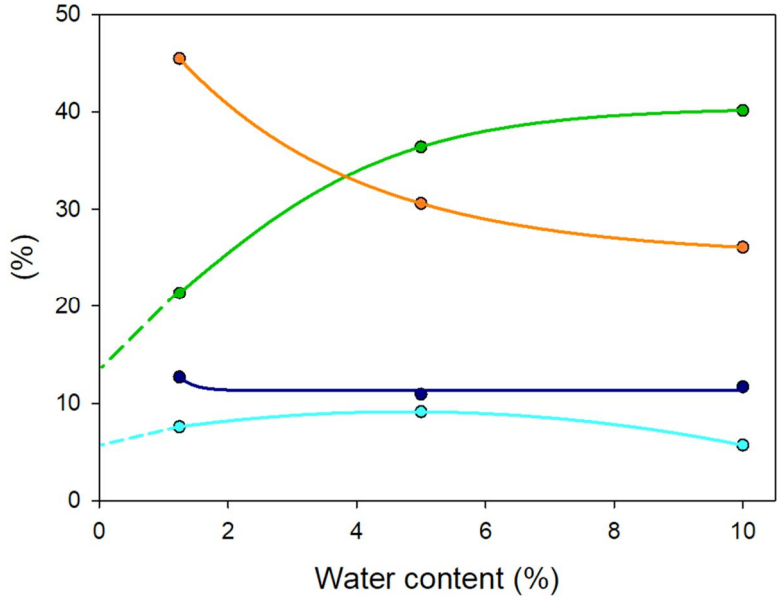

Figure 5.7. Effect of water content in hemicellulose hydrolysis (sum of arabinose and xylose (●), hemicellulose content (sum of arabinan and xylan) in solid (●), hemicellulose conversion to furfural (●), hemicellulose loss (degradation product) (●) at 120 °C /82.1 min. Solid lines are designed by polynomial adjustment to the experimental point.

5.5. Conclusion

Exploitation of lignocellulosic residue potential is an important issue in the context of green chemistry and biorefinery concept. In this work a method of wheat straw pre-treatment using the acidic [bmim][HSO_4] IL was employed. Two independent parameters were optimised using Doehlert statistical model design aiming the maximal xylose and furfural productions. For comparison of the set of experimental data, the severity factor for pre-treatment with [bmim][HSO_4] was proposed. Less severe reaction conditions favour xylose formation and maximum yield of xylose 16.7 mol% was attained at 125 °C/82.1 min. Furfural is mostly formed at more severe conditions and 30.7 mol% was obtained at 161 °C/104.5 min. Variation of water content was studied and an increase of water content to 4.84 wt.% led to the hemicellulose sugar yields of 36.4 mol%. Pre-treatment process using a 9.22 wt.% content resulted in hemicellulose-originated sugars yield of 40.1 mol%. At the same time, conversion to furfural was maintained. The performed experiments allowed for selective removal of hemicellulose from processed biomass confirming that the acidic IL is capable to selectively catalyse hemicellulose within a green and sustainable approach.

To accomplish the comprehensive engineering approach of the presented process, the products recovery as well as recycling and reuse of IL should be considered as shown in Figure 5.8. The efficiency of the process is also connected with further valorisation of biomass besides the production of xylose and furfural. After pre-treatment, the obtained solid can be further fractionated into cellulose and lignin. An effective separation process of the main fractions of lignocellulosic biomass was already presented elsewhere.[18] Furthermore, the formation of humins is an interesting phenomenon and could be examined as the opportunity for the process with [bmim][HSO_4].

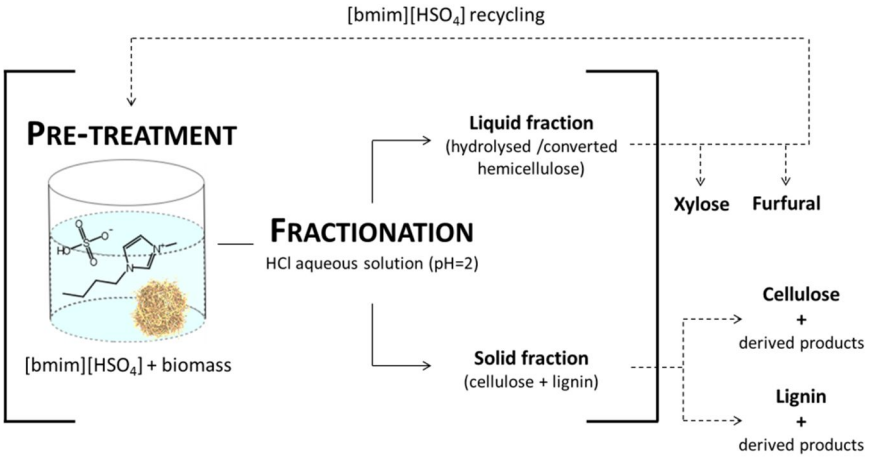

Figure 5.8. The schematic representation of the potential processes of biomass valorisation with [bmim][HSO_4]. The bracket depicts the study being the focus of the work presented in this chapter.

5.6. References

1. M. Foston and A. J. Ragauskas, *Ind. Biotechnol.*, 2012, **8**, 191-208.
2. F. M. Girio, C. Fonseca, F. Carvalheiro, L. C. Duarte, S. Marques and R. Bogel-Lukasik, *Bioresource Technol.*, 2010, **101**, 4775-4800.
3. M. FitzPatrick, P. Champagne, M. F. Cunningham and R. A. Whitney, *Bioresource Technol.*, 2010, **101**, 8915-8922.
4. J. J. Bozell and G. R. Petersen, *Green Chem.*, 2010, **12**, 539-554.
5. V. Menon and M. Rao, *Prog. Energ. Comb. Sci.*, 2012, **38**, 522-550.
6. A. M. da Costa Lopes, K. G. Joao, D. F. Rubik, E. Bogel-Lukasik, L. C. Duarte, J. Andreaus and R. Bogel-Lukasik, *Bioresource Technol.*, 2013, **142**, 198-208.
7. I. Anugwom, V. Eta, P. Virtanen, P. Maki-Arvela, M. Hedenstrom, M. Hummel, H. Sixta and J. P. Mikkola, *ChemSusChem*, 2014, **7**, 1170-1176.
8. A. Brandt, J. Grasvik, J. P. Hallett and T. Welton, *Green Chem.*, 2013, **15**, 550-583.
9. I. Anugwom, V. Eta, P. Virtanen, P. Mäki-Arvela, M. Hedenström, M. Yibo, M. Hummel, H. Sixta and J.-P. Mikkola, *Biomass Bioenerg.*, 2014, **70**, 373-381.
10. A. M. da Costa Lopes, K. G. João, A. R. C. Morais, E. Bogel-Lukasik and R. Bogel-Lukasik, *Sustain. Chem. Process.*, 2013, **1:3**.
11. I. Anugwom, J. P. Mikkola, P. Mäki-Arvela and A. Virtanen, WO2012/059643, 2012.
12. T. Leskinen, A. W. King, I. Kilpeläinen and D. S. Argyropoulos, *Ind. Eng. Chem. Res.*, 2013, **52**, 3958-3966.
13. A. S. da Silva, R. S. S. Teixeira, T. Endo, E. P. S. Bon and S. H. Lee, *Green Chem.*, 2013, **15**, 1991-2001.
14. T. Leskinen, A. W. King, I. Kilpeläinen and D. S. Argyropoulos, *Ind. Eng. Chem. Res.*, 2011, **50**, 12349-12357.
15. S. Hyvärinen, P. Virtanen, D. Yu Murzin and J.-P. Mikkola, *Cellul. Chem. Technol.*, 2010, **44**, 187-195.
16. S. P. Magalhães da Silva, A. M. da Costa Lopes, L. B. Roseiro and R. Bogel-Lukasik, *RSC Adv.*, 2013, **3**, 16040-16050.
17. A. Brandt, J. P. Hallett, D. J. Leak, R. J. Murphy and T. Welton, *Green Chem.*, 2010, **12**, 672-679.
18. A. M. da Costa Lopes, K. G. João, E. Bogel-Lukasik, L. B. Roseiro and R. Bogel-Lukasik, *J. Agric. Food Chem.*, 2013, **61**, 7874-7882.
19. A. M. da Costa Lopes and R. Bogel-Lukasik, *ChemSusChem*, 2015, **8**, 947-965.
20. A. R. C. Morais, A. C. Mata and R. Bogel-Lukasik, *Green Chem.*, 2014, **16**, 4312-4322.
21. S. P. Magalhães da Silva, A. R. C. Morais and R. Bogel-Lukasik, *Green Chem.*, 2014, **16**, 238-246.
22. A. R. C. Morais, A. M. da Costa Lopes and R. Bogel-Lukasik, *Chem. Rev.*, 2015, **115**, 3-27.
23. C. Zetzl, K. Gairola, C. Kirsch, L. Perez-Cantu and I. Smirnova, *Chem. Ing. Tech.*, 2011, **83**, 1016-1025.
24. F. W. Lichtenthaler and S. Peters, *C. R. Chim.*, 2004, **7**, 65-90.
25. Y. U. Paulechka, G. J. Kabo, A. V. Blokhin, O. A. Vydrov, J. W. Magee and M. Frenkel, *J. Chem. Eng. Data*, 2003, **48**, 457-462.
26. U. Domanska and R. Bogel-Lukasik, *J. Phys. Chem. B*, 2005, **109**, 12124-12132.
27. R. Bogel-Lukasik, L. M. N. Goncalves and E. Bogel-Lukasik, *Green Chem.*, 2010, **12**, 1947-1953.
28. J. F. B. Pereira, F. Vicente, V. C. Santos-Ebinuma, J. M. Araujo, A. Pessoa, M. G. Freire and J. A. P. Coutinho, *Process Biochem.*, 2013, **48**, 716-722.
29. R. Bogel-Lukasik, D. Matkowska, M. E. Zakrzewska, E. Bogel-Lukasik and T. Hofman, *Fluid Phase Equilib.*, 2010, **295**, 177-185.
30. M. G. Freire, A. R. R. Teles, M. A. A. Rocha, B. Schroder, C. M. S. S. Neves, P. J. Carvalho, D. V. Evtuguin, L. M. N. B. F. Santos and J. A. P. Coutinho, *J. Chem. Eng. Data*, 2011, **56**, 4813-4822.
31. A. Forte, E. Bogel-Lukasik and R. Bogel-Lukasik, *J. Chem. Eng. Data*, 2011, **56**, 2273-2279.
32. K. Paduszynski, M. Okuniewski and U. Domanska, *J. Phys. Chem. B*, 2013, **117**, 7034-7046.

33. U. Domanska, A. Pobudkowska and P. Bochenska, *J. Chem. Eng. Data*, 2012, **57**, 1894-1898.
34. U. Domanska and R. Bogel-Lukasik, *Fluid Phase Equilib.*, 2005, **233**, 220-227.
35. M. E. Zakrzewska, E. Bogel-Lukasik and R. Bogel-Lukasik, *Energ. Fuel.*, 2010, **24**, 737-745.
36. R. P. Swatloski, S. K. Spear, J. D. Holbrey and R. D. Rogers, *J. Am. Chem. Soc.*, 2002, **124**, 4974-4975.
37. I. A. Kilpeläinen, H. Xie, A. King, M. Granstrom, S. Heikkinen and D. S. Argyropoulos, *J. Agric. Food Chem.*, 2007, **55**, 9142-9148.
38. A. A. Rosatella, R. F. M. Frade and C. A. M. Afonso, *Curr. Org. Synth.*, 2011, **8**, 840-860.
39. O. A. El Seoud, A. Koschella, L. C. Fidale, S. Dorn and T. Heinze, *Biomacromolecules*, 2007, **8**, 2629-2647.
40. Y. Y. Liu, W. W. Xiao, S. Q. Xia and P. S. Ma, *Carbohydr. Polym.*, 2013, **92**, 218-222.
41. A. S. Amarasekara and B. Wiredu, *Int. J. Carbohydr. Chem.*, 2012, **2012**, 1-6.
42. Y. L. Gu, F. Shi and Y. Q. Deng, *Catal. Commun.*, 2003, **4**, 597-601.
43. A. S. Amarasekara and O. S. Owereh, *Ind. Eng. Chem. Res.*, 2009, **48**, 10152-10155.
44. M. E. Zakrzewska, E. Bogel-Lukasik and R. Bogel-Lukasik, *Chem. Rev.*, 2011, **111**, 397-417.
45. A. Brandt, M. J. Ray, T. Q. To, D. J. Leak, R. J. Murphy and T. Welton, *Green Chem.*, 2011, **13**, 2489-2499.
46. L. Chen, M. Sharifzadeh, N. Mac Dowell, T. Welton, N. Shah and J. P. Hallett, *Green Chem.*, 2014, **16**, 3098-3106.
47. A. Sluiter, B. Hames, R. Ruiz, C. Scarlata, J. Sluiter and D. Templeton, *Determination of Sugars, Byproducts, and Degradation Products in Liquid Fraction Process Samples - Laboratory Analytical Procedure (LAP)*, Report NREL/TP-510-42623, National Renewable Energy Laboratory, Colorado, USA, 2008.
48. S. Hyvarinen, J. P. Mikkola, D. Y. Murzin, M. Vaher, M. Kaljurand and M. Koel, *Catal. Today*, 2014, **223**, 18-24.
49. S. Rovio, J. Yli-Kauhaluoma and H. Siren, *Electrophoresis*, 2007, **28**, 3129-3135.
50. D. H. Doehlert, *Roy Stat Soc C-App*, 1970, **19**, 231-239.
51. Z.-D. Ding, J.-C. Shi, J.-J. Xiao, W.-X. Gu, C.-G. Zheng and H.-J. Wang, *Carbohydr. Polym.*, 2012, **90**, 792-798.
52. X. M. Hu, Y. B. Xiao, K. Niu, Y. Zhao, B. X. Zhang and B. Z. Hu, *Carbohydr. Polym.*, 2013, **97**, 172-176.
53. C. Z. Li, Q. Wang and Z. K. Zhao, *Green Chem.*, 2008, **10**, 177-182.
54. N. Abatzoglou, E. Chornet, K. Belkacemi and R. P. Overend, *Chem. Eng. Sci.*, 1992, **47**, 1109-1122.
55. Y. Kim, T. Kreke, N. S. Mosier and M. R. Ladisch, *Biotechnol. Bioeng.*, 2014, **111**, 254-263.
56. F. Carvalheiro, T. Silva-Fernandes, L. C. Duarte and F. M. Gírio, *Appl. Biochem. Biotechnol.*, 2009, **153**, 84-93.
57. H. L. Chum, D. K. Johnson, S. K. Black and R. P. Overend, *Appl. Biochem. Biotechnol.*, 1990, **24-5**, 1-14.
58. F. Carvalheiro, G. Garrote, J. C. Parajo, H. Pereira and F. M. Girio, *Biotechnol. Prog.*, 2005, **21**, 233-243.
59. H. Rasmussen, H. R. Sorensen and A. S. Meyer, *Carbohydr. Res.*, 2014, **385**, 45-57.
60. R. Kumar, F. Hu, P. Sannigrahi, S. Jung, A. J. Ragauskas and C. E. Wyman, *Biotechnol. Bioeng.*, 2013, **110**, 737-753.
61. N. Sun, M. Rahman, Y. Qin, M. L. Maxim, H. Rodriguez and R. D. Rogers, *Green Chem.*, 2009, **11**, 646-655.
62. W. H. Hsu, Y. Y. Lee, W. H. Peng and K. C. W. Wu, *Catal. Today*, 2011, **174**, 65-69.
63. L. J. A. Conceiçao, E. Bogel-Lukasik and R. Bogel-Lukasik, *RSC Adv.*, 2012, **2**, 1846-1855.
64. T. Ahmad, L. Kenne, K. Olsson and O. Theander, *Carbohydr. Res.*, 1995, **276**, 309-320.
65. J. B. Binder, J. J. Blank, A. V. Cefali and R. T. Raines, *ChemSusChem*, 2010, **3**, 1268-1272.
66. V. Choudhary, A. B. Pinar, S. I. Sandler, D. G. Vlachos and R. F. Lobo, *ACS Catal.*, 2011, **1**, 1724-1728.

CHAPTER VI

Biorefinery approach for biomass valorisation with acidic ionic liquid

---

This chapter is based on data and information of the following publication:

A. M. da Costa Lopes, R. M. G. Lins, R. A. Rebelo and R. M. Lukasik, Biorefinery approach for lignocellulosic biomass valorisation with acidic ionic liquid, *Energ. Environ. Sci.*, 2017 (submitted).

6.1. Introduction

The low carbon economy is the main med-century targets of European Union.[1] One of the ways to achieve this objective is the use of renewable carbon sources as alternatives to fossil oil. Abundant lignocellulosic biomass is one from not many available sustainable carbon sources able to play a key role in the achievement of these objectives.[2] Hence, a more extensive valorisation of lignocellulosic biomass, where all fractions are selectively processed towards a variety of products, is needed to accomplish the biorefinery concept. The efficient lignocellulosic biomass processing requires a selection of suitable technologies and strategies that underpin maximal separation of main polymeric fractions of biomass, namely cellulose, hemicellulose and lignin. On the other hand, a very complex inter- and intramolecular network existing between these components makes the fractionation of lignocellulosic biomass a very challenging task.[3] Various physical, chemical and thermal technologies have been widely studied to overcome the biomass recalcitrance.[4] Among conventional treatments are processes involving acids (*e.g.* H_2SO_4) and alkaline reagents (*e.g.* ammonia and NaOH). In general, they guide to a partial biomass fractionation and the recovery of catalysts (acid or base) is still intricate. Alternative solutions are water-based processes, *i.e.* steam explosion and liquid hot water. The advantage of these processes is no need of the addition of chemicals (catalysts). The main shortcoming is that only hemicellulose is extracted (often in oligosaccharide form) and this normally takes place at elevated temperature, *e.g.* 220 °C.[5] Hence, to solve the bottlenecks of current pre-treatment technologies, greener and more sustainable technologies of lignocellulosic biomass conversion are required. In this context ionic liquids,[6] carbon dioxide[7, 8] and bio-based solvents (*e.g.* γ-valerolactone, tetrahydrofuran)[9-12] are often a first choice because allow achieving a selective biomass processing at less sever conditions, although a cost-efficient recovery of this novel solvent/catalyst is still an issue.

Ionic liquids (ILs) are organic salts characterised by low melting point. They are constituted by a large-size organic cation with low charge density that establishes weak electrostatic interactions with an inorganic or organic anion. This makes that ILs possess many intriguing physico-chemical properties, including a great solvent power.[13] Due to these, ILs have been recognised to be good alternatives to volatile organic compounds in many processes including biomass dissolution,[14-16] pre-treatment,[17, 18] extraction,[19, 20] fractionation[21-23] and catalysis.[24]

A partial or total dissolution of lignocellulosic biomass in ILs has been broadly reported in literature in the last decade.[25] This process is based on the basicity of IL anion (*e.g.* acetate or chloride), which allows establishing strong hydrogen bond network with biomass polymers.[26] Therefore, a complete dissolution and subsequent improved biomass fractionation into main constituents can be achieved with alkaline ILs.[22] However, a biomass processing with these ILs produces fractions enveloped in

their polymeric matrix. Consequently, a subsequent chemical or enzymatic hydrolysis is needed to achieve upgradable sugars and aromatic compounds.

More recently, the use of acidic ILs demonstrated the potential to accomplish biomass process intensification. Acidic ILs allowed performing a pre-treatment and hydrolysis of biomass. The pioneer works have proven the catalytic performance of 1-butyl-3-methylimidazolium hydrogensulphate ([bmim][HSO_4]) towards biomass.[27-30] In these processes, the anion delivers the catalytic power to perform the hydrolysis of biomass. Other acidic ILs, *i.e.* 1-H-3-methylimidazolium chloride ([Hmim][Cl]) and 1-butyl-3-H-imidazolium hydrogensulphate ([bHim][HSO_4]) demonstrated the ability to hydrolyse biomass when an acidic proton is present in the cation.[24, 31] Another example are ILs with a sulfonic group (SO_3H) in the cation. The presence of this group increases the acidity of IL and provides additionally catalytic power to the biomass processing.[30, 32] One common drawback of the aforementioned works is low or in the best cases, moderate yields of released monosaccharides. One of the reasons might be a highly acidic character of these ILs. Therefore, learned from those works, a principal challenge in the current research on lignocellulosic biomass valorisation with ILs is the integration of biomass fractionation and depolymerisation of polysaccharides to deliver upgradable monosaccharides as well as aromatic compounds from lignin. Furthermore, considering the major challenge in the IL biomass processing, which is price of IL, developed processes have to demonstrate an efficient recovery and reusability of IL without jeopardising the process performance. One of the forerunner works in this context was recently published by Hallett and co-workers, who demonstrated an integrated processing of *Miscanthus* with the acidic triethylammonium hydrogensulphate ([TEA][HSO_4]) IL.[33] The authors claimed a complete dissolution of hemicellulose and an 85 wt.% lignin extraction to the IL phase at 120 °C for 24h. Therefore, a resulting solid was mainly constituted by cellulose, which after enzymatic saccharification demonstrated 77 wt.% of glucan to glucose yield. Additionally, they showed the possibility of lignin recovery from future upgrading.[33] One of the major weaknesses of the presented work was unsuccessful valorisation of hemicellulose, which constitutes *ca.* 1/5 of dried *Miscanthus*. The main part of this fraction was degraded (furfural) and resulting monosaccharides were never recovered from the IL stream for valorisation.

The present work proposes solutions that encompass these shortcomings and demonstrates a biorefinery concept based on the valorisation of lignocellulosic biomass to pentoses, glucose, lignin and aromatic compounds. The first stage of the process relied on the wheat straw processing with a catalytic system composed of 1-ethyl-3-methylimidazolium hydrogensulphate ([emim][HSO_4]) and H_2O. This system allowed the selective hydrolysis of hemicellulose to pentose characterised by a high yield. The challenge of pentoses and IL separation and recovery as well as reuse of IL was also successfully addressed.

A produced solid, enriched in cellulose and lignin, was subject of the subsequent fractionation. In this context, two different scenarios were evaluated and they considered the lignin extraction followed by

the enzymatic hydrolysis or direct enzymatic saccharification of produced solid. In both scenarios, an upgradable stream of sugar(s) and a solid fraction of lignin were obtained, however in case of process with preceding lignin extraction, the additional fraction of depolymerised aromatic compounds with high value was produced too.

Finally, this work also demonstrates a holistic techno-economic analysis of two potential processes to help to evaluate the feasibility of [emim][HSO_4] use as solvent and catalyst for biomass processing in the biorefinery concept.

6.2. Experimental

6.2.1. Biomass and chemicals

The wheat straw used in this work was received from Estação Nacional de Melhoramento de Plantas (Elvas, Portugal). The biomass was air-dried, grounded with a knife mill IKA® WERKE, MF 10 basic (Germany) to particle size <0.5 mm and stored in glass containers at room temperature. The composition of biomass is given in Table 6.1. The moisture content was 8.3 ± 0.2 wt.% and was determined by AMB-50 moisture analyser.

Table 6.1. Macromolecular composition of wheat straw.[34]

Component	wt.% (dried weight)[a]
Cellulose[b]	38.5 ± 0.1
Hemicellulose	24.9
Arabinoxylan	22.1 ± 0.7
Acetyl groups	2.7 ± 0.2
Klason lignin	17.7 ± 0.1
Ash	10.7 ± 0.1
Proteins	4.7 ± 0.1
Others[c]	3.5

[a] average of two replicates. [b] on glucan basis. [c] determined by difference.

The [emim][HSO_4] IL (99 wt.% of purity) was purchased from Iolitec GmBH (Heilbronn, Germany) and was used in reactions without any further purification. The H_2O content in IL was determined by a volumetric Karl-Fischer titration and was 3796 ppm. Ultrapure H_2O (18.2 MΩ·cm^{-1}) used for biomass fractionation and preparation of acid and alkali solutions was produced by the PURELAB Classic of Elga system. Glucose (≥98 wt.%, Merck, Germany), xylose (≥98 wt.%, Merck, Germany), arabinose (≥ 98 wt.%, Merck, Germany), furfural (99 wt.%, Sigma-Aldrich, Germany), 5-hydroxymethylfurfural

(99 wt.%, Sigma-Aldrich, Germany) and acetic acid (glacial, 99.8 wt.% Merck, Germany) were used for the qualitative and quantitative HPLC analyses of the obtained liquids and solids. Sulphuric acid (96 wt.%, Panreac, Spain) was used to prepare mobile phase for HPLC analyses (5 mM sulphuric acid). NaOH aqueous solutions for lignin extraction as well as for capillary electrophoresis were prepared from NaOH pellets (99 wt.% purity) supplied by Eka Chemicals/Akzonobel - Bohus, Sweden. HCl solution for acidification of lignin-rich solid was prepared from HCl fuming 37 wt.% (Merck, Germany). Potassium bromide (99 wt.% trace metals basis) purchased from Sigma–Aldrich Co. (St. Louis, MO, USA) was used for FTIR analyses.

For IL recycling and purification, column chromatography was prepared using alkaline alumina 90 active I (70-230 mesh, Merck, Germany), and acetonitrile (99.9 wt.% HPLC gradient, Carlo Erba, Italy) in mixture with water (97/3 $w \cdot w^{-1}$) was used as eluent.

The same acetonitrile as well as ethanol (96 vol.%, Merck, Germany) and methanol (99.9 wt.%, CARLO ERBA reagents, Italy) were used for extraction of aromatic compounds prior to capillary electrophoresis analyses. A borate buffer was used for detection of aromatic compounds (in capillary electrophoresis) consisting of 15 mM disodium tetraborate decahydrate (≥99.5 wt.% Merck, Germany) dissolved in 10 vol.% methanol aqueous solution and pH was adjusted to 9.

The enzymatic cocktail of Celli® CTec2 kindly provided by Novozymes (Denmark) was used for enzymatic hydrolysis assays. Aqueous solution of 100 mM acetic acid was used as buffer for enzymatic hydrolysis and sodium azide (99 wt.%, Merck, Germany) solution was used to maintain aseptic medium in the enzymatic hydrolysis.

The Nylon filters (Ø 47 mm, 0.45 mm porosity) from Merck Millipore (Billerica, MA, USA) were also used for all filtrations. Nylon syringe filters (Ø 13 mm, 0.22 mm porosity), purchased from Red® analytical (Cambridgeshire, UK), were used to filter all samples before running on the capillary electrophoresis and HPLC instruments.

Basylone M-350 oil purchased from Bayer (Leverkursen, Germany) was used as the heating medium for reaction experiments. Filtering crucibles equipped with a fritted disc, Gooch with porosity grade 4 from SciLabware (Stone, Staffordshire) were used for the solid analyses.

6.2.2. Biomass processing

The procedure of biomass processing is presented in Figure 6.1. This figure aims guiding through each step of biomass treatment and fractionation from native biomass to the targeted products. All the names of fractions given in italic in this section are used coherently along the entire work with the aim at easy identification of analysed and discussed fractions.

The first step of the process relied on the wheat straw pre-treatment and hydrolysis of hemicellulose performed by the mixture of acidic [emim][HSO_4] and H_2O (indicated as *Reaction* in Figure 6.1.). In

this process, hemicellulose underwent hydrolysis to pentoses (*liquid* in Figure 6.1.), leaving cellulose and lignin as major fractions in the *solid*. The *liquid* was subject of a chromatographic separation of produced pentoses and recovery of IL. Afterwards, the recovered IL was used in a new treatment. The *solid* was studied in two separate manners. Scenario A considered a direct enzymatic hydrolysis of the *solid* and production of *C5/C6 sugars* and *lignin-rich solid A*. Scenario B involved a *lignin extraction* step prior to the enzymatic hydrolysis. The *lignin extraction* produced a *lignin-rich liquid*, which after acidification allowed recovering a *lignin-rich solid B1*. Additionally, after subsequent steps *aromatic compounds* were obtained. The lignin extraction step left cellulose intact producing *cellulose-rich solid*, which was the subject of the enzymatic hydrolysis resulting in *glucose* liquor and *lignin-rich solid B2*.

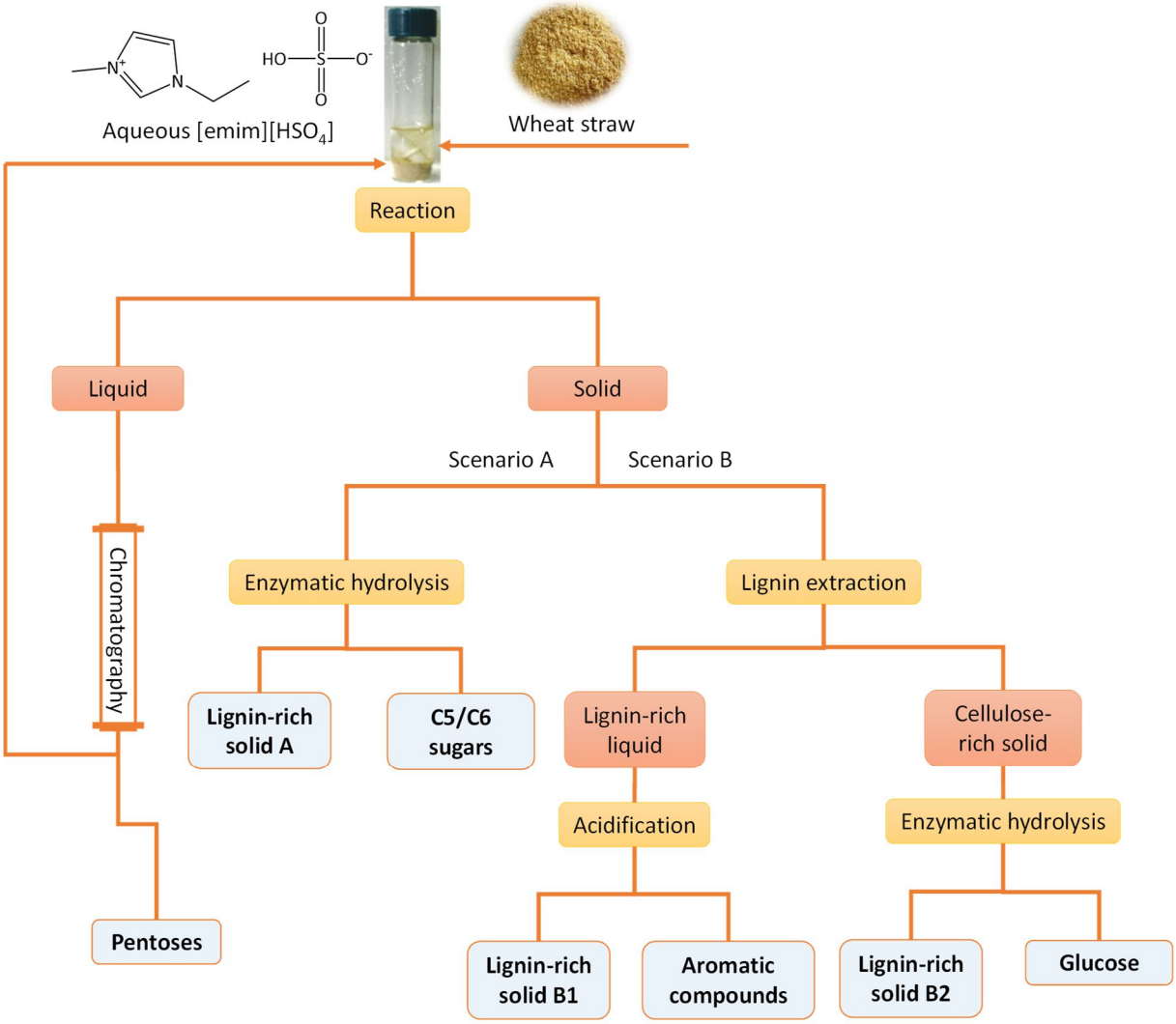

Figure 6.1. Biorefinery concept of wheat straw valorisation with aqueous solution of [emim][HSO_4].

All aforementioned steps are described in detail in the following sections. Analytical techniques, such as high-performance liquid chromatography (HPLC), Fourier Transform Infrared spectroscopy (FTIR) and capillary electrophoresis (CE), were used for quantitative and qualitative characterisations of liquid or solid fractions. Detailed description of each analytical technique is given in this section too.

6.2.2.1. Reaction of wheat straw with aqueous ionic liquid solution

All reactions were performed with a 10 wt.% of dry biomass in the reaction mixture. For this purpose, 0.5 g of dry biomass (≈ 0.545 g wheat straw) and 4.5 g of aqueous ionic liquid solution ([emim][HSO_4]/H_2O) with pre-established composition (see Table 6.2. for details), were put into a 15 mL glass vial (Supelco/Sigma-Aldrich, USA). A vial was placed in the oil bath pre-heated to a desired temperature (according to Table 6.2.), and reactions were carried out for determined period of time (see Table 6.2. for details), under continuous magnetic stirring. After reaction, the mixture was cooled down to room temperature and approximately 5.0 mL of ultrapure H_2O was added to precipitate non-hydrolysed polymers. The resulting mixture was filtered under vacuum using 0.45 μm nylon membrane filters (Merck Millipore, USA). The liquid phase was collected and stored in a freezer, while recovered solid biomass was washed with 100 mL of ultrapure H_2O (in 10 mL portions) to guarantee removal of IL from precipitated solid. Such obtained solid was placed in the oven at 60 °C for 24 hours and afterwards was stored at room temperature for 1 hour to analyse the dry mass content.

6.2.2.2. Experimental design of reactions towards pentose production in the liquid

The reaction conditions were established according to the Doehlert experimental design.[35, 36] For this purpose, an experimental distribution for three variables was considered. Fifteen experiments listed in Table 6.2. were carried out to scrutinise the effect of independent variables, namely temperature (X_1) between 90.0 and 160.0 °C, H_2O content in the mixture with IL (X_2) between 30 wt.% and 70 wt.% and time (X_3) from 60 to 100 minutes on the pentose yield (mol%) - expected output (Y). For the pentose yield calculation, the arabinose and xylose produced as well as the amount of arabinoxylan present in the native dry biomass were considered. Also the correction for dehydration (132/150) was included in the calculations.

Following the preliminary experiments[28, 37] a temperature of 140 °C was initially considered to be the upper limit of X_1 domain. However, along the performed reactions, the obtained results (Y) showed the need of redesigning a X_1 domain to 160 °C (entry 14 - Table 6.2.) to ensure achievement of a maximal response Y. Consequently, X_1 values were recalculated and by this, coded X_1 do not correspond to the original Doehlert matrix.[35, 36]

A second order polynomial ($Y = \beta_0 + \beta_1 X_1 + \beta_2 X_2 + \beta_3 X_3 + \beta_{12} X_1 X_2 + \beta_{13} X_1 X_3 + \beta_{23} X_2 X_3 + \beta_{11} X_1^2 + \beta_{22} X_2^2 + \beta_{33} X_3^2$) was used to express the response (Y). X_n ($n = 1,2\ or\ 3$) are the experimental factor levels

(independent variables expressed as coded units) and β_n ($n = 1, 2\ or\ 3$) are the regression coefficients of the model. The β_0 represents the analysed response in the centre of the experimental domain; β_1, β_2 and β_3 indicate the importance of temperature, H_2O content and time, respectively, on the response; β_{12}, β_{13} and β_{23} are the interaction parameters that indicate how the effect of one factor depends on another factor; β_{11}, β_{22} and β_{33} determine how the response surface folds downward (negative values) or upward (positive values) quadratically.

Table 6.2. Independent variables: temperature (X_1), H_2O content (X_2) and time (X_3) and their respective coded levels for statistical modelling as well as obtained results (Y) and severity factors (R_O) of the performed reactions.

Entry	X_1		X_2		X_3		$logR_O$[a]	Y (mol%)
	T (°C)	coded	H_2O (wt.%)	coded	t (min)	coded		
1	115.0	-0.286	50.4	0.020	80.0	0.000	3.92	54.5
2	140.0	0.429	50.0	0.001	80.0	0.000	5.39	77.5
3	90.0	-1.000	50.1	0.005	80.0	0.000	2.45	20.9
4	127.5	0.071	67.5	0.875	80.0	0.000	4.66	74.4
5	102.5	-0.643	33.1	-0.845	80.0	0.000	3.19	26.4
6	127.5	0.071	32.7	-0.863	80.0	0.000	4.66	67.0
7	102.5	-0.643	67.4	0.868	80.0	0.000	3.19	26.6
8	127.5	0.071	56.0	0.300	96.3	0.817	4.76	76.8
9	102.5	-0.643	44.3	-0.284	63.7	-0.817	3.07	24.7
10	127.5	0.071	44.4	-0.278	63.7	-0.817	4.53	67.5
11	115.0	-0.286	61.7	0.585	63.7	-0.817	3.80	43.7
12	102.5	-0.643	55.7	0.286	96.3	0.817	3.28	28.7
13	115.0	-0.286	38.8	-0.562	96.3	0.817	4.02	56.2
14	160.0	1.000	50.1	0.005	80.0	0.000	6.56	59.1
15	115.0	-0.286	49.9	-0.006	80.0	0.000	3.92	54.1

[a] Severity factor calculated according to a procedure given in Appendix C.

6.2.2.3. Liquid processing: Separation of pentoses and ionic liquid

A preparative chromatography was used to separate pentoses from IL. For this purpose, alumina (> 20 g) was placed in a beaker and stirred with 100 mL of 0.5 M H_2SO_4 aqueous solution at room temperature for 1 h. The solution was decanted and alumina was washed several times with ultrapure

H_2O until supernatant had a neutral pH. Subsequently, the alumina was placed in the oven at 200 °C overnight.

The succeeding steps of stationary phase preparation and procedure of separation of [emim][HSO_4] and pentoses is presented in Figure 6.2. A 20 g of prepared dried alumina was packed in a glass column (25 cm height, 1 cm i.d.) previously filled with acetonitrile. The stationary phase was then rinsed with 100 mL of acetonitrile to guarantee an adequate packing in the column (Figure 6.2. A). Later, 1.9 g [emim][HSO_4] dissolved in 0.2 L of acetonitrile/H_2O (97/3 w·w^{-1}) was placed in the column (Figure 6.2. B). This procedure allows avoiding losses of IL during the elution process.[38] Finally, 1.1 L of acetonitrile/H_2O (97/3 w·w^{-1}) mixture was used as eluent (Figure 6.2. C). Such prepared column was ready for separation of IL and pentoses present in the liquid produced in the reaction at optimal conditions.

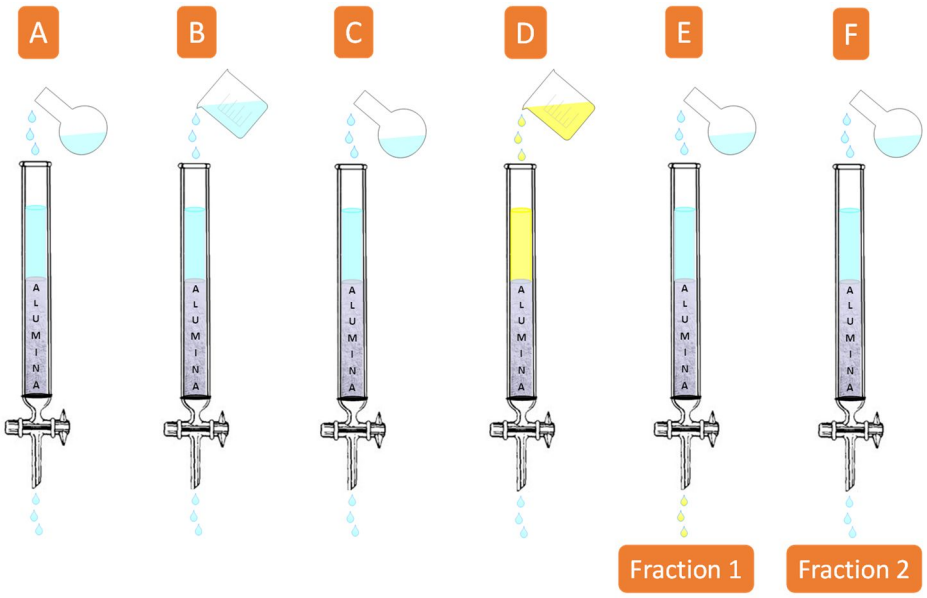

Figure 6.2. Preparative chromatography for the separation of [emim][HSO_4] and pentoses from the liquid. A: packing H_2SO_4 pre-treated stationary phase with acetonitrile; B: elution of [emim][HSO_4] dissolved in acetonitrile/H_2O (97/3 w·w^{-1}); C: washing out the IL excess with acetonitrile/H_2O (97/3 w·w^{-1}); D: addition of reaction liquid dissolved in acetonitrile/H_2O (97/3 w·w^{-1}) in a total volume of 0.2 mL; E: elution of 0.2 L of acetonitrile/H_2O (97/3 w·w^{-1}) for the recovery of IL-rich fraction 1; F: elution of 1.1 L of acetonitrile/H_2O (97/3 w·w^{-1}) for the recovery of pentose-rich fraction 2.

Prior to preparative chromatography, all water from the liquid sample was removed to produce a solution composed solely by IL and biomass hydrolysis products, mainly pentoses. This solution was re-dissolved in 0.2 L of acetonitrile/H_2O (97/3 w·w^{-1}) eluent. After eluting the sample through the column (Figure 6.2. D), more 1.1 L of eluent with same composition was used. On the basis of

previous results[38] two fractions of 0.2 L (Fraction 1 – Figure 6.2. E) and 1.1 L (Fraction 2 – Figure 6.2. F) were collected. After the solvent removal under reduced pressure, the obtained samples were re-dissolved in 2 mL of H_2O, filtered through a 0.45 μm membrane filter syringe and analysed by HPLC according to the procedure described in 6.2.3.1. section.

6.2.2.4. Liquid processing: Reuse of ionic liquid

IL was recovered from eluate samples (Figure 6.2. E) by removing the eluent under reduced pressure (rotatory evapouration under high vacuum). Next, a known amount of H_2O that corresponded to the optimal quantity according to conditions established in 6.2.2.2. section, was added to recovered IL and a such aqueous IL mixture was used in new experiment of biomass reaction performed according to the procedure described in 6.2.2.1. section

6.2.2.5. Solid processing: Scenario A

The solid obtained from the reaction performed at optimal conditions (131.0 °C, 58.7 wt.% H_2O and 88.0 min) was used for enzymatic hydrolysis. The procedure of the enzymatic hydrolysis is presented in 6.2.2.7 section. Enzymatic saccharification resulted in liquid stream of C5/C6 sugars and solid that was filtrated, washed with ultrapure H_2O, and placed in an oven at 60 °C for 24 hours. This solid fraction designated as lignin-rich solid A was characterised by FTIR according to method presented in 6.2.3.3. section.

6.2.2.6. Solid processing: Scenario B

The solid obtained from the reaction performed at optimal conditions was subject of a lignin extraction carried out with an aqueous solution of NaOH (0.75 M) at 70 °C for 1 hour with a solid/liquid ratio of 1:25 ($g_{solid} \cdot (mL_{NaOH\ solution})^{-1}$).[34] The liquid phase resulted from this treatment contained lignin-rich liquid and cellulose-rich solid. Both fractions were separated by filtration and solid was washed with water. The lignin-rich liquid was acidified to pH of 1.5 using an aqueous HCl solution to precipitate lignin. A formed lignin-rich solid B1 was washed with aqueous HCl solution (pH = 2) to avoid any lignin dissolution during this step. The liquid phase from lignin-rich solid B1 precipitation contained aromatic compounds. The last was neutralised with NaOH aqueous solution and water was evapourated under reduced pressure at 50 °C. This caused a solid formation, which contained NaCl and precipitated aromatic compounds, which were analysed according to the method presented in 6.2.3.4. section.

A previously referred cellulose-rich solid underwent enzymatic hydrolysis as described in 6.2.2.7. section. The solid remained after the enzymatic treatment was filtrated, washed with ultrapure H_2O, and placed in an oven for 24 h at 60 °C. This solid fraction designated as lignin-rich solid B2 was characterised by FTIR as described in 6.2.3.3. section.

6.2.2.7. Enzymatic hydrolysis of solids

The digestibility of cellulose present in the solid in scenario A and the cellulose-rich solid in scenario B was evaluated by enzymatic hydrolysis. The assays were performed in 30 mL vials with 2.5 mL of 0.1 M acetate buffer (pH 4.8) and 100 µL of a 2 wt.% sodium azide solution to prevent undesired growth of microorganisms. Distilled water was added to reach 5.0 mL taking into account the volume of enzyme added as the last. An enzymatic solution of 100 $mg \cdot L^{-1}$ prepared from Celli® CTec2 (199.9 $FPU \cdot mL^{-1}$) was added considering a ratio of 100 $mg_{enzyme} \cdot g_{glucan}^{-1}$ content in the examined solid samples. The enzymatic hydrolyses were performed in a shaking incubator (Optic ivymen® system – Spain) at 200 rpm and 50 °C for 72 h. After hydrolysis, enzymes were inactivated by freezing the samples. To measure monosaccharide content, the hydrolysates were filtered under vacuum using nylon filters (pore size of 0.45 µm) and analysed by HPLC according to procedure described in 6.2.3.1. section. The glucose and xylose yields were calculated considering the glucan and xylan contents and factors of (162/180) and (132/150) for dehydration, respectively.

6.2.3. Chemical analyses of solids and liquids

6.2.3.1. HPLC analysis

The analyses of the solid composition (cellulose and hemicellulose content) performed by means of quantitative acid hydrolysis according to the NREL protocol[39] were performed using HPLC. The liquid phases from reactions were directly analysed by HPLC to determine the content of monosaccharides, furans and acetic acid following a procedure described elsewhere.[40] The liquids obtained from enzymatic hydrolysis were analysed also directly in order to determine a release of glucose and xylose.

All HPLC analyses were performed using Agilent 1100 series HPLC system (Agilent Technologies, USA) equipped with Aminex HPX-87H column (Bio-Rad, USA) using a 5 mM H_2SO_4 mobile phase. The column temperature was 50 °C, while injection volume and flow rate of 5 µL and 0.6 $mL \cdot min^{-1}$ were used, respectively. The detection was performed using RID (refractive index detector) for monosaccharides (glucose, xylose and arabinose) and acetic acid and DAD (diode array detector) at 280 nm wavelength for furans (furfural (furan-2-carbaldehyde) and 5-HMF ≡ 5-hydroxymethylfurfural (5-(hydroxymethyl)-2-furaldehyde)). The quantitative analyses were made against the calibration curves produced with external standards of obtained products.

6.2.3.2. Lignin content in solid

The lignin content in solids obtained from reactions was determined gravimetrically following the aforementioned method of quantitative acid hydrolysis according to the NREL protocol.[39]

6.2.3.3. FTIR spectroscopy analysis

Approximately 1.0 mg of each lignin-rich solid (A, B1 and B2) was mixed with 50.0 mg of KBr and grinded in a mortar, until a homogeneous mixture was obtained. The grinding time was 5 min and samples were placed in a press with 8.5 tonnes for 5 min. All spectra were registered using a FTIR spectrometer Spectrum BX, Perkin Elmer, Inc. (San Jose, CA, USA). This instrument was equipped with a DTGS detector and KBr beam splitter. The operating system used was Spectrum software (Version 5.3.1, Perkin Elmer, Inc., San Jose, CA, USA). All FTIR spectra were acquired in the 4000–400 cm^{-1} region, with 16 scans and a resolution of 4 cm^{-1} with a strong apodisation in the absorbance mode. A background air spectrum was subtracted from spectra of analysed samples.

6.2.3.4. Capillary electrophoresis analysis of aromatic compounds

Capillary electrophoresis technique was used to perform analyses of the aromatic compounds. Prior the analysis, the solid produced in the neutralisation with NaOH was subject to consecutive solid-liquid extractions using organic solvents *i.e.* 40 mL of acetonitrile, 20 mL of ethanol and 10 mL of methanol. The organic fraction containing soluble aromatic compounds was decanted and organic solvents were evapourated to produce solid extracts. Those solids were re-dissolved in 0.5 mL water and were subject of the capillary electrophoresis analysis. The analyses were made using an Agilent Technologies CE system (Waldbronn, Germany), equipped with a diode array detector. The Agilent 3D-CE ChemStation data software (Rev B.04.01) was used to perform qualitative and quantitative analyses. An uncoated fused-silica extended light path capillary from Agilent with i.d. 50 μm and 56/64.5 cm length was used. Between runs, the capillary was preconditioned by flushing with 1.0 M NaOH and 0.1 M NaOH, 3 min each, and finally with the electrolyte solution (15 mM borate buffer) for 5 min. Samples were filtered through a 0.45 μm membrane filter and were injected directly for 5 s under the pressure of 50 mbar at the anode of the CE system. The separation voltage applied was +30 kV producing approximately 25 μA of current. Identification of compounds was done by electrophoretic comparison (migration times and spectra) with authentic standards performed using direct UV detection at wavelength of 200 nm with a bandwidth of 10 nm.

6.2.4. Experimental and analytical error analysis

Standard deviation errors (u) were calculated for all obtained results. The applied temperature in reactions demonstrated an u(T)=1 °C. All mass determinations were performed using a Mettler Toledo, XS205 dual range scale (Germany) with a given u(m)=0.1 mg.

In order to estimate the experimental errors of the biomass processing, the experiment at the conditions determined by the centre of Doehlert domains was performed in duplicated (entries 1 and 15 in Table 6.2.).

All analyses were performed at least in duplicate and average results are presented in the following sections.

6.3. Results and Discussion

Figure 6.1. presents a general concept explored in this work, which aimed at wheat straw valorisation via cascade process contemplating fractionation and depolymerisation of all biomass components, *i.e.* cellulose, hemicellulose and lignin. The reactions of biomass processing with aqueous [emim][HSO_4] solutions were performed under conditions presented in Table 6.2. and resulted in liquid and solid (for liquid and solid compositions see Tables C.1. and C.2. in Appendix C), which are discussed in the following sections.

6.3.1. Pentoses as a major product of biomass reaction

The severity factor (R_O) was used to encompass the experimental variables because it allows for transformation of independent variables into a single numerical value for each set of conditions. The methodology employed to determine the severity factor for processes with IL is presented in Appendix C. The products found in liquid were analysed as a function of R_O and are given in Figure 6.3. The analysis of this figure shows that liquid from the reaction of biomass with aqueous [emim][HSO_4] solution contained pentoses (arabinose and xylose) and their degradation product – furfural. Additionally, cellulose-derived products such as glucose and 5-HMF were found too.

A close inspection of Figure 6.3. shows that for the least severe reaction conditions ($logR_O$ = 2.45) a pentose yield of 20.9 mol% was attained. This considerable amount of pentoses in the liquid confirms that acidic [emim][HSO_4] had already a catalytic effect on hemicellulose at temperature as low as 90 °C. Comparing this finding to *e.g.* hydrothermal processes, a significant advance in case of acidic IL can be observed, because in hydrothermal processes the hydrolysis of hemicellulose is considered to begin at temperatures not lower than 100 °C.[41] Even in case of dilute acid hydrolysis of biomass with *e.g.* H_2SO_4, the most commonly employed temperature of the process is not lower than 140 °C as reported in literature.[5]

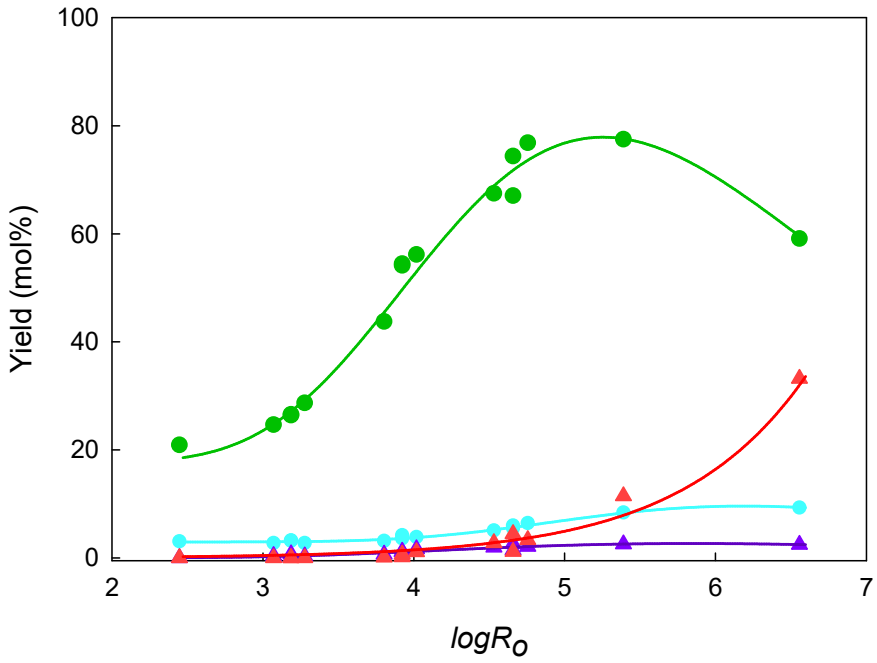

Figure 6.3. The profiles of yields of (●) sum of arabinose and xylose, (▲) furfural, (●) glucose and (▲) 5-HMF as a function of the $logR_O$. Lines are a guide for the eye. For details of quantitative analysis please refer to Appendix C.

An increase in the reaction severity contributed to an increase in pentose yield to a maximum of 77.5 mol% at $logR_O$ = 5.39, 140 °C. Further increase in the reaction severity demonstrated a negative effect on the pentose yield because it promoted the furfural degradation for $logR_O$ > 5.39. At the most severe reaction conditions ($logR_O$ = 6.56, 160 °C), pentoses were still main products (59.1 mol%), however furfural yield sharply increased and constituted already 1/3 of all potential products from hemicellulose hydrolysis. These results are not surprising because a high performance of acidic ILs towards furfural was often reported in literature.[29, 42] For example Brandt *et al.* found that reaction of *Miscanthus* (16 wt.% of water content) with [bmim][HSO_4] at 120 °C during 22 h produced 33 % of furfural.[29] Carvalho *et al.* also found that when using the same IL in the reaction of wheat straw at 160 °C and 156.6 min, as much as 36.2 mol% of furfural can be obtained.[28]

Contrary to a great performance of aqueous [emim][HSO_4] solution in processing hemicellulose, a cellulose hydrolysis with this catalytic system seems to be very inefficient. As it can be observed in Figure 6.3., either glucose or 5-HMF was barely produced for the entire range of reaction severities. The glucose yield maintained constant for the moderate reaction severity. At these conditions, the produced glucose might originate in the hydrolysis of xyloglucans from hemicellulose or amorphous cellulose because crystalline cellulose is practically insoluble in [HSO_4]-based ILs. Acetate (β^{43} = 1.20 for [bmim][OAc][17]) or chloride ILs are good solvents for cellulose, however the [HSO_4] anion is

characterised by poor basicity (β^{43} = 0.67 for [bmim][HSO_4][29]) and [HSO_4]-based ILs are unable to alter the solvation environment of crystalline cellulose.[44]

In order to achieve the best valorisation of the biomass, the maximal removal of hemicellulose from biomass should be sought. The profiles of pentoses shown in Figure 6.3. confirm a possibility to achieve a maximum of selective hydrolysis of hemicellulose to pentoses. Thus, for this purpose, the multiple linear regression analysis of the obtained pentose yields as function of temperature, H_2O content and time was performed according to the methodology presented in 6.2.2.2. section. A response surface model representing the obtained pentose yield as a function of temperature and H_2O content is demonstrated in Figure 6.4.

The statistical modelling analysis performed according to 6.2.2.2. section allowed establishing conditions for maximisation of pentose yield. At conditions of 141.0 °C, 57.8 wt.% H_2O and 90.0 min, a maximum pentose yield of 78.8 mol% was expected to be obtained. The experimental validation gave 81.6 mol% pentose yield that confirms the accuracy of statistical analysis. The liquid and solid compositions obtained at these conditions are given in Tables C.3. and C.4. of Appendix C. The model parameters as well as the statistical analysis (Tables C.5. and C.6. in Appendix C) allowed understanding the significance of the studied temperature, H_2O content and reaction time. The β parameters showed that temperature is the only statistically significant variable while either H_2O content or time or any other combination of these two and temperature have no statistical significance within the range of studied domains. However, a careful analysis of Figure 6.3. and results in Table 6.2. allow finding the effect of H_2O on the obtained pentose yield. For instance, for temperature of 102.5 °C ($logR_O$ = 3.19), the experiments with 33.1 wt.% and 67.4 wt.% H_2O (entries 5 and 7 in Table 6.2.) gave only 0.2 mol% differences in pentose yields. Whereas for the same H_2O contents but for reactions performed at 127.5 °C ($logR_O$ = 4.66), the difference between pentose yields was as high as 7.4 mol% (entries 4 and 6, Table 6.2.). This show that H_2O content might have an impact on pentose production, but it is strongly dependent on temperature that governs the equilibrium of the hemicellulose hydrolysis into pentoses and the subsequent dehydration of pentoses into furfural. Furthermore, in the previous work, the presence of water (up to 10 wt.%) in the reaction of wheat straw with [bmim][HSO_4] revealed an increase in pentose yield and prevention of furfural formation in comparison to biomass treatment solely with IL.[28] Therefore, on the basis of these literature results[28] and those obtained in this work, it can be concluded that certain amount of H_2O is needed to influence significantly the pentose yield, however for amount surpassing this value, the effect of H_2O is statistically insignificant as demonstrated herein.

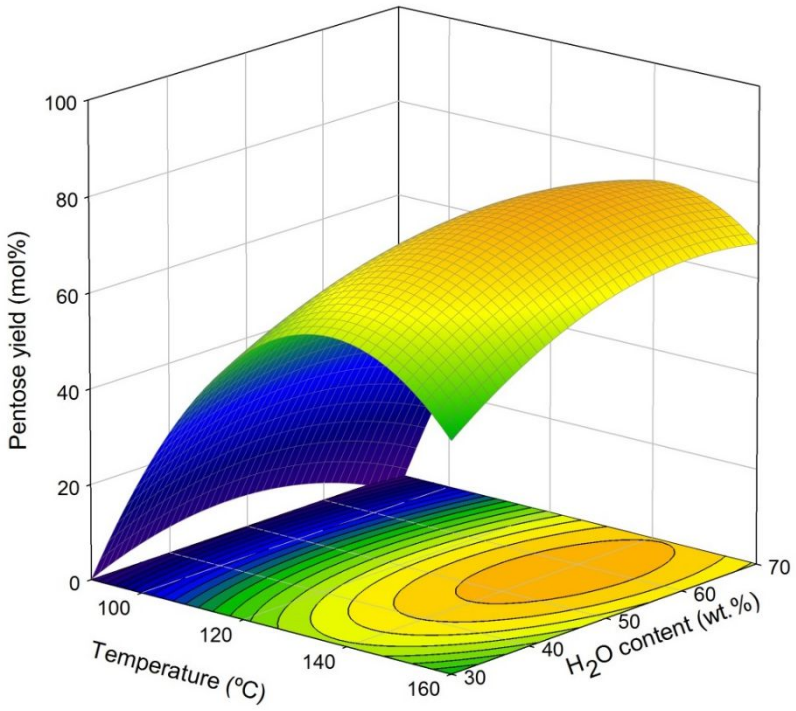

Figure 6.4. The 3D response surface of the pentose yield as a function of temperature and H_2O content for 90 min of reaction time.

Regardless to the statistical analysis, one of the most relevant conclusions is that the pentose yield obtained in this work is at least twice higher than those reported in literature up to date.[24, 28-31] For example, Li *et al.* employed [bmim][HSO_4] or 1-(4-sulfobutyl)-3-methylimidazolium hydrogensulphate ([bSO_3Hmim][HSO_4]) with 0.75 wt.% H_2O in the treatment of corn stalk at 100 °C. At these conditions only 23 % and 15 % reducing sugars, respectively were obtained.[30] Higher temperature (120 °C) and 4 h of *Miscanthus* reaction with [bmim][HSO_4] and 20 vol.% (17 wt.%) of H_2O content produced close to 16 % of hemicellulose sugar monomers.[29] Other work showed that the use of the same IL with 9.22 wt.% H_2O content in treatment of wheat straw (125 °C and 82.1 min) allowed to obtain 40.1 mol% pentose yield.[28] Additionally drawback of all those works is a lack of selectivity toward pentoses because of further degradation resulting in considerably low yields of the products of interest. As it was alleged above, the reason for such moderate pentose yields can be insufficient amount of H_2O present in the reaction systems. At the conditions presented in this work, the H_2O content was as high as 57.8 wt.%, which seems to not only inhibit the dehydration reaction of xylose and arabinose to furfural,[45] but also allows controlling the catalytic effect of IL. On the other hand, it can be expected that excessive amount of H_2O would hamper the catalytic performance of IL. Xu *et al.* found that the eucalyptus treatment catalysed by 0.5 vol.% [bmim][HSO_4] gave only ≈ 25 mol% of pentose yield at 190 °C.[27] This data confirms again that water presence is a very important

factor in the hemicellulose hydrolysis, which can be tuned towards pentoses or furfural production depending on the water content in the reactive system.

The obtained results revealed also one more important aspect. As it was already mentioned, more severe reaction conditions promoted undesired degradation of pentoses to furfural. Therefore, to minimise unproductive valorisation of biomass (formation of furfural), the statistical modelling was reorganised with the aim at maximising the yield of subtraction of pentose and furfural. Such approach showed that the optimal conditions were different (131.0 °C, 58.7 wt.% H_2O and 88.0 min) from the previous one and at these conditions the pentose and furfural yields were 80.5 mol% and 5.3 mol%, respectively (composition of liquids and solids obtained at these conditions please are given in Tables C.7. and C.8. of Appendix C) These surprising results demonstrated that by decreasing a temperature by 10 °C, a very similar pentose yield (80.5 mol% *vs.* 81.6 mol%) was obtained and at the same time, the amount of furfural dropped to a half.

6.3.2. Valorisation of the liquid: separation of pentoses and [emim][HSO$_4$]

One of the major challenges in the IL-based biomass processing is the IL recovery and reuse without a loss of its performance. The separation of the reaction products from IL is also often one of the major concerns.[46] Up to date, the recovery of ILs and products have been thoroughly studied using various separation processes *e.g.* chromatography,[47] ultra- and nanofiltration,[48] liquid-liquid,[49] and supercritical extractions.[22] In this work, the liquid obtained in the reaction contained [emim][HSO_4] and H_2O as solvents, pentoses as a major product, and glucose, furfural, 5-HMF and acetic acid as minority products. Because of similar molecular weights of [emim][HSO_4] (208 g·mol^{-1}) and pentoses (150 g·mol^{-1}) as well as high polarities of [emim][HSO_4], H_2O and pentoses neither ultra- nor nano-filtrations nor liquid-liquid nor supercritical extractions could be used. Therefore, following the literature reports, the preparative chromatography was chosen as the best separation technique for pentose and IL.[50]

Prior to IL and pentose separation, water was removed (vacuum distillation at 50 mbar at 50 °C) from the liquid sample to minimise the obstruction of separation of both chemicals. On the basis of the literature reports[38] it is also known that polarity is a key factor in separation of IL and pentoses. To circumvent this limitation, less polar acetonitrile (dipole moment = 3.91 D[51]) was used as a solvent. However, still negligible amount of water present in the system may produce a biphasic solution caused by the mutual solubility with acetonitrile. To avoid this, acetonitrile was added to the liquid in the amount that constituted a 97 wt.% of the (IL + acetonitrile + H_2O) mixture according to data presented elsewhere.[38] This procedure allowed achieving a good resolution of IL and pentoses because the first fraction (Fraction 1 - Figure 6.2. E) contained as much as 92.6 %(w·w^{-1}) of the initial IL mass used for biomass processing and no traces of pentoses. At the same time 85.4 %(w·w^{-1}) of 5-HMF produced in the reaction was also eluted. The second fraction (Fraction 2 – Figure 6.2. F) was

constituted by 88.6 %(w·w^{-1}) pentose and 10.8 %(w·w^{-1}) IL of the initial contents in the liquid from reaction. The obtained results mean unprecedented achievement regarding the separation of IL and monosaccharides. This subject has been tackled in the last years, and always IL hampered the separation of monosaccharides, either in artificial solutions or in biomass hydrolysates.[48, 52] In this context, different approaches of purification and separation were proposed, *e.g.* column chromatography with ion-exchange resins,[47] alumina,[50] simulated moving bed,[53] and others including anti-solvent precipitation,[54] electrodialysis,[48] aqueous biphasic systems[55] and monosaccharide derivatisation.[52] Most of these works mentioned recovery of ILs and monosaccharides with yields higher than 90 %(w·w^{-1}) however purities of each of separated fraction were practically disregarded. The present work demonstrates a clearly advance in separation of pentoses from IL that is especially noticeable when consider that the liquid of the reaction contained IL and pentoses in mass ratio of 19.0, while after the chromatography a pentose-rich fraction, the same mass ratio was 10-fold lower *i.e.* 1.9. Additionally, one of the major advantages of the developed process is that this significant enrichment was achieved just in one chromatographic run. Possibly, second purification could be further accessed in order to have even higher recovery of IL with no pentose presence. The literature reports confirm this expectation because for simulated moving bed chromatography, a 95 %(w·w^{-1}) IL was recovered in the first run, whereas more 4.5 %(w·w^{-1}) could be recovered in a second run.[53] Nevertheless, one of the main objectives should be always to not compromise a pentose recovery and that recovered IL maintains its catalytic potential. To confirm the last fact, recovered IL was reused in subsequent biomass reaction performed at the same optimal conditions (131.0 °C, 58.7 wt.% H_2O and 88.0 min). The obtained results are presented in Figure 6.5. and show an identical ability of recovered IL to produce pentoses (78.5 mol%) as observed for fresh IL (1st run) that was 80.5 mol%. Also, the composition of the resulting solid is similar to that obtained with fresh IL (see Table C.8. in Appendix C for details).

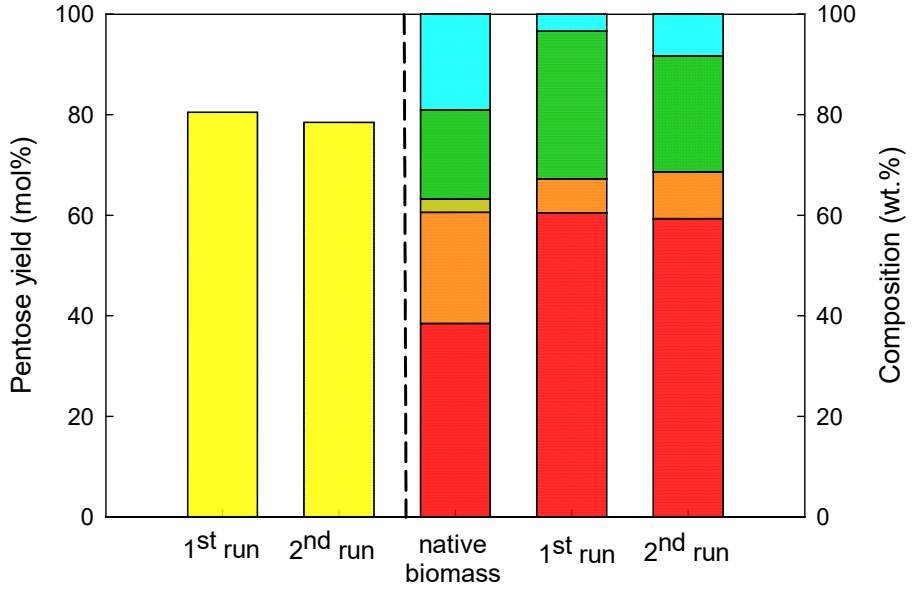

Figure 6.5. Performances of fresh (1st run) and recovered (2nd run) [emim][HSO_4]. Yellow bars indicate the pentose yield in liquid with fresh and recovered IL. Three right bars demonstrate the composition of native biomass (3rd bar from the right), of solid obtained with fresh IL (2nd bar from the right) and of solid from the reaction with recovered IL (1st bar from the right). The stacked bar corresponds to (■) glucan, (■) arabinoxylan, (■) acetyl groups, (■) Klason lignin and (■) others (*i.e.* extractives, ash, proteins, etc.).

6.3.3. Solid enrichment in cellulose and lignin

The above-discussed selective removal of hemicellulose constituents from biomass provides significant changes in the chemical composition of the obtained solids as shown in Figure 6.6.

The analysis of the composition of solids shows that with an increase in the reaction severity either cellulose (estimated as glucan) or lignin contents increased. This effect is directly related to the progressive removal of hemicellulose (arabinoxylan and acetyl group) to the liquids. For instance, at optimal conditions for pentose formation (131.0 °C, 58.7 wt.% H_2O and 88.0 min) the arabinoxylan content was reduced from the original 22.1 wt.% to 6.7 wt.%, whereas cellulose content raised up from 38.5 wt.% to 60.6 wt.% and lignin content increased from 17.7 wt.% to 29.3 wt.%. Also with an increase in the reaction severity the acetyl groups bonded to polysaccharides structure were completely removed from the solid and the corresponding acetic acid was found in the liquids as given in Table C.1. of Appendix C. Additionally, the removal of hemicellulose components from biomass can also be confirmed by the solid recovery yield presented in Figure 6.6. An increase in $logR_O$ reduced the solid yield from 82.7 %(w·w^{-1}) for the least severe reaction conditions to 56.3 %(w·w^{-1}) for $logR_O$ = 6.56. Considering the recovery of each fraction in solid presented in Table C.2. of

Appendix C, it can be stated that the cellulose contents in solids corresponded to more than 90 %(w·w^{-1}) of the cellulose in native wheat straw. This result once again confirms the results obtained for glucose and 5-HMF in the reaction liquid (Figure 6.3.) and corroborates the catalytic effect of [emim][HSO_4] on the hemicellulose (arabinoxylan and acetyl groups) fraction.

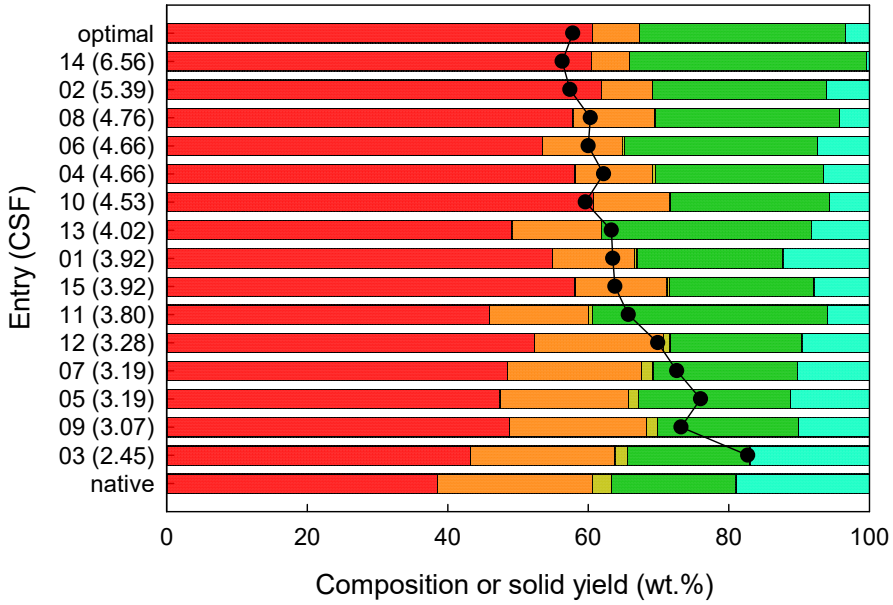

Figure 6.6. The composition in (■) glucan, (■) arabinoxylan, (■) acetyl groups, (■) Klason lignin and (■) others (*i.e.* extractives, ash, proteins, etc.) of produced solids at different $logR_O$. The optimal conditions mean 131.0 °C, 58.7 wt.% H_2O and 88.0 min. The composition of native wheat straw is shown for comparison. The solid line with points represents the recovered solid yield (%(w·w^{-1})) for all performed reactions.

Contrary to cellulose, significant variations in the lignin recovery yield were observed. In order to better analyse the aforementioned variations, a 3D surface presenting the yields of recovered lignin as a function of temperature and H_2O content is presented in Figure 6.7. The results demonstrate an approximation to a quadratic 3D surface suggesting two opposite phenomena: i) delignification and/or depolymerisation resulting in lignin recovery yield in the solid and ii) condensation of hydrolysis products (sugars and furans) into so-called humins occurred under more severe reaction conditions, which contribute to an increase in the lignin recovery yield.[56, 57] The first phenomenon, marked by yellow zone in the near plan, might be the effect of reactions between lignin and acidic ILs as reported elsewhere.[58, 59] In the presence of acidic ILs, covalent bonds between lignin units, such as β-O-4 ether linkages, might undergo hydrolysis[58] resulting in lower lignin recovery (at the range of 74 %(w·w^{-1}) for temperatures between 102.5 °C and 115 °C for H_2O contents between 49.9 wt.% and 55.7 wt.%) observed in this work. On the other hand, the more acidic environment caused by high IL

concentration (lower H_2O content) and high temperatures, the higher amount of furans was found and consequently the more side reactions between sugars and furans could take place. In general, those reactions guide to the formation of insoluble polymers called humins, which are quantified as lignin.[57] That is why at the most severe reaction conditions ($logR_O$ = 6.56), marked by red zone in the near plan in Figure 6.7., the lignin recovery yield increased achieving yield even above 100 %(w·w^{-1}) for the most severe reaction conditions. For example, at these conditions, the obtained solid was composed by 33.7 wt.% of lignin that is as much as 107.4 %(w·w^{-1}) of the lignin content in native biomass.

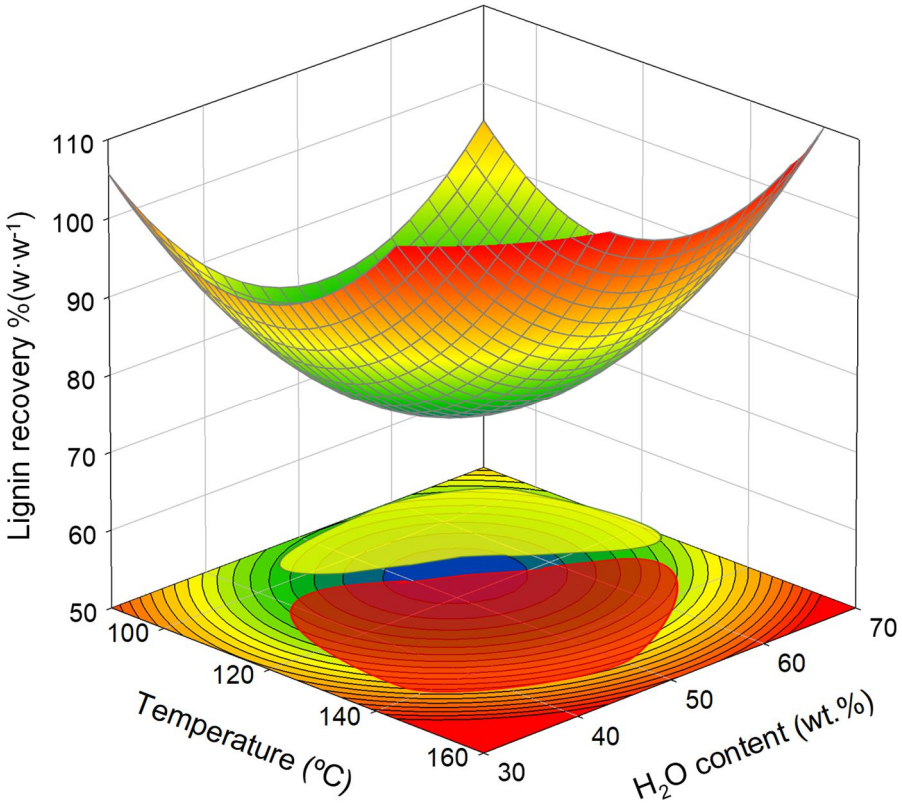

Figure 6.7. The 3D surface representing a statistical approximation of the yields of recovered lignin in the obtained solids as function of temperature and H_2O content for reaction time of 80 min. For description of yellow and red zones in the near plan please refer to the text.

6.3.4. Valorisation of the reaction solid: production of glucose, lignin and aromatic compounds

A successful hydrolysis of hemicellulose into pentoses mediated by acidic IL produced a solid rich in cellulose (60.6 wt.%) and lignin (29.3 wt.%). To accomplish a biorefinery approach, this work aimed at the valorisation of this reaction solid. In this context, two scenarios (A and B) as described in experimental section were scrutinised. Scenario A considered a direct enzymatic hydrolysis of

obtained solid whereas scenario B involved a lignin extraction prior to enzymatic hydrolysis of resulting solid.

The obtained results for both scenarios are depicted in Figure 6.8. In scenario A, the reaction solid was submitted to enzymatic hydrolysis and a glucan to glucose yield of 75.8 mol% was obtained. Furthermore, xylose was also detected in the hydrolysate as a result of the hydrolysis of residual xylan still present in the solid (6.7 wt.% xylan in solid, 20.4 %(w·w^{-1}) of initial xylan content in native wheat straw). A complete hydrolysis of xylan was accomplished (97.6 mol%) mostly because of the xylanase activity of Celli® CTec2 enzymatic cocktail used. The second product of the scenario A is a lignin-rich solid A, which characterisation is discussed below.

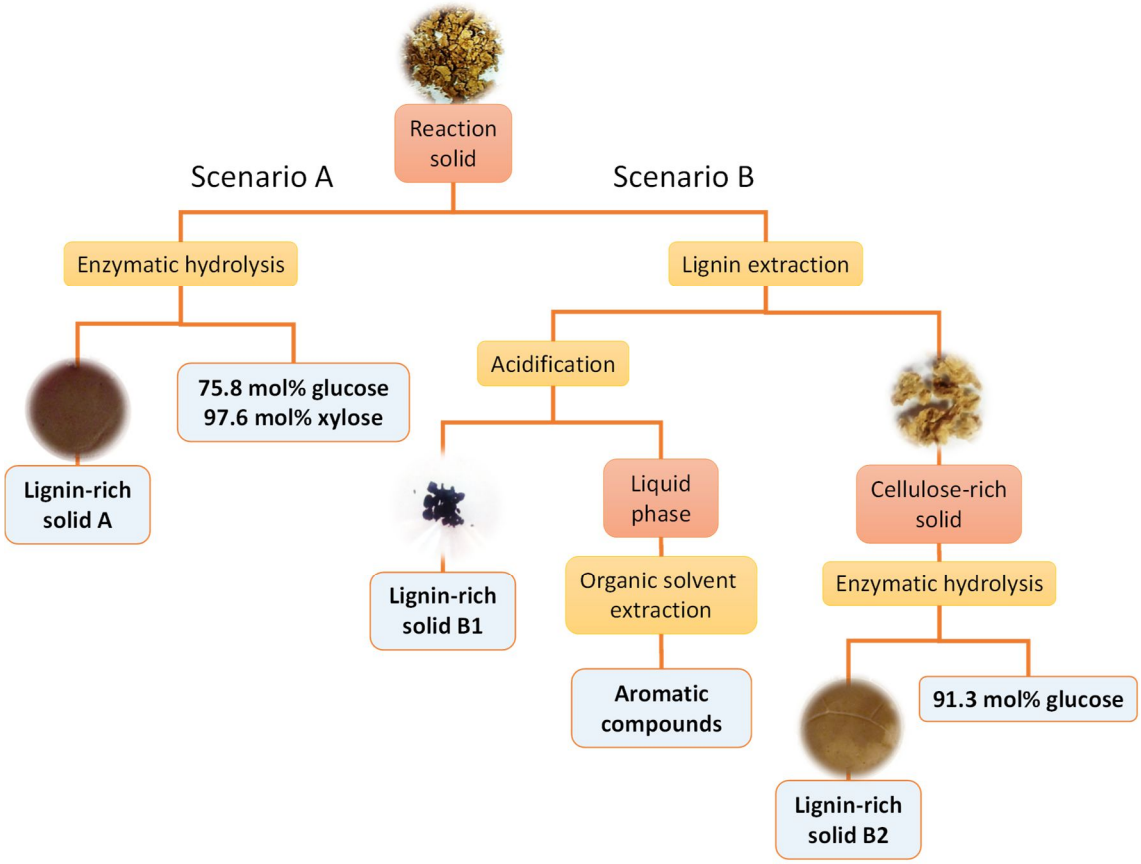

Figure 6.8. The two scenarios approached in this work for the valorisation of the reaction solid.

In scenario B, the extraction of lignin was performed first using an alkaline treatment. This allowed enriching the resulting solid (called cellulose-rich solid) in cellulose from 60.6 wt.% to 89.2 wt.%. The alkali treatment of lignin affected also the hemicellulose because no xylan was found in the resulting solid. The obtained cellulose-rich solid was submitted to enzymatic hydrolysis performed at the same conditions as those applied in scenario A and a 91.3 mol% of potential glucose was yielded.

At the first glance the obtained results for both scenarios demonstrate that extraction of lignin (scenario B) contributed to a higher glucose yield in enzymatic hydrolysis. However, considering the yields of total upgradable sugars (glucose and xylose), both scenarios gave similar results as shown in Figure 6.8. This allows concluding that the process of lignin removal is beneficial for cellulose digestibility, however, it has a negative effect on hemicellulose because leads to its loss.

Regardless of the enzymatic digestibility performance, the extraction of lignin prior to enzymatic hydrolysis offers some advantages. The extracted lignin was recovered as a solid (lignin-rich solid B1). This precipitated fraction represented 42.6 %($w \cdot w^{-1}$) of the lignin content in native wheat straw. FTIR analysis presented in Figure 6.9. demonstrates that this solid is of a high purity especially when compared to lignin-rich solids A and B2. The FTIR spectra show characteristic bands for lignin (solid lines in Figure 6.9.) and for cellulose (dashed lines in Figure 6.9.). A lignin-rich solid B1 has a very distinct spectrum (spectrum c) in Figure 6.9.) from spectra of lignin-rich solids A and B2 (spectra a) and b), respectively). Spectrum c) revealed a strong absorbance of lignin aromatic skeleton vibrations at 1597, 1508, 1458 and 1420 cm^{-1}, which is not evident for lignin-rich solids A and B2. Furthermore, the appearance of sharp and distinct lignin characteristic vibration bands, *i.e*. 840, 1127, 1235 and 1262 cm^{-1} in spectrum c) and their absence in spectra a) and b) also corroborates the increased lignin content. In fact, the bands at 840, 1127 and 1235 cm^{-1} corresponds to structure vibrations of syringyl units,[21] which are exposed after removal of cellulose. In contrast, several cellulose vibration bands of glucose unit (998, 1035, 1065, and 1161 cm^{-1}) and β-glycoside bonds existing in cellulose (898 cm^{-1}), are very noticeable in lignin rich-solids A and B2, once incomplete hydrolysis of glucan was attained. Therefore, besides the separated fractions of pentoses and glucose obtained in scenario B, due to its high purity, the lignin-rich solid B1 can also be considered as a value-added product of the developed process. This opens room for its valorisation different than energy purposes.

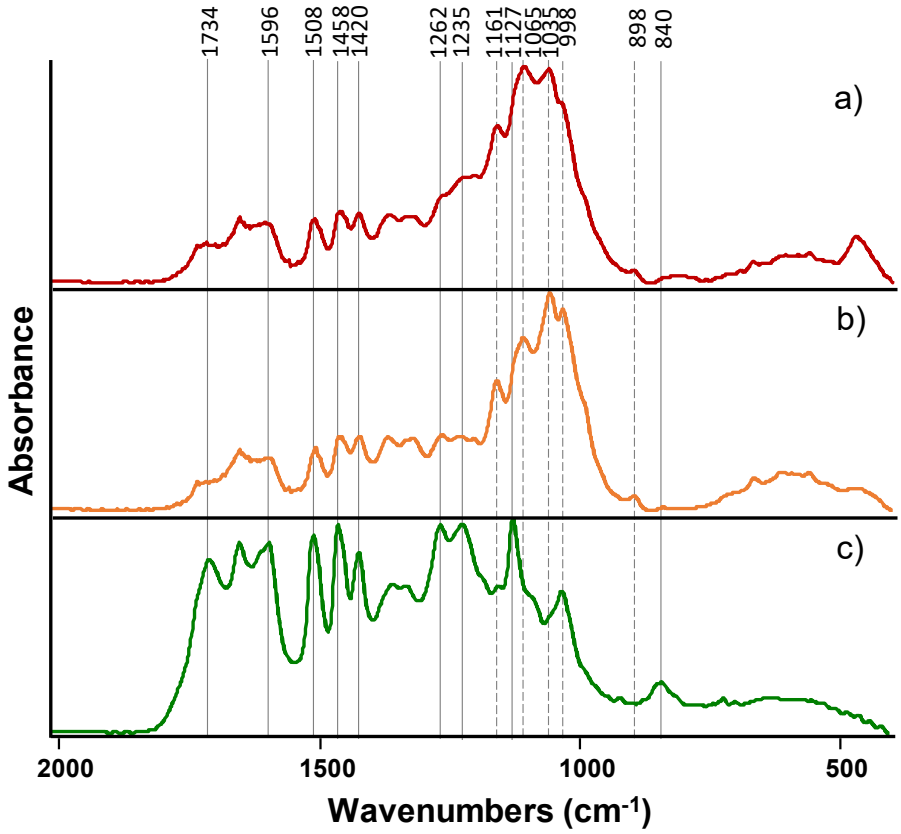

Figure 6.9. FTIR spectra of a) lignin-rich solid A; b) lignin-rich solid B2; and c) lignin-rich solid B1. Solid vertical lines indicate characteristic bands for lignin while dashed lines depict characteristic bands for cellulose.

As mentioned before, a vast part of lignin extracted with alkaline treatment from solid was recovered as high purity lignin (lignin-rich solid B1). However, still some lignin fragments remained soluble in the reaction medium. To scrutinise this fact, the extraction procedure described in experimental section was performed and obtained extracts were analysed by capillary electrophoresis. The electropherograms of aromatic compounds extracted with acetonitrile, ethanol and methanol are shown in Figure 6.10.

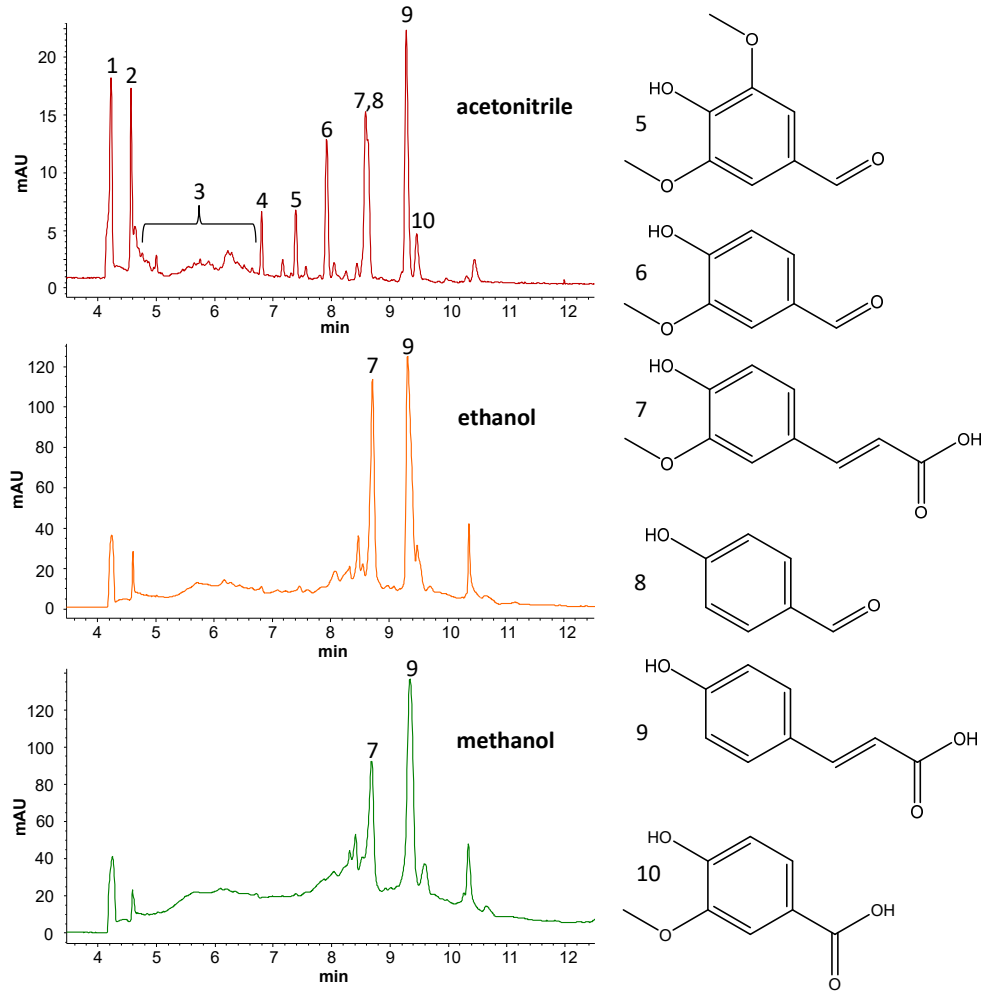

Figure 6.10. Electropherograms recorded at 200 nm showing the aromatic compounds profile after consecutive extraction with acetonitrile, ethanol and methanol. 1) electroosmotic flow; 2: unidentified compound; 3) catchins; 4) vanillin/syringaldehyde derivative; 5) syringaldehyde; 6) vanillin; 7) ferulic acid; 8) 4-hydroxybenzaldehyde; 9) coumaric acid; 10) vanillic acid.

The comparison of the obtained electropherograms with standards of aromatic compounds, confirmed the presence of lignin-derived aromatic compounds obtained from partial lignin depolymerisation during the biomass processing. Acetonitrile was good solvent for a large variety of aromatic compounds. Among them can be mentioned aromatic aldehydes (syringaldehyde, vanillin and 4-hydroxybenzaldehyde) and aromatic acids (ferulic, coumaric and vanillic). Both alcohols used for extraction (*i.e.* ethanol and methanol) were more selective solvents for aromatic acids, such as ferulic and coumaric acids. However, the electropherograms of extracts obtained with ethanol and methanol showed a wide and undefined band between 4 and 7 minutes of the electrophoretic runs. This region is characteristic *e.g.* for catechins (see the electropherogram of acetonitrile extract) and for other aromatic compounds with large molecular weight. Catechins are flavonoids with several hydroxyl

groups hence despite a high molecular weight, to some extend are soluble in polar solvents like ethanol or methanol.

Regardless of this, the obtained results show that beside a high purity lignin-rich solid B1 also aromatic compounds obtained in this stage can be considered as additional products with high commercial value.[60]

6.3.5. Process consideration for acidic ionic liquid biorefinery

This work also aims at the analysis of the proposed processes, especially differences between scenarios A and B, in terms of material and economic efficiencies.

The mass balances of the entire processes were calculated on the basis of obtained results and are presented in detail in Appendix C (Figures C.1. and C.2., Tables C.9. and C.10.). A linear increment of scale to 1 kg of processed wheat straw was performed for both scenarios.

Considering the material efficiencies of both processes, scenario A seems to be more efficient than scenario B because 90.9 %($w \cdot w^{-1}$) of initial glucan, pentosan and lignin contents were recovered as final products. In scenario B this value was only 77.8 %($w \cdot w^{-1}$). The main reason for this difference can be associated to the recovery of lignin-rich solid A (256 g) that is almost 4 times higher than in case of scenario B. However, it cannot be also overlooked that in the native wheat straw the amount of lignin is only 177 g. This confirms again that lignin-rich solid A contains still large amount of impurities namely polysaccharides, which did not undergo enzymatic hydrolysis. In scenario B, the extraction of lignin showed to be beneficial towards a high purity lignin-rich solid B1, although with low mass recovery (75 g). This, in turn contributed to higher glucose recovery in scenario B (355 g) than in scenario A (277 g). The process of pentose production directly associated to IL performance over biomass is common for both scenarios and it stands for 179 g of pentose per 221 g of theoretical arabinoxylan. Furthermore, the recovery of IL is high (92.6 %($w \cdot w^{-1}$)), free of sugars, and recovered IL can be reused without losing its efficiency in a new reaction run.

The mass balance was used to proceed with economic feasibility of the proposed processes. The details of simplified techno-economic analysis for both scenarios are given in Tables C.11.-C.17. and Figures C.3. and C.4. of Appendix C. To approximate the developed process to industrial reality the economic calculations were performed for 9900 tonnes$\cdot$year^{-1} scale with 20 years of operation. The structure of the techno-economic analysis was relied on the estimation of capital expenditures (CAPEX) including the investment in facilities and operating expenses (OPEX) that encompasses the costs for feedstock (biomass, IL, enzyme, etc.), energetic requirements of each unit operation (*e.g.* biomass reaction, enzymatic hydrolysis, solvent distillation) and finally labour costs. The estimated values for CAPEX and OPEX were counterbalanced by the revenues of generated products (pentoses, glucose and lignin) but also with further integration of derived valuable compounds, exemplary

products *e.g.* xylitol (obtained from the xylose by hydrogenation) and succinic acid (product of glucose fermentation). The production of aromatic compounds and the revenues from them were not considered in scenario B, since the separation and purification of those compounds is difficult to assess and would introduce high level of uncertainties.

Inbicon installation facility has similar production scale as this considered in this work thus its CAPEX was also considered herein.[61] However it must be taken into consideration that the CAPEX strongly depends on the investment in high-pressure and high-temperature (≥ 200 °C) resistant reactors to process biomass, which in case of reactions with IL might not be needed due to low operational temperature (131 °C). In case of feedstock prices, a value of 1 €·kg^{-1} was considered for IL, which is in agreement with the previous reports considering either a foreseen large scale of the process as well as type of IL.[33, 62] A higher value was estimated for enzyme cocktail used for enzymatic saccharification (4 €·kg^{-1}).[63] The cost of other utilities was taken from the SuperproDesigner software.[64] The energetic requirements (MJ) were determined for several unit operations that requires heating, such as biomass reaction, distillation of solvents, alkaline extraction, acidification and enzymatic hydrolysis and considering 0.158 € per 1 kWh of electricity needed to supress the required energy. Finally, to conclude the OPEX calculations, labour costs were estimated by assuming the need for 4 persons per unit operation with an average salary of 2500 €·month^{-1}.[64]

The revenues of biomass processing were calculated on the basis of products obtained in a biorefinery considered in scenarios A and B. In both cases biomass was considered to be fractionated and transformed into monomeric units, such as pentoses and glucose, which are subsequently transformed into xylitol and succinic acid. Lignin was considered as final product, but price varies from scenarios A and B regarding the different purities obtained for this fraction. The values of these products were estimated on the basis of their current world sales. (Tables C.16. and C.17. in Appendix C)

The results of techno-economic analyses showed that for both scenarios feedstocks constitute the major share of annual cost with 62.7 % and 59.5 % for scenarios A and B, respectively. In both cases the cost of IL constitutes ∽50 % of this share. Enzymes with ∽25 % of share constitute the second major fraction of feedstock fraction. These numbers are not surprising since pre-treatment and enzymatic hydrolysis are normally considered to be the most cost extensive parts of biomass processing. The loss of 7.4 %(w·w^{-1}) IL shows that IL recovery is desirable to be significantly higher and the enzyme loading should be much lower. Nevertheless, it is important to point out that a free sugar recovered IL was claimed herein. From the industrial perspective point of view, this might not be as relevant because if loss of 9.7 mol% of pentoses[38] would be considered the IL recovery could be as high as 95 %(w·w^{-1}). This would allow the feedstock cost reduction by 15 %.

The second field where some reduction can be achieved is the enzyme charge. The reduction of enzymes from 17 FPU·g^{-1} glucan currently used to half dosage would allow also a significant cost

reduction. However, in this case lower yield of enzymatic hydrolysis might be achieved which can compromise the revenues obtained.

On the revenues side, when comparing techno-economic analysis for both scenarios A and B, one of the major differences appears in the succinic acid (Tables C.16. and C.17. in Appendix C) which is directly related to the yield of enzymatic hydrolysis in both scenarios. The second major difference is associated to the recovered lignin. The scenario B allowed producing a high purity lignin (lignin-rich solid B1), which together with higher glucose availability for succinic acid production opens a possibility to achieve an increase of revenues by 14 % when compared to scenario A. Considering the 20 years of investment the net present value curves for scenario A and B were determined and are presented in Figure 6.11. In case of scenario A, "pay-back period" is only achieved after 16 years of operation, while scenario B allows reducing it to 12 years of industrial activity.

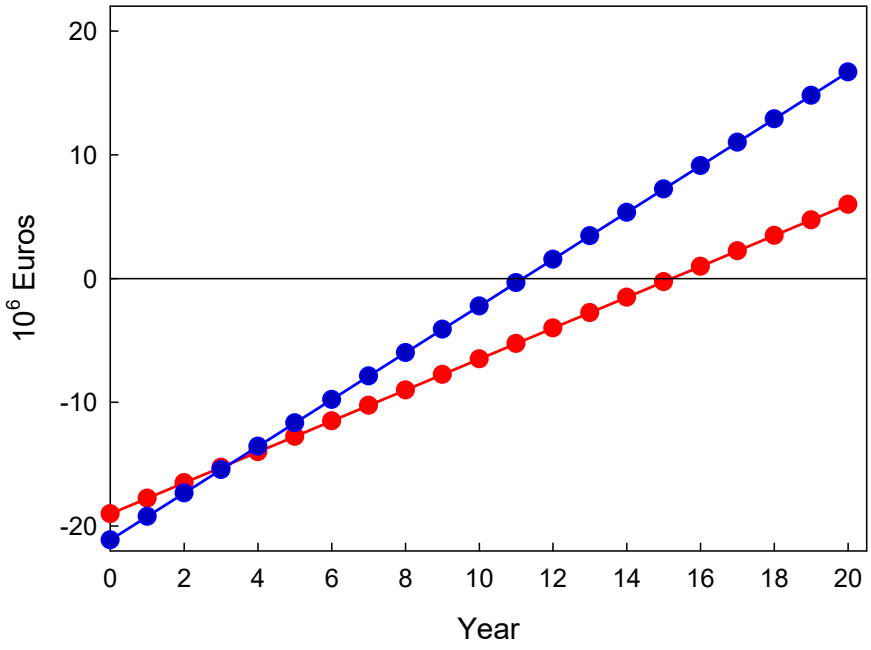

Figure 6.11. The predicted net present value curves for 20 years of operation period of the forecasted scenarios A (●) and B (●).

6.4. Conclusion

A successful multi-step process for an effective separation and transformation of main lignocellulosic biomass components within the biorefinery concept was presented in this work. A focal point of the biomass processing was the development of the selective hydrolysis of hemicellulose by aqueous acidic [emim][HSO_4] IL to produce as much as 80.5 mol% pentose yield. This result places the proposed methodology among the top, the most efficient methods of biomass processing in delivery of

pentoses. Simultaneously, the proposed approach delivered a solid enriched in cellulose and lignin which can be further valorised. Two distinct scenarios for solid valorisation were examined and showed that removal of lignin from the solid prior to enzymatic hydrolysis permits to obtain highly digestible fraction. The glucan to glucose yield above 90 mol% was obtained, while in case of direct enzymatic hydrolysis, the same yield was only ∽76 mol%. Additionally, the lignin extraction step produced high purity lignin which contributes to the economics of the process. The sustainability of the process is also enhanced by recycling of IL with high yield (92.6 %($w \cdot w^{-1}$)) and reusing it without losing the performance on the selective hydrolysis of hemicellulose. The proof of concept of pentose recovery was also demonstrated and opens room for valorisation of such produced stream of pentoses.

The use of moderate temperature to obtain pentose stream, the efficient separation of pentoses and IL, the separation of lignin and cellulose, the production of glucose with high yield in the enzymatic saccharification, the possibility of IL catalyst recovery and reuse without the loss of its performance, turns this technology in the path of a sustainable and efficient biomass process to realise the bioeconomy. This was also confirmed by the heuristic techno-economic analyses, which integrated the conversion of produced streams of sugars and lignin into valuable products.

6.5. References

1. *A Roadmap for moving to a competitive low carbon economy in 2050*, European Commission, Brussels, Belgium, 2011.
2. *Paris Agreement*, The 21st Conference of the Parties (COP) of the United Nations Framework Convention on Climate Change, Paris, 2015.
3. X. Zhao, L. Zhang and D. Liu, *Biofuels Bioprod. Biorefining*, 2012, **6**, 561-579.
4. M. S. Singhvi, S. Chaudhari and D. V. Gokhale, *RSC Adv.*, 2014, **4**, 8271-8277.
5. M. H. L. Silveira, A. R. C. Morais, A. M. da Costa Lopes, D. N. Olekszyszen, R. Bogel-Lukasik, J. Andreaus and L. Pereira Ramos, *ChemSusChem*, 2015, **8**, 3366-3390.
6. A. M. da Costa Lopes and R. Bogel-Lukasik, *ChemSusChem*, 2015, **8**, 947-965.
7. A. R. C. Morais, A. M. da Costa Lopes and R. Bogel-Lukasik, *Chem. Rev.*, 2015, **115**, 3-27.
8. A. R. C. Morais, A. C. Mata and R. Bogel-Lukasik, *Green Chem.*, 2014, **16**, 4312-4322.
9. J. S. Luterbacher, J. M. Rand, D. M. Alonso, J. Han, J. T. Youngquist, C. T. Maravelias, B. F. Pfleger and J. A. Dumesic, *Science*, 2014, **343**, 277-280.
10. A. R. C. Morais and R. Bogel-Lukasik, *Green Chem.*, 2016, **18**, 2331-2334.
11. A. R. C. Morais, M. D. J. Matuchaki, J. Andreaus and R. Bogel-Lukasik, *Green Chem.*, 2016, **18**, 2985-2994.
12. W. Schutyser, S. Van den Bosch, T. Renders, T. De Boe, S.-F. Koelewijn, A. Dewaele, T. Ennaert, O. Verkinderen, B. Goderis and C. Courtin, *Green Chem.*, 2015, **17**, 5035-5045.
13. J. P. Hallett and T. Welton, *Chem. Rev.*, 2011, **111**, 3508-3576.
14. N. Sun, M. Rahman, Y. Qin, M. L. Maxim, H. Rodriguez and R. D. Rogers, *Green Chem.*, 2009, **11**, 646-655.
15. I. A. Kilpeläinen, H. Xie, A. King, M. Granstrom, S. Heikkinen and D. S. Argyropoulos, *J. Agric. Food Chem.*, 2007, **55**, 9142-9148.
16. P. Mäki-Arvela, I. Anugwom, P. Virtanen, R. Sjoholm and J. P. Mikkola, *Ind. Crop. Product.*, 2010, **32**, 175-201.
17. A. Brandt, J. P. Hallett, D. J. Leak, R. J. Murphy and T. Welton, *Green Chem.*, 2010, **12**, 672-679.
18. R. Pezoa, V. Cortinez, S. Hyvarinen, M. Reunanen, J. Hemming, M. E. Lienqueo, O. Salazar, R. Carmona, A. Garcia, D. Y. Murzin and J. P. Mikkola, *Cellul. Chem. Technol.*, 2010, **44**, 165-172.
19. A. M. da Costa Lopes, L. B. Roseiro and R. Bogel-Lukasik, in *Ionic Liquids in the Biorefinery Concept : Challenges and Perspectives*, ed. R. Bogel-lukasik, RSC, 2015, pp. 121-167.
20. I. Anugwom, P. Maki-Arvela, P. Virtanen, S. Willfor, R. Sjoholm and J. P. Mikkola, *Carbohydr. Polym.*, 2012, **87**, 2005-2011.
21. A. M. da Costa Lopes, K. G. Joao, D. F. Rubik, E. Bogel-Lukasik, L. C. Duarte, J. Andreaus and R. Bogel-Lukasik, *Bioresource Technol.*, 2013, **142**, 198-208.
22. A. M. da Costa Lopes, M. Brenner, P. Fale, L. B. Roseiro and R. Bogel-Lukasik, *ACS Sustain. Chem. Eng.*, 2016, **4**, 3357-3367.
23. V. Eta, I. Anugwom, P. Virtanen, P. Maki-Arvela and J. P. Mikkola, *Ind. Crop. Product.*, 2014, **55**, 109-115.
24. P. Verdia, A. Brandt, J. P. Hallett, M. J. Ray and T. Welton, *Green Chem.*, 2014, **16**, 1617-1627.
25. R. P. Swatloski, S. K. Spear, J. D. Holbrey and R. D. Rogers, *J. Am. Chem. Soc.*, 2002, **124**, 4974-4975.
26. R. C. Remsing, R. P. Swatloski, R. D. Rogers and G. Moyna, *Chem. Commun.*, 2006, 1271-1273.
27. J.-K. Xu, J.-H. Chen and R.-C. Sun, *Bioresource Technol.*, 2015, **193**, 119-127.
28. A. V. Carvalho, A. M. da Costa Lopes and R. Bogel-Lukasik, *RSC Adv.*, 2015, **5**, 47153-47164.
29. A. Brandt, M. J. Ray, T. Q. To, D. J. Leak, R. J. Murphy and T. Welton, *Green Chem.*, 2011, **13**, 2489-2499.
30. C. Z. Li, Q. Wang and Z. K. Zhao, *Green Chem.*, 2008, **10**, 177-182.
31. X. M. Hu, Y. B. Xiao, K. Niu, Y. Zhao, B. X. Zhang and B. Z. Hu, *Carbohydr. Polym.*, 2013, **97**, 172-176.
32. A. S. Amarasekara and P. Shanbhag, *Bioenerg. Res.*, 2013, **6**, 719-724.
33. A. Brandt, F. Gschwend, P. Fennell, T. Lammens, B. Tan, J. Weale and J. Hallett, *Green Chem.*, 2017, **19**, 3078-3102.

34. S. P. Magalhães da Silva, A. M. da Costa Lopes, L. B. Roseiro and R. Bogel-Lukasik, *RSC Adv.*, 2013, **3**, 16040-16050.
35. D. H. Doehlert, *Roy. Stat. Soc. C*, 1970, **19**, 231-239.
36. S. L. Ferreira, W. N. Dos Santos, C. M. Quintella, B. c. B. Neto and J. M. Bosque-Sendra, *Talanta*, 2004, **63**, 1061-1067.
37. M. Almenara Rodrigues, A. M. da Costa Lopes and R. Bogel-Lukasik, *unpublished data*, 2016.
38. A. M. da Costa Lopes and R. M. Lukasik, *Chem. Eng. J.*, 2017. (submitted).
39. A. Sluiter, B. Hames, R. Ruiz, C. Scarlata, J. Sluiter, D. Templeton and D. Crocker, *Determination of structural carbohydrates and lignin in biomass - Laboratory Analytical Procedure (LAP)*, Report NREL/TP-510-42618, National Renewable Energy Laboratory, Colorado, USA, 2011.
40. A. Sluiter, B. Hames, R. Ruiz, C. Scarlata, J. Sluiter and D. Templeton, *Determination of Sugars, Byproducts, and Degradation Products in Liquid Fraction Process Samples - Laboratory Analytical Procedure (LAP)*, Report NREL/TP-510-42623, National Renewable Energy Laboratory, Colorado, USA, 2008.
41. G. Garrote, R. Yáñez, J. L. Alonso and J. C. Parajó, *Ind. Eng. Chem. Res.*, 2008, **47**, 1336-1345.
42. S. Peleteiro, A. M. da Costa Lopes, G. Garrote, J. C. Parajó and R. Bogel-Łukasik, *Ind. Eng. Chem. Res.*, 2015, **54**, 8368-8373.
43. M. J. Kamlet and R. W. Taft, *J. Am. Chem. Soc.*, 1976, **98**, 377-383.
44. Y. T. Xiao, W. L. Chin and S. B. Abd Hamid, *Adv. Mater. Research*, 2015, **1087**, 106-110.
45. J. B. Binder, J. J. Blank, A. V. Cefali and R. T. Raines, *ChemSusChem*, 2010, **3**, 1268-1272.
46. A. M. da Costa Lopes and R. Bogel-Łukasik, in *Ionic-Liquid-Based Aqueous Biphasic Systems*, ed. M. G. Freire, Springer, 2016, pp. 37-60.
47. J. B. Binder and R. T. Raines, *Proc. Natl. Acad. Sci. U. S. A.*, 2010, **107**, 4516-4521.
48. C. Abels, K. Thimm, H. Wulfhorst, A. C. Spiess and M. Wessling, *Bioresource Technol.*, 2013, **149**, 58-64.
49. D. C. Dibble, C. L. Li, L. Sun, A. George, A. R. L. Cheng, O. P. Cetinkol, P. Benke, B. M. Holmes, S. Singh and B. A. Simmons, *Green Chem.*, 2011, **13**, 3255-3264.
50. D. Feng, L. Li, F. Yang, W. Tan, G. Zhao, H. Zou, M. Xian and Y. Zhang, *Appl. Microbiol. Biotechnol.*, 2011, **91**, 399-405.
51. P. A. Steiner and W. Gordy, *J. Mol. Spectrosc.*, 1966, **21**, 291-301.
52. N. Sun, H. Liu, N. Sathitsuksanoh, V. Stavila, M. Sawant, A. Bonito, K. Tran, A. George, K. L. Sale and S. Singh, *Biotechnol. Biofuels*, 2013, **6**, 1-15.
53. B. R. Caes, T. R. Van Oosbree, F. Lu, J. Ralph, C. T. Maravelias and R. T. Raines, *ChemSusChem*, 2013, **6**, 2083-2089.
54. A. P. Carneiro, O. Rodríguez and E. A. Macedo, *Sep. Purif. Technol.*, 2014, **132**, 496-504.
55. K. M. Lee, G. C. Ngoh and A. S. M. Chua, *Ind. Crop. Product.*, 2015, **77**, 415-423.
56. B. Danon, G. Marcotullio and W. de Jong, *Green Chem.*, 2014, **16**, 39-54.
57. P. Sannigrahi, D. H. Kim, S. Jung and A. Ragauskas, *Energ. Environ. Sci.*, 2011, **4**, 1306-1310.
58. B. J. Cox, S. Y. Jia, Z. C. Zhang and J. G. Ekerdt, *Polym. Degrad. Stab.*, 2011, **96**, 426-431.
59. B. J. Cox and J. G. Ekerdt, *Bioresource Technol.*, 2013, **134**, 59-65.
60. P. Varanasi, P. Singh, M. Auer, P. D. Adams, B. A. Simmons and S. Singh, *Biotechnol. Biofuels*, 2013, **6**.
61. M. Persson, *Inbicon demonstration plant*, Brussels, Belgium, 2010.
62. A. George, A. Brandt, K. Tran, S. N. S. M. S. Zahari, D. Klein-Marcuschamer, N. Sun, N. Sathitsuksanoh, J. Shi, V. Stavila, R. Parthasarathi, S. Singh, B. M. Holmes, T. Welton, B. A. Simmons and J. P. Hallett, *Green Chem.*, 2015, **17**, 1728-1734.
63. L. da Costa Sousa, M. Jin, S. P. Chundawat, V. Bokade, X. Tang, A. Azarpira, F. Lu, U. Avci, J. Humpula and N. Uppugundla, *Energ. Environ. Sci.*, 2016, **9**, 1215-1223.
64. Intelligen, Inc. SuperPro Designer, V8.5 Build 7, Special Build 3550 edn., 2013.

CHAPTER VII

Separation and recovery of pentoses and acidic ionic liquid

This chapter is based on data and information of the following publication:

A. M. da Costa Lopes and R. M. Lukasik, A comprehensive study for the separation and recovery of hemicellulose-derived sugar produced from biomass hydrolysis by acidic ionic liquid, *ACS Sus. Chem. Eng.*, 2017 (submitted).

7.1. Introduction

Carbohydrates are an ample class of organic and natural compounds, widespread in nature and responsible for structural and energy source functions in biological systems.[1] One of the most important features of carbohydrates is their easy assimilation by microorganisms and facile conversion to a series of valuable compounds used in pharmaceutical and cosmetic applications,[2, 3] food formulations,[4] biomedical devices[5], nanomaterials[6] and biotechnological processes.[7] The later has been intensively explored in the frame of the biorefinery concept and it consists of using microorganisms to convert monosaccharides, *e.g.* glucose and xylose, into a myriad of chemicals, fuels and value-added commodities. However, a price and availability of monosaccharides are key issues for a cost-effective accomplishment of this concept. Cereals are examples of biomass materials rich in fermentable carbohydrates, but *food vs. fuel* concerns and land use issues restrict their use for these purposes.[8] In this context, other feedstocks containing easily available carbohydrates have been sought. One of them is lignocellulosic biomass, which comprehends in its composition even up to 80 wt.% of polymeric carbohydrates mostly in the form of cellulose (or starch) and hemicellulose.[9]

The physical, chemical, physicochemical and/or biological treatments of lignocellulosic biomass allow obtaining the required monosaccharides in upgradable forms.[10] Acid hydrolysis treatment stands as one of the principal options to achieve that. Nevertheless, this technology requires specialised high temperature, pressure and corrosion-resistant reactors. Additionally, the acid neutralisation affects negatively the environmental aspects of the biomass processing. Therefore, other, greener and more sustainable technologies, *e.g.* use of ILs have been emerged.[10-13] Ionic liquids (ILs) are organic salts and due to numerous potential combinations of cations and anions, ILs are called "designer solvents".[14] This allows constructing IL with task-specific and unique properties, such as high thermal stability, non-flammability, wide range of polarity, acidity and basicity, among others.[15, 16] Additionally, ILs possess a great solvent power towards a large variety of chemicals and more complex polymeric matrixes.[17-19] All these features have been driving to the full exploitation of ILs in diverse field including a biomass processing.[20-23] In this context, one of the most recent trends is the biomass process intensification *i.e.* integration of biomass dissolution and hydrolysis by the use of acidic ILs.[24-28] However, similarly to other applications of ILs, two main challenges remain, *i.e.* a separation of products from IL post-reaction liquid as well as recycle and reuse of IL. Particularly, interactions established between biomass-derived products and ILs are generally strong, hampering their separation in an efficient way. Also, one of the requirements of the separation processes is that they should not influence the IL performance, *i.e.* the properties of IL must be retained. Furthermore, a choice of a separation methodology is highly dependent on the physicochemical properties, namely polarity and molecular weight of IL and products. This all makes the separation and recovery of monosaccharides and IL a challenging issue. Therefore, a separation of monosaccharides and ILs has been thoroughly studied by applying different strategies.[29-31]

The present work aims to address also this challenge and demonstrates an innovative approach for the separation of xylose from the acidic 1-ethyl-3-methylimidazolium hydrogensulphate ([emim][HSO_4]) IL by using preparative chromatography approach. This work responds to a need for efficient separation of acidic IL and pentoses produced by the selective hydrolysis of hemicellulosic fraction of wheat straw.[25] The referred process demonstrated a potential to produce in the IL liquor as much as 80.5 % of the theoretical amount of these carbohydrates.[25] However, as separation of both monosaccharides and [emim][HSO_4] was never reported, this work encompasses a comprehensive study of xylose and [emim][HSO_4] separation by means of fine-tuning of eluent polarity and adequate adjustment of stationary phase of preparative chromatography.

7.2. Experimental

7.2.1. Materials

[emim][HSO_4] IL (≥99 wt.%, Iolitec GmBH, Heilbronn, Germany), xylose (≥98 wt.%, Merck, Germany), acetonitrile (99.9 wt.% HPLC gradient, Carlo Erba, Italy) and ultrapure water (18.2 MΩ·cm^{-1}, PURELAB Classic of Elga system) were used in this study. The water content of IL was determined prior to its use by a volumetric Karl-Fischer titration and was 3796 ppm. For the chromatographic study, a glass column (25 cm height, 1 cm *i.d.*) was used and alkali alumina 90 active I (70-230 mesh, Merck, Germany) was employed as a stationary phase. Finally, sulphuric acid (96 wt.%, Panreac, Spain) was used for alumina treatment and to prepare 5 mM concentration of mobile phase for HPLC analyses.

7.2.2. Phase diagram and tie-lines' determination for ionic liquid + water + acetonitrile ternary system

The phase envelope of [emim][HSO_4] + water + acetonitrile ternary system was determined at 21 °C and under atmospheric pressure using two distinct methods. The first one was a cloud point determination method performed according to the following approach. To the solutions with a known concentration of [emim][HSO_4] and water, as small as possible amounts of pure acetonitrile were added and the mixture was stirred for 5 min. Next, the mixture was left for 30 min to achieve equilibrium to observe an existence of cloud point (two-phase region). When this was not observed, the procedure was repeated. Once a cloud point was determined, a known amount of water was added to return to one-phase region. The same approach was used for [emim][HSO_4] + acetonitrile system with a use of water as phase splitting agent. The amount of added water or acetonitrile was controlled using Mettler Toledo balance, XS205 dual range scale (Germany).

The second method relied on the tie-line determination. For tie-line determination, biphasic solutions composed of [emim][HSO_4] + water + acetonitrile were prepared, vigorously stirred and left for 30 min to achieve equilibrium. Next, both liquid phases were separately collected and composition of each phase was determined. Water contents were determined by Karl-Fisher titration, while [emim][HSO_4]

contents were analysed by weighing after evapouration of water and acetonitrile from the sample at 100 °C for 24 h. Finally, acetonitrile contents were determined by mass difference.

7.2.3. Xylose adsorption on alumina

A 50 mg of xylose was dissolved in known amounts of water and [emim][HSO_4]. Next, a known amount of acetonitrile was added considering the phase diagram determined as presented in section 2.2. Mixtures comprising different mass contents of [emim][HSO_4] (between 1.6 and 4.6 wt.%), water (between 0.6 and 13.9 wt.%) and acetonitrile (between 81.5 and 97.9 wt.%) were studied. Afterwards, 2.0 g of dried alumina was added to Erlenmeyer flask and placed in a shaker (Optic ivymen® system – Spain) to proceed with adsorption experiments. The experiments were carried out for 90 min and 1 mL aliquots of the solution were collected at 5, 10, 15, 30, 60 and 90 min. The collected samples were placed in an oven at 100 °C for 24 h to evapourate water and acetonitrile and resulting samples were re-dissolved in 1 mL of water, filtered through a 0.45 μm membrane filter syringe and analysed by HPLC as described in section 2.5.

7.2.4. Separation and recovery of xylose and ionic liquid through alumina column chromatography

The xylose and [emim][HSO_4] separation studies were performed using preparative column chromatography with alumina as a stationary phase.

7.2.4.1. Experimental design of reactions towards pentose production in the liquid

Alumina was used for the chromatographic experiments in the following scenarios: A) no treatment; B) treatment with H_2SO_4 aqueous solution; and C) treatment with H_2SO_4 aqueous solution followed by a second treatment with [emim][HSO_4].

In the first case (scenario A), alumina was dried in a muffle at 200 °C overnight before being packed into a glass column previously filled with acetonitrile. For scenarios B and C, known amounts of alumina were placed into a glass beaker and stirred with 100 mL of 0.5 M H_2SO_4 aqueous solution at room temperature for 1 h. Next, the solution was decanted and alumina was washed several times with water until the solution pH was equal to that of water. Such processed alumina was next placed in a muffle at 200 °C overnight. Dried alumina was packed in a glass column previously filled with acetonitrile. The alumina was then rinsed with 100 mL acetonitrile for adequate packing. To complete alumina treatment for scenario C, 1.9 g [emim][HSO_4] dissolved in 200 mL of acetonitrile + water (97:3 $w \cdot w^{-1}$) eluent was eluted through packed alumina and next eluted with extra 1100 mL of the same eluent to guarantee the removal of all unlinked IL.

7.2.4.2. Sample elution

A known amount of xylose was dissolved in [emim][HSO_4] + water (42:58 w·w^{-1}). Subsequently, acetonitrile was added and the resulting mixture was stirred until a clear solution was obtained. The sample (examined compositions are listed in Table 7.1.) was then eluted through a chromatography column. After loading the entire sample to the column, acetonitrile-based eluent with fixed water composition (Table 7.1.) was used for elution. A flux of 2 mL·min^{-1} was maintained during the elution process and fractions with known volumes were collected. Next, the last were next evapourated and resulting dried solids were re-dissolved in a known amount of water, filtered through a 0.45 μm membrane filter syringe and analysed by HPLC following the procedure described in section 2.5.

Table 7.1. Conditions applied in the alumina column chromatography study.

Entry	Sample composition			Alumina		H_2O in eluent (wt.%)
	Xylose (g)	[emim][HSO_4] (g)	acetonitrile (g)	amount (g)	treatment applied	
C1	0.05	0.95	80.0	10.0	-	0.0
C2	0.05	0.95	80.0	10.0	-	1.6
C3	0.05	0.95	80.0	10.0	-	5.0
C4	0.05	0.95	80.0	10.0	H_2SO_4	1.6
C5	0.05	0.95	80.0	10.0	H_2SO_4	3.0
C6	0.10	1.90	160.0	20.0	H_2SO_4	3.0
C7	0.10	1.90	80.0	20.0	H_2SO_4	3.0
C8	0.10	1.90	160.0	20.0	-	3.0
C9	0.10	1.90	160.0	20.0	H_2O	3.0
C10	0.10	1.90	160.0	20.0	H_2SO_4/[emim][HSO_4]	3.0

7.2.5. HPLC analysis of chromatographic fractions

HPLC analyses were made using Agilent 1100 series HPLC system (Agilent Technologies, USA) equipped with Aminex HPX-87H column (Bio-Rad, USA) with a 5 mM H_2SO_4 used as a mobile phase. The column temperature was 50 °C, while injection volume and flow rate of 5 μL and 0.6 mL·min^{-1} were used, respectively. The detection was performed using RID (refractive index detector) for both xylose and [emim][HSO_4] and calibration curves of corresponding standards were used for the quantitative analysis.

7.2.6. Experimental and analytical error analysis

Standard deviation errors (u) were calculated for all obtained results. All mass determinations were performed using a Mettler Toledo, XS205 dual range scale (Germany) with a given u(m)= 0.1 mg. All analyses were performed at least in duplicate and average results are presented in the following sections.

7.3. Results and Discussion

Biomass hydrolysis catalysed by acidic IL ([emim][HSO_4]) drives to the formation of liquid phase constituted chiefly by pentoses (xylose and arabinose), water and IL. A highly-polar system hampers the separation of xylose and IL, once xylose, as most of monosaccharides, is soluble in water in very high concentrations. Also IL and water are fully miscible and solid-liquid equilibrium data for xylose + 1-ethyl-3-methylimidazolium ethylsulphate (no literature data for xylose + [emim][HSO_4] are available) system shows that at 25 °C the solubility of xylose is as high as $x_1 = 0.205$ (x_1 means mass fraction of solute).[32] Thus, at this condition a direct separation of pentoses and IL is impossible. To overcome this limitation, a medium-polarity solvent such as acetonitrile (dipole moment = 3.91 D[33]) was used.

7.3.1. Phase diagram of ionic liquid + water + acetonitrile ternary system

Due to moderate polarity of acetonitrile, this solvent was used to change the polarity of the system and to separate xylose and IL. However, to establish the most adequate conditions for this, knowledge about the solubility of water, IL and xylose in acetonitrile is needed. Both water and studied ionic liquid are fully miscible in acetonitrile and the solubility of xylose in acetonitrile at 22 °C is 0.61 $g \cdot L^{-1}$, *i.e.* $x_1 = 0.775 \cdot 10^{-3}$.[34] To scrutinise the use of acetonitrile as potential solvent for xylose and IL separation, the ternary phase diagram for system containing water, [emim][HSO_4] and acetonitrile was determined and is shown in Figure 7.1. The obtained phase diagram shows that for $x_{water} < 0.33$ a wide range of IL mass fraction exists for which a miscibility gap can be found. Considering that liquid obtained from the biomass hydrolysis contains as much as 58.7 wt.% of water,[25] an addition of acetonitrile to achieve low polarity of the system drives to the formation of two liquid phases (region marked by the red line in Figure 7.1.). Consequently, this causes a partition of ionic liquid between two distinct liquid phases. Hence, to avoid this and at the same time, achieve a sufficiently low polarity of the system, $x_{acetonitrile}$ should be as high as possible and certainly above 0.9.

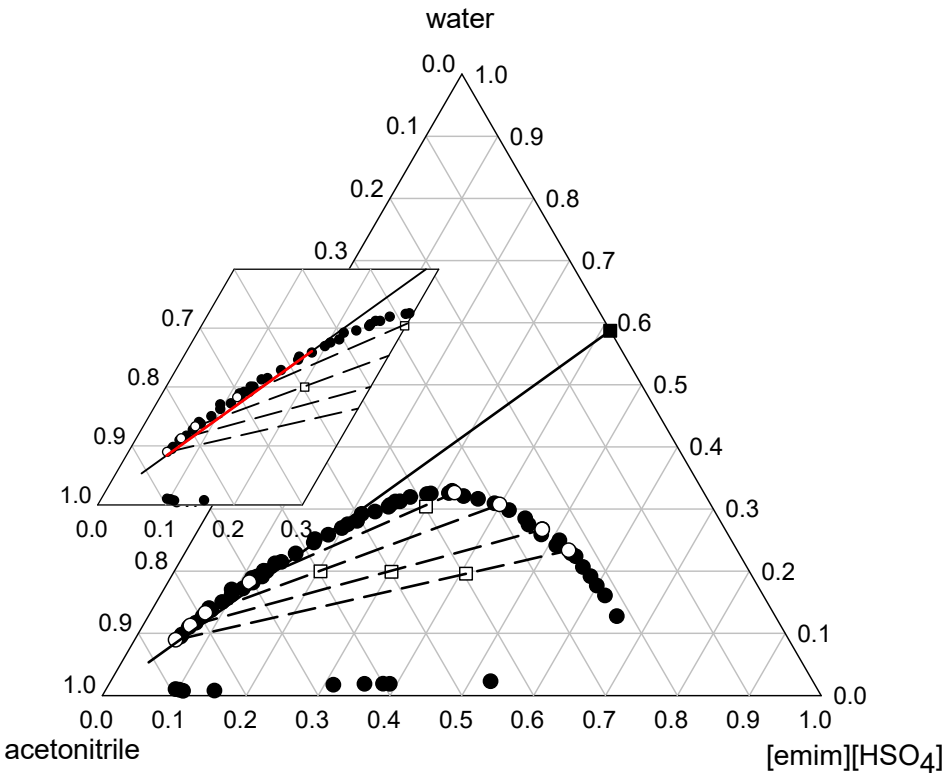

Figure 7.1. Ternary phase diagram (in mass fraction) of ([emim][HSO_4] + water + acetonitrile) obtained at 21 °C and 1 atm. Full circles represent a binodal curve obtained by a cloud point determination method. Open squares represent the overall composition of mixtures used to determine the tie-lines (dashed lines) drawn on the basis of the composition of two liquid phases represented by open circles for each overall composition. The black solid line demonstrates the direction of the change of the composition of the ternary mixture initially constituted by IL and water with subsequent addition of acetonitrile. This line was designed taking into a consideration an initial composition (full square) of the liquid obtained from the biomass hydrolysis with [emim][HSO_4].[25] The red solid line represents the region of compositions at which two-phase region is formed when acetonitrile is added to the mixture.

7.3.2. Xylose adsorption performance of alumina in [emim][HSO_4] + water + acetonitrile media

The phase equilibrium presented in Figure 7.1. demonstrates that satisfactory resolution of xylose and IL by liquid-liquid separation of water-rich phase containing xylose and acetonitrile-rich phase containing IL is impossible. Therefore, batch experiments for xylose adsorption on alumina in [emim][HSO_4] + water + acetonitrile system were performed and results are presented in Figure 7.2. At first glance, a fast xylose adsorption on alumina occurred and after 30 minutes no further enhancement was observed. The efficiency of xylose adsorption was however dependent on the polarity of the system, or in other words, on acetonitrile content in the solution. An increase in acetonitrile content from 88.6

wt.% (blue) to 95.8 wt.% (red) in the mixture promoted an increase in xylose adsorption on alumina from 40.2 %(w·w^{-1}) to 72.1 %(w·w^{-1}). However, the recovery of adsorbed xylose with water revealed that IL was also adsorbed on alumina. To explore this phenomenon, a series of experiments evaluating the selective adsorption of xylose and [emim][HSO_4] on alumina from solutions with different contents of [emim][HSO_4] + water + acetonitrile were performed and results are listed in Table 7.2.

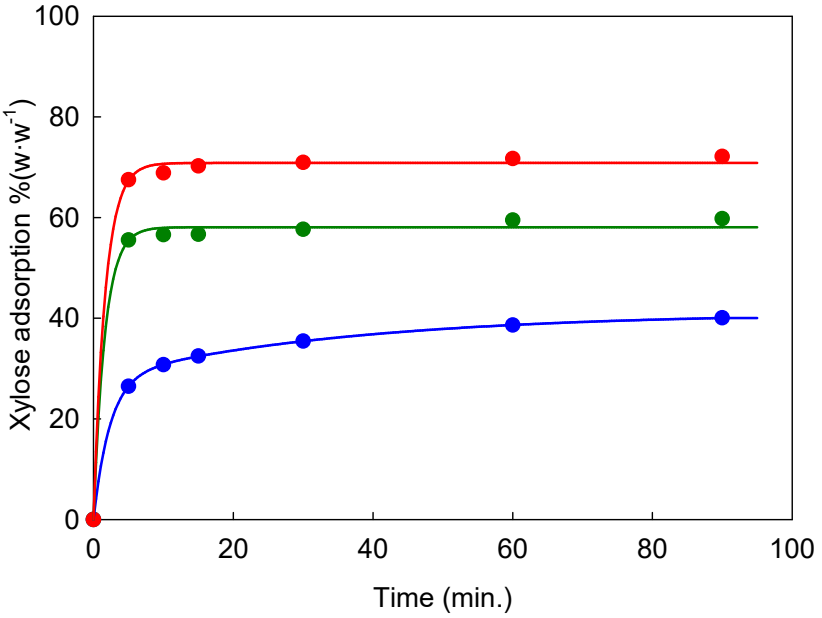

Figure 7.2. Profiles of xylose adsorption on alumina from solutions containing 2.8 wt.% [emim][HSO_4] + 8.5 wt.% water + 88.6 wt.% acetonitrile (blue); 2.5 wt.% [emim][HSO_4] + 3.6 wt.% water + 93.1 wt.% acetonitrile (green) and 3.1 wt.% [emim][HSO_4] + 1.1 wt.% water + 95.8 wt.% acetonitrile (red) obtained in batch systems with 50 mg xylose, 2.0 g alumina, 45 mL total volume of solution at 21 °C.

Obtained results shows that for the fixed initial water content, the amount of acetonitrile added to the system provoked a decrease in the adsorption performance of either xylose or IL. One of the reasons for this might be the dilution of the system because a fixed amount of alumina (2 g) was used in all trials. Although the adsorption performances of xylose and IL were observed to be lower for more diluted systems, the selectivity of xylose adsorption in comparison to IL was higher. Another important conclusion is that a decrease of water content in the final solution accompanied by an increase of acetonitrile content favours selectivity of xylose adsorption on alumina. For the most apolar system (97.9 wt.% of acetonitrile and 1.6 wt.% water) as much as 2/3 of initial xylose was adsorbed on alumina and only 1/5 of initial IL. This gave a maximum selectivity of 3.32. These results show that more apolar

system is adequate to achieve higher selectivity. The reason for this might be a decrease of xylose solubility in solution containing low water content, which consequently favours interactions of the monosaccharide with alumina.

Table 7.2. Performance of alumina (2.0 g) for the adsorption of xylose and [emim][HSO_4] in solutions containing different contents of [emim][HSO_4] + water + acetonitrile. Adsorption trials were performed at 21 °C and 90 min and using 50 mg xylose.

$H_2O_{initial}$ (wt.%)[a]	Acetonitrile added (g)	Final composition (wt.%)[b]			Adsorption performance (%(w·w^{-1}))		Selectivity
		IL	H_2O	acetonitrile	xylose	IL	
75.0	20.0	4.6	13.9	81.5	49.1	36.9	1.33
75.0	35.0	2.8	8.5	88.6	40.1	27.7	1.45
58.0	20.0	4.2	5.9	89.9	71.2	46.1	1.54
58.0	35.0	2.5	3.6	93.9	59.8	33.9	1.76
26.0	35.0	3.1	1.1	95.8	72.1	26.9	2.68
26.0	70.0	1.6	0.6	97.9	66.5	20.0	3.32

[a] initial water content in solution with [emim][HSO_4] before the addition of acetonitrile; [b] composition of final solution after the addition of acetonitrile; $Adsorption\ performance = \frac{m_{xylose\ or\ IL_{initial}} - m_{xylose\ or\ IL_{final}}}{m_{xylose\ or\ IL_{initial}}}$, $Selectivity = \frac{Adsorption\ performance_{xylose}}{Adsorption\ performance_{IL}}$.

7.3.3. Preparative chromatography for xylose and [emim][HSO_4] separation

The aforementioned batch experiments allowed formulating the principles for selective adsorption of xylose and IL on alumina in presence of acetonitrile. This knowledge was employed in the preparative chromatography trials with alumina as a stationary phase. To optimise the separation of both xylose and IL, a series of variables *i.e.* water content in the eluent, type of alumina treatment, effect of the amount of stationary phase and sample used, were studied (Table 7.1.).

The preliminary tests (Figure 7.3.) showed the influence of water content in the acetonitrile eluent on IL elution. For each performed experiment (Table 7.1., entries C1-C3), [emim][HSO_4] started to be collected only after 100 mL of elution reaching very sharply a maximum and, afterwards, the amount of eluted IL was slowly reduced until practically no IL was collected. The data shows that by using acetonitrile as eluent only 28.5 %(w·w^{-1}) of the initial IL was recovered after 400 mL of elution volume. An increase in eluent polarity enhanced either individual or accumulated IL contents in the samples. For 5 wt.% of water content in acetonitrile eluent, 44.7 %(w·w^{-1}) of the initial IL was recovered after 350

mL of elution volume. Nevertheless, more than a half of IL was still retained on the stationary phase. Only due to the change of eluent polarity from 10 wt.% to 75 wt.% of water content, an increase of IL recovery yield up to 66.8 %(w·w^{-1}) (green open squares) was achieved. Thus, these results show that although [emim][HSO_4] is well soluble in acetonitrile, it is also able to form strong interactions with the stationary phase (alumina) preventing it from efficient elution. Even an increase in eluent polarity, a quantitative recovery of IL was not achieved. This may suggest that part of IL might be chemically bonded to the alumina. Bearing in mind the acidic character of [emim][HSO_4], it can be expected that IL might interact with alumina in the presence of water.[35] Santacesaria *et al.* found that in the presence of water Lewis sites on alumina are transformed into Brönsted sites, which in the presence of strong acids reacts as alkali.[35] In order to verify this hypothesis and to circumvent the loss of IL, an alumina treatment with H_2SO_4 was performed before using it as a stationary phase in the preparative chromatography. Figure 7.4. shows the elution profiles of IL with treated (orange circles) and untreated stationary phase (blue circles).

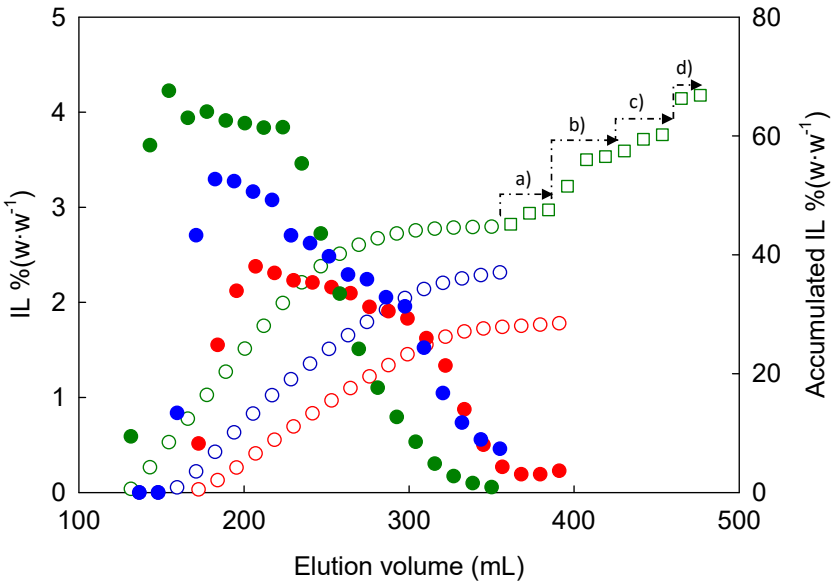

Figure 7.3. The elution profile of [emim][HSO_4] obtained for eluents with different composition: acetonitrile (Table 7.1., entry C1: ●), acetonitrile with 1.6 wt.% water content (Table 7.1., entry C2: ●) and acetonitrile with 5.0 wt.% water content (Table 7.1., entry C3: ●). The respective accumulated mass yields of [emim][HSO_4] for each experiment is depicted as open symbols. Open squares represent accumulated IL of entry C3 with a gradual increase in water content in eluent composition as the following: a) 10 wt.%; b) 25 wt.%; c) 50 wt.%; and d) 75 wt.%.

The obtained data shows clearly that treatment of alumina with H_2SO_4 enhanced the elution of IL when compared to experiment with untreated alumina. Additionally, the elution of IL started with lower

elution volume and the maximal recovery of IL after approximately of 430 mL elution volume was as high as 68.5 %(w·w^{-1}). At the same time, co-elution of xylose was not observed.

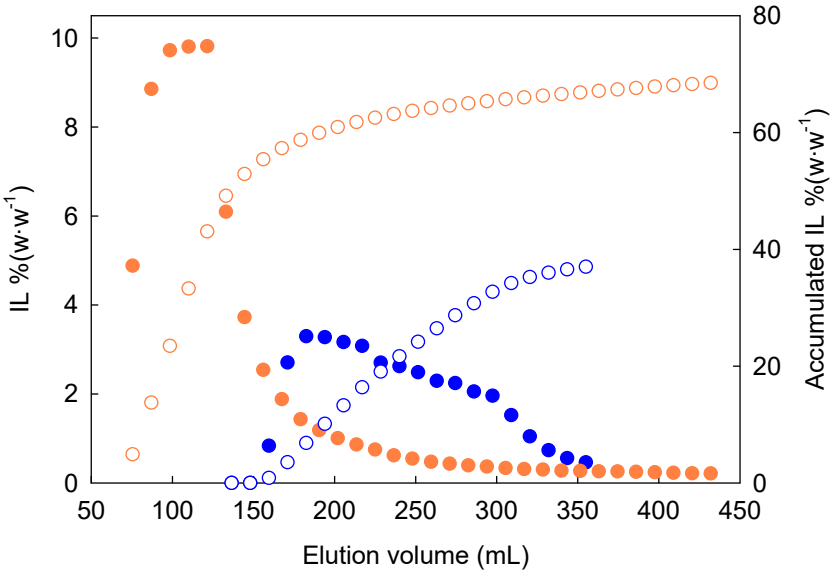

Figure 7.4. The elution profiles of [emim][HSO_4] for untreated alumina (Table 7.1., entry C2: ●) and for H_2SO_4 treated alumina (Table 7.1., entry C4: ●). The accumulated [emim][HSO_4] mass yields for untreated (○) and treated (○) alumina experiments are also depicted.

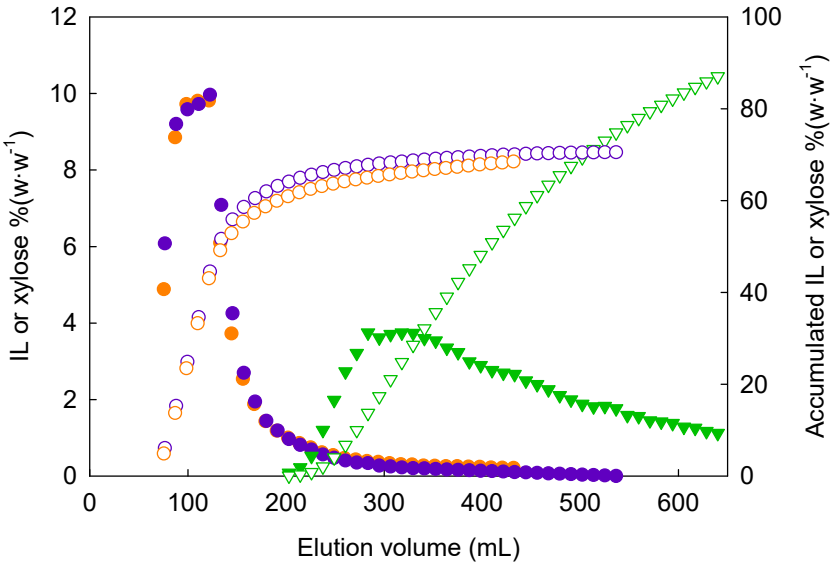

Figure 7.5. The elution profiles of [emim][HSO_4] and xylose with H_2SO_4-treated alumina for 1.6 wt.% water content in eluent (Table 7.1., entry C4: [emim][HSO_4] ●) and 3.0 wt.% water content in eluent (Table 7.1., entry C5: [emim][HSO_4] ●; xylose ▼). The accumulated mass yields of [emim][HSO_4] and xylose for each entry are depicted by the corresponding open symbols.

With the aim to use lower volumes of eluent, the polarity of eluent was increased to a 3 wt.% of water content in the acetonitrile-based eluent. The obtained elution profile is presented in Figure 7.5. and shows that elution of IL did not suffer a significant improvement, *i.e.* a maximum of 70 %(w·w^{-1}) of accumulated yield was achieved, however, xylose was started to be detected already with 200 mL elution volume. Nevertheless, the first 200 mL fraction free of xylose contained a 65.7 %(w·w^{-1}) of initial IL, while a residual amount of IL (4.8 %(w·w^{-1})) was co-eluted with xylose in the rest of the chromatographic run.

An increase of the scale of the separation process was considered also in this work. For this purpose, twice higher amount of alumina and xylose and IL concentrations were used (Table 7.1., entry C6). The obtained results are presented in Figure 7.6. As it could be expected, for the same geometry of chromatography column, the elution of both IL and xylose was delayed, which means that larger volume of eluent was needed. Furthermore, the elution profiles for IL and xylose were similar for both experiments (Table 7.1., entries C5 and C6), however due to a higher concentration of xylose and IL used in entry C6 than in entry C5, a maximum concentration of both compounds in individual samples was also higher. The achieved separation of IL and xylose was similar to those observed in case of smaller scale (Table 7.1., entry C5), *i.e.* the first fraction contained as much as 64.8 %(w·w^{-1}) of IL, free of monosaccharides, while in the second fraction a 94.4 %(w·w^{-1}) of initial xylose and 9.8 %(w·w^{-1}) of IL was collected. Nevertheless, it can be stated that contrary to IL, xylose recovery was nearly quantitative, reaching 94.4 %(w·w^{-1}) of initial xylose (open orange symbols – Figure 7.6.). This may indicate that the interaction of xylose with alumina is rather mediated by physical interactions than covalent bonding as it is a case of IL.

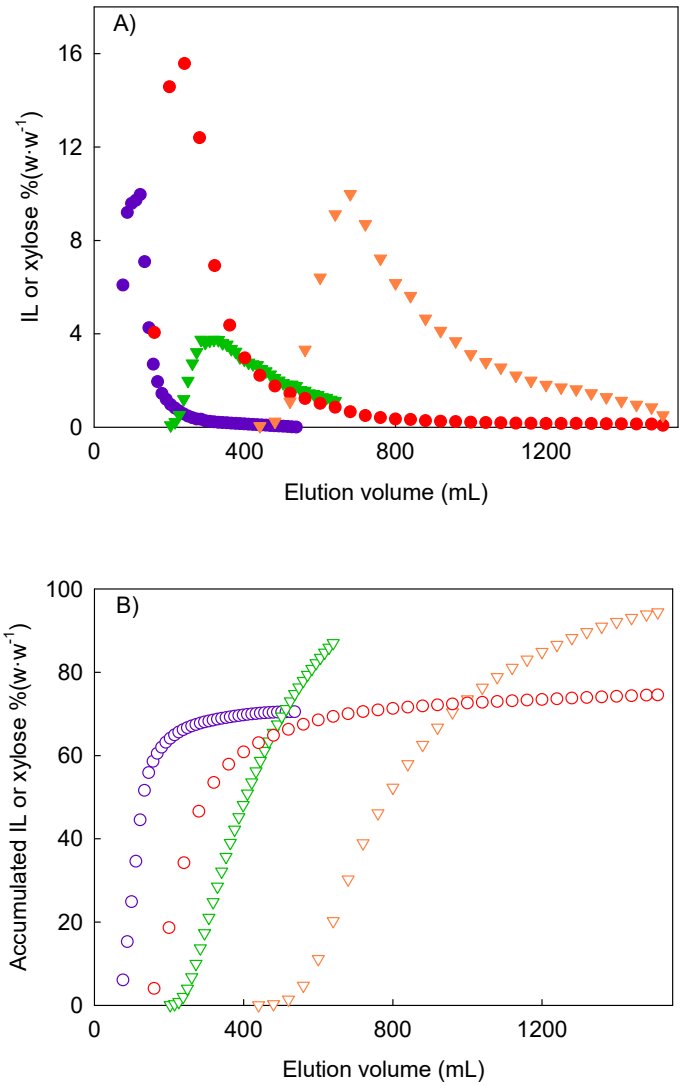

Figure 7.6. A) The elution profiles of [emim][HSO_4] and xylose for 10.0 g (Table 7.1., entry C5: [emim][HSO_4] ●; xylose ▼) and 20.0 g (Table 7.1., entry C6: [emim][HSO_4] ●; xylose ▼) of H_2SO_4 treated alumina. B) The corresponding accumulated mass yields of [emim][HSO_4] and xylose for C5 and C6 entries are presented by the respective opened symbols.

As it was stated above, to avoid the two-phase formation and to achieve a sufficiently low polarity of the system, the $x_{acetonitrile}$ in the sample should be somewhere above 0.9. This means that a large volume of acetonitrile must be used. Hence, with the aim of reducing the amount of acetonitrile, an additional experiment was performed (Table 7.1., entry C7) in which concentrations of IL and xylose in the sample were doubled. As it could be expected, the elution of both IL and xylose started with lower volume of eluent, but recovery of IL was slightly lower when compared to entry C6. Additionally, the resolution between IL and xylose was also lower as it is demonstrated in Figure 7.7. The fact that IL at higher concentration was placed in contact with stationary phase caused an increase in covalent bonding

capacity between IL and alumina. This, in turn, resulted in lower recovery yield (66.0 %(w·w^{-1})) than in case of entry C6 where 71.3 %(w·w^{-1}) for the same eluent volume (800 mL) was obtained.

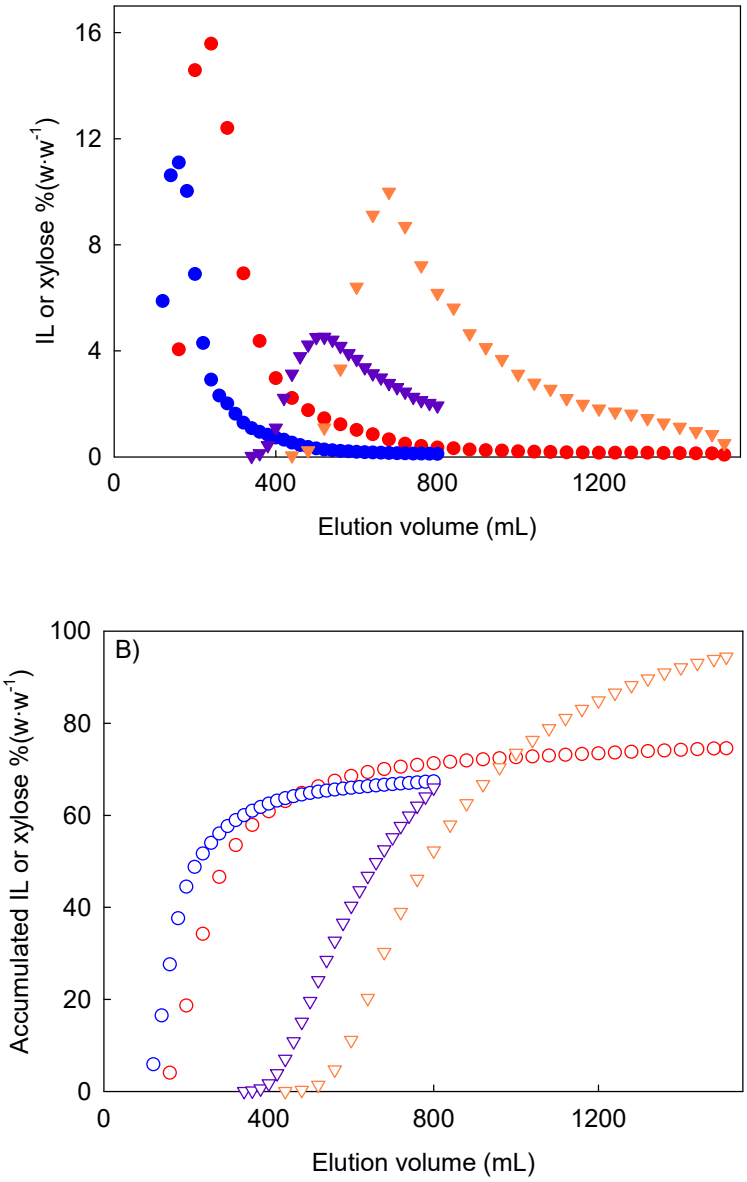

Figure 7.7. A) The elution profiles of [emim][HSO_4] and xylose obtained using a sample constituted by 160.0 g acetonitrile (Table 7.1., entry C6: [emim][HSO_4] ●; xylose ▼) and by 80.0 g acetonitrile (Table 7.1., entry C7: [emim][HSO_4] ●; xylose ▼) loaded on H_2SO_4 treated alumina. B) The accumulated mass yields of [emim][HSO_4] and xylose for each entry are represented by the corresponding open symbols.

All the aforementioned systems, although led to a significant improvement in the xylose and IL separation and the recovery of both, the limitations in the IL recovery were still evident. At the best case scenario, as much as 25.4 %(w·w^{-1}) of the initial [emim][HSO_4] was still retained in the column (Table

7.1., entry C6) even when *ca.* 1500 mL of elution volume was used. The plausible reason is a covalent bonding between IL and alumina as it was explained already above. A way to achieve a high IL recovery yield is an adequate processing of alumina prior to a chromatographic run, which could reduce the retention of IL on the column. The results presented until now showed that the use of H_2SO_4 is a correct method, however still another approach was needed. Therefore, a process of alumina treatment with H_2SO_4 and fresh [emim][HSO_4] was studied. The efficiency of this methodology can be analysed on Figure 7.8. where the IL elution profiles for untreated alumina (green symbols), alumina washed with water (red symbols), H_2SO_4 treated alumina (orange symbols) and H_2SO_4/[emim][HSO_4] treated alumina (blue symbols) are shown.

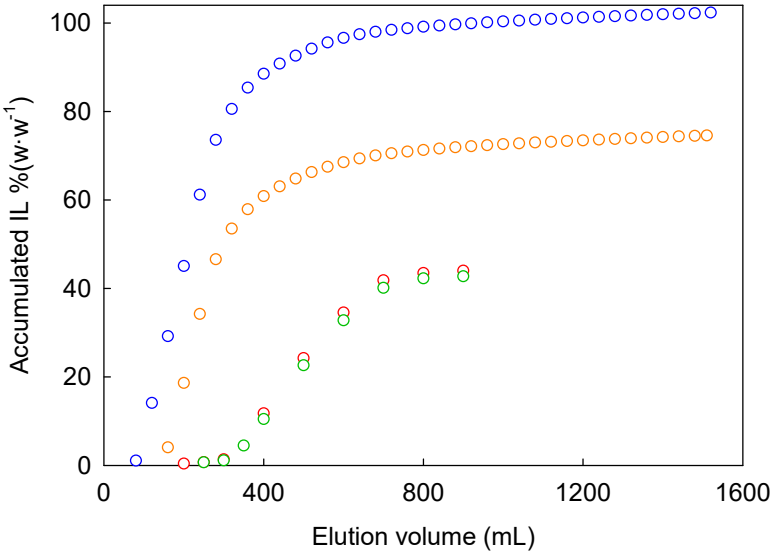

Figure 7.8. The elution profiles of accumulated [emim][HSO_4] on untreated alumina (Table 7.1., entry C8: ○), on alumina washed with water (Table 7.1., entry C9: ○), on H_2SO_4 treated alumina (Table 7.1., entry C6: ○) and on H_2SO_4/[emim][HSO_4] treated alumina (Table 7.1., entry C10 experiment: ○). For clarity of the figure, the xylose elution profiles are not demonstrated.

The presented data demonstrates that either untreated alumina (Table 7.1., entry C8) or alumina washed with water (Table 7.1., entry C9) retained more than 50 %(w·w^{-1}) of the initial IL. Furthermore, the elution of IL occurred only with much higher elution volumes, probably due to the strong acid-base interactions between IL and (untreated or water-washed) alumina. As it was described above, the treatment of alumina with H_2SO_4 (Table 7.1., entry C6) enhanced the IL recovery yield, but still 1/4 of initial IL was retained on the column. One of the advantages of this process, in comparison to the previous, was the need for lower elution volumes, nevertheless, obtained results were unsatisfactory in terms of IL recovery. Hence, to overcome this limitation, treatment of alumina with H_2SO_4 followed by treated with pure [emim][HSO_4] (Table 7.1., entry C10) was performed before eluting the sample. As it

can be seen in Figure 7.8., this approach allowed achieving quantitative IL recovery with elution volume similar to those used in other experiments (*ca.* 800 mL). This result shows that IL recovery is possible to be obtained, however the separation of IL and xylose must be accomplished as well. Figure 7.9. shows this issue, *i.e.* it demonstrates the elution profiles for xylose and IL in a chromatographic run with stationary phase treated by H_2SO_4 and [emim][HSO_4]. The obtained results show that an IL-rich fraction contained 90.8 %(w·w^{-1}) of the initial IL mass while the xylose-rich-fraction contained as much as 98.1 %(w·w^{-1}) of xylose yield and the remaining IL. Obtained results showed that a satisfactory separation of monosaccharides and IL as well as recovery yields of both in separate fractions is possible to be achieved.

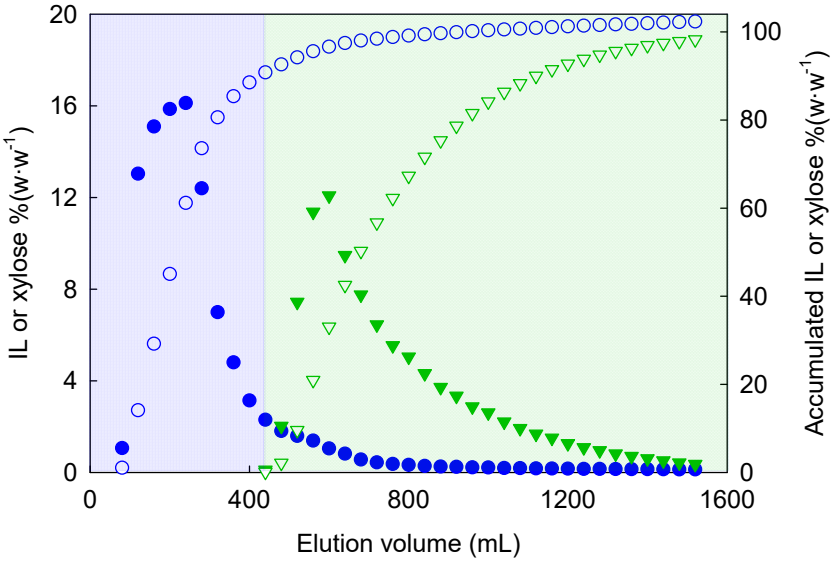

Figure 7.9. The elution profiles of [emim][HSO_4] and xylose obtained on H_2SO_4/[emim][HSO_4] treated alumina (Table 7.1., entry C10: [emim][HSO_4] ●; xylose ▼) and their respective accumulated mass yields elution profiles (respective open symbols). The blue and green zones indicate the IL-rich and xylose-rich fractions, respectively.

A separation of monosaccharides and ILs also have been thoroughly studied in the literature.[36] One of the most commonly used methodologies was the use of anti-solvent character of some organic solvents (*e.g.* acetonitrile, ethanol, acetone and dichloromethane), aiming to achieve monosaccharide precipitation.[31] One of the drawbacks is a need for use of anhydrous antisolvents to achieve an adequate efficiency of the process. Another widely explored option is the monosaccharide derivatisation method, which helps to change the mutual solubility of derivatised monosaccharide and IL, and potentially allows for liquid-liquid extraction with *e.g.* organic solvents.[29] An alternative strategy is the employment of physical separation processes. A combination of ultrafiltration, nanofiltration and electrodialysis was applied in a process of IL-based treatment of cellulose, aiming the production and purification of

glucose.[37] Glucose obtained from cellulose treatment with 1,3-dimethylimidazolium dimethylphosphate IL and posterior enzymatic hydrolysis was separated by membrane ultrafiltration and, subsequently, by nanofiltration allowed separation of glucose from intermediary products (*e.g.* cellobiose). At the final step, glucose and remaining IL were separated by electrodialysis taking advantage of charged and uncharged character of IL and glucose, respectively. One of the burdens in the practical application of this method is its cost.[37] Still, the most traditional but effective methodology for the desired separation of monosaccharides and ILs is the chromatography approach.[30, 38, 39] This type of separation can be tuned by choosing and modifying both stationary and mobile phases. For instance, a Dowex 50 resin was used for the separation of glucose from 1-ethyl-3-methylimidazolium chloride allowing recovering 70-80 wt.% of the glucose from biomass hydrolysate containing IL.[38] Also Dowex-based resins demonstrated > 95 %($w \cdot w^{-1}$) recovery of the initial IL mass in biomass hydrolysate.[30, 38] Other literature report showed that alumina can be efficiently used to separate biomass-derived monosaccharides from *N*-methyl-*N*-methylimidazolium dimethylphosphate by adequate adjustment of eluent constituted by methanol and water.[39] The reported recovery yields were as high as 93.4 %($w \cdot w^{-1}$) and 90.1 %($w \cdot w^{-1}$) for IL and glucose, correspondingly.[39]

One of the common characteristics of all demonstrated examples is high recovery yields for both monosaccharides and ILs, however the separation efficiency was barely reported. In this context, the present work discloses unparalleled results. The initial IL/xylose mass ratio was 19 that is similar to IL/pentose mass ratio obtained in the reaction of wheat straw with [emim][HSO_4] presented elsewhere.[25] After the chromatographic separation of IL and xylose, the aforementioned ratio in the xylose-rich fraction abruptly reduced to approximately 1.9. Also, the IL-rich fraction contained 90.8 %($w \cdot w^{-1}$) of the initial IL mass with no traces of xylose. Furthermore, recovery yields of both xylose and [emim][HSO_4] were quantitative demonstrating the potentiality of the developed technology in terms of material efficiency.

7.4. Conclusion

The separation and recovery of both monosaccharides and ILs have been a challenge in the IL-based biomass processing. This work demonstrated a comprehensive study focused on the development of a simple alumina chromatographic approach allowing separation of pentoses (xylose) from an acidic IL (1-ethyl-3-methylimidazolium hydrogensulphate). The breakthrough in the separation of these highly-polar compounds was achieved by the change of system polarity. High acetonitrile content in the sample favoured the interaction of xylose with stationary phase (alumina) in detriment of IL. Furthermore, a treatment of alumina with both H_2SO_4 and IL permitted to achieve quantitative recovery of xylose and IL as well as satisfactory separation of IL and xylose. As much as 90 %($w \cdot w^{-1}$) of the initial IL was obtained in the first fraction free of xylose and 98 %($w \cdot w^{-1}$) of xylose was collected in the second fraction.

7.5. References

1. J. F. Robyt, *Essentials of carbohydrate chemistry*, Springer, 1998.
2. A. Ahmed, M. Adel, P. Karimi and M. Peidayesh, *Adv. Food Nutr. Res.*, 2014, **73**, 197-220.
3. P. Laurienzo, *Mar. Drugs*, 2010, **8**, 2435-2465.
4. M. Fathi, A. Martin and D. J. McClements, *Trends Food Sci. Technol.*, 2014, **39**, 18-39.
5. R. Jayakumar, M. Prabaharan, S. V. Nair, S. Tokura, H. Tamura and N. Selvamurugan, *Prog. Mater. Sci.*, 2010, **55**, 675-709.
6. I. Siró and D. Plackett, *Cellulose*, 2010, **17**, 459-494.
7. P. F. Stanbury, A. Whitaker and S. J. Hall, *Principles of fermentation technology*, Elsevier, 2013.
8. S. N. Naik, V. V. Goud, P. K. Rout and A. K. Dalai, *Renew. Sust. Energ. Rev.*, 2010, **14**, 578-597.
9. Z. Anwar, M. Gulfraz and M. Irshad, *J. Radiat. Res. Appl. Sci.*, 2014, **7**, 163-173.
10. M. H. L. Silveira, A. R. C. Morais, A. M. da Costa Lopes, D. N. Olekszyszen, R. Bogel-Lukasik, J. Andreaus and L. P. Ramos, *ChemSusChem*, 2015, **8**, 3366-3390.
11. A. R. C. Morais, A. M. da Costa Lopes and R. Bogel-Lukasik, *Chem. Rev.*, 2015, **115**, 3-27.
12. A. M. da Costa Lopes and R. Bogel-Lukasik, *ChemSusChem*, 2015, **8**, 947-965.
13. S. Hyvärinen, P. Damlin, J. Gräsvik, D. Y. Murzin and J.-P. Mikkola, *Cellul. Chem. Technol.*, 2011, **45**, 483-486.
14. N. V. Plechkova and K. R. Seddon, in *Methods and Reagents for Green Chemistry*, ed. P. Tundo, John Wiley & Sons, Inc., 2007, pp. 103-130.
15. J. P. Hallett and T. Welton, *Chem. Rev.*, 2011, **111**, 3508-3576.
16. U. Domanska and R. Bogel-Lukasik, *J. Phys. Chem. B*, 2005, **109**, 12124-12132.
17. R. Bogel-Lukasik, L. M. N. Goncalves and E. Bogel-Lukasik, *Green Chem.*, 2010, **12**, 1947-1953.
18. M. E. Zakrzewska, E. Bogel-Lukasik and R. Bogel-Lukasik, *Energ. Fuel.*, 2010, **24**, 737-745.
19. K. Paduszynski, M. Okuniewski and U. Domanska, *J. Phys. Chem. B*, 2013, **117**, 7034-7046.
20. I. A. Kilpeläinen, H. Xie, A. King, M. Granstrom, S. Heikkinen and D. S. Argyropoulos, *J. Agric. Food Chem.*, 2007, **55**, 9142-9148.
21. I. Anugwom, V. Eta, P. Virtanen, P. Maki-Arvela, M. Hedenstrom, M. Hummel, H. Sixta and J. P. Mikkola, *ChemSusChem*, 2014, **7**, 1170-1176.
22. N. V. Plechkova and K. R. Seddon, *Chem. Soc. Rev.*, 2008, **37**, 123-150.
23. V. Eta, I. Anugwom, P. Virtanen, K. Eränen, P. Mäki-Arvela and J.-P. Mikkola, *Chem. Eng. J.*, 2014, **238**, 242-248.
24. A. V. Carvalho, A. M. da Costa Lopes and R. Bogel-Lukasik, *RSC Adv.*, 2015, **5**, 47153-47164.
25. A. M. da Costa Lopes, R. M. G. Lins, R. A. Rebelo and R. M. Lukasik, *Energ. Environ. Sci.*, 2017 (submitted).
26. I. Anugwom, P. Maki-Arvela, P. Virtanen, S. Willfor, R. Sjoholm and J. P. Mikkola, *Carbohydr. Polym.*, 2012, **87**, 2005-2011.
27. L. Chen, M. Sharifzadeh, N. Mac Dowell, T. Welton, N. Shah and J. P. Hallett, *Green Chem.*, 2014, **16**, 3098-3106.
28. P. Verdia, A. Brandt, J. P. Hallett, M. J. Ray and T. Welton, *Green Chem.*, 2014, **16**, 1617-1627.
29. T. C. R. Brennan, S. Datta, H. W. Blanch, B. A. Simmons and B. M. Holmes, *Bioenerg.Res.*, 2010, **3**, 123-133.
30. B. R. Caes, T. R. Van Oosbree, F. Lu, J. Ralph, C. T. Maravelias and R. T. Raines, *ChemSusChem*, 2013, **6**, 2083-2089.
31. A. P. Carneiro, O. Rodríguez and E. A. Macedo, *Sep. Purif. Technol.*, 2014, **132**, 496-504.
32. A. P. Carneiro, O. Rodríguez and E. A. Macedo, *Fluid Phase Equilib.*, 2012, **314**, 22-28.
33. P. A. Steiner and W. Gordy, *J. Mol. Spectrosc.*, 1966, **21**, 291-301.
34. H. Zhang, E. C. Brace and A. S. Engelberth, *J. Liq. Chromatogr. Relat. Technol.*, 2016, **39**, 666-673.
35. E. Santacesaria, D. Gelosa and S. Carrà, *Ind. Eng. Chem. Prod. RD.*, 1977, **16**, 45-47.
36. N. L. Mai, K. Ahn and Y.-M. Koo, *Process Biochem.*, 2014, **49**, 872-881.
37. C. Abels, K. Thimm, H. Wulfhorst, A. C. Spiess and M. Wessling, *Bioresour. Technol.*, 2013, **149**, 58-64.
38. J. B. Binder and R. T. Raines, *Proc. Natl. Acad. Sci. USA*, 2010, **107**, 4516-4521.

39. D. Feng, L. Li, F. Yang, W. Tan, G. Zhao, H. Zou, M. Xian and Y. Zhang, *Appl. Microbiol. Biotechnol.*, 2011, **91**, 399-405.

CHAPTER VIII

Conclusions

8.1. Conclusions and outlook

The disclosed thesis demonstrated a comprehensive study in the development of two distinct IL-based technologies that aimed at maximal valorisation of lignocellulosic biomass. A biomass fractionation in the frame of the biorefinery concept is one of most important achievements underpinned in this study. Biomass processing into high quality fractions was approached in each of the developed technologies by using either alkaline or acidic character of selected ILs.

8.1.1. The alkaline IL-based technology

The processing of wheat straw with alkaline [emim][OAc] allowed biomass dissolution and fractionation into cellulose-, hemicellulose- and lignin-rich fractions under mild conditions. The recalcitrance of the lignocellulosic matrix was overcome by alteration of strong network of intra- and intermolecular bonds existing in biomass. This alteration was essentially mediated by the alkaline character of IL anion (acetate), however, a polymeric form of those components was maintained. Variations of temperature and time in the dissolution of biomass with [emim][OAc] have an impact on the fractionation efficiency especially on the purity and recovery yields of macromolecular components. Conditions of 140 °C, 6 h and a biomass content of 5 %($w \cdot w^{-1}$) were found to be optimal for the production of high purity biomass fractions. On the other hand, for high recovery yields of cellulose and hemicellulose (>90 %($w \cdot w^{-1}$)) optimal conditions of 140 °C, 6 h and a biomass content of 5 %($w \cdot w^{-1}$) were determined. Nevertheless, nearly 50 %($w \cdot w^{-1}$) of the initial lignin content was lost. A potential depolymerisation of lignin was checked to explain such result and it was confirmed by evidencing the presence of phenolic compounds with low molecular mass, such as vanillin, syringaldehyde, *p*-coumaric acid, tricin, etc. soluble in the recovered IL.

A scale-up of the process did not influence the efficiency of the fractionation process and provided [emim][OAc] with a required amount of phenolic compounds in order to study their purification by extraction from recovered IL. An approach based on the adsorption of phenolic compounds through the employment of polymeric resins resulted in the production of a phenolic-rich sample, but with traces of IL content. Tested polymeric resins (Amberlite XADs and Polyvinylpolypyrrolidone) demonstrated different selectivities towards phenolic compounds. Among examined resins, the most efficient in phenolic extraction was Amberlite XAD-7. However, the presence of IL in phenolic extracts was still observed, which enforce the employment of an additional purification step. For this purpose, the successfully application of supercritical CO_2 extraction was carried out and sample of IL-free phenolics was obtained.

The potential scale up of the developed fractionation process with [emim][OAc] would allow transformation of wheat straw into bulky but high-quality cellulose, hemicellulose and lignin products readily available for further processing and valorisation. Additionally, the biorefinery concept with

alkaline IL would be potentiated by the valorisation of phenolic-rich fraction, which represents a low-volume but high-value product.

8.1.2. The acidic IL-based technology

A second strategy relied on the processing of wheat straw with acidic HSO_4-based ILs. This approach allowed the integration of biomass pre-treatment, hydrolysis and conversion into a single step process. The acidic character of [HSO_4] anion of IL, promoted a selective processing of hemicellulose fraction and the resulting products (mainly pentoses and furfural) were dissolved in the liquid phase. The advance in the hemicellulose hydrolysis was tailored by temperature and time of the reaction. Besides, the avoidance of unproductive formation of humins was mitigated by the controlled acidity of the reaction medium, namely by the use of an aqueous HSO_4-based IL system instead of using pure IL. This approach revealed a favourable production of pentoses in detriment of furfural. The presence of water in the system allowed avoiding the dehydration of pentoses into furfural and consequently, high pentose yield was possible to be obtained. At optimal (mild) conditions, approximately 80 mol% pentose yield was achieved placing this technology among the most efficient for this purpose. However, the production of pentoses, even with high yield, put another challenge on the process, that is an efficient removal of pentoses from the IL media. The separation of pentoses from IL was accomplished by the use of preparative chromatography approach. Highly polar character of IL media containing xylose, water and IL was changed by aprotic and less polar acetonitrile. Afterwards, the preparative chromatography with preconditioned alumina allowed efficient separation of IL and pentose streams. The first fraction comprised more than 90 %($w \cdot w^{-1}$) of the initial IL mass and no trace of sugar were observed. The second fraction was constituted by monosaccharides and a residual content of IL.

The solids produced in the HSO_4-based ILs process were constituted by cellulose and lignin and were subject to further fractionation and valorisation. Two scenarios were developed and consisted of lignin extraction prior to enzymatic hydrolysis of cellulose-rich sample or a direct enzymatic hydrolysis of the solid constituted by both cellulose and lignin. The first scenario produced higher glucose to glucan yield (> 90 mol%) in comparison to scenario without lignin removal ($\backsim$76 mol%). Furthermore, in the first case, a high pure fraction of lignin was obtained. Similar to alkaline IL, some depolymerisation of lignin was observed with HSO_4-based ILs allowing production of aromatic compounds with no presence of IL.

Therefore, an integrated process for wheat straw valorisation with HSO_4-based ILs was herein demonstrated and comprised (i) the production of pentoses in the liquid phase, (ii) the recovery and separation of those sugars from HSO_4-based IL, (iii) the separation of lignin and cellulose from obtained solid, (iii) the production of glucose via enzymatic hydrolysis of cellulose fraction, (iv) the production of high purity lignin and (v) simultaneous production of aromatic compounds. The recovery of HSO_4-

based IL was also successfully achieved and a reuse of IL revealed that this novel solvent maintained its performance in biomass processing.

The developed IL-based technologies might offer advantages in creating value from low-cost biomass and their application depends on targeted biorefinery approach. For instance, the alkaline IL-based technology involves the treatment and separation of major biomass components, which in turn, can be used as feedstocks for further processing either for the creation of novel bio-based materials or for the depolymerisation into compounds useful for the production of biofuels and chemicals. For instance, the obtained hemicellulose fraction that presents a morphological and mechanical behaviour similar to a glue is appellative for the production of polymers and hydrogels. On the contrary, the developed acidic IL-based technology offers the possibility to hydrolyse hemicellulose in a one-step process. The produced pentoses can be further used as high quality substrate for biological conversion towards a wide variety of value-added compounds (*e.g.* xylitol and polyhydroxyalkanoates). The same technology can be also tailored to produce furfural, which is one of the main building blocks for a wide portfolio of chemicals.

Furthermore, the disclosed multi-step technologies meet the main objectives of both green chemistry and biorefinery concepts. For instance, the valorisation of lignocellulosic residues, such as wheat straw, was accomplished by producing several high quality fractions. Furthermore, it should be underlined that developed technologies are characterised by a high efficiency in recovery of major biomass fractions and minimisation of waste disposal. These are indicators of good practices and as such follow both bioeconomy and circular economy frameworks propelled by European Commission. Additionally, the high recyclability of ILs in both developed technologies demonstrated to be a key aspect for accomplishment of the green chemistry strategy. This is also important regarding to the economic aspects of the process, where the reuse of the IL solvent and/or catalyst for a next subsequent run is highly demanding. Moreover, it will also put the end about the myth of IL price, which actually limits the potential of IL use in the biomass valorisation.

The obtained results demonstrate an elevated impact regarding to research in biomass processing and valorisation. The work demonstrated in this thesis activate the projects, which obtained national (FCT) and international (*e.g.* from European Commission within the Horizon 2020 calls, CAPES) financial support.[1] It can be expected that in a near future, these works will contribute to the development of energy- and cost-saving IL-based technologies at higher TRLs (Technology Readiness Levels) for tangible application in biorefineries.

Therefore, the present thesis shows that IL-based technologies can be a solid alternative to current industrial processes of biomass upgrading. The described IL-based technologies could be frontrunners

[1] a) P2020-SAICT-45-2016-01 BBRI nº 22059; b) INFRAIA-01-2016-2017 BRISK2; c) LCE-33-2016 AMBITION; d) Pesquisador Visitante Especial CAPES project; 5) SMIBIO – ERANET-LAC.

in future biorefineries and, in medium-term, can be competitive with products obtained from fossil refineries.

APPENDIX A

Additional information supporting

CHAPTER IV

This appendix is based on data of the following publication:

A. M. da Costa Lopes, M. Brenner, P. Fale, L. B. Roseiro and R. Bogel-Lukasik, Extraction and purification of phenolic compounds from lignocellulosic biomass assisted by ionic liquid, polymeric resins and supercritical CO_2, *ACS Sustain. Chem. Eng.*, 2016, **4**, 3357-3367.

Table A.1. Doehlert experimental design applied for the corresponding experimental responses Y_1 (total phenolic extraction yield) and Y_2 (vanillin extraction yield).

Entry	Coded variables		Responses	
	X_1	X_2	Y_1 (%)	Y_2 (μg·$g_{biomass}^{-1}$)
A	-0.03	-0.40	74	456
B	0.83	-0.40	73	502
C	-0.90	-0.40	50	292
D	0.40	0.12	79	485
E	-0.47	0.92	54	386
F	0.40	0.92	73	488
G	-0.47	0.12	66	482
H	-0.90	0.80	43	265

Table A.2. Parameters of the polynomial models representing the studied response Y_1 (total phenolic extraction yield) and Y_2 (vanillin extraction yield). The adequacy of the models to fit the sets of data was performed using Fisher test (F-test) for the effectiveness of the factors.

Model parameters (MP)	Y_1		Y_2	
	MP	*p*	*MP*	*p*
β_0	76.54	0.00	497.65	0.00
β_1	11.27	0.00	73.00	0.04
β_2	-3.70	0.28	-42.92	0.34
β_{12}	-6.24	0.20	-58.60	0.36
β_{11}	-18.24	0.00	-131.40	0.01
β_{22}	-15.37	0.00	-92.97	0.11
F-test				
Effectiveness of the parameters	48.66		13.55	
Significance level (p<0.05)	0.00		0.00	
R^2	0.96		0.87	

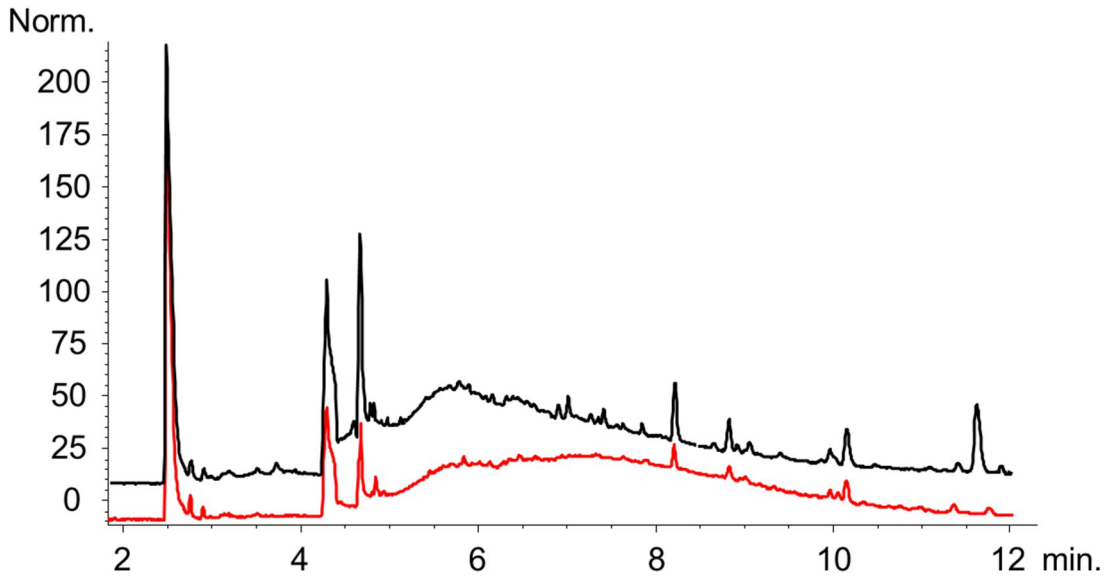

Figure A.1. Phenolic adsorption profiles of the original sample placed on the pressure vessel before (black) and after (red) CO_2 extraction, both recorded at 200 nm wavelength.

APPENDIX B

Additional information supporting

CHAPTER V

This appendix is based on data of the following publication:

A. V. Carvalho, A. M. da Costa Lopes and R. Bogel-Lukasik, Relevance of the acidic 1-butyl-3-methylimidazolium hydrogen sulphate ionic liquid in the selective catalysis of biomass hemicellulose fraction, *RSC Adv.*, 2015, **5**, 47153-47164.

Table B.1. Pre-treatment temperatures and times studied in this work and respective coded levels for statistical modelling.

T **(°C)**	***t*** **(min)**	**Coded levels (xylose)**		**Coded levels (furfural)**	
		X_1	X_2	X_1	X_2
85	113.3	-0.67	+0.87	-	-
100	70.0	-0.33	0.00	-	-
115	26.7	0.00	-0.87	-1.00	-
	113.3	0.00	+0.87	-1.00	0.00
130	70.0	+0.33	0.00	-0.50	-
	156.6	+0.33	-	-0.50	+0.87
145	26.7	+0.67	-0.87	0.00	-
	113.3	+0.67	+0.87	0.00	0.00
160	70.0	-	-	+0.50	-0.87
	156.6		-	+0.50	+0.87
175	63.3	-	-	+1.00	-1.00
	163.3		-	+1.00	+1.00
	113.3		-	+1.00	0.00

Table B.2. Doehlert experimental design applied for the corresponding experimental responses Y_1 (xylan hydrolysis to xylose).

Run	**Coded variables**		**Response**
	X_1	X_2	Y_1
A	-0.33	0.00	1.9
B	0.33	0.00	18.9
C	0.00	0.87	15.4
D	0.00	-0.87	4.5
E	-0.67	0.87	0.0
F	0.67	-0.87	12.9
G	0.67	0.87	3.8

Table B.3. Doehlert experimental design applied for the corresponding experimental responses Y_2 (sum of arabinan and xylan conversion to furfural).

Run	Coded variables		Response
	X_1	X_2	Y_2 (mol%)
A	-0.50	-0.87	14.3
B	-1.00	0.00	3.1
C	0.00	0.00	26.1
D	1.00	0.00	34.4
E	0.50	0.87	36.2
F	0.50	-0.87	30.7
G	-0.50	0.87	23.4
H	1.00	1.00	15.6
I	1.00	-1.00	30.6

Table B.4. Parameters of the polynomial models representing the studied response Y_1 (xylan hydrolysis to xylose) and Y_2 (hemicellulose sugar hydrolysis to furfural); The adequacy of the models to fit the sets of data was performing using Fisher test (F-test) for the effectiveness.

Model parameters (MP)	Y_1 (mol%)		Y_2 (mol%)	
	MP	*p*	*MP*	*p*
β_0	13.82	0.01	30.16	0.00
β_1	19.77	0.02	12.89	0.01
β_2	7.04	0.04	2.81	0.40
β_{12}	-18.29	0.03	-7.94	0.12
β_{11}	-32.00	0.03	-13.70	0.05
β_{22}	-5.19	0.16	-3.36	0.49
F-test				
Effectiveness of the parameters	16.23		5.49	
Significance level	0.06		0.06	
R^2	0.99		0.93	

Table B.5. Analysis of the liquid fraction produced in experiments performed at the optimum conditions for xylose and furfural production.

T (°C)	*t* (min)	Yield (mol%)							
		xylose[a]	arabinose[b]	furfural[c]	glucose[d]	HMF[e]	acetic acid[f]	formic acid[g]	levulinic acid[h]
125	82.1	16.7	10.9	7.6	0.9	1.1	40.8	0.0	0.0
161	104.5	0.0	0.0	30.7	0.9	1.4	67.9	0.9	2.1

a) $\frac{m_{xylose}}{m_{xylan_{native}}} \times \frac{132}{150} \times 100$; b) $\frac{m_{arabinose}}{m_{arabinan_{native}}} \times \frac{132}{150} \times 100$ c) $\frac{m_{glucose}}{m_{glucan_{native}}} \times \frac{162}{180} \times 100$; d) $\frac{m_{furfural}}{m_{(xylan+arabinan)_{native}}} \times \frac{132}{96} \times 100$; e) $\frac{m_{HMF}}{m_{glucan_{native}}} \times \frac{162}{126} \times 100$; f) $\frac{m_{acetic\ acid}}{m_{acetyl\ groups_{native}}} \times \frac{59}{60} \times 100$; g) $\frac{m_{formic\ acid}}{m_{(xylan+arabinan)_{native}}} \times \frac{132}{46} \times 100$; h) $\frac{m_{levulinic\ acid}}{m_{glucan_{native}}} \times \frac{162}{116} \times 100$.

Table B.6. Analysis of the solid produced from wheat straw pre-treatment at optimum conditions for xylose and furfural production obtained from statistical modelling.

T (°C)	*t* (min)	Solid composition (wt.%)[a]							Recovery yield (%(w·w^{-1})	
		xylan	arabinan	acetyl	glucan	lignin	ash	SY (%)	hemicellulose	cellulose
125	82.1	12.4	0.3	0.5	55.3	20.1	6.1	64.4	54.5	81.1
161	104.5	0.0	0.0	1.0	47.5	40.5	6.4	62.8	38.4	71.4

a) The oven-dried solid phase composition; SY - solid yield %(w·w^{-1}).

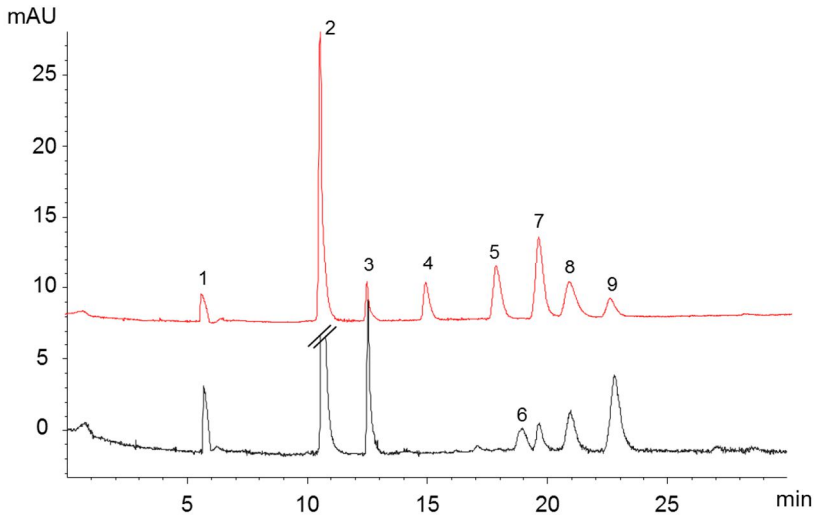

Figure B.1. CE electropherograms recorded at 270 nm demonstrating the detection and separation of [bmim][HSO_4], furans and sugars of standard solution (red) and liquid phase from a pre-treatment sample (black). Analytes: 1) [bmim][HSO_4]; 2) furfural; 3) HMF; 4) sucrose (internal standard); 5) cellobiose; 6) unidentified compound; 7) glucose; 8) arabinose; and 9) xylose.

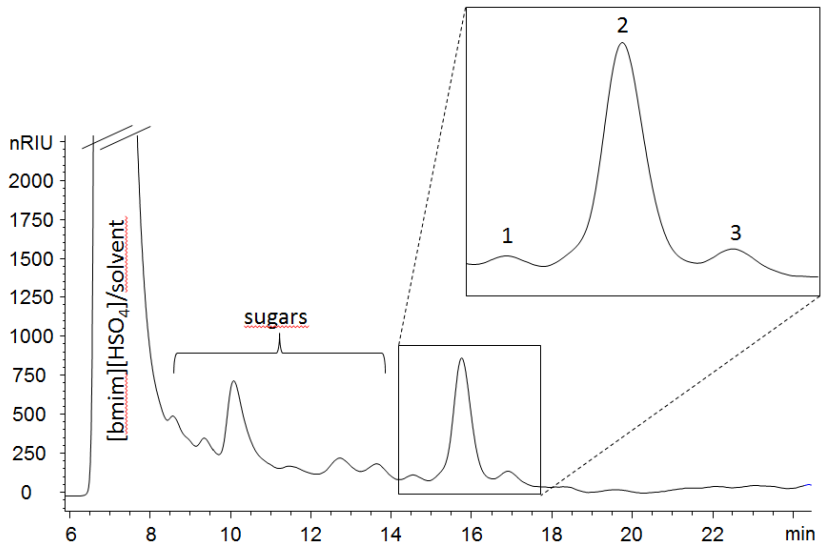

Figure B.2. HPLC chromatogram acquired with refractive index detector demonstrating the separation of [bmim][HSO_4], sugars and organic acids of liquid phase from a pre-treatment sample. Analytes: 1) formic acid; 2) acetic acid; and 3) levulinic acid.

APPENDIX C

Additional information supporting

CHAPTER VI

This appendix is based on data of the following publication:

A. M. da Costa Lopes, R. M. G. Lins, R. A. Rebelo and R. M. Lukasik, Biorefinery approach for lignocellulosic biomass valorisation with acidic ionic liquid, *Energ. Environ. Sci.*, 2017 (submitted).

Table C.1. The yields of main products, *i.e.* pentoses (sum of arabinose and xylose), furfural, glucose, 5-hydroxymethylfurfural (5-HMF) and acetic acid found in the liquids produced in the biomass reactions.

Entry[a]	$logR_O$	Yield (mol%)[b]				
		Pentoses	**Furfural**	**Glucose**	**5-HMF**	**Acetic acid**
3	2.45	20.9	0.0	3.1	0.0	36.3
9	3.07	24.7	0.0	2.7	0.4	50.0
5	3.19	26.4	0.0	3.2	0.7	43.5
7	3.19	26.6	0.0	3.2	0.1	50.2
12	3.28	28.7	0.0	2.7	0.3	54.5
11	3.80	43.7	0.1	3.2	0.6	61.2
15	3.92	54.1	0.6	3.6	1.1	73.5
1	3.92	54.5	0.2	4.2	1.2	78.2
13	4.02	56.2	1.1	3.8	1.6	81.2
10	4.53	67.5	2.8	5.1	1.9	85.7
4	4.66	74.4	1.1	5.5	1.4	86.5
6	4.66	67.0	4.5	6.0	2.6	92.4
8	4.76	76.8	3.4	6.4	2.1	91.1
2	5.39	77.5	11.4	8.4	2.5	102.3
14	6.56	59.1	33.2	9.3	2.5	103.4

[a] the entry according to Table 6.2.; [b] For quantification please refer to next sections.

Table C.2. The yield of recovered solid (SY) and composition of solid and recovery yields of main components *i.e.* arabinoxylan (sum of xylan and arabinan), acetyl groups, glucan, Klason lignin and ash produced in biomass reactions.

Entry[a]	*logRo*	SY %(w·w^{-1})	Composition (wt.%)[b] (recovery yield %(w·w^{-1})[b]				
			Arabinoxylan	Acetyl groups	Glucan	Klason Lignin	Ash
native	-	100.0	22.1 (100.0)	2.7 (100.0)	38.5 (100.0)	17.7 (100.0)	10.7 (100.0)
3	2.45	82.7	20.6 (77.1)	1.8 (54.6)	43.2 (92.8)	17.4 (81.1)	3.9 (29.9)
9	3.07	73.2	19.5 (64.7)	1.5 (39.8)	48.8 (92.8)	20.1 (83.1)	4.1 (28.0)
5	3.19	76.0	18.3 (63.1)	1.5 (40.9)	47.4 (93.6)	21.6 (92.9)	3.7 (26.3)
7	3.19	72.6	19.1 (62.7)	1.6 (42.1)	48.5 (91.5)	20.6 (84.6)	3.4 (22.9)
12	3.28	69.9	18.4 (58.3)	0.9 (23.5)	52.3 (94.5)	18.8 (74.2)	4.3 (28.1)
11	3.80	65.7	14.1 (42.0)	0.6 (15.2)	45.9 (78.4)	33.4 (124.0)	4.8 (29.4)
15	3.92	63.8	13.1 (37.9)	0.3 (7.7)	58.1 (96.2)	20.6 (74.1)	5.0 (30.1)
1	3.92	63.5	11.6 (33.2)	0.4 (8.9)	54.9 (90.5)	20.8 (74.6)	5.0 (29.9)
13	4.02	63.3	12.7 (36.4)	0.1 (2.8)	49.1 (80.7)	29.8 (106.5)	5.4 (32.1)
10	4.53	59.6	10.9 (29.5)	0.0 (0.0)	60.7 (93.9)	22.7 (76.4)	2.8 (15.6)
4	4.66	62.2	11.0 (30.8)	0.4 (9.5)	58.1 (93.8)	24.0 (84.3)	4.4 (25.3)
6	4.66	60.0	11.3 (30.6)	0.3 (7.5)	53.5 (83.4)	27.5 (93.1)	4.2 (23.4)
8	4.76	60.3	11.6 (31.7)	0.2 (5.6)	57.8 (90.6)	26.1 (89.1)	4.1 (23.1)
2	5.39	57.4	7.2 (18.8)	0.0 (0.0)	61.9 (92.4)	24.8 (80.5)	5.7 (30.7)
14	6.56	56.3	5.5 (14.0)	0.0 (0.0)	60.4 (88.3)	33.7 (107.4)	6.1 (32.0)

[a] the entry according to Table 6.2.; [b] For quantification please refer to next sections.

Table C.3. The yields of main products, *i.e.* pentoses (sum of arabinose and xylose), furfural, glucose, 5-HMF and acetic acid found in liquid from reaction at conditions of 141.0 °C, 57.8 wt.% H_2O and 90.0 min.

Yield (mol%)[a]				
Pentoses	Furfural	Glucose	5-HMF	Acetic acid
81.6	11.2	8.8	2.0	105.5

[a] For quantification please refer to next sections.

Table C.4. The yield of recovered solid (SY) and composition of solid and recovery yields of main components *i.e.* arabinoxylan (sum of xylan and arabinan), acetyl groups, glucan, Klason lignin and ash produced in biomass reaction at conditions of 141.0 °C, 57.8 wt.% H_2O and 90.0 min.

SY %(w·w^{-1})	Composition (wt.%)[a] (recovery yield %(w·w^{-1}))[a]				
	Arabinoxylan	Acetyl groups	Glucan	KL	Ash
55.8	6.6 (16.7)	0.0 (0.0)	65.6 (95.0)	27.2 (85.7)	6.8 (35.3)

[a] For quantification please refer to next sections.

Table C.5. The coefficients of model parameters and their statistical significance.

Model parameters	β_0	β_1	β_2	β_3	β_{11}	β_{22}	β_{33}	β_{12}	β_{13}	β_{23}
Coefficients	70.36	28.33	2.59	5.95	-34.95	-8.43	-8.20	5.76	2.59	2.69
***p*-value**	0.00	0.00	0.72	0.45	0.01	0.44	0.42	0.74	0.89	0.84
R^2	0.91									

Table C.6. Statistical approach of ANOVA performed to data obtained from experimental design.

Source of variation	DF[a]	SS[b]	MS[c]	*F-value*	*p-value*
Regression	9	5400.50	600.06	5.90	0.03
Residual Error	5	508.49	101.70	-	-
Total	14	5908.99	-	-	-

[a] Degrees of freedom; [b] Sum of squares; [c] Mean square.

Table C.7. The yields of main products, *i.e.* pentoses (sum of arabinose and xylose), furfural, glucose, 5-HMF and acetic acid found in liquid from reactions at optimal conditions (131.0 °C, 58.7 wt.% H_2O and 88.0 min) with fresh IL and with recovered IL.

Entry	Yield (mol%)[a]				
	Pentoses	Furfural	Glucose	5-HMF	Acetic acid
Fresh IL	80.5	5.3	7.3	1.7	100.7
Recovered IL	78.5	4.0	5.4	3.2	121.8

[a] For quantification please refer to next sections.

Table C.8. The yield of recovered solid (SY) and composition of solid and recovery yields of main components *i.e.* arabinoxylan (sum of xylan and arabinan), acetyl groups, glucan, Klason lignin and ash produced in biomass reactions at optimal conditions (131.0 °C, 58.7 wt.% H_2O and 88.0 min) with fresh IL and with recovered IL.

Entry	SY %(w·w^{-1})	Composition (wt.%)[a] (recovery yield %(w·w^{-1}))[a]				
		Arabinoxylan	Acetyl groups	Glucan	KL	Ash
Fresh IL	57.8	6.7 (17.6)	0.0 (0.0)	60.6 (90.9)	29.3 (95.7)	3.4 (18.4)
Recovered IL	60.2	9.3 (25.3)	0.0 (0.0)	59.4 (92.9)	23.1 (78.5)	5.2 (29.0)

[a] For quantification please refer to next sections.

Determination of severity factor ($logR_o$)

For comparison purposes and to provide a mathematic tool for direct analysis of the influence of three studied parameters a severity factor ($logR_O$) for reactions with catalysts was calculated using the following equation: $logR_O = log_{10}\left(e^{\left(\frac{T_r - T_b}{\omega}\right)} \times \Delta t\right)$, where T_r and T_b are absolute reaction temperature and reference temperature when hydrolysis initiates with [emim][HSO_4], respectively, and are expressed in °C, and ω is a dimensionless constant that translates the effect of the temperature in the conversion. Yields of hemicellulose hydrolysis with [emim][HSO_4] obtained in this work were used to estimate the values of T_b and ω.

The value of T_b was attained by applying the equation below obtained from Doehlert experimental design (section 2.4 of the article) for all the hemicellulose hydrolysis experiments examined. The point (x,0,0) represents the value of T_b and by solving the equation obtained from experimental design in the following form $Y = 77.01 + 30.83X_1 - 0.59X_2 - 0.62X_1X_2 - 21.20{X_1}^2 - 11.00{X_2}^2$, where Y is the percentage of hemicellulose hydrolysis and X_1, X_2 are the temperature (°C) and H_2O content (wt%), respectively. The result gave T_b= 80.25 °C.

The value of ω was attained by representation of the experimental results using the following equation: $Y = mX + B$, where $Y = \ln(-\ln(1-\alpha))$, where α is the hydrolysis of hemicellulose and X is the severity factor calculated in the following manner: $X = logR_O = log_{10}\left(R_{o_{heating}} + R_{o_{isothermal}}\right)$, where $R_{o_{heating}}$ is the severity factor for heating and $R_{0_{isothermal}}$ is the severity factor for isothermal condition process. Hence the value of ω was 7.2, obtained by maximisation of R^2.

Therefore, $logR_O$ for each reaction was calculated through the following equation: $logR_O = log_{10}\left(e^{\left(\frac{T_r - 80.25}{7.2}\right)} \times \Delta t\right)$.

Calculations of the yields of products in the liquid samples

$$pentose\ yield\ (mol\%) = \frac{m_{pentose}}{m_{arabinoxylan_{native}}} \times \frac{132}{150} \times 100$$

$$glucose\ yield\ (mol\%) = \frac{m_{glucose}}{m_{glucan_{native}}} \times \frac{162}{180} \times 100$$

$$furfural\ yield\ (mol\%) = \frac{m_{furfural}}{m_{arabinoxylan_{native}}} \times \frac{132}{96} \times 100$$

$$HMF\ yield\ (mol\%) = \frac{m_{5-HMF}}{m_{glucan_{native}}} \times \frac{162}{126} \times 100$$

$$acetic\ acid\ yield\ (mol\%) = \frac{m_{acetic\ acid}}{m_{acetyl\ group_{native}}} \times \frac{59}{60} \times 100$$

native means the amount of fraction in native biomass

Calculations of the recovery yields in the solid phase samples

$$solid\ recovery\ yield\ (wt.\%) = \frac{m_{dry\ biomass_{initial}}}{m_{dry\ biomass_{after\ reaction}}} \times 100$$

$$arabinoxylan\ recovery\ yield\ (wt.\%) = \frac{m_{arabinoxylan}}{m_{arabinoxylan_{native}}} \times 100$$

$$acetyl\ groups'recovery\ yield\ (wt.\%) = \frac{m_{acetyl\ groups}}{m_{acetyl\ groups_{native}}} \times 100$$

$$glucan\ recovery\ yield\ (wt.\%) = \frac{m_{glucan}}{m_{glucan_{native}}} \times 100$$

$$lignin\ recovery\ yield\ (wt.\%) = \frac{m_{lignin}}{m_{lignin_{native}}} \times 100$$

$$ash\ recovery\ yield\ (wt.\%) = \frac{m_{ash}}{m_{ash_{native}}} \times 100$$

native means the amount of fraction in native biomass; *initial* means the amount of biomass used in the reaction; *after reaction* means the amount of biomass recovered after the reaction;

Calculations of the solid phase samples' composition

$$arabinoxylan\ content\ (wt.\%) = \frac{m_{arabinoxylan}}{m_{recovered\ biomass}} \times 100$$

$$acetyl\ groups\ content\ (wt.\%) = \frac{m_{acetyl\ groups}}{m_{recovered\ biomass}} \times 100$$

$$glucan\ content\ (wt.\%) = \frac{m_{glucan}}{m_{recovered\ biomass}} \times 100$$

$$lignin\ content\ (wt.\%) = \frac{m_{lignin}}{m_{recovered\ biomass}} \times 100$$

$$ash\ content\ (wt.\%) = \frac{m_{ash}}{m_{recovered\ biomass}} \times 100$$

Mass Balances: Scenario A

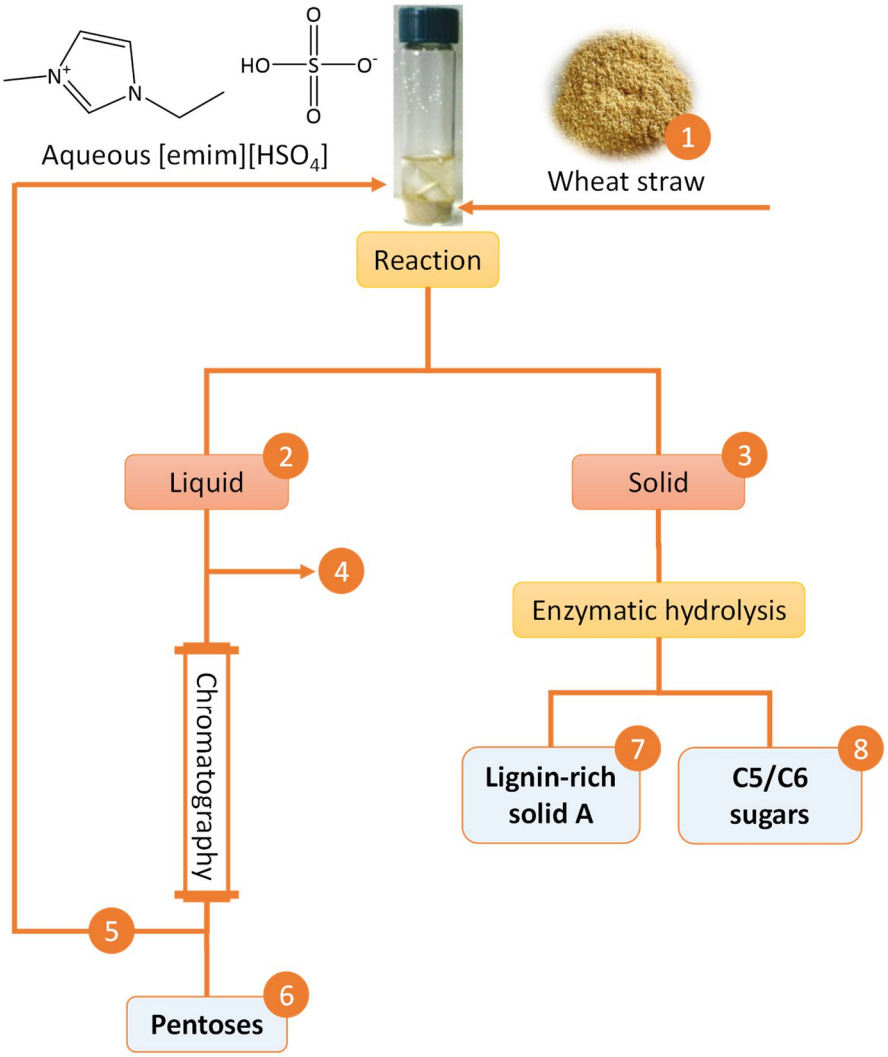

Figure C.1. Flowchart of scenario A process.

Table C.9. Mass balance (g) for streams of scenario A (Figure C.1.) on the basis of 1 kg of wheat straw.

	Scenario A							
Components	**1**	**2**	**3**	**4**	**5**	**6**	**7**	**8**
Glucan	385.0		350.1				84.8	
Xylan	191.0		38.9				0.9	
Arabinan	30.0		0.0				0.0	
Arabinoxylan	221.0		38.9				0.9	
Acetyl groups	27.0		0.0			-		
Lignin	177.0		169.5			-	150.5	
Ash	107.0		19.7			-	19.7	
Others	83.0					-		
Glucose		31.1				6.1		294.9
Xylose		168.6				148.5		43.2
Arabinose		33.5				30.5		0.0
Pentoses		202.1				179.0		43.2
Acetic acid		27.6		18.6		-		
5-HMF		5.3		-	5.3	-		
Furfural		8.5		8.3		-		

Mass Balances: Scenario B

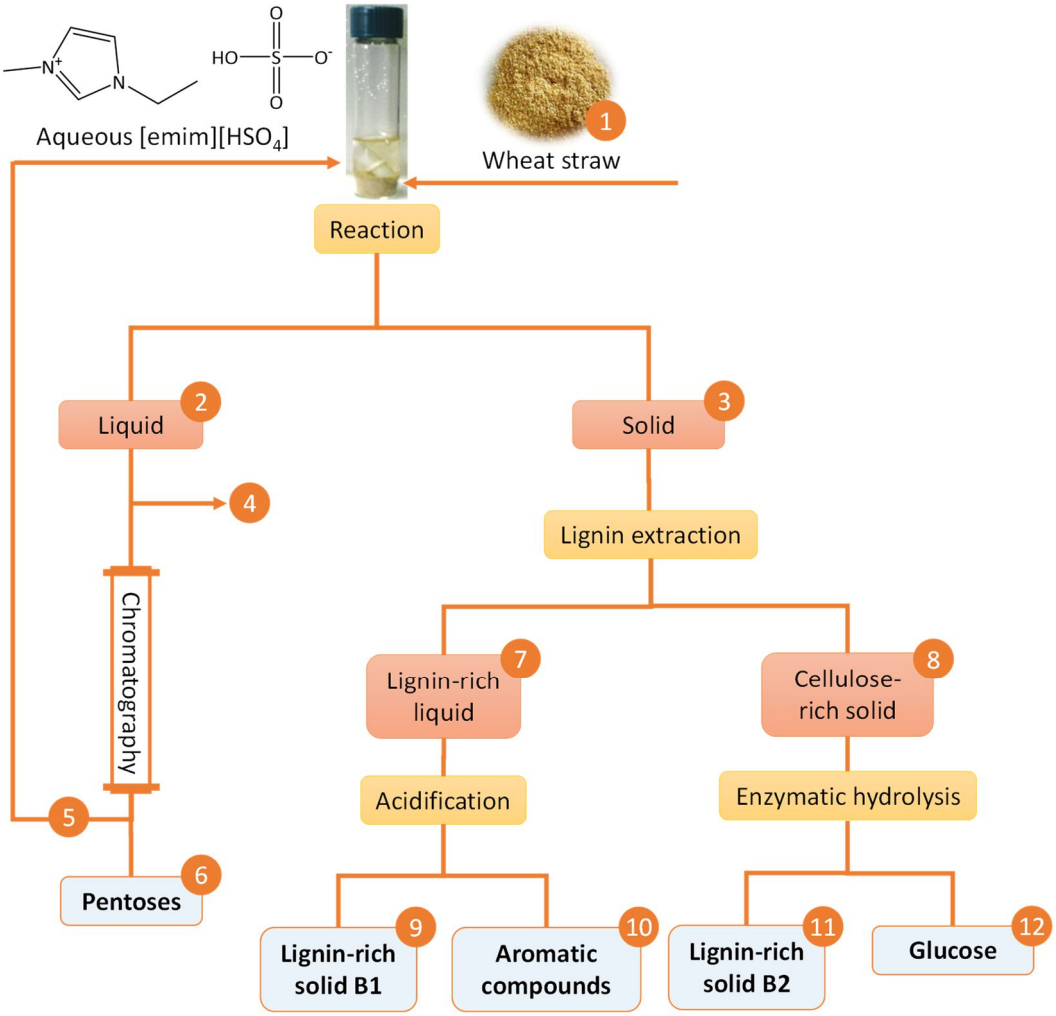

Figure C.2. Flowchart of scenario B process.

Table C.10. Mass balance (g) for streams of scenario B (Figure C.2.) on the basis of 1 kg of wheat straw.

	Scenario B									
Components	**1**	**2**	**3**	**4**	**5**	**6**	**9**	**10**	**11**	**12**
Glucan	385.0		350.1						30.6	
Xylan	191.0		38.9							
Arabinan	30.0		0.0							
Arabinoxylan	221.0		38.9							
Acetyl groups	27.0		0.0							
Lignin	177.0		169.5				75.4			
Ash	107.0		19.7							
Others	83.0									
Glucose		31.1				6.1				355.0
Xylose		168.6				148.5				
Arabinose		33.5				30.5				
Pentoses		202.1				179.0				
Acetic acid		27.6		18.6						
5-HMF		5.3			5.3					
Furfural		8.5		8.3						
Aromatic compounds								traces		

Table C.11. Main assumptions regarding the prices of feedstocks, products and utilities, settings of labour and technical issues as well as heat capacity constants for used solvents.

Feedstocks	**€·kg^{-1}**	**Labour**	
Wheat straw	0.045	Human resources per unit operation	4[1]
Ionic Liquid	1.000[2]	Salary (€/person)	2500[1]
Water	0.100 (**€·m^{-3}**)[1]	Working time (days/year)	330[1]
Enzyme	4.000[3]	**Technical**	
Acetonitrile	0.400[1]	acetonitrile/biomass ratio (w·w^{-1})	100
NaOH	0.100[1]	Enzyme loading (g_{enzyme}·g_{glucan}^{-1})	0.10
HCl	0.100[1]	Yield ($g_{pentoses}$·$g_{xylitol}^{-1}$)	0.76
Products	**€·kg^{-1}**	Yield ($g_{glucose}$·$g_{succinic\ acid}^{-1}$)	0.89
Pentoses	0.285[1]	**Energy balance**	
Glucose	0.296[1]	$h_{(H2O)}$ @ 25 °C (kJ·kg^{-1})[4]	4.180
Lignin	0.143[5]	$h_{(H2O)}$ @ 50 °C (kJ·kg^{-1})[4]	4.182
High purity lignin	0.800[6]	$h_{(H2O)}$ @ 70 °C (kJ·kg^{-1})[4]	4.191
Xylitol	2.709[7]	$h_{(H2O)}$ @ 130 °C (kJ·kg^{-1})[4]	4.270
Succinic acid	1.987[8]	$Cp_{(IL)}$ @ 25 °C (kJ·K·kmol^{-1})[a]	1.817
Utilities		$Cp_{(IL)}$ @ 130 °C (kJ·K·kmol^{-1})[a]	1.923
Electricity (€·kWh^{-1})	0.158[1]	$Cp_{(acetonitrile)}$ @ 25 °C (kJ·K·kmol^{-1})[9]	93.0
		$Cp_{(acetonitrile)}$ @ 40 °C (kJ·K·kmol^{-1})[9]	91.7

[a] there is no literature data for [emim][HSO_4] thus data for [emim][$EtSO_4$] from [10] were used in this work, h – specific enthalpy, Cp – heat capacity.

[1] Intelligen, Inc. SuperPro Designer, V8.5 Build 7, Special Build 3550 edn., 2013.
[2] A. Brandt, F. Gschwend, P. Fennell, T. Lammens, B. Tan, J. Weale and J. Hallett, *Green Chem.*, 2017, **19**, 3078-3102.
[3] L. da Costa Sousa, M. Jin, S. P. Chundawat, V. Bokade, X. Tang, A. Azarpira, F. Lu, U. Avci, J. Humpula and N. Uppugundla, *Energ. Environ. Sci.*, 2016, **9**, 1215-1223.
[4] The Engineering ToolBox, http://www.engineeringtoolbox.com/.
[5] Technical lignin, http://www.alibaba.com/.
[6] High purity lignin (90%), http://www.alibaba.com/.
[7] Xylitol (purity > 99 %) avarage price, http://www.alibaba.com/.
[8] Succinic acid (99.5% purity) average price, http://www.alibaba.com/.
[9] P. J. Linstrom and W. G. Mallard, Book of the NIST Chemistry Web, http://webbook.nist.gov/chemistry/fluid.
[10] Z.-H. Zhang, Z.-C. Tan, L.-X. Sun, Y. Jia-Zhen, X.-C. Lv and Q. Shi, *Thermochim. Acta*, 2006, **447**, 141-146.

Table C.12. The CAPEX for biorefinery infrastructures with capacity of 99000 tonne/year for both scenarios.

	Scenario A	**Scenario B**
CAPEX (€)[11a]	19 008 000	21 120 000

[a] an additional investment for xylitol and succinic acid production on the basis of unit operation was considered, *i.e.* feedstock receive, pentose hydrogenation and xylitol purification, glucose fermentation and succinic acid purification, respectively.

Table C.13. The OPEX of production part for both scenarios.

Feedstock	**Scenario A**	**Scenario B**
	Cost (€/year)	
Wheat straw	445 500	445 500
Water	20 378	21 813
Ionic Liquid	2 733 400	2 733 400
Enzyme	1 386 792	1 386 792
acetonitrile	515 880	515 880
NaOH	-	84 645
HCl	-	77 220
Others[a]	450 160	449 057
Total OPEX (€/year)	5 552 110	5 714 306

[a] other utilities for xylitol and succinic acid production and purification.

[11] M. Persson, Inbicon demonstration plant, *in European Biofuels Technology Platform*, 3rd Stakeholder Plenary Meeting, Brussels, Belgium, 2010.

Table C.14. The OPEX for energetic requirements for scenario A.

Scenario A							
Operation Unit	**T (K)**	**ΔT (K)**	**Component**	**Mass (kg)**	**ΔH (MJ)**	**ΔH (kWh^{-1}/year)**	**Cost(€/year)**
Reaction	404.15	111.0	Water	158 490	1 583.3	145 137	22 932
	404.15	111.0	Ionic Liquid	111 510	1 309.2	120 007	18 961
Distillation	373.15	80.0	Water	6 158 490	19 214.5	1 761 328	278 290
Enzymatic hydrolysis	323.15	30.0	Water	173 400	10.4	954	151
Distillation	313.15	20.0	acetonitrile	990 000	1 883.4	172 646	27 278
Xylitol purification	-	-	-	-	-	-	334 005[a]
Succinic acid purification	-	-	-	-	-	-	471 291[b]
Total OPEX (€/year)							1 152 908

[a] cost includes all intermediary unit operation *i.e.* feedstock receive, pentose hydrogenation and xylitol purification; [b] cost includes all intermediary unit operation *i.e.* feedstock receive, glucose fermentation and succinic acid purification.

Table C.15. The OPEX for energetic requirements for scenario B.

Scenario B							
Operation Unit	**T (K)**	**ΔT (K)**	**Component**	**Mass (kg)**	**ΔH (MJ)**	**ΔH (kWh^{-1}/year)**	**Cost(€/year)**
Reaction	404.15	111.0	Water	158 490	1 583.3	145 137	22 932
	404.15	111.0	Ionic Liquid	111 510	1 309.2	120 007	18 961
Distillation	373.15	80.0	Water	6 158 490	19 214.5	1 761 328	278 290
Alkaline extraction	343.15	50.0	Water	433 500	238.4	21 856	3 453
Acidification	343.15	50.0	Water	3 000 000	1 650.0	151 250	23 898
Enzymatic hydrolysis	323.15	30.0	Water	120 000	7.2	660	104
Distillation	313.15	20.0	acetonitrile	990 000	1 883.4	172 646	27 278
Xylitol purification	-	-	-	-	-	-	334 005[a]
Succinic acid purification	-	-	-	-	-	-	567 466[b]
Total OPEX (€/year)							1 276 387

[a] cost includes all intermediary unit operation *i.e.* feedstock receive, pentose hydrogenation and xylitol purification; [b] cost includes all intermediary unit operation *i.e.* feedstock receive, glucose fermentation and succinic acid purification.

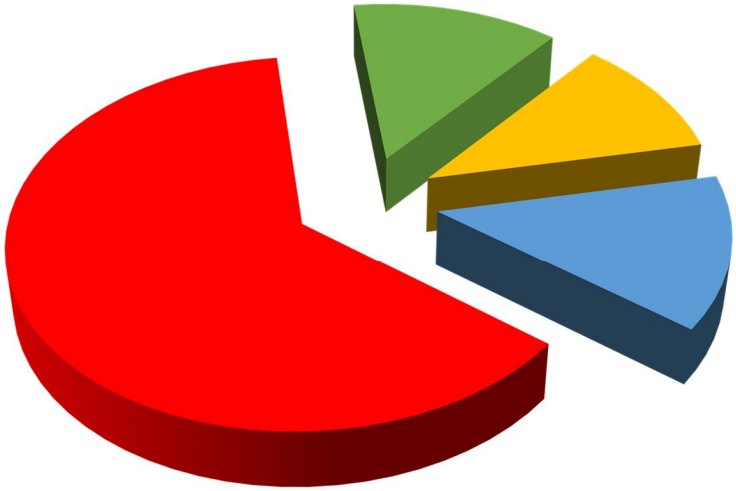

Figure C.3. Cost breakdown for scenario A. Red part represents feedstock (62.7 %), blue part corresponds to labour costs (13.6 %), orange part represents the depreciation cost (10.7 %) and green part demonstrates the cost of utilities (13.0 %).

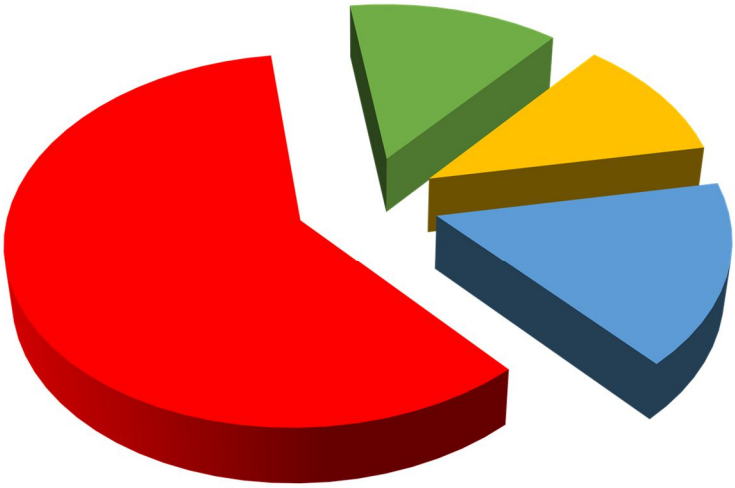

Figure C.4. Cost breakdown for scenario B. Red part represents feedstock (59.5 %), blue part corresponds to labour costs (16.2 %), orange part represents the depreciation cost (11.0 %) and green part demonstrates the cost of utilities (13.3 %).

Table C.16. Revenues for scenario A considering the hydrogenation of pentoses into xylitol (76% mass yield)[12] and fermentation of glucose into succinic acid (89% mass yield).[13]

Scenario A				
Products$_{(practical)}$	**Mass (kg)**	**Products$_{(theoretical)}$**	**Mass (kg)**	**Revenue (€/year)**
Pentoses	5 370	Xylitol	4 081	3 648 156
Glucose	8 850	Succinic acid	7 847	5 145 162
Low purity lignin	7 680	High purity lignin	7 680	361 152
Total revenue (€/year)				9 154 470

Table C.17. Revenue for scenario B considering the hydrogenation of pentoses into xylitol (76% mass yield)[12] and fermentation of glucose into succinic acid (89% mass yield).[13]

Scenario B				
Products$_{(practical)}$	**Mass (kg)**	**Products$_{(theoretical)}$**	**Mass (kg)**	**Revenue (€/year)**
Pentoses	5 370	Xylitol	4 081	3 648 156
Glucose	10 656	Succinic acid	9 448	6 195 124
High purity lignin	2 262	High purity lignin	2 262	597 168
Total revenue (€/year)				10 440 448

[12] A. J. Melaja and L. Hamalainen, US4008285A, 1977.
[13] C. Pateraki, M. Patsalou, A. Vlysidis, N. Kopsahelis, C. Webb, A. A. Koutinas and M. Koutinas, *Biochem. Eng. J.*, 2016, **112**, 285-303.